# THE LARGE AMPLITUDE VIBRATION OF MULTI-ROTOR SYSTEMS SUPPORTED UPON OIL-FILM BEARINGS

by

ANDREW GORDON HOLMES

A thesis submitted for the degree of
Doctor of Philosophy
of the
University of London
and also for the
Diploma of Imperial College

November 1977

Applied Mechanics Group
Department of Mechanical Engineering
Imperial College of Science & Technology
London SW7 2BX

## ABSTRACT

The self-excited flexural vibration of a multi-rotor system due to vertical misalignment of the support bearings was investigated using numerical initial-value-problem techniques. The equations of motion are expressed in terms of the free-free modes of the shaft, and the modal coefficients propagated in time.

The method was used to study a two rotor, four bearing system subjected to vertical misalignment of one of the central bearings. Previous authors have reported that, for single rotor systems supported upon bearings with circular symmetry, the speed of the shaft had to be increased beyond twice its first pinned critical speed, and external damping applied to the shaft, in order to predict the finite amplitude whirl, at frequencies less than half shaft rotational frequency, that has been observed in practice. This was confirmed for the two rotor system but it was found that, by using a non-circular lemon-bore bearing model, realistic limit cycle motion was obtained, which was in agreement with the amplitude and the frequency of the motion observed for large turbogenerators, without the need to apply heavy (and quite arbitrary) damping to the shaft.

The method is general and may be used for any rotor geometry for which the free-free modes and natural frequencies are known, and for any number of bearings. Any bearing configuration for which there is a suitable computational model for the oil-film forces may be included.

In addition, the basic method was adapted to calculate the bearing settings required to align the system; the equilibrium position of the rotating shaft; the stability of the equilibrium position; and the forced response of the linearised system.

ACKNOWLEDGEMENTS

I wish to express my gratitude to the following:

Dr C. Ettles for giving me the opportunity to conduct this research, and for his advice and encouragement during its execution.

The Central Electricity Generating Board for providing me with a bursary.

The staff of the Midlands Region Scientific Services Department of the Central Electricity Generating Board, especially Dr I. Mayes, for stimulating discussions and many helpful suggestions.

Mr N. James for his advice on computer programming techniques.

Miss E.A. Quin for her efficient typing of this thesis.

Finally, my wife, Denise, for her unfailing support and encouragement.

CONTENTS

Page

APPENDICES

## LIST OF FIGURES

# LIST OF TABLES

## NOTATION

| Symbol | | Description |
|---|---|---|
| $a_{R_i}$, $a_{I_i}$ | : | transformed modal coefficients (6.9) |
| $A_R$, $A_I$ | : | modal sums of transformed modal coefficients (6.12, 6.13) |
| $A_\varepsilon$ | : | (7.24) |
| $B$ | : | length of bearing |
| $B_\varepsilon$ | : | (7.25) |
| $C$ | : | arc radial clearance |
| $C_D(Z)$ | : | coefficient of viscous damping |
| $c_d(s)$ | : | non-dimensional coefficient of viscous damping (2.17) |
| $c_m$ | : | minimum radial clearance in bearing |
| $c_r$ | : | reference radial clearance of system |
| $[C_{xx}]$, $[C_{xy}]$, etc. | : | matrices containing modal sums of linearised bearing forces (5.38 - 5.41) |
| $d$ | : | geometric preset of arc (see Figure 7.1) |
| $e$ | : | eccentricity of journal relative to arc centre |
| $\overline{e}$ | : | eccentricity of journal relative to bearing centre |
| $EI(Z)$ | : | flexural rigidity of shaft |
| $E_c$ | : | cumulative energy input to shaft from a bearing |
| $F_u^{(j)}$ | : | $j$th point unbalance force |
| $F_{u\xi}^{(j)}$, $F_{u\eta}^{(j)}$ | : | components of $j$th point unbalance force in $\xi,\eta$ directions |
| $F_{x_k}$, $F_{y_k}$ | : | forces exerted by $k$th bearing in $X,Y$ directions |
| $f_{x_k}$, $f_{y_k}$ | : | non-dimensional forces exerted by $k$th bearing (2.19, 2.20) |

| Symbol | | Description |
|---|---|---|
| $F_{\varepsilon_k}$, $F_{\psi_k}$ | : | forces exerted by $k$th bearing in $\varepsilon,\psi$ directions |
| $f_{\varepsilon_k}$, $f_{\psi_k}$ | : | non-dimensional forces exerted by $k$th bearing (3.18, 3.19) |
| $g$ | : | gravitational constant |
| $g_c$ | : | non-dimensional geometric preset of arc (7.6,7.7) |
| $h$ | : | film thickness (3.2) |
| $h^*$ | : | non-dimensional film thickness (3.6) |
| $I_m$ | : | non-dimensional mass moment of inertia of shaft (2.55) |
| $\underline{i}$ | : | $\sqrt{-1}$ |
| $K_s$ | : | simple spring constant |
| $[K_{xx}]$, $[K_{xy}]$, etc. | : | matrices containing modal sums of linearised bearing forces (5.42 - 5.45) |
| $L$ | : | total length of shaft |
| $M$ | : | total mass of shaft |
| $m_l(s)$ | : | non-dimensional mass per unit length of shaft |
| $m$ | : | number of free-free modes in modal expansion |
| $n$ | : | number of bearings in system |
| $P$ | : | oil-film pressure |
| $P^*$, $\overline{P}$ | : | non-dimensional pressure (3.8) |
| $P_a$ | : | non-dimensional mean axial pressure |
| $P_c$ | : | non-dimensional centre line pressure |
| $P_l$ | : | non-dimensional pressure according to long bearing approximation |
| $Q_{\xi_i}$, $Q_{\eta_i}$ | : | generalised unbalance components (2.67,2.68) |
| $q_{x_i}$, $q_{y_i}$ | : | modal coefficients (2.61,2.62) |
| $\{q\}$ | : | vector containing modal coefficients $q_{x_i}$,$q_{y_i}$ (5.17) |

| Symbol | | Description |
|---|---|---|
| $\{q_x\}$ | : | vector containing modal coefficients $q_{x_i}$ (5.60) |
| $\{\bar{q}\}$ | : | vector defined by (5.48) |
| $r_\xi(Z)$, $r_\eta(Z)$ | : | displacement of mass centre of shaft from geometric centre measured relative to coordinate system $OZ$ (see Figure 2.2) |
| $R$ | : | journal radius |
| $s$ | : | non-dimensional coordinate along axis of shaft (2.8) |
| $s_k$ | : | non-dimensional displacement along shaft to $k$th bearing (2.9) |
| $s_g$ | : | non-dimensional displacement along shaft to centre of mass (2.54) |
| $S_t$ | : | stability parameter |
| $t$ | : | time |
| $u_\xi(s)$, $u_\eta(s)$ | : | non-dimensional displacement of mass centre of shaft from geometric centre (2.15,2.16) |
| $u_{x_i}$, $u_{y_i}$ | : | derivatives of modal coefficients $q_{x_i}$,$q_{y_i}$ (2.72, 2.73) |
| $\{u\}$ | : | vector containing modal coefficients $u_{x_i}$,$u_{y_i}$, $q_{x_i}$,$q_{y_i}$ (5.24) |
| $\{\bar{u}\}$ | : | vector defined by (5.27) |
| $V_\varepsilon(\theta)$ | : | (7.30) |
| $W_k$ | : | non-dimensional load carried by $k$th bearing in an aligned system (5.4) |
| $W_\varepsilon(\theta)$ | : | equivalent "wedge" term in Reynolds equation (7.26) |
| $X$, $Y$ | : | coordinates perpendicular to axis of shaft (see Figure 2.1) |

| Symbol | | Description |
|---|---|---|
| $x$, $y$ | : | non-dimensional coordinates perpendicular to axis of shaft (2.4,2.5) |
| $X_{b_k}$, $Y_{b_k}$ | : | displacement of $k$th bearing centre relative to datum (see Figure 2.1) |
| $x_{b_k}$, $y_{b_k}$ | : | non-dimensional displacement of $k$th bearing centre relative to datum (2.6,2.7) |
| $Z$ | : | coordinate along axis of shaft (see Figure 2.1) |
| $Z_k$ | : | displacement along shaft to centre of $k$th bearing (see Figure 2.1) |
| $\overline{z}$ | : | axial coordinate measured from mid-plane of bearing |
| $z^*$ | : | non-dimensional axial coordinate measured from mid-plane of bearing (3.7) |
| $\alpha$ | : | (diameter/length) ratio of bearing (3.9) |
| $\beta$ | : | bearing parameter (3.20) |
| $\gamma$ | : | critical damping ratio (2.26) |
| $\delta(Z)$, $\delta(S)$ | : | Dirac delta function (2.3,2.21) |
| $\delta_{ij}$ | : | Kronecker delta (2.43) |
| $\Delta x_{b_k}$, $\Delta y_{b_k}$ | : | non-dimensional misalignment of $k$th bearing from aligned condition (5.13,5.14) |
| $\varepsilon$ | : | non-dimensional eccentricity of journal relative to arc centre, $e/C$ |
| $\overline{\varepsilon}$ | : | non-dimensional eccentricity of journal relative to bearing centre (7.11) |
| $\eta_e$ | : | effective viscosity of oil |
| $\theta$ | : | circumferential coordinate measured relative to line of centres (see Figures 3.1 and 7.2) |

| Symbol | | Description |
|---|---|---|
| $\theta_1$, $\theta_2$ | : | oil-film in $\theta$ coordinate |
| $\theta_s$, $\theta_f$ | : | start and finish of arc in $\theta$ coordinate |
| $\theta_c$ | : | point of cavitation in $\theta$ coordinate |
| $\theta_m$ | : | point of maximum pressure in $\theta$ coordinate |
| $\bar{\theta}$ | : | circumferential coordinate measure relative to fixed axis through bearing centre (see Figure 7.2) |
| $\bar{\theta}_1$, $\bar{\theta}_2$ | : | oil-film limits in $\bar{\theta}$ coordinate |
| $\bar{\theta}_s$, $\bar{\theta}_f$ | : | start and finish of arc in $\bar{\theta}$ coordinate |
| $\kappa$ | : | side leakage correction factor |
| $\lambda_i$ | : | an eigenvalue of the linearised system |
| $\mu_i^2$ | : | non-dimensional free-free natural frequency of a uniform shaft (4.4) |
| $\nu_{f_i}$ | : | non-dimensional free-free natural frequency of shaft, $\omega_{f_i}/\omega$ |
| $\nu_{p_i}$ | : | non-dimensional pinned natural frequency of shaft, $\omega_{p_i}/\omega$ |
| $\nu_{w_i}$ | : | non-dimensional steady-state whirl frequency, $\omega_{w_i}/\omega$ |
| $\rho A(Z)$ | : | mass per unit length of shaft |
| $\rho_i$ | : | complex modal coefficient (6.7) |
| $\sigma(s)$ | : | non-dimensional flexural rigidity of shaft (2.13) |
| $\tau$ | : | non-dimensional time (2.10) |
| $\phi_i(s)$ | : | non-dimensional free-free mode shape of shaft (i.e. an eigenfunction of equation 2.29) |
| $\psi$ | : | attitude angle of journal relative to arc centre (see Figures 3.1 and 7.2) |
| $\omega$ | : | shaft rotational speed |
| $\omega_d$ | : | design rotational speed of shaft |

| Symbol | | Description |
|---|---|---|
| $\omega_{f_i}$ | : | free-free natural frequency of shaft |
| $\omega_{p_i}$ | : | pinned natural frequency of shaft |
| $\omega_{w_i}$ | : | steady-state whirl frequency |
| $(\dot{})$ | : | denotes differentiation with respect to $\tau$, i.e. $d/d\tau$ or $\partial/\partial\tau$ |

Subscripts

| | | |
|---|---|---|
| $()_a$ | : | denotes aligned condition |
| $()_o$ | : | denotes equilibrium condition |
| $()_k$ | : | denotes $k$th bearing |

# CHAPTER 1

# INTRODUCTION

## 1.1 STATEMENT OF PROBLEM

Vertical misalignment of the support bearings due to the differential thermal expansion of the bearing pedestals is considered to be one of the principal causes of the non-synchronous flexural vibration exhibited by large turbogenerators. Although operational experience has shown that the amplitude of the vibration is not always large enough to cause loss on internal clearance or bearing damage, its non-synchronous nature is undesirable as the shaft is subjected to cyclic stresses which may propagate fatigue cracks. Such vibration sometimes continues for several hours which, because of its finite amplitude and non-synchronous frequency, is a non-linear phenomenon normally attributable to the oil-film bearings.

The non-linear behaviour of the generic rotor system, comprising a rotor supported by two bearings, has been the subject of a number of previous investigations. However, with only two bearings, it is not possible to consider the effect of misalignment.

### 1.1.1 Terms of Reference

(1) To develop a computer based method for predicting the non-linear flexural vibrations of a shaft supported upon oil-film bearings. The method should be capable of treating a shaft having any realistic distribution of mass and flexural stiffness and supported upon any number of bearings. A facility must be available for introducing parallel misalignment (both horizontal and vertical) to any of the bearings.

(2) The method should be used to study the non-linear behaviour of a simple two rotor, four bearing system subjected to vertical misalignment of the bearings. The objective being to gain a better understanding of misalignment induced large amplitude vibration by obtaining qualitative information about the non-linear behaviour of the simple system, rather than detailed quantitative information.

## 1.2 PRELIMINARY DISCUSSION

It has been recognised for more than fifty years that, under certain conditions, the interaction of the journal bearing oil-film forces and the shafts they support may be responsible for violent vibration in rotating machinery, at frequencies not predicted by consideration of the shaft alone. Although the dynamic characteristics of flexible shafts are, to a close approximation, linear and thus amenable to analysis, two factors have impaired progress towards a full understanding and prediction of the behaviour of rotating shafts supported upon journal bearings.

The first concerns the calculation of the oil-film forces, which requires the solution of the Reynolds equation for the pressure field generated in the bearing. Unfortunately, a solution to this equation is not available, even for the comparatively simple geometry of a plane circular bore bearing, without recourse to numerical techniques and modern computational aids. This difficulty has, however, been overcome in many studies by the use of approximate solutions of which the "long" bearing and "short" bearing solutions are well known.

The second and more fundamental difficulty is that the oil-film forces are non-linear functions of the velocity and displacement of the journal within the bearing. Incorporation of these forces into an analysis of the shaft motion produce non-linear equations of motion. Because numerical and analogue methods are the only means generally available for obtaining solutions to non-linear differential equations, the investigation of the non-linear effects of the oil-film force had to await the advent of the modern computer.

In the majority of theoretical investigations reported in the literature, it is assumed that the excursion of the journal about its equilibrium position is small so that the oil-film force, in each of two

perpendicular directions, may be approximated as a linear function of the velocity and displacement, relative to the equilibrium position, in each of the two perpendicular directions. (The oil-film force acting on the journal is, for a given bearing configuration and at a given equilibrium position, thus determined by eight linearised bearing coefficients, usually known as the stiffness and damping coefficients of the bearing.) This assumption yields linear equations of motion which are amenable to well established techniques of analysis. But, although a linearised analysis is valuable for determining the stability of the equilibrium position of the rotating shaft, or the forced response of the system to unbalance excitation, it is unable to account for finite amplitude self-excited vibration (or a subharmonic response to unbalance excitation), the study of which is the purpose of this work.

## 1.3 LITERATURE SURVEY

### 1.3.1 Early Studies

Newkirk & Taylor (1925) were the first to identify and investigate journal bearing induced instability in rotating systems. A comprehensive review of the studies, both experimental and theoretical, conducted during the following thirty five years, is given in review papers by Newkirk (1957) and Sternlicht (1967). A summary of some of the principal experimental findings of this period will now be given.

(1) If self-excited vibration developed, the motion was observed to be one of two types: the first, known as *resonant whirl*, occurred when the shaft was rotating at speeds in excess of twice its first pinned (i.e. simply supported) critical speed. The amplitude of vibration in this case was large and the whirl frequency was approximately equal to the first pinned natural frequency of the shaft. The second type of self-excited motion, known as *half frequency whirl*, occurred at speeds below twice the first pinned critical speed, when the shaft was lightly loaded. In this case, the vibration was not as violent as for resonant whirl and the frequency was approximately equal to, but always slightly less than, half the rotational frequency.

(2) Heavy bearing loads promoted stable motion. For rotors supported upon more than two bearings, whirling sometimes developed if misalignment reduced the load carried by one of the bearings.

(3) Newkirk & Taylor (1925) reported that, once whirl had developed, it persisted at all higher speeds. Pinkus (1956), however, reported a case where resonant whirl died out at speeds exceeding three times the lowest pinned critical speed.

(4) The onset and intensity of self-excited vibration is almost unaffected by rotor unbalance.

(5) A hysteresis (or inertia) effect was sometimes observed. That is, when the rotational speed of the shaft was decreased, self-excited vibrations persisted down to a speed lower than that at which self-excited vibration started when the speed was increased. The ability to induce whirl in a shaft by subjecting it to a sudden blow, reported by Newkirk & Taylor (1925), is another facet of this phenomenon.

(6) Some bearing configurations exhibited a greater resistance to the onset of self-excited vibrations than did others. The plain circular bore bearing was the most susceptible to self-excited vibrations, whilst lemon-bore ("elliptical"), three lobe, and tilting pad bearings generally exhibited increasing stability, in that order.

The few theoretical investigations conducted during this period were usually based upon the long bearing approximation to the circular-bore bearing. But, because the effects of cavitation were often ignored, the rotor systems were predicted to be inherently unstable, which did not accord with the experimental evidence.

### 1.3.2 Recent Studies

The late 1950s saw the start of a new era in the study of rotor dynamics. The general availability of the modern electronic computer and the recent development of the short bearing approximation, due to Ocvirk (1952), provided the impetus for a whole series of papers on the theoretical prediction of rotor behaviour. It should, however, be added that not all the subsequent theoretical studies depended upon these two factors.

The recent literature will be reviewed under four broad headings: (1) the determination of linearised bearing coefficients; (2) the prediction of non-linear behaviour; (3) methods used to represent the dynamic characteristics of shafts; (4) bearing induced instability in large turbogenerators. No attempt has been made to give a complete bibliography; such a task would not serve a useful purpose here.

#### 1.3.2.1 The determination of linearised bearing coefficients

Sternlicht (1959) determined the stiffness and damping coefficients for a finite width circular bore bearing using numerical techniques. The pressure field for the bearing was solved using finite difference techniques and cavitation of the oil-film was allowed for.

Before this date, the only linearised bearing coefficients available had been those corresponding to a long circular bore bearing - and cavitation effects were often ignored. Hagg & Sankey (1956,1958) had determined stiffness and damping coefficients for commonly occurring bearing configurations, from unbalance response experiments. But, as only four of the eight linearised coefficients may be found in such a manner, they ignored cross coupling effects and postulated a direct stiffness and a direct damping coefficient along each of the principal axes of the elliptical orbit of the journal. These apparent out-of-

balance coefficients (to use Smith's (1969) terminology) are not properties of the bearing alone, and give an imperfect representation of the dynamic properties of the bearing, which make them unsuitable for stability calculations.

Holmes (1960) calculated the eight stiffness and damping coefficients for a short circular bearing having a film extent of $180^{o}$. The linearised coefficients were used to determine the stability profile of a rigid shaft supported upon short circular bearings. Mitchell et al (1965-66) determined the spring stiffness coefficients of a short circular bearing experimentally from the static loading locus of the journal and found good agreement between experiment and theory. The eight stiffness and damping coefficients for several common bearing designs were determined experimentally by Glienecke (1966-67). For this, two different sinusoidal loads (in addition to a static load to alter the equilibrium position of the shaft) were imposed, in turn, upon the bearing, and measurements of the phase and amplitude of the resulting elliptical orbits and the imposed load gave sufficient information for the eight unknown coefficients to be determined by the solution of two sets of four simultaneous equations. Later, Woodcock & Holmes (1969-70) claimed that, because of the ill conditioning inherent in Glienecke's method, more accurate results could be obtained by first obtaining the four stiffness coefficients from the static loading locus (i.e. the method of Mitchell et al) which then allows the four damping coefficients to be determined from a single unbalance test.

Lund (1964) gave theoretically evaluated stiffness and damping coefficients for a tilting pad journal bearing.

Morton (1971) used a similar technique to Glienecke to measure the stiffness and damping coefficients of large turbogenerator

bearings. He found that the predictions based upon theory considerably under-estimate the stability of a system, and over-estimate the stiffness of a bearing. A technique for determining the linearised coefficients of a bearing, in situ, by applying a transient force to the rotating shaft is described by Morton (1974). Again, it was reported that stability calculations based upon theoretically predicted bearing coefficients are generally pessimistic.

#### 1.3.2.2 The prediction of non-linear behaviour

The first comprehensive explanation of the phenomenon of journal bearing induced whirl was given by Hori (1959). Hori studied the behaviour of a single disc (represented as a point mass) mounted at the centre of a light flexible shaft supported upon "long" circular bore bearings. The stability of the equilibrium position of the rotating shaft was assessed, and by considering much simplified equations of motion, it was shown that large amplitude self-excited motion (i.e. resonant whirl) could not exist at speeds below twice the pinned critical speed of the shaft.

Hori argued that, if the equilibrium position of a shaft becomes unstable, when the rotational speed is less than twice the first pinned critical speed, then the self-excited vibration is of small amplitude, the bending of the shaft is slight, and the frequency is approximately equal to half the rotational frequency. When, however, the speed reaches twice the pinned critical speed, large amplitude vibration develops at a frequency approximately equal to the pinned natural frequency of the system.

The hysteresis phenomenon, observed experimentally, was also explained by postulating a situation in which the equilibrium position of the shaft does not become unstable until a speed beyond twice

the critical speed is reached. If, for this situation, the speed is increased, self-excited vibration does not occur until the equilibrium position becomes unstable; and then large amplitude vibration develops immediately. However, once the large amplitude vibration has developed, it persists, even if the equilibrium position is stable, until the speed is reduced to below twice the pinned critical speed.

Hori conducted a series of experimental tests to substantiate his assertions. These also revealed that, under certain conditions, the amplitude of the resonant whirl may decrease, accompanied by an increase in whirl frequency, as the rotational speed is increased. Some aspects of Hori's explanation for this effect were questioned by Tondl (1965). Tondl studied the same system as Hori but assumed that the shaft was vertical, and solved less simplified equations of motion. Tondl showed that a source of external damping was necessary to limit the amplitude of the mid-span of the shaft during resonant whirl, and was also able to give a more satisfactory explanation for the decrease in resonant whirl amplitude with increasing speed.

With the advent of the modern computer, numerical *initial-value-problem* techniques (e.g. Runge-Kutta type methods) became widely used for the solution of the non-linear equation of motion for shafts supported upon journal bearings. Reddi & Trumpler (1962), who were the first to use these techniques to study journal bearing induced instability, investigated the symmetrical motion of a rigid shaft supported upon circular bore bearings. The oil-film forces for this were obtained using the long bearing approximation together with a side leakage correction factor.

Someya (1963-64) used numerical initial-value-problem techniques to study the behaviour of a horizontal flexible shaft supported

upon circular bore bearings. The shaft was represented by three point masses (one situated at each of the journal positions and one at the mid-span of the shaft) connected by light flexible shaft elements. The oil-film forces for a finite width bearing were obtained using a series solution to the Reynolds equation. Although not stated, it is assumed that cavitation was allowed for by neglecting negative pressures when the oil-film forces were calculated. Only symmetric motion of the shaft was considered, which reduced the number of equations of motion to be solved. Someya found that, when the equilibrium position of the shaft became unstable at speeds below twice the pinned critical speed, the motion of shaft centre and disc remained bounded and had a frequency approximately equal to half the rotational frequency. If, however, the speed was greater than twice the pinned critical speed, then whirl developed at a frequency approximately equal to the pinned natural frequency of the shaft, but the mid-span amplitude of the shaft grew incessantly. In order to obtain the finite amplitude resonant whirl observed in practice, Someya proposed that an external damping force, proportional to the square of the velocity of the shaft centre, should act upon the shaft; but he did not identify the physical mechanisms involved.

The short bearing approximation has been used by several authors to study the symmetric motion of a rigid shaft supported upon circular bore bearings. Jennings & Ocvirk (1962) and Huggins (1963-64) used an analogue computer to solve the equations of motion as an initial-value-problem. The analogue computer is ideally suited to transient analyses but, unfortunately, with this device it is difficult to adequately simulate the complex nature of the oil-film forces. Later, Badgley & Booker (1969) and Holmes (1970) solved the equations of motion using Runge-Kutta techniques with the aid of a digitial computer.

An alternative approach was adopted by Lund (1966) who obtained the (symmetric) steady-state, self-excited motion of a rigid shaft, supported by short circular bearings, directly by applying the *method of averaging* to the equations of motion. It was assumed that the motion was dominated by its fundamental frequency component and so only motion due to a single frequency component was permitted in the analysis. This method, although elegant, becomes unmanageable if more than one frequency component is included, or if any but the simplest of systems is considered.

All the aforementioned studies were for single rotor systems. To the best of the author's knowledge, no theoretical study of the non-linear behaviour of shafts supported upon more than two bearings has, to date, been published.

#### 1.3.2.3 Methods used to represent the dynamic characteristics of shafts

In theoretical investigations into the behaviour of shafts supported upon journal bearings, three methods have generally been used to represent the linear dynamic characteristics of the shafts. They are:

(a) lumped mass method;

(b) transfer matrix method (Myklestad-Prohl method)

(c) assumed modes method (Rayleigh-Ritz method)

In the lumped mass method, the shaft is represented by a series of point masses (or, more generally, by localised inertias) connected by light flexible shaft elements. The equations of motion are applied directly at each mass station along the shaft. Such a method was

used by Someya (1963-64) in his study of the non-linear behaviour of a single rotor system. The principal disadvantage of this method is that, in order to adequately represent the dynamic characteristics of a shaft, a large number of mass stations are required, which in a linearised analysis (say) necessitates the manipulation of matrix equations of large order. This method is discussed further in Chapter 2.

The transfer matrix method has been used by several authors to investigate the linearised properties (i.e. stability and forced response) of single and multi-rotor systems (see, for example, Lund & Orcutt (1967), Lund (1974), and Dostal et al (1974)). Although the transfer matrix method is similar to the lumped mass method in that the shaft is represented by a series of mass (or inertia) stations connected by uniform shaft elements (which are normally considered to be inertialess), it has the advantage that large matrices are not generated. (In a rotor dynamics calculation, the maximum size of a matrix would normally be 8 by 8.) Unfortunately, however, the transfer matrix method does readily lend itself to the prediction of the non-linear behaviour of rotor systems.

The assumed modes method was the most recent of the above methods to be applied to the study of shafts supported upon journal bearings. It was first used by Morton (1965-66) to predict the behaviour of large turbogenerator rotors, and later by Black et al (1972) and Black & Loch (1973) to study pump rotor dynamics. The method effectively reduces the number of degrees of freedom needed to represent the dynamic characteristics of a shaft by expressing the deflection of the shaft as a linear combination of a suitable set of its modes shapes obtained for a simpler situation. To date, no work has been published in which this method is used in a study of non-linear shaft motion. There is, however, no reason why this method should not be used for such a study.

1.3.2.4 Bearing induced instability in large turbogenerators

Although it has been recognised for many years that vertical misalignment of journal bearings may be the cause of large amplitude whirl in large turbogenerators, little information (e.g. frequency of vibration and its amplitude at various stations) has been published about this problem. Two reasons are responsible for this. The first is that only recently has it become design policy to install vibration monitoring devices at each bearing, station and at strategic rotor locations, as standard equipment on operational machinery. Before this, such devices were only installed in exceptional circumstances. Secondly, those whose responsibility it is to operate large turbogenerators are, quite reasonably, only willing to publish information couched in very general terms, on what will effectively be viewed as a machine fault, for fear of identifying and embarrassing a manufacturer. Therefore, much of the data used in this work is unpublished data supplied by the Central Electricity Generating Board.

A number of papers have been published on methods of detecting vertical misalignments of bearings, and on methods for determining the remedial action to be taken to cure rotor instability. These include Seery et al (1972), Wronski et al (1973) and Ettles et al (1974). An important point made in Wronski's paper is that changes in the thermal environment may alter bearing pedestal heights by as much as 0.100 inches.

## 1.4 THE METHOD TO BE ADOPTED

The method to be adopted will be to represent the linear dynamic characteristics of the shaft using an assumed modes method based upon the free-free normal modes of the shaft. (The reason for choosing the free-free modes will be discussed later.) The resulting system of non-linear ordinary differential equations will then be solved using numerical initial-value-problem techniques.

# CHAPTER 2

# MATHEMATICAL MODEL

## 2.1 THE EQUATIONS OF MOTION FOR THE FLEXURAL VIBRATIONS OF A ROTATING SHAFT

### 2.1.1 Description of the Rotor System to be Modelled

The rotor system to be modelled comprises a number of flexible rotors coupled together to form a continuous shaft, of total length $L$, whose undeflected axis is parallel to the $OZ$ direction of a fixed rectangular coordinate system $OZXY$. The $OY$ axis is chosen to coincide with vertical (upwards) direction and displacement of the shaft centreline parallel to the $OX$ and $OY$ axes is denoted by $X$ and $Y$, respectively (see Figure 2.1). The shaft has a circular cross-section, the diameter of which may vary along its length, and is supported upon $n$ journal bearings. The location of the centre of the $k$th bearing relative to the frame of reference $OZXY$ is given by $(Z_k, X_{b_k}, Y_{b_k})$.

### 2.1.2 Statement of Equations

Subject to the assumptions stated in the next section, the equations of motion for the flexural vibrations of the rotating shaft are:

$$\left.\begin{aligned} &\frac{\partial^2}{\partial Z^2}\left[EI(Z)\,\frac{\partial^2 X}{\partial Z^2}\right] + C_D(Z)\,\frac{\partial X}{\partial t} + \rho A(Z)\,\frac{\partial^2 X}{\partial t^2} \\ &= \sum_{k=1}^{n} \delta(Z-Z_k)\,F_{x_k} + \rho A(Z)\,\omega^2\left[r_\xi(Z)\cos\omega t - r_\eta(Z)\sin\omega t\right] \\ &\frac{\partial^2}{\partial Z^2}\left[EI(Z)\,\frac{\partial^2 Y}{\partial Z^2}\right] + C_D(Z)\,\frac{\partial Y}{\partial t} + \rho A(Z)\,\frac{\partial^2 Y}{\partial t^2} \\ &= \sum_{k=1}^{n} \delta(Z-Z_k)\,F_{y_k} + \rho A(Z)\,\omega^2\left[r_\xi(Z)\sin\omega t + r_\eta(Z)\cos\omega t\right] - \rho A(Z)\,g \end{aligned}\right\} \quad 2.1$$

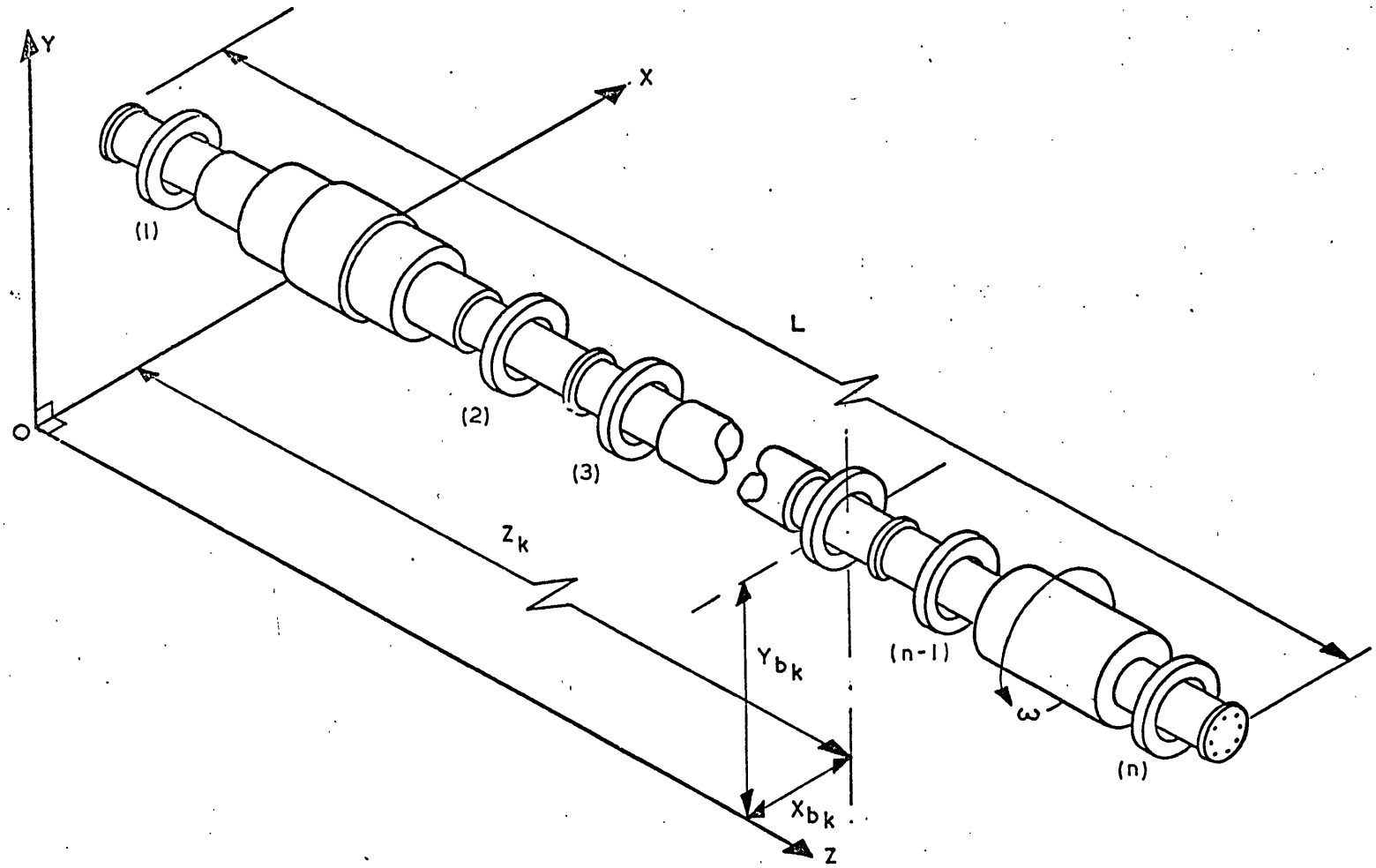


Figure 2.1: A multi-rotor system supported upon $n$ journal bearings

where:

$$\left.\begin{aligned} F_{x_k} &= F_x\left[\frac{\partial X}{\partial t}\,,\ (X-X_{b_k})\,,\ \frac{\partial Y}{\partial t}\,,\ (Y-Y_{b_k})\right]_{Z=Z_k} \\ F_{y_k} &= F_y\left[\frac{\partial X}{\partial t}\,,\ (X-X_{b_k})\,,\ \frac{\partial Y}{\partial t}\,,\ (Y-Y_{b_k})\right]_{Z=Z_k} \end{aligned}\right\} \qquad 2.2$$

The Dirac delta function, $\delta(Z-Z_k)$, is defined as:

$$\left.\begin{aligned} \delta(Z-Z_k) &= 0 \quad , \quad Z \neq Z_k \\ \int_0^L \delta(Z-Z_k)\,dZ &= 1 \end{aligned}\right\} \qquad 2.3$$

and $r_\xi(Z)$ and $r_\eta(Z)$ are the displacements of the mass centre ($M_c$) of the shaft from its geometric centre ($G_c$) measured, as shown in Figure 2.2, relative to the rectangular coordinate system $OZ\xi\eta$, which rotates about $OZ$ at shaft speed $\omega$.

Equations 2.1 are well known, and their derivation, which is achieved by considering the dynamic equilibrium of an elemental slice of the shaft, is described by several authors, including Gladwell & Bishop (1959), Dimentberg (1961) and Tondl (1965).

### 2.1.3 Assumptions

The following assumptions are made about the properties of the rotor system:

(1) The inter-rotor couplings are rigid so that the coupled rotor train may be treated as one continuous shaft.

(2) The shaft is thin so that the effects of rotary inertia and gyroscopic forces upon an element of the shaft, and deformation

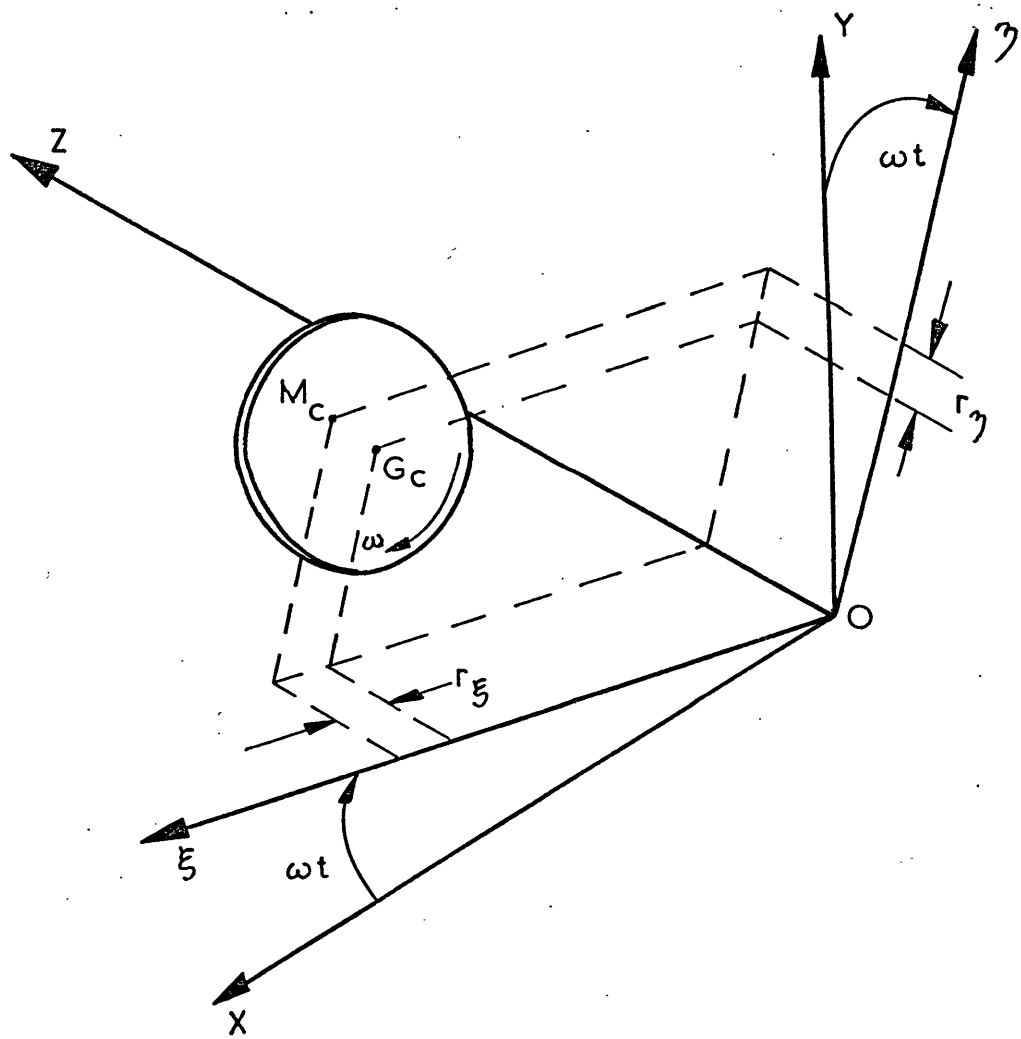


Figure 2.2: The rotating coordinate system $OZ\xi\eta$

due to shear may be neglected.

(3) The shaft, when straight, is free from residual bending stresses, i.e. the shaft does not have a permanent bend.

(4) The shaft has the same flexural rigidity in all directions normal to its axis, i.e. the shaft is axially symmetric.

(5) Internal damping within the shaft due to shrink fits and hysteretic damping is negligible.

(6) The journal bearings are self-aligning, and so do not exert a bending moment upon the shaft.

(7) The journal bearing oil film forces $F_{x_k}$ and $F_{y_k}$ act through the mid axial plane ($Z = Z_k$) of each bearing and are functions of the displacement and velocity of the shaft centre, at this axial plane, relative to the bearing centre.

(8) Fluid forces generated in seals, glands, etc., may be neglected.

(9) The pedestals upon which the bearings are mounted are rigid so that there is no relative motion between the bearing shells and the frame of reference *OZXY*.

(10) Any external damping acting upon the shaft is of a linear viscous nature.

These assumptions are made for the following reasons:

Firstly, the principal objective of this work is to study the non-linear large amplitude vibrations induced in multi-rotor systems by parallel misalignment of the bearings. This behaviour, which results from the interaction of the bearing oil-film forces and the rotating shaft, is in itself a complex phenomenon, the study of which would not be facilitated if further factors were allowed to influence the motion of

the shaft.

It is acknowledged that steam forces in fine clearances are sometimes a cause of instability in large turbogenerators (Greathead (1976)) and that internal friction forces in a rotating shaft can also cause instability (see, for example, Gunter (1967)). However, it is known that, in many instances, instability results from the journal bearings alone. Mayes (1974), from operational experience on 500 MW generating sets, reported that large amplitude vibration, the principal component of which was usually in the range 20-25 Hz, sometimes developed when the machine had reached its operating speed of 3000 rpm after run up, but whilst still running with zero load. Under these conditions, the steam flow is very low and it is unlikely that steam forces are the cause of the excitation. Further, as the instability did not develop when the system passed through its lower critical speeds (a turbogenerator of this size operates in the region of twice its first critical speed), this suggested that internal friction forces were not the cause.

(It should be added that, if desired, the fluid forces generated in the seals and glands can be incorporated into the equations of motion in a similar manner to that used for the bearing forces.)

Secondly, many of the assumptions are mathematically expedient and may only be relaxed at the expense of increasing the complexity of the equations of motion. Although the resulting equations would not be intractable, their solution would be more difficult and, as computers are to be employed for this purpose, more costly.

For example, including the effect of shear, deformation introduces terms that have a fourth order time derivative and, as will be seen later, would double the number of ordinary (non-linear) differential equations to be solved by numerical integration. Whilst several authors

have accounted for shear deformation, rotary inertia and gyroscopic effects in their analyses of rotor systems (see, for example, Lund (1974)), they have also assumed that the motion is of small amplitude so that the bearing forces may be approximated by linear functions - such an assumption would not be meaningful here.

It should be emphasised that most of the assumptions listed above are closely approximated to in turbogenerators and if relaxed would only have a secondary influence upon the behaviour of the system.

Morton (1967-68) in a series of tests on turbogenerator alternator rotors showed that the internal damping was not significant, and that the difference in flexural stiffness between the two principal planes (which, because of the winding slots, it would be reasonable to assume would be greatest in the alternator rotor of a generator set) was always less than 5%.

The assumption that the bearing forces act in a single plane of the shaft is justifiable in view of the ratio of shaft span to bearing length and the axial distribution of the pressure developed in the bearings. The self-aligning condition of the bearings is approximated to in practice by mounting the bearings in spherical seats.

Assumption (10) needs further explanation: several authors, notably Tondl (1965) and Someya (1963-64), have shown that, for a single rotor supported in axisymmetric bearings, a source of damping, other than that provided by the bearings, is needed in order to maintain at a finite level any self-excited oscillations whose frequency is less than half shaft speed. As the frequency of unstable motion in large turbogenerator is normally less than half speed, it was decided to incorporate into the model a facility for providing external linear viscous damping to the shaft, should this be required.

### 2.1.4 The Non-Dimensionalised Equations

The number of independent variables needed to describe the rotor system may be reduced by casting the equations of motion into non-dimensional form. This is achieved by first introducing the following dimensionless variables:

$$x = X/c_r \tag{2.4}$$

$$y = Y/c_r \tag{2.5}$$

$$x_{b_k} = X_{b_k}/c_r \tag{2.6}$$

$$y_{b_k} = Y_{b_k}/c_r \tag{2.7}$$

$$s = Z/L \tag{2.8}$$

$$s_k = Z_k/L \tag{2.9}$$

$$\tau = \omega t \tag{2.10}$$

where $c_r$ is a reference dimension of the system comparable in magnitude to the amplitude of vibration, and is defined here to be the minimum radial clearance of all the bearings in the system.

These are substituted into equations 2.1 and the equations are rendered dimensionless by dividing through by $M\, c_r\, \omega^2/L$, where $M$ is the total mass of the coupled rotors, i.e.

$$M = \int_0^L \rho A(Z)\, dZ \tag{2.11}$$

The resulting non-dimensional equations are:

$$\left.\begin{aligned} &\frac{\partial^2}{\partial s^2}\left[\sigma(s)\,\frac{\partial^2 x}{\partial s^2}\right] + c_d(s)\,\frac{\partial x}{\partial \tau} + m_l(s)\,\frac{\partial^2 x}{\partial \tau^2} \\ &= \sum_{k=1}^{n} \delta(s-s_k)\, f_{x_k} + m_l(s)\left[u_\xi(s)\cos\tau - u_\eta(s)\sin\tau\right] \\ &\frac{\partial^2}{\partial s^2}\left[\sigma(s)\,\frac{\partial^2 y}{\partial s^2}\right] + c_d(s)\,\frac{\partial y}{\partial \tau} + m_l(s)\,\frac{\partial^2 y}{\partial \tau^2} \\ &= \sum_{k=1}^{n} \delta(s-s_k)\, f_{y_k} + m_l(s)\left[u_\xi(s)\sin\tau + u_\eta(s)\cos\tau\right] - m_l(s)\,S_t \end{aligned}\right\} \quad 2.12$$

where:

$$\sigma(s) = \frac{EI}{M\,L^3\,\omega^2} \quad 2.13$$

$$m_l(s) = \frac{\rho A}{M/L} \quad 2.14$$

$$u_\xi(s) = \frac{r_\xi}{c_r} \quad 2.15$$

$$u_\eta(s) = \frac{r_\eta}{c_r} \quad 2.16$$

$$c_d(s) = \frac{C_D}{\omega\,M/L} \quad 2.17$$

$$S_t = \frac{g}{c_r\,\omega^2} \quad 2.18$$

$$f_{x_k} = f_x\left[\frac{\partial x}{\partial \tau},\ (x-x_{b_k}),\ \frac{\partial y}{\partial \tau},\ (y-y_{b_k})\right]_{s=s_k} = \frac{F_{x_k}}{M\,c_r\,\omega^2} \quad 2.19$$

$$f_{y_k} = f_y\left[\frac{\partial x}{\partial \tau},\ (x-x_{b_k}),\ \frac{\partial y}{\partial \tau},\ (y-y_{b_k})\right]_{s=s_k} = \frac{F_{y_k}}{M\,c_r\,\omega^2} \quad 2.20$$

$$\left.\begin{aligned} &\delta(s-s_k) = 0 \quad , \quad s \neq s_k \\ &\int_0^1 \delta(s-s_k)\,ds = 1 \end{aligned}\right\} \quad 2.21$$

## 2.2 THE NATURAL MODES OF VIBRATION OF THE FREE SHAFT

### 2.2.1 Separation of the Variables

The equations of motion 2.12 for the rotor system are non-linear and coupled in the horizontal and vertical directions due to the oil-film forces $f_x$ and $f_y$. Before considering the proposed method for solving these, it is necessary to review the properties of the solution to the reduced problem of the free unconstrained, or *free-free*, motion of the shaft in a viscous medium. This is described by the homogeneous form of equations 2.12 and is given below by equations 2.22 and 2.23:

$$\frac{\partial^2}{\partial s^2}\left(\sigma(s)\,\frac{\partial^2 x}{\partial s^2}\right) + c_d(s)\,\frac{\partial x}{\partial \tau} + m_l(s)\,\frac{\partial^2 x}{\partial \tau^2} = 0 \qquad 2.22$$

$$\frac{\partial^2}{\partial s^2}\left(\sigma(s)\,\frac{\partial^2 y}{\partial s^2}\right) + c_d(s)\,\frac{\partial y}{\partial \tau} + m_l(s)\,\frac{\partial^2 y}{\partial \tau^2} = 0 \qquad 2.23$$

It may be seen that the equations for the horizontal and vertical directions are uncoupled and identical and so only equation 2.22 for the horizontal direction will be considered.

A solution is sought according to the method of *separation of variables*. To this end, assume a solution of the form:

$$x = T(\tau)\,\phi(s) \qquad 2.24$$

which, after substituting into equation 2.22 and dividing through by $T(\tau)\,\phi(s)\,m_l(s)$, leads to:

$$\frac{1}{m_l(s)\,\phi(s)}\,\frac{d^2}{ds^2}\left(\sigma(s)\,\frac{d^2\phi}{ds^2}\right) = -\frac{1}{T(\tau)}\left(\frac{c_d(s)}{m_l(s)}\,\frac{dT}{d\tau} + \frac{d^2T}{d\tau^2}\right) \qquad 2.25$$

The separation of the variable may be effected if the damping is

proportional to the mass distribution along the length of the shaft, i.e. if:

$$\frac{c_d(s)}{m_l(s)} = constant = 2\gamma \qquad 2.26$$

Under this assumption, the left hand side of equation 2.25 is a function of $s$ alone and the right hand side is a function of $\tau$ alone, and so both sides must be equal to a constant, i.e.

$$\frac{1}{m_l(s)\ \phi_s}\frac{d^2}{ds^2}\left[\sigma(s)\ \frac{d^2\phi}{ds^2}\right] = -\frac{1}{T(\tau)}\left[2\gamma\ \frac{dT}{d\tau} + \frac{d^2T}{d\tau^2}\right] = \nu_f^2 \qquad 2.27$$

where $\nu_f$ is an as yet undetermined constant. After rearranging, this leads to two ordinary differential equations:

$$\frac{d^2T}{d\tau} + 2\gamma\ \frac{dT}{d\tau} + \nu_f^2 = 0 \qquad 2.28$$

$$\frac{d^2}{ds^2}\left[\sigma(s)\ \frac{d^2\phi}{ds^2}\right] - \nu_f^2\ m_l(s)\ \phi(s) = 0 \qquad 2.29$$

The solution to the first of these equations is well known, i.e.

$$T(\tau) = e^{-\gamma\tau}\left[A_1\ cos\ (\nu_f^2 - \gamma^2)^{\frac{1}{2}}\ \tau + A_2\ sin\ (\nu_f^2 - \gamma^2)^{\frac{1}{2}}\ \tau\right] \qquad 2.30$$

where $A_1$ and $A_2$ are constants determined by the initial conditions. For the second equation, a solution must not only satisfy the differential equation but must be such that for all values of $\tau$ the boundary conditions at the ends of the shaft are satisfied. For a free-free shaft, the requirement is that the bending moment and shear force at the ends of the shaft should be zero, i.e.

$$EI(Z) \left.\frac{\partial^2 X}{\partial Z^2}\right|_{Z=0,L} = 0 \qquad 2.31$$

$$\frac{\partial}{\partial Z}\left[EI(Z) \frac{\partial^2 X}{\partial Z^2}\right]_{Z=0,L} = 0 \qquad 2.32$$

After non-dimensionalisation and substituting from equation 2.24 for the assumed solution, the above conditions are equivalent to:

$$\left.\frac{d^2\phi}{ds^2}\right|_{s=0,1} = 0 \qquad 2.33$$

$$\frac{d}{ds}\left[\sigma(s) \frac{d^2\phi}{ds^2}\right]_{s=0,1} = 0 \qquad 2.34$$

A solution to equation 2.29 which satisfies both the differential equation and the boundary condition only exists for certain values of the constant $\nu_f$. Such a solution $\phi_i$ is known as an eigenfunction or mode and the associated value of $\nu_{f_i}$ is known as an eigenvalue or natural frequency. The eigenfunctions corresponding to different eigenvalues are mutually orthogonal, a property that will now be demonstrated.

### 2.2.2 Properties of the Normal Modes

Consider two different eigenfunctions $\phi_i(s)$ and $\phi_j(s)$, both of which satisfy equation 2.29, i.e.

$$\frac{d}{ds^2}\left[\sigma(s) \frac{d^2\phi_i}{ds^2}\right] - \nu_{f_i}{}^2 m_l(s) \phi_i = 0 \qquad 2.35$$

$$\frac{d}{ds^2}\left[\sigma(s) \frac{d^2\phi_j}{ds^2}\right] - \nu_{f_j}{}^2 m_l(s) \phi_j = 0 \qquad 2.36$$

Multiplying the first of these equations by $\phi_j$ and the second by $\phi_i$ and

integrating along the length of the shaft gives:

$$\int_0^1 \phi_j \frac{d}{ds^2}\left[\sigma(s)\frac{d^2\phi_i}{ds^2}\right] ds = \nu_{f_i}^2 \int_0^1 \phi_j\, m_l(s)\, \phi_i\, ds \qquad 2.37$$

$$\int_0^1 \phi_i \frac{d}{ds^2}\left[\sigma(s)\frac{d^2\phi_j}{ds^2}\right] ds = \nu_{f_j}^2 \int_0^1 \phi_i\, m_l(s)\, \phi_j\, ds \qquad 2.38$$

Integration by parts leads to:

$$\left[\phi_j \frac{d}{ds}\left\{\sigma(s)\frac{d^2\phi_i}{ds^2}\right\}\right]_0^1 - \left[\frac{d\phi_j}{ds}\sigma(s)\frac{d^2\phi_i}{ds^2}\right]_0^1 + \int_0^1 \frac{d^2\phi_j}{ds^2}\sigma(s)\frac{d^2\phi_i}{ds^2} ds$$

$$= \nu_{f_i}^2 \int_0^1 \phi_j\, m_l(s)\, \phi_i\, ds \qquad 2.39$$

$$\left[\phi_i \frac{d}{ds}\left\{\sigma(s)\frac{d^2\phi_j}{ds^2}\right\}\right]_0^1 - \left[\frac{d\phi_i}{ds}\sigma(s)\frac{d^2\phi_j}{ds^2}\right]_0^1 + \int_0^1 \frac{d^2\phi_i}{ds^2}\sigma(s)\frac{d^2\phi_j}{ds^2} ds$$

$$= \nu_{f_j}^2 \int_0^1 \phi_j\, m_l(s)\, \phi_i\, ds \qquad 2.40$$

The first two terms in each of the above equations are zero as a result of the boundary conditions given by equations 2.33 and 2.34. Subtracting equation 2.40 from equation 2.39 gives:

$$(\nu_{f_i}^2 - \nu_{f_j}^2) \int_0^1 \phi_i\, m_l(s)\, \phi_j\, ds = 0 \qquad 2.41$$

When $\nu_{f_i}^2 \neq \nu_{f_j}^2$, the integral must be equal to zero, but for $\nu_{f_i}^2 = \nu_{f_j}^2$, the integral is equal to a non-zero constant $c_1$ which, because the differential equation 2.29 is linear and homogeneous with linear homogeneous boundary conditions*, is of arbitrary value. Hence, the

---

* If $\phi_i$ is a solution, so also is $A\phi_i$, where $A$ is a constant.

eigenfunctions are mutually orthogonal with respect to the mass distribution and are normalised here by setting $c_1$ to unity, i.e.

$$\int_0^1 \phi_i \, m_l(s) \, \phi_j \, ds = \delta_{ij} \qquad 2.42$$

where $\delta_{ij}$ is the Kronecker delta, defined as:

$$\delta_{ij} = \begin{cases} 0 & \text{when } i \neq j \\ 1 & \text{when } i = j \end{cases} \qquad 2.43$$

Two further important properties of the normalised eigenfunctions, or normal modes, follow immediately. From equations 2.37 or 2.38:

$$\int_0^1 \phi_j \frac{d^2}{ds^2}\left[\sigma(s) \frac{d^2\phi_i}{ds^2}\right] ds = \delta_{ij} \, \nu_{f_i}^2 \qquad 2.44$$

and from equations 2.39 or 2.40:

$$\int_0^1 \frac{d^2\phi_i}{ds^2} \sigma(s) \frac{d^2\phi_j}{ds^2} ds = \delta_{ij} \, \nu_{f_i}^2 \qquad 2.45$$

### 2.2.3 Rigid-Body Modes

It is possible for a free-free shaft to undergo a non-oscillatory motion for which the natural frequency $\nu_f$ is zero and equation 2.29 reduces to:

$$\frac{d^2}{ds^2}\left[\sigma(s) \frac{d^2\phi}{ds^2}\right] = 0 \qquad 2.46$$

Performing repeated integration upon this equation whilst observing the boundary conditions 2.33 and 2.34 leads to:

$$\phi_i = a_i + b_i s \tag{2.47}$$

where $a_i$ and $b_i$ are constants of integration. From this it may be seen that any rigid body displacement of the shaft is an eigenfunction of equation 2.29 and is therefore also orthogonal to all the flexural modes. Two such linearly independent, rigid body modes are necessary to describe any rigid body displacement of the shaft in space. Let these be:

$$\phi_1 = a_1 \tag{2.48}$$

$$\phi_2 = a_2 (1 + b_2 s) \tag{2.49}$$

If it is required that these be mutually orthogonal with respect to the mass distribution, and normalised in the same manner as the flexural modes, then this produces three equations from which the three constants $a_1$, $a_2$ and $b_2$ may be determined, i.e.

$$\int_0^1 (\phi_1)^2 m_l(s)\, ds = a_1^2 \int_0^1 m_l(s)\, ds = 1 \tag{2.50}$$

$$\int_0^1 \phi_1 m_l(s) \phi_2\, ds = a_1 a_2 \int_0^1 (1 + b_2 s) m_l(s)\, ds = 0 \tag{2.51}$$

$$\int_0^1 (\phi_2)^2 m_l(s)\, ds = a_2^2 \int_0^1 (1 + b_2 s)^2 m_l(s)\, ds = 1 \tag{2.52}$$

After noting from the non-dimensionalised form of equation 2.11 that:

$$\int_0^1 m_l(s)\, ds = 1.0 \tag{2.53}$$

and defining the following properties of the shaft:

$$s_g = \int_0^1 s\, m_l(s)\, ds \qquad 2.54$$

$$I_m = \int_0^1 s^2\, m_l(s)\, ds \qquad 2.55$$

where $s_g$ is the non-dimensional displacement along the shaft to the centre of mass, and $I_m$ is the non-dimensional mass moment of inertia* about an axis at $s = 0.0$, the solution of equations 2.50 to 2.52 giving the values of the constants to be:

$$a_1 = 1 \qquad 2.56$$

$$a_2 = s_g / \sqrt{I_m - s_g^2} \qquad 2.57$$

$$b_2 = -1.0/s_g \qquad 2.58$$

Hence, the mutually orthogonal and normalised rigid body modes are:

$$\phi_1 = 1 \qquad 2.59$$

$$\phi_2 = (s_g - s)/\sqrt{I_m - s_g^2} \qquad 2.60$$

It may be seen that $\phi_1$ describes pure translational motion of the shaft whilst $\phi_2$ describes a rotation, without translation, about the mass centre. It should be noted that the term $(I_m - s_g^2)$ in the denomenator of equation 2.60 is, by the parallel axis theorem, equal to the non-dimensional mass moment of inertia about an axis ($s = s_g$) through the mass centre of the shaft.

---

* Made non-dimensional by dividing by $M L^2$.

### 2.2.4 Methods for Determining the Normal Modes

In order to determine the normal modes of a shaft and their associated frequencies, it is necessary, except for the special case of a uniform shaft which is discussed in section 4.2 of Chapter 4, to make recourse to numerical techniques. The Mykelstad-Prohl approach which, when cast into matrix form is known as the *transfer matrix method*, is one such technique, a description of which is given by Pestel & Leckie (1963) and Meirovitch (1967). Another approach, developed by Witte (1968), effectively discretises equation 2.20, by means of finite difference approximations, to form stiffness and mass matrices from which the eigenvalues and associated eigenvectors may be determined by standard techniques.

Both of the above methods are, in essence, lumped mass approximations in which the shaft is represented by a series of point masses connected by light flexible shaft elements. It should be noted that, in order to obtain a realistic estimate of the $m$th mode, the number of mass stations must greatly exceed $m$. Morton (1972) used some 250 mass stations to calculate, by the Mykelstad-Prohl method, the first dozen free-free modes of the coupled rotors of a 500 MW turbogenerator.

The details of the procedures for obtaining the normal modes and natural frequencies will not be discussed further here as it is outside the terms of reference for this work.

## 2.3 THE PROPOSED METHOD FOR TREATING A MULTI-ROTOR SYSTEM SUPPORTED UPON JOURNAL BEARINGS

### 2.3.1 The Transformation of the Equations of Motion Using the Free-Free Modes

The infinite family of eigenfunctions for the free-free shaft, which satisfy equation 2.42, constitute a complete set of orthonormal modes. Any function satisfying the homogeneous boundary conditions given by equations 2.31 and 2.32 may, according to the *expansion theorem* (see Meirovitch (1967)), be represented as a linear combination of these. The shaft system depicted in Figure 2.1 does not have a bending moment or a shear force imposed at its ends and so the deflected shape of the shaft $X(Z,t)$ and $Y(Z,t)$ must, at all times, automatically satisfy equations 2.31 and 2.32. Therefore, assume a solution of the non-dimensional equations of motion 2.12 to be of the form:

$$x(s,\tau) = \sum_{i=1}^{\infty} q_{x_i}(\tau)\ \phi_i(s) \qquad 2.61$$

$$y(s,\tau) = \sum_{i=1}^{\infty} q_{y_i}(\tau)\ \phi_i(s) \qquad 2.62$$

from which it follows that:

$$\frac{\partial x}{\partial \tau} = \sum_{i=1}^{\infty} \frac{dq_{x_i}}{d\tau}\ \phi_i(s) \qquad 2.63$$

$$\frac{\partial y}{\partial \tau} = \sum_{i=1}^{\infty} \frac{dq_{y_i}}{d\tau}\ \phi_i(s) \qquad 2.64$$

etc.

The assumption made in the previous section concerning the distribution of the external damping, and expressed by equation 2.26, will

also be made here.

Substituting the above expressions into equations 2.12, multiplying through each equation by $\phi_j(s)$, and integrating along the shaft leads to:

$$\left.\begin{aligned}
&\sum_{i=1}^{\infty} \left\{ q_{x_i} \int_0^1 \phi_j \frac{d^2}{ds^2}\left[\sigma(s) \frac{d^2\phi_i}{ds^2}\right] ds + \left(2\gamma \frac{dq_{x_i}}{d\tau} + \frac{d^2 q_{x_i}}{d\tau^2}\right) \right. \\
&\left. \int_0^1 \phi_j \, m_l(s) \, \phi_i \, ds \right\} = \sum_{k=1}^{n} \{\phi_j(s_k) \, f_{x_k}\} + \\
&\cos\tau \int_0^1 \phi_j \, m_l(s) \, u_\xi(s) \, ds - \sin\tau \int_0^1 \phi_j \, m_l(s) \, u_\eta(s) \, ds \\
&\sum_{i=1}^{\infty} \left\{ q_{y_i} \int_0^1 \phi_j \frac{d^2}{ds^2}\left[\sigma(s) \frac{d^2\phi_i}{ds^2}\right] ds + \left(2\gamma \frac{dq_{y_i}}{d\tau} + \frac{d^2 q_{y_i}}{d\tau^2}\right) \right. \\
&\left. \int_0^1 \phi_j \, m_l(s) \, \phi_i \, ds \right\} = \sum_{k=1}^{n} \{\phi_j(s_k) \, f_{x_k}\} + \\
&\sin\tau \int_0^1 \phi_j \, m_l(s) \, u_\xi(s) \, ds + \cos\tau \int_0^1 \phi_j \, m_l(s) \, u_\eta(s) \, ds - \\
&S_t \int_0^1 \phi_j \, m_l(s) \, ds
\end{aligned}\right\} \quad 2.65$$

By invoking the properties of the normal modes, given by equations 2.42 and 2.44, the above equations may be reduced to:

$$\left.\begin{aligned}
&\frac{d^2 q_{x_i}}{d\tau^2} + 2\gamma \frac{dq_{x_i}}{d\tau} + \nu_{f_i}^{\,2}\, q_{x_i} \\
&= \sum_{k=1}^{n} \{\phi_i\,(s_k)\, f_{x_k}\} + Q_{\xi_i} \cos\tau - Q_{\eta_i} \sin\tau \\
&\frac{d^2 q_{y_i}}{d\tau^2} + 2\gamma \frac{dq_{y_i}}{d\tau} + \nu_{f_i}^{\,2}\, q_{y_i} = \sum_{k=1}^{n} \{\phi_i\,(s_k)\, f_{y_k}\} + \\
&Q_{\xi_i} \sin\tau + Q_{\eta_i} \cos\tau - \delta_{i1}\, S_t \qquad , \qquad (i = 1, 2, .., \infty)
\end{aligned}\right\} \quad 2.66$$

where $Q_{\xi_i}$ and $Q_{\eta_i}$ are the generalised unbalance components given by:

$$Q_{\xi_i} = \int_0^1 \phi_i(s)\, m_l(s)\, u_\xi(s)\, ds \qquad 2.67$$

$$Q_{\eta_i} = \int_0^1 \phi_i(s)\, m_l(s)\, u_\eta(s)\, ds \qquad 2.68$$

and the integral:

$$\int_0^1 \phi_i\, m_l(s)\, ds \;\left(= \int_0^1 \phi_i\, m_l(s)\, \phi_1\, ds\right) = \delta_{i1} \qquad 2.69$$

may be evaluated as shown because the rigid body mode, $\phi_1$, has a constant value equal to unity. Thus, it may be seen that the two partial differential equations 2.12 describing the motion of the shaft have been transformed into an infinite system of ordinary differential equations in terms of the modal coefficients $q_{x_i}$ and $q_{y_i}$. These equations are coupled through the oil-film forces $f_{x_k}$ and $f_{y_k}$ which, from equations 2.61 to 2.64, now become functions of the modal coefficients and their derivatives, i.e.

$$f_{x_k} = f_x \left[ \dot{x}(\dot{q}_{x_i}) \, , \, \{x(q_{x_i}) - x_{b_k}\} \, , \, \dot{y}(\dot{q}_{y_i}) \, , \, \{y(q_{y_i}) - y_{b_k}\} \right]_{s=s_k} \qquad 2.70$$

$$f_{y_k} = f_y \left[ \dot{x}(\dot{q}_{x_i}) \, , \, \{x(q_{x_i}) - x_{b_k}\} \, , \, \dot{y}(\dot{q}_{y_i}) \, , \, \{y(q_{y_i}) - y_{b_k}\} \right]_{s=s_k} \qquad 2.71$$

($\dot{}$ denotes differentiation with respect to $\tau$)

### 2.3.2 Method of Solution

Large turbogenerators do not normally operate at speeds beyond their third or fourth free-free (flexural) natural frequency. It is, therefore, reasonable to assume that the higher frequency modes make little contribution to the motion and that it is justifiable to truncate the modal expansion (equations 2.61 and 2.62) after $m$ terms, thus reducing equations 2.66 to a finite system suitable for solution by numerical *initial-value-problem* techniques. The difficulty lies in determining *a priori* the term at which the truncation may be made. This problem, however, may be overcome empirically. First, a solution is obtained using $m$ modes and then re-solved using $(m+2)$ modes. If there are significant differences between the two solutions, then further pairs of terms are added to the modal expansion until the difference between successive solutions is reduced to an acceptable level. Terms are added in pairs because the addition of a single anti-symmetric mode for a motion that was predominantly symmetric in nature (or vice versa) would have little effect upon the solution and thus might falsely indicate that convergence had been achieved.

Most numerical methods for integrating a system of ordinary differential equations require the equations to be of first order. By

defining the new variables:

$$u_{x_i} = \frac{dq_{x_i}}{d\tau} \qquad 2.72$$

$$u_{y_i} = \frac{dq_{y_i}}{d\tau} \qquad 2.73$$

The system of $2m$ second order equations, arrived at by truncating the modal expansion, is converted into a system of $4m$ first order equations in a form suitable for numerical integration, i.e.

$$\left.\begin{aligned}
\frac{du_{x_i}}{d\tau} &= \sum_{k=1}^{n} \{\phi_i(s_k) f_{x_k}\} - 2\gamma u_{x_i} - \nu_{f_i}^2 q_{x_i} + Q_{\xi_i} \cos\tau - Q_{\eta_i} \sin\tau \\
\frac{dq_{x_i}}{d\tau} &= u_{x_i} \\
\frac{du_{y_i}}{d\tau} &= \sum_{k=1}^{n} \{\phi_i(s_k) f_{y_k}\} - 2\gamma u_{y_i} - \nu_{f_i}^2 q_{y_i} + Q_{\xi_i} \sin\tau + Q_{\eta_i} \cos\tau \\
&\quad - \delta_{i1} S_t \\
\frac{dq_{y_i}}{d\tau} &= u_{y_i} \qquad , \qquad (i = 1, 2, \ldots, m)
\end{aligned}\right\} \qquad 2.74$$

The $4m$ initial conditions needed for the solution procedure are discussed later.

### 2.3.3 Point Unbalance Forces

It is sometimes more convenient to represent the unbalance force acting on a shaft by a set of point unbalance forces rather than a

distributed unbalance. Let $F_u^{(j)}$ be the $j$th point unbalance force, acting at station $s = s_j$, and let the components of this force in the directions $\xi$ and $\eta$ of the rotating coordinate system $OZ\xi\eta$ (see Figure 2.2) be $F_{u\xi}^{(j)}$ and $F_{u\eta}^{(j)}$, respectively. For this situation, the generalised unbalance components in equations 2.66 and 2.74 become:

$$Q_{\xi_i} = \sum_j \left\{ \frac{F_{u\xi}^{(j)}}{M c_r \omega^2} \phi_i (s_j) \right\} \qquad 2.75$$

$$Q_{\eta_i} = \sum_j \left\{ \frac{F_{u\eta}^{(j)}}{M c_r \omega^2} \phi_i (s_j) \right\} \qquad 2.76$$

## 2.4 DISCUSSION

The principal objective in this work was the study of the vibrations resulting from the interaction between the non-linear oil-film bearings and the rotating shaft. The modal method described above effectively separates the dynamic characteristics of the shaft, which is essentially a linear element and thus amenable to analytical treatment, from those of the bearings.

### 2.4.1 The Case for Employing Free-Free Modes

In general, the dynamic behaviour of a shaft may be characterised by a set of normal modes and natural frequencies of the free vibration of the shaft when supported upon idealised bearings. In the foregoing analysis, the displacement of the shaft was expressed in terms of the free-free modes, but several authors have shown that, for the linearised analysis of multi-rotor systems, other sets of assumed modes may be successfully employed. Morton (1972), when considering a turbo-generator, used a combination of free-free modes and the modes obtained if the coupled rotors are "pinned" at each bearing. Whilst Black & Loch (1973) for an analysis of a four bearing pump suggested that high accuracy could be achieved by using the modes obtained by supporting the shaft in *single stiffness* bearings. However, the use of the free-free modes, besides being the natural choice of assumed modes from a mathematical viewpoint (as they are the eigenfunctions of the homogeneous form of the equations of motion 2.12) was desirable in this work for the following reasons.

First, if a system of second order ordinary differential equations is to be solved by numerical integration techniques, it is necessary for the inertia matrix (i.e. the matrix of coefficients for the

second order terms) to be diagonal. As may be seen from equations 2.65 and 2.66, this condition is satisfied if the free-free modes are used as these are orthogonal with respect to the mass distribution along the shaft.

Second, it is advantageous to choose the free-free modes as they are a property of the shaft alone, determined by the distribution of mass and flexural stiffness along its length, and are independent of the locations of the bearings or their characteristics. Hence, the relocation, insertion, removal, or modification of a bearing for an existing shaft (assuming this to be physically reasonable) may be accommodated for in the method without the need to calculate a new set of modes.

Although the modes suggested by Black & Loch (cited above) result in off-diagonal terms in the inertia matrix, this does not present a difficulty with a linearised analysis. Brown (1977), when extending the work of Black & Loch to include the non-linear effects of the journal bearings, needed to diagonalise the inertia matrix in order that the equations should be amenable to solution by numerical integration techniques. To achieve this, he used the modes resulting from supporting the shaft in very soft single stiffness bearings - and which thus closely approximate its free-free modes. (The effect of fluid inertia in the ring seals was not included, as it had been in the linearised analysis, because they give rise to off-diagonal terms in the inertia matrix, irrespective of the system of assumed modes employed.)

### 2.4.2 Comparison with the Direct Lumped Mass Approach

Equations of motion for a shaft supported upon journal bearings may, alternatively, be developed by direct consideration of the lumped mass approximation.

If a shaft is represented by $p$ lumped masses connected by light, elastic shaft sections, then a system of $2p$ ordinary differential equations may be derived by considering the dynamic equilibrium of each mass. The equations obtained, which are given in Appendix 1 by equations A1.1 together with an outline of their derivation, are in a form suitable for solution by numerical initial-value-problem techniques. This approach, however, has a major disadvantage for, in order to adequately represent the lower frequency dynamic characteristics of the shaft, a large number of mass stations must be employed, but in doing this higher frequency modes, which make an insignificant contribution to the motion of the shaft, are also allowed for and an unnecessarily large system of non-linear equations must be solved.

With the modal method, this problem does not arise since the lower frequency characteristics of the shaft are contained in the normal modes and natural frequencies. For, whilst it is recognised that the lower frequency modes, for realistic shafts, may only be determined by allowing an approximate shaft model a sufficiently large number of degrees of freedom, such a calculation is linear in nature, need only be performed once for a given shaft, and does not necessitate the inclusion of unnecessary high frequency characteristics in the non-linear solution procedure.

These assertions may be verified if the systems of equations for the two approaches are compared in a common form. In Appendix 1, it is shown that equations A1.1 for the lumped mass system may be transformed, without affecting their accuracy, into a system of $2p$ equations in terms of the free-free modes of the lumped mass shaft. The resulting equations A1.25 are identical in form to the system of equations 2.66 for the continuous shaft (if the latter are truncated), differing only in the

value of the free-free frequencies and the value of the modes at each shaft station. It may thus be seen that, for a given number of degrees of freedom, the modal method would be better able to represent the dynamic characteristics of the shaft as it employs more accurate estimates of the normal modes and natural frequencies of the shaft.

The direct lumped mass approach suffers from a further disadvantage: in order to ensure that the equations of motion for the shaft are explicit, a mass station must exist at each bearing location. If it is subsequently decided to change the location of a bearing, it may be necessary, unless the new locations happen to coincide with a mass station, to modify the distribution of the point masses; this would be difficult to achieve without altering the dynamic characteristics of the shaft model.

### 2.4.3 Conclusions

A method has been developed for predicting the non-linear flexural vibrations of a multi-rotor system supported upon journal bearings. The equations of motion for the system are in terms of the free-free modes of the coupled rotors. The method is applicable (subject to the conditions given in section 2.1.3 of this chapter) to a rotor system having any realistic distribution of mass and flexural stiffness and supported upon any number of journal bearings.

# CHAPTER 3

# THE JOURNAL BEARINGS

## 3.1 INTRODUCTION

Consideration has, so far, not been given to the type of bearings to be used in the computer model of the multi-rotor system. The method for treating the shaft, discussed in Chapter 2, is not restricted to a single type of bearing. For example, circular-bore, lemon-bore, three lobe or pivoted pad bearings, each with realistic design features such as feed ports, recesses, scallops, etc., could all, in principle, be incorporated into the model.

The bearing forces that act upon a shaft result from the pressure generated in the oil film contained between the rotating journal and stationary bearing surfaces. The pressure distribution in the bearing is, under the assumption of laminar flow, governed by Reynolds equation. The Reynolds equation is described fully by Pinkus & Sternlicht (1961). To calculate the oil-film forces, the Reynolds equation must first be solved for the bearing geometry under consideration, and then the resulting pressure distribution integrated over the surface of the journal to give the required forces. Unfortunately, analytical solutions to the Reynolds equation do not exist in closed form even for the special case of a plain circular-bore bearing. For static bearing calculations, this difficulty is normally overcome by solving the Reynolds equation numerically using finite difference techniques. This approach, however, makes heavy demands upon computer time and is therefore normally considered unsuitable for use in a numerical integration procedure for which the oil-film forces must be recomputed at each time step.

Recourse is therefore normally made to approximate solutions of which

the long and short bearing approximations are well known. Of these, the short bearing approximation is the one normally adopted in the study of rotor dynamics because, for practical bearings, it is the more realistic of the two assumptions to make. An unfortunate property of the short bearing approximation is that it has pre-determined circumferential boundary conditions which limit its applicability to plain circular-bore bearings. The short circular-bore bearing approximation was successfully employed by Badgley & Booker (1969) and Holmes (1970) to study, using digital techniques, the symmetric, non-linear motion of a rigid shaft supported upon two bearings.

Although a plain circular-bore is a somewhat idealised configuration, the speed at which the bearing forces may be computed using the short bearing approximation recommended it for use in the computer model of the multi-rotor system - at least during the development stages of the work.

## 3.2 THE OIL-FILM FORCES FOR A CIRCULAR-BORE BEARING

### 3.2.1 The Reynolds Equation for a Circular-Bore Bearing

The geometry of a circular-bore bearing is shown in Figure 3.1. The Reynolds equation for this configuration is derived by Pinkus & Sternlicht (1961), and is given below by equation 3.1. It is assumed that the lubricant is isoviscous with an effective viscosity $\eta_e$:

$$\frac{1}{R^2}\frac{\partial}{\partial\theta}\left(h^3\frac{\partial P}{\partial\theta}\right) + h^3\frac{\partial^2 P}{\partial\bar{z}^2} = 6\eta_e\left[\left(\omega - 2\frac{d\psi}{d\tau}\right)(-e\sin\theta) + 2\frac{de}{dt}\cos\theta\right] \qquad 3.1$$

The axial coordinate, $\bar{z}$, is measured from the mid-plane of each bearing, and the film thickness, $h$, is given by:

$$h = C + e\cos\theta \qquad 3.2$$

where $C$ is the radial clearance.

As in the previous chapter, it is convenient to reduce the equations to non-dimensional form. This is achieved by first introducing the following non-dimensional variables:

$$\varepsilon = \frac{e}{C} \qquad 3.3$$

$$\dot{\varepsilon} = \frac{1}{\omega C}\frac{de}{dt} \qquad 3.4$$

$$\dot{\psi} = \frac{1}{\omega}\frac{d\psi}{dt} \qquad 3.5$$

$$h^* = \frac{h}{C} = 1. + \varepsilon\cos\theta \qquad 3.6$$

$$z^* = \frac{\bar{z}}{B/2} \qquad 3.7$$

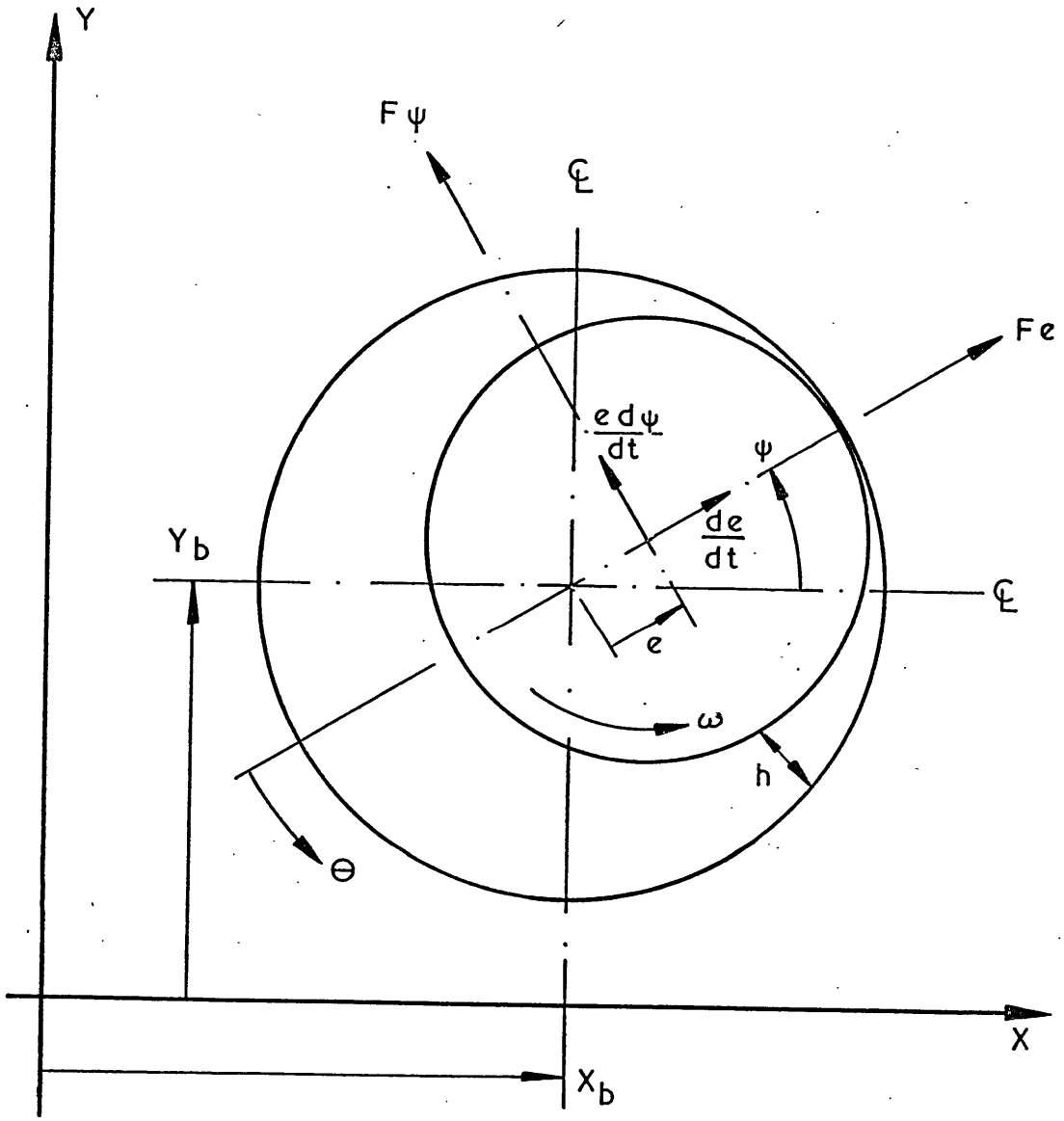


Figure 3.1: The geometry of a circular bore bearing

$$P^* = \frac{P}{12\eta_e R^2 \omega/C^2} \tag{3.8}$$

$$\alpha = \frac{2R}{B} \tag{3.9}$$

These are then substituted into equation 3.1 to give the following non-dimensional form of the Reynolds equation:

$$\frac{\partial}{\partial\theta}\left(h^{*3}\frac{\partial P^*}{\partial\theta}\right) + \alpha^2 h^{*3}\frac{\partial^2 P^*}{\partial z^{*2}} = -\varepsilon\,(0.5 - \dot{\psi})\sin\theta + \dot{\varepsilon}\cos\theta \tag{3.10}$$

It is important to note that $e$ and $de/dt$ are made non-dimensional by using the bearing (or arc) clearance $C$ and not the reference clearance of the system, $c_r$. This must be taken into account when converting from the cartesian coordinates of the shaft equations (2.44 and 2.45) to the polar coordinates of the bearing equations for evaluation of the oil-film forces, i.e.

$$\varepsilon = \left(\frac{c_r}{C}\right)\sqrt{(x - x_b)^2 + (y - y_b)^2} \tag{3.11}$$

$$\cos\psi = \left(\frac{c_r}{C}\right)\frac{(x - x_b)}{\varepsilon} \tag{3.12}$$

$$\sin\psi = \left(\frac{c_r}{C}\right)\frac{(y - y_b)}{\varepsilon} \tag{3.13}$$

$$\dot{\varepsilon} = \left(\frac{c_r}{C}\right)(\dot{x}\cos\psi + \dot{y}\sin\psi) \tag{3.14}$$

$$\dot{\psi} = \left(\frac{c_r}{C}\right)\frac{(\dot{y}\cos\psi - \dot{x}\sin\psi)}{\varepsilon} \tag{3.15}$$

### 3.2.2 The Non-Dimensional Oil-Film Forces

The oil-film forces $F_e$ and $F_\psi$ along and perpendicular to the line of centres (see Figure 3.1) are obtained by integration as follows:

$$F_e = \int_{-B/2}^{B/2} \int_{\theta_1}^{\theta_2} P \cos\theta \, R \, d\theta \, d\bar{z} \qquad 3.16$$

$$F_\psi = \int_{-B/2}^{B/2} \int_{\theta_1}^{\theta_2} P \sin\theta \, R \, d\theta \, d\bar{z} \qquad 3.17$$

where $\theta_1$ and $\theta_2$ are the start and finish, respectively, of the uncavitated oil-film. The non-dimensional oil-film force $f_e$ and $f_\psi$ are defined as:

$$f_e = \frac{F_e}{M c_r \omega^2} = \frac{3}{2} \alpha^2 \beta \left(\frac{c_r}{C}\right)^2 \int_{-1}^{1} \int_{\theta_1}^{\theta_2} P^* \cos\theta \, d\theta \, dz^* \qquad 3.18$$

$$f_\psi = \frac{F_\psi}{M c_r \omega^2} = \frac{3}{2} \alpha^2 \beta \left(\frac{c_r}{C}\right)^2 \int_{-1}^{1} \int_{\theta_1}^{\theta_2} P^* \sin\theta \, d\theta \, dz^* \qquad 3.19$$

where:

$$\beta = \frac{\eta_e R B^3}{M c_r^3 \omega} \qquad 3.20$$

It may be seen that the definition of $f_e$ and $f_\psi$ is consistent with the definition of the non-dimensional bearing forces $f_x$ and $f_y$ given in Chapter 2 (equations 2.19 and 2.20). The forces for the two coordinate systems are related as follows:

$$f_x = f_e \cos\psi - f_\psi \sin\psi \qquad 3.21$$

$$f_y = f_e \sin\psi + f_\psi \cos\psi \qquad 3.22$$

### 3.2.3 The Short Bearing Approximation

In the short bearing approximation, it is assumed that:

$$\frac{\partial}{\partial\theta}\left(h^{*3}\frac{\partial P^*}{\partial\theta}\right) \ll h^{*3}\frac{\partial^2 P^*}{\partial z^{*2}} \qquad 3.23$$

That is, the pressure induced flow in the circumferential direction is much less than that in the axial direction. The Reynolds equation thus reduces to:

$$\frac{d^2P^*}{dz^{*2}} = \frac{(0.5-\dot{\psi})(-\varepsilon\sin\theta)+\dot{\varepsilon}\cos\theta}{\alpha^2 h^{*3}} \qquad 3.24$$

which may be integrated directly to give the pressure distribution. If it is assumed that the pressure is zero at the sides of the bearing ($z^* = \pm 1.0$), then the resulting pressure distribution is given by:

$$P^* = \frac{\left[(0.5-\dot{\psi})(-\varepsilon\sin\theta)+\dot{\varepsilon}\cos\theta\right](z^{*2}-1)}{2\alpha^2 h^{*3}} \qquad 3.25$$

Substituting this expression into equations 3.18 and 3.19 gives the non-dimensional oil-film forces, i.e.

$$f_e = \beta\left(\frac{c_r}{C}\right)^2\left\{\varepsilon(0.5-\dot{\psi})A_3^{11}-\dot{\varepsilon}A_3^{20}\right\} \qquad 3.26$$

$$f_\psi = \beta\left(\frac{c_r}{C}\right)^2\left\{\varepsilon(0.5-\dot{\psi})A_3^{20}-\dot{\varepsilon}A_3^{11}\right\} \qquad 3.27$$

where:

$$A_n^{ij} = \int_{\theta_1}^{\theta_2}\frac{\sin^i\theta\cos^j\theta}{(1+\varepsilon\cos\theta)^n}\,d\theta \qquad 3.28$$

The definite integrals $A_n^{ij}$ may be evaluated using Booker's (1965) table of journal bearing integrals. The oil-film is assumed to cavitate in the region of negative pressure (half Sommerfeld condition) and so, from

equation 3.25, the oil-film limits are given by:

$$\theta_1 = tan^{-1} \frac{\dot{\varepsilon}}{\varepsilon\ (0.5 - \psi)} \qquad 3.29$$

$$\theta_2 = \theta_1 + \pi \qquad 3.30$$

To ensure that the region of positive, and not negative, pressure is selected, the sign of the pressure at $\theta_1 + \pi/2$ should be checked.

# CHAPTER 4

# THE MULTI-ROTOR CONFIGURATION INVESTIGATED

## 4.1 THE TWO ROTOR, FOUR BEARING SYSTEM

The large turbogenerators used in the British power generating industry normally consist of a number of turbine rotors and an alternator rotor, each supported near its ends upon journal bearings, and rigidly bolted together to form one continuous shaft. The large amplitude vibration of a single rotor supported upon journal bearings - which is the basic unit of which the multi-rotor system is composed - has been the subject of a number of previous studies (see, for example, Hori (1959), Someya (1963-64)). However, with a two bearing system it is not possible to investigate the effects of parallel misalignment of the bearings. For this reason, the behaviour of a simple two rotor, four bearing system was to be investigated - this being the lowest multiple of the basic unit that may suffer from parallel misalignment of the bearings.

The shape of the rotor to be used in the investigation was arbitrary and so, for simplicity, the system chosen comprised two equal, rigidly coupled uniform rotors each supported symmetrically upon two bearings (see Figure 4.1). The positions of the bearings is typical of the coupled low pressure turbines of a 500 MW generating set. Although a uniform shaft is an idealised shape, it has the essential properties of distributed mass and stiffness and is convenient to use as its normal modes and natural frequencies may be obtained analytically.

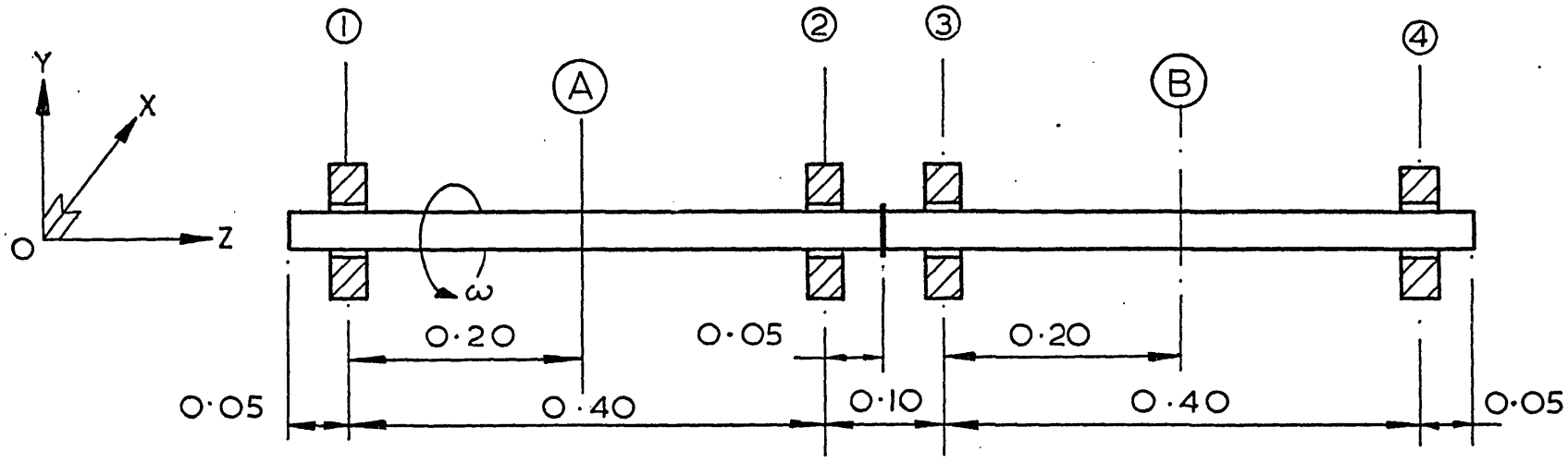


Figure 4.1: Two rotor, four bearing system

## 4.2 THE FREE-FREE MODES OF A UNIFORM SHAFT

For a uniform shaft, the non-dimensional flexural rigidity $\sigma$ and mass distribution $m_l$ assume constant values. From equation 2.13:

$$\sigma = constant = \frac{EI}{M L^3 \omega^2} \qquad 4.1$$

and from equation 2.14:

$$m_l = constant = \frac{\rho A}{M/L} = 1.0 \qquad 4.2$$

and, hence, equation 2.29 reduces to:

$$\frac{d^4\phi(s)}{ds^4} - \mu^4 \phi(s) = 0 \qquad 4.3$$

where:

$$\mu^4 = \nu_f^2 \frac{M L^3 \omega^2}{EI} \qquad 4.4$$

Equation 4.3 may be integrated directly and, for $\mu \neq 0$ (i.e. $\nu_f \neq 0$), the general solution is:

$$\phi(s) = A_1 \cos \mu s + A_2 \cosh \mu s + A_3 \sin \mu s + A_4 \sinh \mu s \qquad 4.5$$

where $A_1$ to $A_4$ are constants of integration. Applying the boundary conditions for a free-free shaft (equations 2.33 and 2.34) leads to four algebraic homogeneous equations in terms of the constants $A_1$ to $A_4$. These equations only have a non-trivial solution if:

$$\cos \mu \cosh \mu = 1 \qquad 4.6$$

The roots of this transcendental equation reveal, via equation 4.4, the free-free natural frequencies of the shaft. It should be noted that the root $\mu = 0$ corresponds to the rigid body modes (see section 2.2.3 of Chapter 2). For flexural modes, the roots, which are given approximately by:

$$\mu_i \simeq (2i - 3)\,\pi/2 \quad , \quad (i = 3, 4, \ldots) \tag{4.7}$$

may be obtained numerically using Newton's method.

The constants $A_1$ to $A_4$ are found from the boundary conditions to within an arbitrary constant, but this is fixed by imposing the orthogonality condition expressed by equation 2.42. The complete set of free-free normal modes for a uniform shaft are then given by:

$$\left.\begin{aligned} \phi_1 &= 1 \quad , \quad (\nu_{f_1} = 0) \\ \phi_2 &= \sqrt{3}\,(1 - 2s) \quad , \quad (\nu_{f_2} = 0) \\ \phi_i &= (\cos \mu_i s + \cosh \mu_i s) - \left(\frac{\cos \mu_i - \cosh \mu_i}{\sin \mu_i - \sinh \mu_i}\right) \\ &\quad (\sin \mu_i s + \sinh \mu_i s) \quad , \quad (i = 3, 4, \ldots) \end{aligned}\right\} \tag{4.8}$$

# CHAPTER 5

# STATIC AND LINEAR CONSIDERATIONS

## 5.1 INTRODUCTION

Before a study of the effect of bearing misalignment upon the non-linear dynamic behaviour of a multi-rotor system can be undertaken, it is necessary to first know the correct alignment for the system. The equilibrium position of the rotating shaft for a given set of bearing alignments, and the stability of the equilibrium position, are also required.

These properties of a rotor system, together with the response of the linearised system to unbalance excitation and the natural frequencies of the coupled rotors if "pinned" at each bearing, may be determined from the modal equations of motion (2.66 or 2.74) and are discussed in this chapter for a general multi-rotor system.

## 5.2 SYSTEM ALIGNMENT

For this section only, the assumption is made that each rotor is supported upon two bearings; therefore, if a system has $n$ bearings, then there are $(n - 2)/2$ couplings.

In this work, a correctly aligned system will be defined as one in which zero bending moment and shear force act through each coupling when the shaft is running at design speed. This differs from industrial practice where, to facilitate assembly of the system, the aligned condition refers to a non-rotating shaft resting at the bottom of each bearing. However, for this situation, bending moment and shear force acting through the couplings remains small even when the shaft is running at design speed as the displacement of the shaft in each bearing due to hydrodynamic "lift" is approximately the same - and hence the distribution of bearing loads remains almost unchanged.

The equations for the static deflection of the shaft, which may be obtained from equations 2.74 by removing acceleration, velocity and unbalance terms, are given by:

$$\left.\begin{aligned} \sum_{k=1}^{n} \left\{ \phi_i(s_k)\, f_x \left[ (x - x_{b_k}),\ (y - y_{b_k}) \right]_{s=s_k} \right\} - \nu_{f_i}{}^2\, q_{x_i} &= 0 \\ \sum_{k=1}^{n} \left\{ \phi_i(s_k)\, f_y \left[ (x - x_{b_k}),\ (y - y_{b_k}) \right]_{s=s_k} \right\} - \nu_{f_i}{}^2\, q_{y_i} &= \delta_{i1}\, S_t \\ , \qquad (i = 1,\ 2,\ \ldots,\ m) & \end{aligned}\right\} \quad 5.1$$

where:
$$x(s_k) = \sum_{i=1}^{m} q_{x_i}\, \phi_i(s_k) \qquad 5.2$$

and:
$$y(s_k) = \sum_{i=1}^{m} q_{y_i}\, \phi_i(s_k) \qquad 5.3$$

Consideration of the free body diagram of a single rotor shows that, for an aligned system, no forces act upon the shaft in the horizontal direction and so:

$$\left.\begin{aligned} f_x\left[(x - x_{b_k}),\ (y - y_{b_k})\right]_{s=s_k} &= 0 \\ f_y\left[(x - x_{b_k}),\ (y - y_{b_k})\right]_{s=s_k} &= W_k \quad , \quad (k = 1, 2, \ldots, n) \end{aligned}\right\} \quad 5.4$$

where $W_k$ is the bearing load at the $k$th station. It may thus be seen that, because $\nu_{f_1} = \nu_{f_2} = 0$, the equations for the horizontal direction are satisfied if the shaft lies in any vertical plane, i.e. if:

$$q_{x_3} = q_{x_4} = \ldots\ldots = q_{x_m} = 0 \quad 5.5$$

The plane $OZY$ is chosen here, so that:

$$x(s) = 0 \quad 5.6$$

and hence:

$$q_{x_1} = q_{x_2} = 0 \quad 5.7$$

The equations for the vertical direction may be written as:

$$\sum_{k=1}^{n} \{\phi_i(s_k)\ W_k\} - \nu_{f_i}{}^2\ q_{y_i} = \delta_{i1}\ S_t \quad , \quad (i = 1, 2, \ldots, m) \quad 5.8$$

This is a set of $m$ linear equations in $(m+n)$ unknowns ($q_{y_1}$, ..., $q_{y_m}$, $W_1$, ..., $W_n$); $n$ further equations are required.

$(n-2)$ equations arise from the requirement for zero bending moment and shear force at the $(n-2)/2$ couplings. Expressions for the bending

moment and shear force at any station along the shaft may be obtained by differentiation of the modal series, but this approach will not be used here for the following reasons. Firstly, as discussed by Bishop & Johnson (1960), the rate of convergence of the modal series becomes progressively worse each time it is differentiated, and so a truncated series, which converges adequately for displacement, may give rise to serious errors for the bending moment and shear force. Secondly, it is difficult for realistic rotors, whose modes are found by approximate methods, to obtain accurate estimates of the derivatives required.

Instead, the desired equations are obtained by "resolving and taking moments" at each coupling, or more formally by integration of the static version of equation 2.12 (only the equation for the vertical direction is considered), which gives:

$$\left.\begin{aligned} \sum_{k=1}^{n} H(s_j - s_k)\, W_k &= S_t \int_o^{s_j} m_l(\eta)\, d\eta \\ \sum_{k=1}^{n} R(s_j - s_k)\, W_k &= S_t \int_o^{s_j} \int_o^{\xi} m_l(\eta)\, d\eta\, d\xi \end{aligned}\right\} \quad 5.9$$

$$, \qquad (j = 1, 2, \ldots, (n-2)/2)$$

where:
$$H(s_j - s_k) = \begin{cases} 0 & , \text{ if } s_j < s_k \\ 1 & , \text{ if } s_j > s_k \end{cases} \quad 5.10$$

$$R(s_j - s_k) = \begin{cases} 0 & , \text{ if } s_j < s_k \\ s_j - s_k & , \text{ if } s_j > s_k \end{cases} \quad 5.11$$

and $s_j$ is the non-dimensional displacement along the shaft to the $j$th coupling.

The final two equations required are obtained by fixing the vertical displacement of two stations along the shaft in order to orientate the

whole system with respect to the datum *OZXY*. For this purpose, the displacement of the shaft at bearing stations 1 and $n$ is set to zero, i.e.

$$\sum_{i=1}^{n} q_{y_i} \phi_i(s_k) = 0 \quad , \quad k = 1, n \qquad 5.12$$

Equations 5.8, 5.9 and 5.12 give a system of *(m+n)* linear equations in *(m+n)* unknowns, which may be solved to yield the bearing loads $W_k$ and the aligned static modal coefficients $q_{y_i}$ for the shaft.

Once the displacement of the aligned shaft and the bearing loads are known, the required position of the bearings relative to the datum may be found. This may be achieved for each bearing by solving the two simultaneous non-linear equations 5.4 for the two unknowns $x_{b_k}$ and $y_{b_k}$. The position of the bearings relative to the datum when the system is aligned will be denoted by $(x_{b_k})_a$ and $(y_{b_k})_a$ and the misalignments of a bearing from the aligned condition, denoted by $\Delta x_{b_k}$ and $\Delta y_{b_k}$, are defined as:

$$\Delta x_{b_k} = x_{b_k} - (x_{b_k})_a \qquad 5.13$$

$$\Delta y_{b_k} = y_{b_k} - (y_{b_k})_a \qquad 5.14$$

(If desired, the whole system may be reoriented by suitable modifications to $q_{x_1}$, $q_{x_2}$, $q_{y_1}$ and $q_{y_2}$, so that the centreline of the two end bearings, 1 and $n$, lie on the datum. The bearing locations $x_{b_k}$ and $y_{b_k}$ must be adjusted accordingly.)

## 5.3 THE EQUILIBRIUM POSITION OF THE ROTATING SHAFT

(It should be noted that, in the matrix equations appearing in this and the following sections, { } denotes a column vector and [ ] a square matrix.)

The equilibrium position of the rotating shaft for a given set of bearing alignments ($x_{b_k}$, $y_{b_k}$) is governed by equations 5.1 which, for convenience, are re-ordered in the following manner:

$$\left.\begin{aligned} &\sum_{k=1}^{n} \{\phi_i(s_k)\, f_{x_k}\} - \nu_{f_i}^{\,2}\, q_{x_i} = H_i = 0 \\ &\qquad , \qquad (i = 1, 2, \ldots, m) \\ &\sum_{k=1}^{n} \{\phi_i(s_k)\, f_{y_k}\} - \nu_{f_i}^{\,2}\, q_{y_i} - \delta_{i1}\, S_t = H_{m+i} = 0 \\ &\qquad , \qquad (i = 1, 2, \ldots, m) \end{aligned}\right\} \quad 5.15$$

and may be written in matrix form as:

$$\{H(\{q\}_o)\} = 0 \qquad 5.16$$

where:

$$\{q\}_o = \begin{Bmatrix} q_{x_1} \\ \vdots \\ q_{x_m} \\ \hline q_{y_1} \\ \vdots \\ q_{y_m} \end{Bmatrix}_o \qquad 5.17$$

and the subscript $\{\ \}_o$ is used to denote the equilibrium state.

Equation 5.16 is a system of $2m$ non-linear algebraic equations, in terms of the $2m$ static modal coefficients $\{q\}_o$, which may be solved

iteratively using the Newton-Raphson technique, that is:

$$\{q\}_{p+1} = \{q\}_p - [J]^{-1} \{H(\{q\}_p)\} \qquad 5.18$$

where $\{q\}_p$ is the $p$th estimate of the solution, and $[J]$ is the jacobean matrix whose elements are given by:

$$J_{ij} = \left.\frac{\partial H_i}{\partial q_i}\right|_p \qquad 5.19$$

The matrix $[J]$ is discussed in more detail in the next section.

The initial estimate of the solution vector $\{q\}_1$ was obtained by choosing the first $n$ modal coefficients for each direction so that the shaft passed through each of the $n$ bearings at a suitable eccentricity. This is achieved by solving the following two sets of $n$ simultaneous linear equations:

$$\sum_{i=1}^{n} q_{x_i} \phi_i(s_k) = x_{b_k} + a \quad , \quad (k = 1, 2, \ldots, n) \qquad 5.20$$

$$\sum_{i=1}^{n} q_{y_i} \phi_i(s_k) = y_{b_k} + b \quad , \quad (k = 1, 2, \ldots, n) \qquad 5.21$$

for $(q_{x_1}, \ldots, q_{x_n})$ and $(q_{y_1}, \ldots, q_{y_n})$; the remaining modal coefficients are set to zero. For most alignment conditions, convergence was achieved if $a \simeq 0.5$ and $b \simeq -0.5$. Occasionally, for extreme misalignment of the bearings, the solution procedure failed during the first few iterations as the shaft was predicted to lie outside one of the bearings. This difficulty could normally be overcome by suitable adjustments to $a$ and $b$.

The iteration procedure was continued until the elements of $\{q\}$ had converged to a desired accuracy.

## 5.4 THE STABILITY OF THE EQUILIBRIUM STATE

The stability of the equilibrium position of the shaft may be determined from the linearised form of equations 2.74.

Firstly, after discounting the unbalance terms, equations 2.74 are, for convenience, re-ordered as follows:

$$\left.\begin{aligned}
\frac{du_{x_i}}{d\tau} &= \sum_{k=1}^{n} \{\phi_i(s_k)\, f_{x_k}\} - 2\gamma\, u_{x_i} - \nu_{f_i}^{\,2}\, q_{x_i} = G_i \\
&\qquad , \qquad (i = 1, 2, \ldots, m) \\
\frac{du_{y_i}}{d\tau} &= \sum_{k=1}^{n} \{\phi_i(s_k)\, f_{y_k}\} - 2\gamma\, u_{y_i} - \nu_{f_i}^{\,2}\, q_{y_i} - \delta_{i1}\, S_t = G_{m+i} \\
&\qquad , \qquad (i = 1, 2, \ldots, m) \\
\frac{dq_{x_i}}{d\tau} &= u_{x_i} = G_{2m+i} \qquad , \qquad (i = 1, 2, \ldots, m) \\
\frac{dq_{y_i}}{d\tau} &= u_{y_i} = G_{3m+i} \qquad , \qquad (i = 1, 2, \ldots, m)
\end{aligned}\right\} \quad 5.22$$

This system of equations may be written in matrix form as:

$$\frac{d\{u\}}{d\tau} = \{G(\{u\})\} \quad 5.23$$

where:

$$\{u\} = \begin{Bmatrix} u_{x_1} \\ \dot{u}_{x_m} \\ \hline u_{y_1} \\ \dot{u}_{y_m} \\ \hline q_{x_1} \\ \dot{q}_{x_m} \\ \hline q_{y_1} \\ \dot{q}_{y_m} \end{Bmatrix} \quad 5.24$$

By expanding the non-linear functions $G_i(\{u\})$ about the equilibrium position $\{u\}_o$, this system of non-linear ordinary differential equations may be approximated to by a system of linear equations with constant coefficients:

$$\frac{d\{\bar{u}\}}{d\tau} = [A]\ \{\bar{u}\} \qquad 5.25$$

where the $(4m \times 4m)$ matrix $[A]$ has elements:

$$A_{ij} = \left.\frac{\partial G_i}{\partial u_j}\right|_o \qquad 5.26$$

and:

$$\{\bar{u}\} = \{u\} - \{u\}_o \qquad 5.27$$

Equation 5.25 is valid for small excursions of the shaft about the equilibrium position. From the theory of ordinary differential equations with constant coefficients, it is known that if the eigenvalues $(\lambda_i)$ of $[A]$ have negative real parts, i.e. if:

$$Max\ Re\ (\lambda_i) < 0 \qquad 5.28$$

then any small disturbance the shaft is subjected to decays and hence the shaft is stable at its equilibrium position. For the large order system under consideration here, the most practical method for assessing the stability of the system is to calculate all the eigenvalues of $[A]$ and inspect the sign of the real parts. In this work, a NAG (1973) library subroutine suitable for real non-symmetric matrices was used to find the eigenvalues of $[A]$.

The matrix $[A]$ will now be considered in more detail. To develop $[A]$, the derivatives $\partial f_x/\partial u_{x_j}$, $\partial f_x/\partial q_{x_j}$, etc., are required. From the

modal expansions (equations 2.61 and 2.64) it may be shown, by applying the rules for differentiating a function of a function, that:

$$\frac{\partial f_x}{\partial u_{x_j}} = \phi_j \frac{\partial f_x}{\partial \dot{x}} \qquad 5.29$$

$$\frac{\partial f_x}{\partial q_{x_j}} = \phi_j \frac{\partial f_x}{\partial x} \qquad 5.30$$

$$\frac{\partial f_x}{\partial u_{y_j}} = \phi_j \frac{\partial f_x}{\partial \dot{y}} \qquad 5.31$$

$$\frac{\partial f_x}{\partial q_{y_j}} = \phi_j \frac{\partial f_x}{\partial y} \qquad 5.32$$

$$\frac{\partial f_y}{\partial u_{x_j}} = \phi_j \frac{\partial f_y}{\partial \dot{x}} \qquad 5.33$$

$$\frac{\partial f_y}{\partial q_{x_j}} = \phi_j \frac{\partial f_y}{\partial x} \qquad 5.34$$

$$\frac{\partial f_y}{\partial u_{y_j}} = \phi_j \frac{\partial f_y}{\partial \dot{y}} \qquad 5.35$$

$$\frac{\partial f_y}{\partial q_{y_j}} = \phi_j \frac{\partial f_y}{\partial y} \qquad 5.36$$

where $-\partial f_x/\partial \dot{x}$, $-\partial f_x/\partial x$, ..., $-\partial f_y/\partial y$ are the eight stiffness and damping coefficients for each bearing, and may be obtained by numerical differencing. It should be noted that the stiffness and damping coefficients generally given in the literature (for example, those given by Smith (1969) for a short bearing) are for bearing supporting vertical loads. In a misaligned multi-rotor system, the bearing load vectors are seldom vertical and so these coefficients are either not valid or, for the special case of axisymmetric bearings, must be modified before they may be employed. Such difficulties do not arise if the coefficients are found

by numerical differencing.

Because of the order of equations 5.22, the matrix $[A]$ may be conveniently partitioned into a number of square submatrices:

$$[A] = \left[\begin{array}{c|c|c|c} [C_{xx}] & [C_{xy}] & [K_{xx}] & [K_{xy}] \\ \hline [C_{yx}] & [C_{yy}] & [K_{yx}] & [K_{yy}] \\ \hline \multicolumn{2}{c|}{[I]} & \multicolumn{2}{c}{[O]} \end{array}\right] \qquad 5.37$$

where the $(m \times m)$ matrices $[C_{xx}]$, $[K_{xx}]$, etc., have the elements:

$$C_{xx_{ij}} = \sum_{k=1}^{n} \{\phi_i \, \phi_j \frac{\partial f_x}{\partial x}\}_{s_k} - \delta_{ij} \, 2\gamma \qquad 5.38$$

$$C_{xy_{ij}} = \sum_{k=1}^{n} \{\phi_i \, \phi_j \frac{\partial f_x}{\partial y}\}_{s_k} \qquad 5.39$$

$$C_{yx_{ij}} = \sum_{k=1}^{n} \{\phi_i \, \phi_j \frac{\partial f_y}{\partial x}\}_{s_k} \qquad 5.40$$

$$C_{yy_{ij}} = \sum_{k=1}^{n} \{\phi_i \, \phi_j \frac{\partial f_y}{\partial y}\}_{s_k} - \delta_{ij} \, 2\gamma \qquad 5.41$$

$$K_{xx_{ij}} = \sum_{k=1}^{n} \{\phi_i \, \phi_j \frac{\partial f_x}{\partial x}\}_{s_k} - \delta_{ij} \, \nu {f_i}^2 \qquad 5.42$$

$$K_{xy_{ij}} = \sum_{k=1}^{n} \{\phi_i \, \phi_j \frac{\partial f_x}{\partial y}\}_{s_k} \qquad 5.43$$

$$K_{yx_{ij}} = \sum_{k=1}^{n} \{\phi_i \, \phi_j \frac{\partial f_y}{\partial x}\}_{s_k} \qquad 5.44$$

$$K_{yy_{ij}} = \sum_{k=1}^{n} \{\phi_i \, \phi_j \frac{\partial f_y}{\partial y}\}_{s_k} - \delta_{ij} \, \nu {f_i}^2 \qquad 5.45$$

and $[I]$ is the $(2m \times 2m)$ unit matrix, and $[O]$ is a $(2n \times 2m)$ zero matrix.

Finally, returning to the problem of finding the equilibrium position of the shaft discussed in the previous section. The jacobean matrix $[J]$ required in the Newton-Raphson procedure is given by:

$$[J] = \left[\begin{array}{c|c} [K_{xx}] & [K_{xy}] \\ \hline [K_{yx}] & [K_{yy}] \end{array}\right] \qquad 5.46$$

where the partial derivatives $\partial f_x/\partial x$, $\partial f_x/\partial y$, $\partial f_y/\partial x$ and $\partial f_y/\partial y$ are evaluated not at the unknown equilibrium position, but at the latest estimate of the solution $\{q\}_p$.

## 5.5 THE FORCED RESPONSE OF THE LINEARISED SYSTEM

If the equilibrium position of the shaft is stable, then equations 5.25 may be used to determine the response of the linearised system to unbalance excitation. For this, equations 5.25 are re-synthesised to a system of $2m$ second order differential equations and the terms for unbalance re-introduced. That is:

$$\frac{d^2\{\bar{q}\}}{d\tau^2} = [C]\frac{d\{\bar{q}\}}{d\tau} + [K]\{\bar{q}\} + Re\left(\{\{Q_c\} + \underline{i}\{Q_s\}\}\, e^{\underline{i}\tau}\right) \qquad 5.47$$

where:
$$\{\bar{q}\} = \{q\} - \{q\}_o \qquad 5.48$$

(see equation 5.17 for the definition of $\{q\}$)

$$[C] = \left[\begin{array}{c|c} [C_{xx}] & [C_{xy}] \\ \hline [C_{yx}] & [C_{yy}] \end{array}\right] \qquad 5.49$$

$$[K] = \left[\begin{array}{c|c} [K_{xx}] & [K_{xy}] \\ \hline [K_{yx}] & [K_{yy}] \end{array}\right] \qquad 5.50$$

$$\{Q_c\} = \left\{\begin{array}{c} Q_{\xi_1} \\ \vdots \\ Q_{\xi_m} \\ \hline Q_{\eta_1} \\ \vdots \\ Q_{\eta_m} \end{array}\right\} \qquad 5.51$$

$$\{Q_s\} = \left\{\begin{array}{c} Q_{\eta_1} \\ \vdots \\ Q_{\eta_m} \\ \hline -Q_{\xi_1} \\ \vdots \\ -Q_{\xi_m} \end{array}\right\} \qquad 5.52$$

The steady-state response of a linear system is at a single frequency if the excitation force contains a single frequency. Therefore, assume the steady-state solution of equation 5.47 to be of the form:

$$\{\bar{q}\} = \{\{\bar{q}_R\} + \underline{i}\{\bar{q}_I\}\}\, e^{\underline{i}\tau} \qquad 5.53$$

where the vectors $\{\bar{q}_R\}$ and $\{\bar{q}_I\}$ are not functions of $\tau$. By substituting equation 5.53 into 5.47 and equating real and imaginery parts, the system of $4m$ linear algebraic equations:

$$\begin{bmatrix} [K] + [I] & -[C] \\ [C] & [K] + [I] \end{bmatrix} \begin{Bmatrix} \{\bar{q}_R\} \\ \{\bar{q}_I\} \end{Bmatrix} = \begin{Bmatrix} -\{Q_c\} \\ -\{Q_s\} \end{Bmatrix} \qquad 5.54$$

is obtained. The solution of equations 5.54 yields $\{\bar{q}_R\}$ and $\{\bar{q}_I\}$ which, if the real part of the assumed solution 5.53 is taken, give the motion of the shaft at any station due to the unbalance excitation, i.e.

$$\bar{x}(s) = x(s) - x_o(s) = \Big(\sum_{i=1}^{m} \bar{q}_{R_i}\phi_i(s)\Big)\cos\tau - \Big(\sum_{i=1}^{m} \bar{q}_{I_i}\phi_i(s)\Big)\sin\tau \qquad 5.55$$

$$\bar{y}(s) = y(s) - y_o(s) = \Big(\sum_{i=1}^{m} \bar{q}_{R_{m+i}}\phi_i(s)\Big)\cos\tau - \Big(\sum_{i=1}^{m} \bar{q}_{I_{m+i}}\phi_i(s)\Big)\sin\tau \qquad 5.56$$

From equations 5.55 and 5.56 it may be seen that the shaft describes an ellipse about the equilibrium position $(x_o, y_o)$. A scheme is presented in Appendix 2 for determining the magnitude and orientation of these elliptic orbits at a given shaft station.

As an example of the application of this method, the response of the two rotor system supported upon four identical short journal bearings is shown in Figure 5.1. The system was aligned and the shaft had a uniform

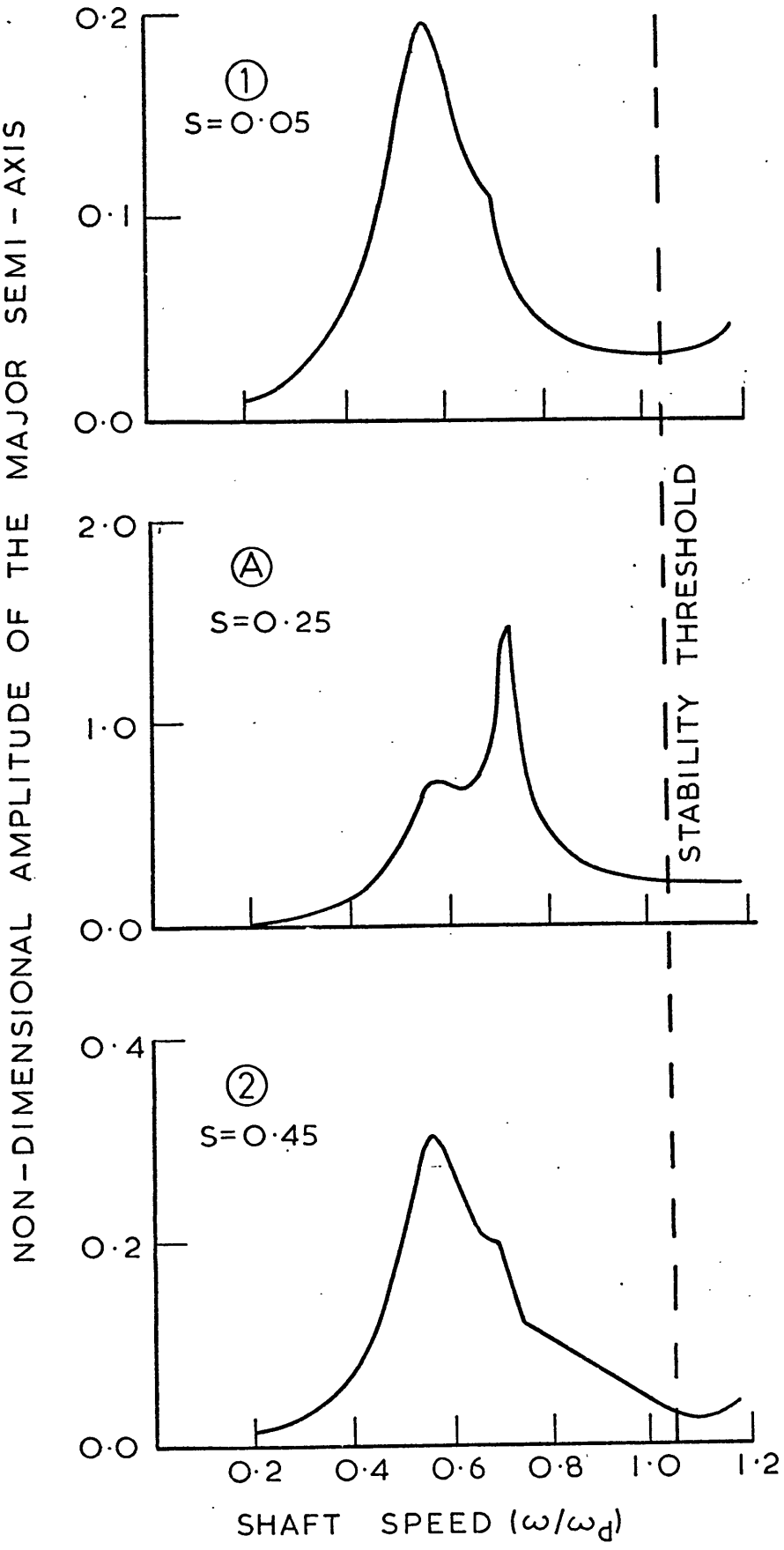


Figure 5.1: The response of the aligned two rotor system to a uniform unbalance distribution

distribution of unbalance along its length, i.e. $Q_{\xi_1} = 0.1$, $Q_{\xi_1} = \ldots = Q_{\xi_m} = Q_{\eta_1} = \ldots = Q_{\eta_m} = 0$. When operating at design speed ($\omega_d$), the equilibrium eccentricity ratio of the bearings is given by $\varepsilon_o = 0.62$, the lowest flexural free-free natural frequency of the shaft $\nu_{f_3} = 0.2$, and the stability parameter $S_t = 0.4$. Eight modes were used in the modal expansion (i.e. $m = 8$) and external damping was ignored. It should be noted that, as the system is symmetric, the behaviour for the first rotor, shown in Figure 5.1, is identical with that predicted for the second rotor. The system has two resonances in the speed range shown, one at $\omega/\omega_d \simeq 0.55$ and the other at $\omega/\omega_d \simeq 0.7$. Between these two speeds, the shaft exhibited "backward" procession.

## 5.6 THE "PINNED" NATURAL FREQUENCIES OF A MULTI-ROTOR SYSTEM

It is well known that the lowest natural frequency of a single rotor system when "pinned" (simply supported) at its bearings is an important parameter governing the vibrational behaviour of the system. Whether the pinned natural frequencies of a multi-rotor system assume a similar importance was a matter to be investigated, but for this purpose it was necessary to have a means of determining these frequencies.

The method proposed for doing this was to replace the journal bearing forces in the linearised system by simple springs, i.e.

$$f_{x_k} = - K_s \, x \qquad 5.57$$

$$f_{y_k} = - K_s \, y \qquad 5.58$$

and to increase $K_s$, the spring constant, until the lower natural frequencies of the system had converged to the corresponding pinned natural frequencies. If, for this situation, the unbalance terms in equation 5.47 are omitted, then the equations for the $X$ and $Y$ directions are decoupled and identical. The equations for the $X$ direction are:

$$\frac{d^2\{q_x\}}{d\tau^2} = [K_{xx}] \, \{q_x\} \qquad 5.59$$

where:

$$\{q_x\} = \begin{Bmatrix} q_{x_1} \\ \vdots \\ q_{x_m} \end{Bmatrix} \qquad 5.60$$

and the elements of $[K_{xx}]$:

$$K_{xx_{ij}} = -K_s \sum_{k=1}^{n} \{\phi_i(s_k)\ \phi_j(s_k)\} - \delta_{ij}\ \nu_{f_i}^2 \qquad 5.61$$

The (square root of the) eigenvalues of the symmetric matrix $[K_{xx}]$ yield the natural frequencies of the system.

The method was tested by finding the first four natural frequencies of a uniform beam pinned at distances 0, $\frac{1}{3}L$, $\frac{2}{3}L$ and $L$ along its length. An exact solution to this problem is given by MacDuff & Felgar (1957). The magnitude of $K_s$ was increased until the first four natural frequencies had converged to five significant figures. The errors resulting from representing the shaft by 8, 10, 12, 14 and 16 free-free modes are given in Table 5.1.

TABLE 5.1

Percentage errors in the calculation of the pinned natural frequencies ($\omega_{p_i}$) of a three span continuous beam

| Number of Free-Free Modes | $\omega_{p_1}$ | $\omega_{p_2}$ | $\omega_{p_3}$ | $\omega_{p_4}$ |
|---|---|---|---|---|
| 8 | 0.85 | 1.50 | 1.66 | 2.12 |
| 10 | 0.39 | 1.49 | 1.28 | 1.13 |
| 12 | 0.21 | 0.77 | 1.26 | 0.62 |
| 14 | 0.12 | 0.60 | 0.08 | 0.37 |
| 16 | 0.08 | 0.60 | 0.05 | 0.24 |

Predicting the pinned natural frequencies of a shaft using the free-free modes is an extreme test for the modal method, but it may be seen from Table 5.1 that good estimates of the pinned natural frequencies were obtained by employing only eight free-free modes (two rigid body plus six

flexural).

The first four pinned natural frequencies of the two rotor system (Figure 4.1), and their associated mode shapes, were found using the above method and are given in Figure 5.2.

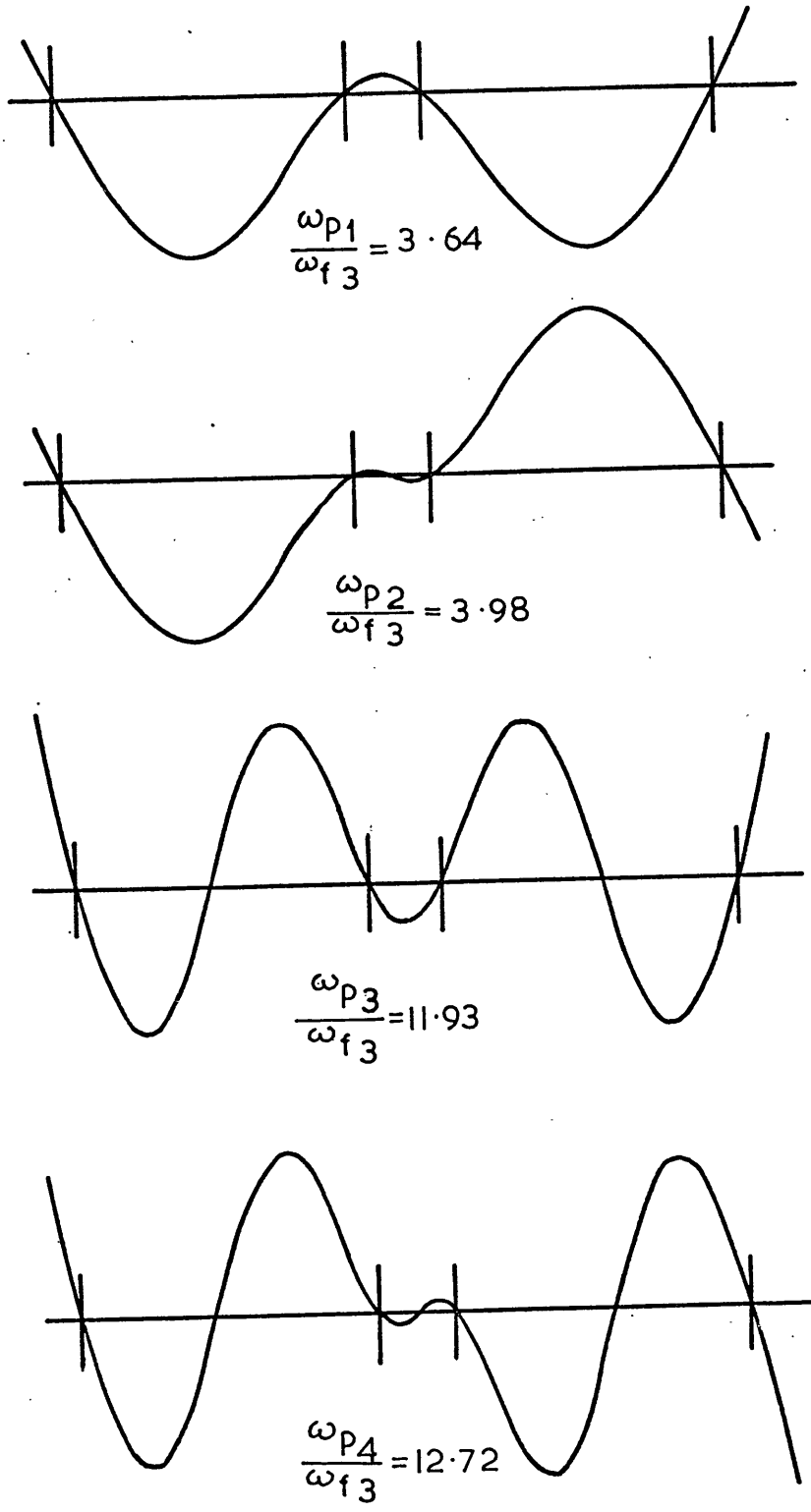


Figure 5.2: The first four pinned modes and natural frequencies of the two rotor system

# CHAPTER 6

# TWO ROTOR SYSTEM SUPPORTED UPON SHORT CIRCULAR BEARINGS

## 6.1 COMPUTATIONAL PROCEDURE

### 6.1.1 Numerical Integration of the Equations of Motion

A computer program was developed, which employed a NAG (1973) library subroutine based upon the Runge-Kutta-Merson method, to integrate the equations of motion (2.74) for the flexural vibrations of a multi-rotor system. For a given interval over which the equations were to be integrated, the NAG subroutine automatically adjusted the size of the time steps within the interval so that a specified bound on the local truncation error was not exceeded. This enabled the results to be obtained at uniform time intervals without recourse to interpolation. The short bearing approximation was used to obtain the bearing forces $f_x$ and $f_y$; these are given, via equations 3.21 and 3.22, by equations 3.26 and 3.27.

The computer program was tested by predicting the symmetric motion of a uniform, rigid shaft supported at its ends in identical bearings. (Such a system is simply modelled by setting $m = 1$ and $n = 2$ in equations 2.74.) The trajectories resulting from giving the balanced shaft a small displacement from its equilibrium position were found either to converge on the equilibrium position or tend to closed orbits of finite amplitude, depending upon whether the operating state was predicted by linear theory to be respectively stable or unstable. As a further check, a number of the whirl orbits given by Holmes (1970) for unbalance excitation were reproduced.

Unless otherwise stated, the initial conditions used in the solution procedure were, for a balanced shaft, those corresponding to

giving the shaft a small rigid body translation from its equilibrium position but without imparting a velocity to it, i.e.

$$q_{x_1} = (q_{x_1})_o + a \qquad 6.1$$

$$q_{y_1} = (q_{y_1})_o + b \qquad 6.2$$

where $0.05 < |a| < 0.1$ and $0.05 < |b| < 0.1$. For a shaft experiencing unbalance forces, the (rotating) shaft was initially at rest at its equilibrium position. Also, unless otherwise stated, eight modes were used in the modal expansion, i.e. $m = 8$ in equations 2.74.

### 6.1.2 Frequency Analysis

Plotting the steady-state orbit of the shaft centre, as has been the practice in much previous work, only provides a limited amount of information about the nature of the motion, especially when the orbits are complicated due to the presence of a number of frequency components. The use of "time markers" to determine the frequency of the motion may lead to confusion if more than one component is present. Therefore, frequency analysis, which is widely used as a diagnostic technique in practice, was used to determine the constituents of the predicted steady-state motion.

For this, a NAG (1973) subroutine based upon the *fast fourier transform* algorithm was employed to analyse the shaft centre displacement in the $X$ and $Y$ directions, at the six stations 1, 2, 3, 4, A and B shown in Figure 4.1, once the steady-state, determined by inspection of the trajectories at these stations, had been attained. The accuracy with which the frequency of each component may be determined, i.e. the resolution, depends upon the sample length, $T$, that is upon the length of

the period of analysis. However, consideration had to be given to the computer time required to generate the data. As a compromise, a period of 64 revolutions of the shaft was chosen which, whilst not making excessive demands upon computer time, gave an accurate equivalent to ±0.39 Hz for a shaft rotating at 50 Hz.

For frequency analysis, the sampling frequency, $N/T$, where $N$ is the number of intervals into which the sample is divided, has to be at least twice the frequency of the highest significant component appearing in the signal. Initially, to ensure this, a very high sampling frequency of 256 $\omega$ (i.e. 256 data intervals per shaft revolution) was used, but later, as the highest significant component in the motion was always found to be less than 4 $\omega$, the sampling frequency was reduced to 16 $\omega$ - which still allowed for a margin of safety. It should be noted that fast fourier transform algorithm requires the total number of data intervals ($N$) to be an integer power of 2, i.e. $N = 2^i$, $i = 2, 3, 4, \ldots$ .

The sample length ($T$) was chosen to be an integer number of shaft revolutions so that a synchronous component present in the motion due to unbalance excitation (this being the only component whose frequency may be predicted *a priori*) would be a multiple of the base frequency $1/T$ and its amplitude given directly from the frequency spectrum by the component at $64/T$. Determining the amplitude of a component whose frequency does not coincide with a multiple of the base frequency requires further discussion.

Consider the frequency analysis of a signal containing a single component of amplitude $\chi$ and frequency $\Omega$. If $\Omega$ is not an exact multiple of the base frequency, $1/T$, then the signal appears as more than one component in the frequency spectrum. The maximum component occurs at the frequency ($p/T$) that is closest to $\Omega$, but the amplitude of this

component, denoted by $a_p$, may considerably under-estimate the signal amplitude $\chi$. For the worst situation when the signal frequency falls mid way between two spectrum frequencies, the maximum component has an amplitude of only 0.64 $\chi$. However, from Parseval's theorem (see Sneddon (1961)), it is known that the sum of the squares of the components in the spectrum is equal to the square of the amplitude of the original signal. This gives a method for determining the signal amplitude $\chi$ from the components in the spectrum. In practice, it is not necessary to carry out the summation process over the whole spectrum as, after only a small number of components on either side of the maximum, the contributions become negligible. By considering only seven components, i.e.

$$\chi \simeq \sqrt{a_{p-3}^2 + a_{p-2}^2 + a_{p-1}^2 + a_p^2 + a_{p+1}^2 + a_{p+2}^2 + a_{p+3}^2} \qquad 6.3$$

the amplitude, for the worst situation, is not under-estimated by more than 3%. It follows from the last argument that the correction formula may also be used for signals containing more than one frequency component if the frequencies are well separated with respect to the resolution.

### 6.1.3 Parameters Governing the System

Misalignment of any of the bearings in the two rotor system may, by translation and rotation of the whole system, be reduced to an equivalent misalignment of the two central bearings. Even with this simplification, it is impractical to make a complete study of all possible misalignment conditions. For this reason, the investigation was restricted to the upward vertical misalignment of bearing number 2.

In order to reduce the number of variables needed to describe the system, it was further decided to make the four bearings identical and

so for each bearing $c_r/C = 1$. For this situation, the system, with the exception of the unbalance distribution, is uniquely described by the following non-dimensional parameters:

$\nu_{f_3}$ : lowest flexural free-free natural frequency of the coupled rotors

$(\varepsilon_o)_a$ : equilibrium eccentricity ratio of the bearings for the aligned system

$S_t$ : stability parameter

$\Delta y_{b_2}$ : vertical misalignment of bearing number 2

($\gamma$ : external damping factor)

For the low pressure turbines of a typical 500 MW turbogenerator, $0.6 < (\varepsilon_o)_a < 0.7$ and $S_t = 0.4$; the value of the other parameters will be discussed later.

The non-dimensional pinned natural frequencies $\nu_{p_i}$ of the system are given by:

$$\nu_{p_i} = \frac{\omega_{p_i}}{\omega} = \frac{\omega_{p_i}}{\omega_{f_3}} \frac{\omega_{f_3}}{\omega} = \frac{\omega_{p_i}}{\omega_{f_3}} \nu_{f_3} \qquad 6.4$$

and so, from Figure 5.2:

$$\frac{1}{\nu_{p_1}} = \frac{\omega}{\omega_{p_1}} = \frac{1}{3.64\ \nu_{f_3}} \qquad 6.5$$

The reciprocal of $\nu_{p_1}$ will be used here in order to conform with the practice of previous literature.

## 6.2 INITIAL INVESTIGATION

For the first series of tests, the first free-free (flexural) natural frequency of each rotor of the two rotor system was made to coincide with the first free-free (flexural) natural frequency of a typical low pressure turbine from a 500 MW generating set. This gave $\nu_{f_3} = 0.2$ and $\omega/\omega_{p_1} = 1.37$. The shaft was considered to be perfectly balanced and not acted upon by external damping.

Examples of steady-state orbits obtained for misalignments of $\Delta y_{b_2} = 0.5$ and $\Delta y_{b_2} = 2.0$ are shown in Figures 6.1 and 6.2. For bearing stations 1, 2, 3 and 4, the shaft centre orbits are shown within the bearing clearance circles, whilst for the mid-span stations A and B the small circles indicate, for comparison, the size and position of the clearance circles of the two end bearings. The small vertical crosses show the equilibrium position of the shaft and the diagonal crosses give a single time marker.

It may be seen that, for both alignment conditions, the bearing exhibiting the largest whirl orbit was the deloaded bearing number 3. Frequency analysis revealed that the fundamental steady-state whirl frequency, $\omega_{w_1}$, occurred at 0.5 $\omega$. Whirl frequencies lower than this were not induced for any misalignment of bearing number 2.

Operational experience on large turbogenerators has shown that steady-state whirl occurs at frequencies in the range 0.4 $\omega$ - 0.5 $\omega$; but usually towards the lower end of this range. To induce whirl in the two rotor system at frequencies lower than 0.5 $\omega$, and closer to those occurring in practice, the flexibility of the shaft had to be increased until the rotational speed was greater than the first pinned critical speed of the system, i.e. $\omega/\omega_{p_1} > 2$. For this situation, the whirl developed at a frequency approximately equal to $\omega_{p_1}$, but the mid-span amplitude grew

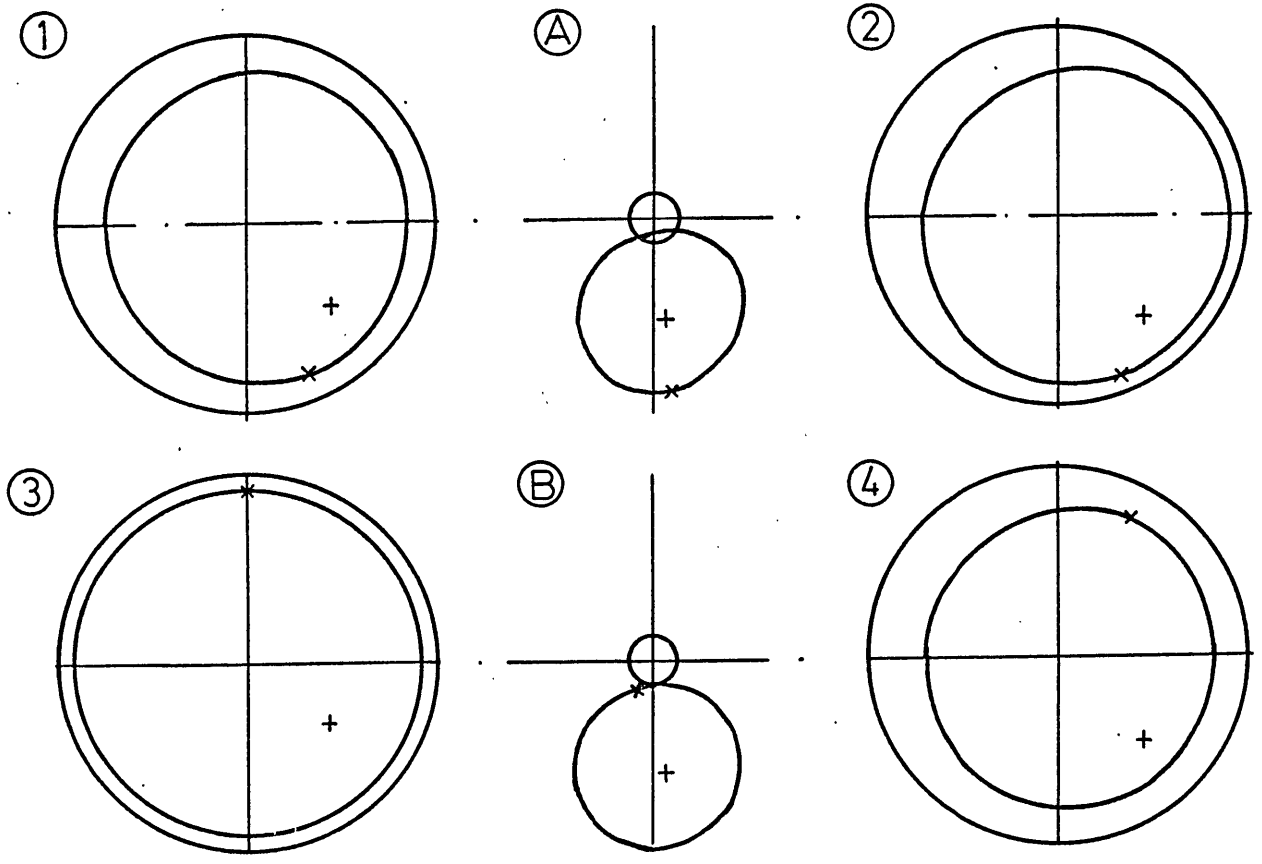


Figure 6.1: The steady-state whirl orbits for the misaligned two rotor system. Balanced shaft, $\Delta y_{b_2} = 0.5$, $\nu_{f_3} = 0.2$, $(\varepsilon_o)_a = 0.62$, $S_t = 0.4$, $\gamma = 0.0$.

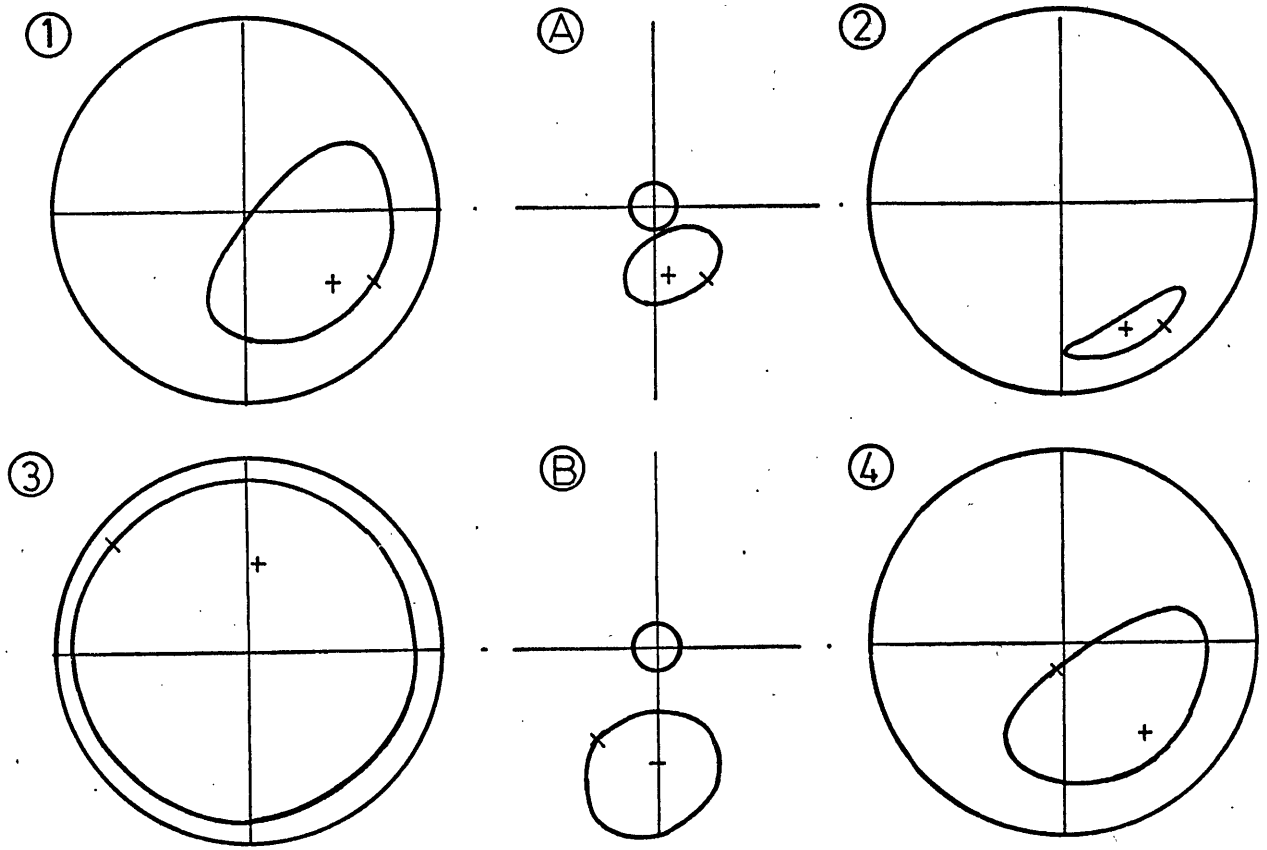


Figure 6.2: The steady-state whirl orbits for the misaligned two rotor system. Balanced shaft, $\Delta y_{b_2} = 0.2$, $(\varepsilon_o)_a = 0.62$, $S_t = 0.4$, $\gamma = 0.0$.

indefinitely whilst the journals moved in approximately circular orbits very close to and approaching the bearing surfaces. An example of a shaft exhibiting divergent whirl is shown in Figure 6.3.

The above results revealed that the behaviour of the two rotor system supported upon short circular bearings was, even for a misaligned system, essentially the same as that reported by Someya (1963-64) for a single rotor supported upon finite width axisymmetric journal bearings. That is, when the shaft is operating below twice its first pinned critical speed and the system becomes unstable, steady-state whirl orbits are obtained at a frequency of 0.5 $\omega$. But if the speed is in excess of twice the first pinned critical speed, then whirl develops at a frequency below 0.5 $\omega$, at a frequency approximately equal to the first pinned natural frequency, but steady-state motion is not obtained as the amplitude of the shaft continuously increases. This was explained by Someya, who argued that if the journal moves in a concentric circular orbit within a circular bearing at a frequency below half the rotational speed of the shaft, then the oil-film forces continuously supply energy to the vibrating shaft and external damping is necessary to dissipate this. (It may be seen from equations 6.21 and 6.22 for a short circular bearing in which the journal executes a circular orbit, that if the precession rate $\dot{\psi}$ (= $\nu_w$) < 0.5 then the tangential force $f_\psi$ is positive for all eccentricities, which for forward precession acts in the direction of motion and therefore "drives" the vibrating shaft.) It, therefore, appeared to be necessary to include a source of external damping in the rotor model in order to simulate the steady-state whirl exhibited by turbogenerators. Before considering this further, a number of interesting observations made during the above tests will be briefly discussed.

Firstly, it may be seen from the time markers on Figures 6.1 to 6.3

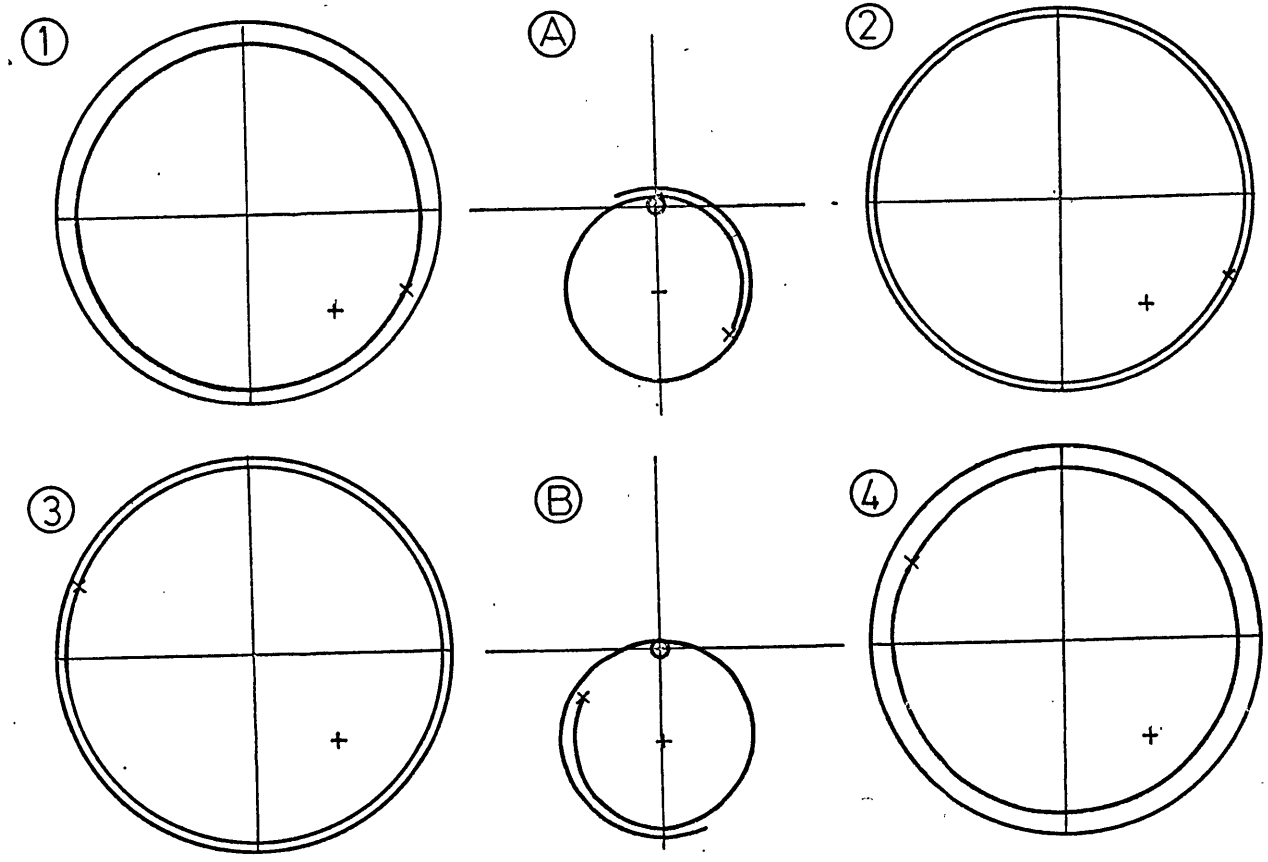


Figure 6.3: The shaft trajectories for the misaligned two rotor system. Balanced shaft, $\Delta y_{b_2} = 0.5$, $\nu_{f_3} = 0.128$, $(\varepsilon_o)_a = 0.673$, $S_t = 0.4$, $\gamma = 0.0$.

that, for both $\nu_{f_3} = 0.2$ and $\nu_{f_3} = 0.128$, the self-excited motion of the shaft assumed on anti-symmetric "mode" shape. This anti-symmetric behaviour was also observed when the system, operating above twice its first pinned critical speed, became unstable in the aligned condition when the system was nominally symmetrical about the coupling; and even when the shaft was acted upon by the uniform unbalance distribution, $Q_{\xi_1} = 0.1$, $Q_{\xi_2} = \ldots = Q_{\xi_m} = Q_{\eta_1} = \ldots = Q_{\eta_m} = 0$. (It should be added that, if for the aligned condition, the initial conditions were symmetric, then the anti-symmetric large amplitude motion took considerable time to develop as it had to grow from small asymmetries in the system due to round off errors. Therefore, a small asymmetry was added to the initial conditions for the aligned system in order to accelerate the development of the instability.)

Secondly, if the motion was such that $\varepsilon > 0.9$ in any of the bearings, then the equations of motion became *stiff*, which required very small time steps to be taken by the solution procedure, and hence increased the computational costs. Even using a method due to Gear (1971) suitable for systems of stiff equations; it became impractical to solve the equations of motion for more than a few revolutions of the shaft if $\varepsilon > 0.95$ in any of the bearings.

## 6.3 VERTICAL SHAFT MODEL

### 6.3.1 Introduction

Tondl (1965) in an analysis of a simple two bearing system, showed the need for external damping to limit the rotor amplitude and give steady-state motion. In order to gain a better understanding of the two rotor system, it was decided to extend Tondl's analysis to treat the case of a vertical shaft supported by more than two bearings, and was to be based upon the modal method. Although this analysis assumes circular motion (a reasonable assumption for a vertical shaft supported by concentric circular bore bearings), when a horizontal rotor executes large amplitude vibration, the centrifugal force acting on the rotor is much greater than the force due to gravity and the motion is approximately circular. Therefore, useful information for the horizontal shaft situation could be inferred from the computationally simpler vertical shaft system which required only the solution of a system of algebraic non-linear equations.

### 6.3.2 Transformation of the Modal Equations of Motion

From equations 2.66, 3.21 and 3.22, the equations of motion for a balanced, vertical shaft are:

$$\left.\begin{aligned} \ddot{q}_{x_i} + 2\gamma\,\dot{q}_{x_i} + \nu_{f_i}^2\, q_{x_i} &= \sum_{k=1}^{n} \left(\phi_i\, f_x\right)_{s_k} = \sum_{k=1}^{n} \left(\phi_i\,(f_e \cos\psi - f_\psi \sin\psi)\right)_{s_k} \\ \ddot{q}_{y_i} + 2\gamma\,\dot{q}_{y_i} + \nu_{f_i}^2\, q_{y_i} &= \sum_{k=1}^{n} \left(\phi_i\, f_y\right)_{s_k} = \sum_{k=1}^{n} \left(\phi_i\,(f_e \sin\psi + f_\psi \cos\psi)\right)_{s_k} \end{aligned}\right\} \quad 6.6$$

$$, \qquad (i = 1, 2, \ldots, m)$$

By defining:

$$\rho_i = q_{x_i} + \underline{i}\, q_{y_i} \tag{6.7}$$

where $\underline{i} = \sqrt{-1}$, the $2m$ equations of motion may be written as the $2m$ complex equations:

$$\ddot{\rho}_i + 2\gamma\, \dot{\rho}_i + \nu_{f_i}\, \rho_i = \sum_{k=1}^{n} \left[\phi_i\, (f_e + \underline{i}\, f_\psi)\, e^{\underline{i}\psi}\right]_{s_k} \tag{6.8}$$

It will be assumed that the $n$ bearings are concentric and therefore $x_{b_k} = y_{b_k} = 0$. (As in section 6.1.3, it is assumed, for simplicity, that the $n$ bearings are identical, and so for each bearing $c_r/C = 1$.)

Equations 6.8 are to be transformed by making the substitution:

$$\rho_i = (a_{R_i}(\tau) + \underline{i}\, a_{I_i}(\tau))\, e^{\underline{i}\nu_w \tau} \tag{6.9}$$

which, it should be noted, does not involve any assumption about the motion of the shaft. From this and from equations 2.61, 2.62, 3.11, 3.12, 3.13 and 6.7, it follows that for the $k$th bearing:

$$e^{\underline{i}\psi} = \cos\psi + \underline{i}\sin\psi = \frac{x + \underline{i}\, y}{\varepsilon} = \frac{(A_R + \underline{i}\, A_I)}{\varepsilon}\, e^{\underline{i}\nu_w \tau} \tag{6.10}$$

in which:
$$\varepsilon = \sqrt{A_R^2 + A_I^2} \tag{6.11}$$

where:
$$A_R = \sum_{i=1}^{m} a_{R_i}\, \phi_i(s_k) \tag{6.12}$$

and:
$$A_I = \sum_{i=1}^{m} a_{I_i}\, \phi_i(s_k) \tag{6.13}$$

It also follows from equations 3.14 and 3.15 that:

$$\dot{\varepsilon} = \frac{A_R \dot{A}_R + A_I \dot{A}_I}{\varepsilon} \qquad 6.14$$

and:

$$\dot{\psi} = \nu_w + \frac{A_R \dot{A}_I - A_I \dot{A}_R}{\varepsilon^2} \qquad 6.15$$

where:

$$\dot{A}_R = \sum_{i=1}^{m} \dot{a}_{R_i} \phi_i(s_k) \qquad 6.16$$

and:

$$\dot{A}_I = \sum_{i=1}^{m} \dot{a}_{I_i} \phi_i(s_k) \qquad 6.17$$

Substituting 6.9 and 6.10 into 6.8, and separating into real and imaginary parts leads to the following system of $2m$ ordinary differential equations in terms of $a_{R_i}$ and $a_{I_i}$:

$$\left.\begin{aligned} \ddot{a}_{R_i} &= -2\gamma \dot{a}_{R_i} + 2\nu_w \dot{a}_{I_i} + (\nu_w^2 - \nu_{f_i}^2) a_{R_i} + 2\gamma \nu_w a_{I_i} \\ &\quad + \sum_{k=1}^{n} \left[ \phi_i \frac{(A_R f_e - A_I f_\psi)}{\varepsilon} \right]_{s_k} = g_{R_i} \\ \ddot{a}_{I_i} &= -2\nu_w \dot{a}_{R_i} - 2\gamma \dot{a}_{I_i} - 2\gamma \nu_w a_{R_i} + (\nu_w^2 - \nu_{f_i}^2) a_{I_i} \\ &\quad + \sum_{k=1}^{n} \left[ \phi_i \frac{(A_I f_e + A_R f_\psi)}{\varepsilon} \right]_{s_k} = g_{I_i} \\ &\quad , \qquad (i = 1, 2, \ldots, m) \end{aligned}\right\} \qquad 6.18$$

### 6.3.3 The Equations for Circular Motion

It will now be assumed that, at all stations, the shaft executes circular orbits, concentric with the bearings, at a non-dimensional angular frequency, $\nu_w$. It, therefore, follows from equation 6.9 that

$a_{R_i} \neq a_{R_i}(\tau)$ and $a_{I_i} \neq a_{I_i}(\tau)$, and so equations 6.18 reduce to:

$$\left.\begin{aligned} (\nu_w^2 - \nu_{f_i}^2)\, a_{R_i} + 2\gamma\, \nu_w\, a_{I_i} + \sum_{k=1}^{n} \left[\frac{\phi_i\,(A_R\, f_e - A_I\, f_\psi)}{\varepsilon}\right]_{s_k} &= h_{R_i} = 0 \\ -2\gamma\, \nu_w\, a_{R_i} + (\nu_w^2 - \nu_{f_i}^2)\, a_{I_i} + \sum_{k=1}^{n} \left[\frac{\phi_i\,(A_I\, f_e + A_R\, f_\psi)}{\varepsilon}\right]_{s_k} &= h_{I_i} = 0 \end{aligned}\right\} \quad 6.19$$

which is a system of $2m$ non-linear algebraic equations in the $(2m+1)$ unknowns $(a_{R_1}, \ldots, a_{R_m}, a_{I_1}, \ldots, a_{I_m}, \nu_w)$. However, as equations 6.18 are autonomous, the phase of the shaft relative to a fixed datum is arbitrary, but for the purposes of finding a solution, the phase must be fixed. This may be achieved by fixing the phase of a single mode, and so for the $p$th mode set:

$$a_{I_p} = 0 \quad 6.20$$

which, hence, reduces the number of unknowns to $2m$, i.e.

$(a_{R_1}, \ldots, a_{R_m}, a_{I_1}, \ldots, a_{I_{p-1}}, \nu_w, a_{I_{p+1}}, \ldots, a_{I_m})$.

For each bearing, $\dot{\varepsilon} = 0$ and $\psi = \nu_w$ and so the oil-film forces for a short circular bearing (see section 3.2.3) are:

$$f_e = -\beta\,(0.5 - \nu_w)\,\frac{2\varepsilon^2}{(1-\varepsilon^2)^2} \quad 6.21$$

$$f_\psi = \beta\,(0.5 - \nu_w)\,\frac{\pi\,\varepsilon}{2\,(1-\varepsilon^2)^{3/2}} \quad 6.22$$

### 6.3.4 Solution Procedure

Inspection of equations 6.19 reveals that the vertical two rotor system is uniquely described by the non-dimensional parameters, $\nu_{f_3}$, $\beta$ and $\gamma$. In contrast to the horizontal system, the bearing

parameter $\beta$ (defined by equation 3.20) is used to describe the bearings instead of the equilibrium eccentricity ratio $\varepsilon_o$, as use of the latter is not meaningful for a vertical system.

Equations 6.19 were re-ordered and solved, using the Newton-Raphson method, in a similar manner to that described in section 5.3 for a static shaft. The partial derivatives $\partial h_{R_i}/\partial a_{R_j}$, $\partial h_{R_i}/\partial a_{I_j}$, $\partial h_{R_i}/\partial \nu_w$, etc., needed to form the jacobean matrix are given in Appendix 3. Because equations 6.19 are non-linear, they may, for a given set of system parameters, possess more than one solution, the one converged on by the solution procedure being determined by the initial estimate of the solution.

For the two rotor system, three types of solution were found; the shape of the shaft for each is shown diagrammatically in Figure 6.4. These solutions were obtained by using, as initial estimates, the three lowest mode shapes (suitably scaled) of the coupled rotors when supported upon simple springs of typical bearing stiffness, and with the whirl frequency initially set to a value in the range $0.3 < \nu_w < 0.5$. It should be noted that, for all three types of solution, the shaft does not lie in a single plane but "twisted" in three dimensions. Higher order solutions than the ones found may exist but these were not sought.

Two difficulties were encountered whilst attempting to find examples of each solution type. First, during the first few iterations, the solution procedure sometimes failed because the shaft was predicted to be outside one, or more, of the bearings. This problem was overcome by under-relaxing the solution procedure so that only a fraction (sometimes as low as 10%) of the predicted change was made to the solution vector at each iteration. Secondly, the solution procedure occasionally convered on the trivial solution $a_{R_1} = \ldots = a_{R_m} = a_{I_1} = \ldots = a_{I_m} = 0$, but this could usually be prevented by solving the modified system of equations:

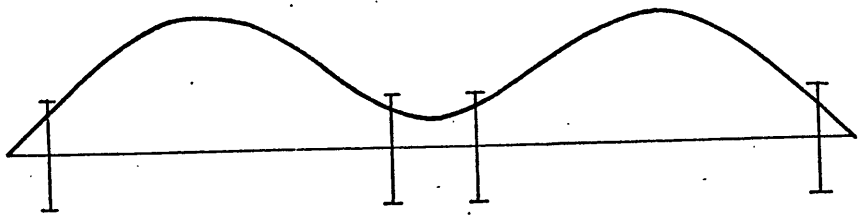

a) 1st SYMMETRIC SOLUTION

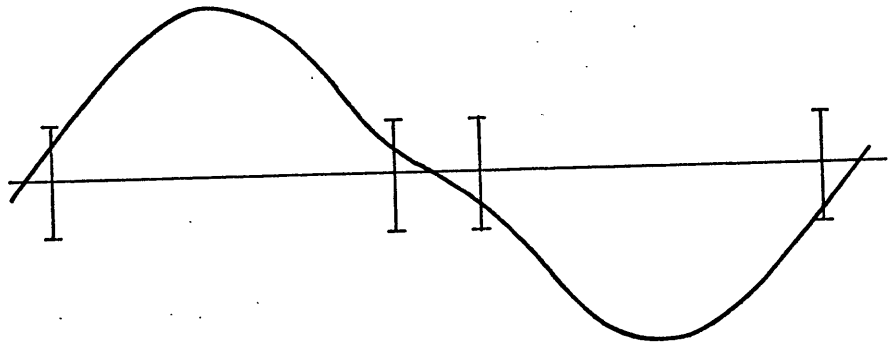

b) 1st ANTISYMMETRIC SOLUTION

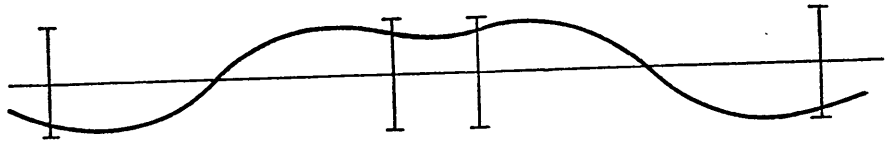

c) 2nd SYMMETRIC SOLUTION

Figure 6.4: The approximate shape of the shaft for the three types of solution found

$$\left.\begin{aligned} \overline{h}_{R_i} &= \frac{h_{R_i}}{a_{R_p}} = 0 \\ \overline{h}_{I_i} &= \frac{h_{I_i}}{a_{R_p}} = 0 \end{aligned}\right\} \quad 6.23$$

$$, \qquad (i = 1, 2, \ldots, m)$$

in which $p$ was chosen such that $a_{R_p} \neq 0$.

Once an example of a solution type had been obtained, all solutions of that type but for other values of the system parameters were obtained by changing the value of the parameters in small steps and using a known neighbouring solution as the initial estimate of the required solution.

### 6.3.5 Stability of the Circular Motion

The circular motion of the shaft is stable if the shaft, when subjected to a small disturbance sufficient to cause it to deviate slightly from its circular orbit, returns to its original orbit. During the motion resulting from such a disturbance, the modal coefficients $a_{R_i}$ and $a_{I_i}$ are not constant, and so the full equations of motion (6.18) must be considered. The stability of the orbit may be assessed by linearising equations 6.18 and evaluating the eigenvalues of the resulting linear system at a point on the orbit. For, if any of the eigenvalues have positive real parts, then the small changes to $a_{R_i}$ and $a_{I_i}$, resulting from the disturbance, grow and hence the orbit is unstable.

The procedure for linearising equations 6.18 and finding the

eigenvalues was similar to that described in section 5.4; the required partial derivatives $\partial g_{R_i}/\partial \dot{a}_{R_i}$, $\partial g_{R_i}/\partial a_{R_i}$, etc., are given in Appendix 3. It should be added that, as the phase of the shaft is arbitrary, the linearised system possesses a zero eigenvalue. Although, as a result, $a_{R_i}$ and $a_{I_i}$ may be permanently changed by a disturbance, the circular orbit, as a configuration, is unaltered and only the phase of the shaft is modified. Therefore, the zero eigenvalue was not considered when assessing the stability of the motion.

### 6.3.6 Properties of the Vertical Two Rotor System

The behaviour of the vertical two rotor system was investigated for a range of shaft stiffnesses. For this the bearing parameter $\beta = 0.05$ (which gave $(\varepsilon_o)_a = 0.673$ for the horizontal system when $S_t = 0.4$) and the external damping factor $\gamma = 0.025$. For the anti-symmetric motion, a second level of damping, $\gamma = 0.01$, was also considered. Ten modes were used in the modal expansion, i.e. $m = 10$. The effect of shaft stiffness upon the whirl frequency, the mid-span amplitude and the amplitude at the bearings is illustrated in Figures 6.5 and 6.6. Only the results for stable circular motion are shown.

It may be seen that the symmetric motion of the first type is only stable for very stiff shafts, i.e. for low values of $\omega/\omega_{p_1}$) and, as might be expected for a stiff shaft, the amplitude at the mid-span is almost the same as that at the bearings. The whirl frequency is slightly less than 0.5 $\omega$ but by not more than 0.05%. It should be noted that, because the bearing forces contain the factor $(0.5 - \nu_w)$, they would disappear if $\nu_w = 0.5$. This also explains why the amplitude at the bearings is always large when the circular motion has a frequency close to 0.5 $\omega$.

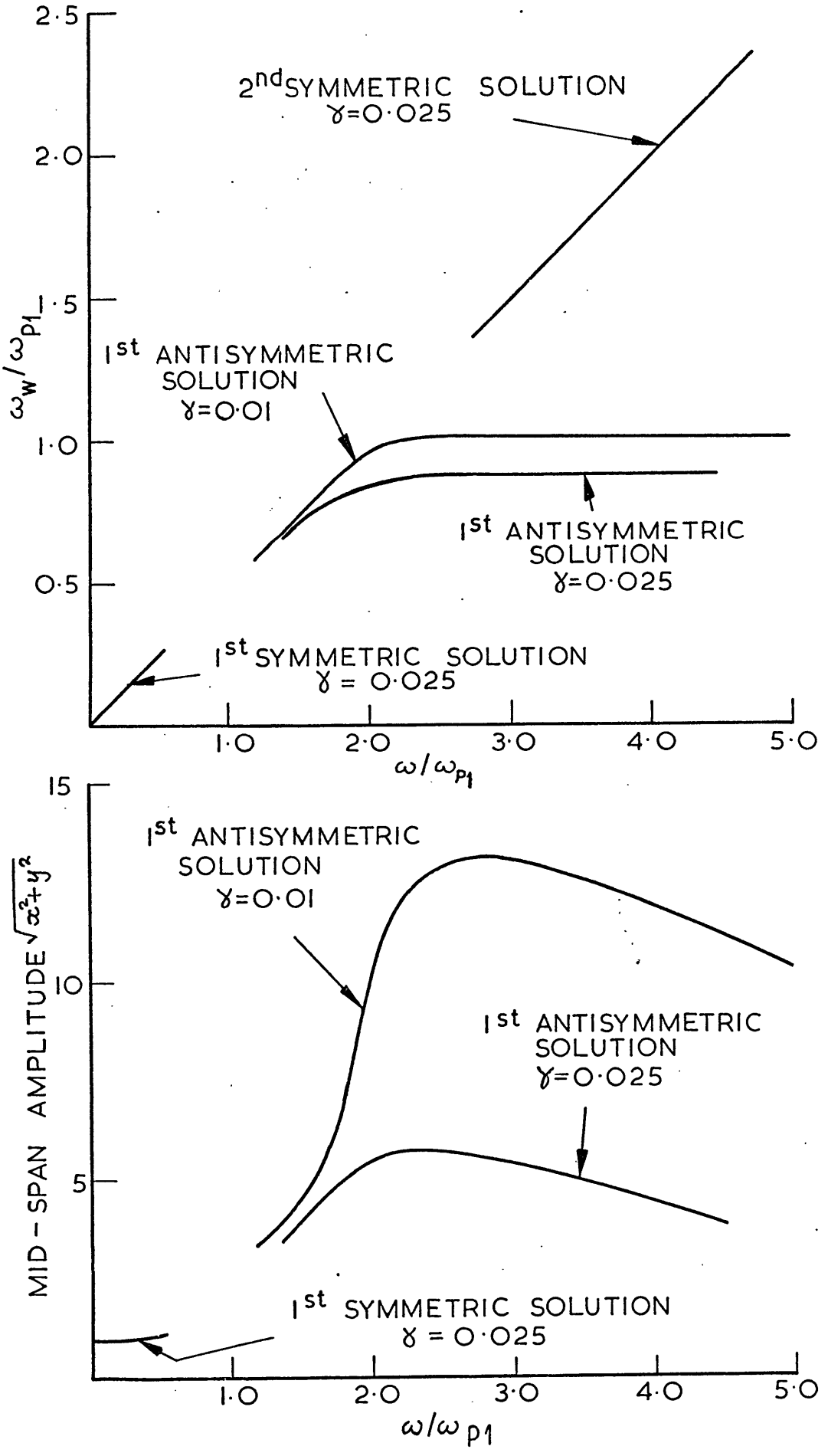


Figure 6.5: The whirl frequency and mid-span amplitude of the vertical two rotor system ($\beta$ = 0.05)

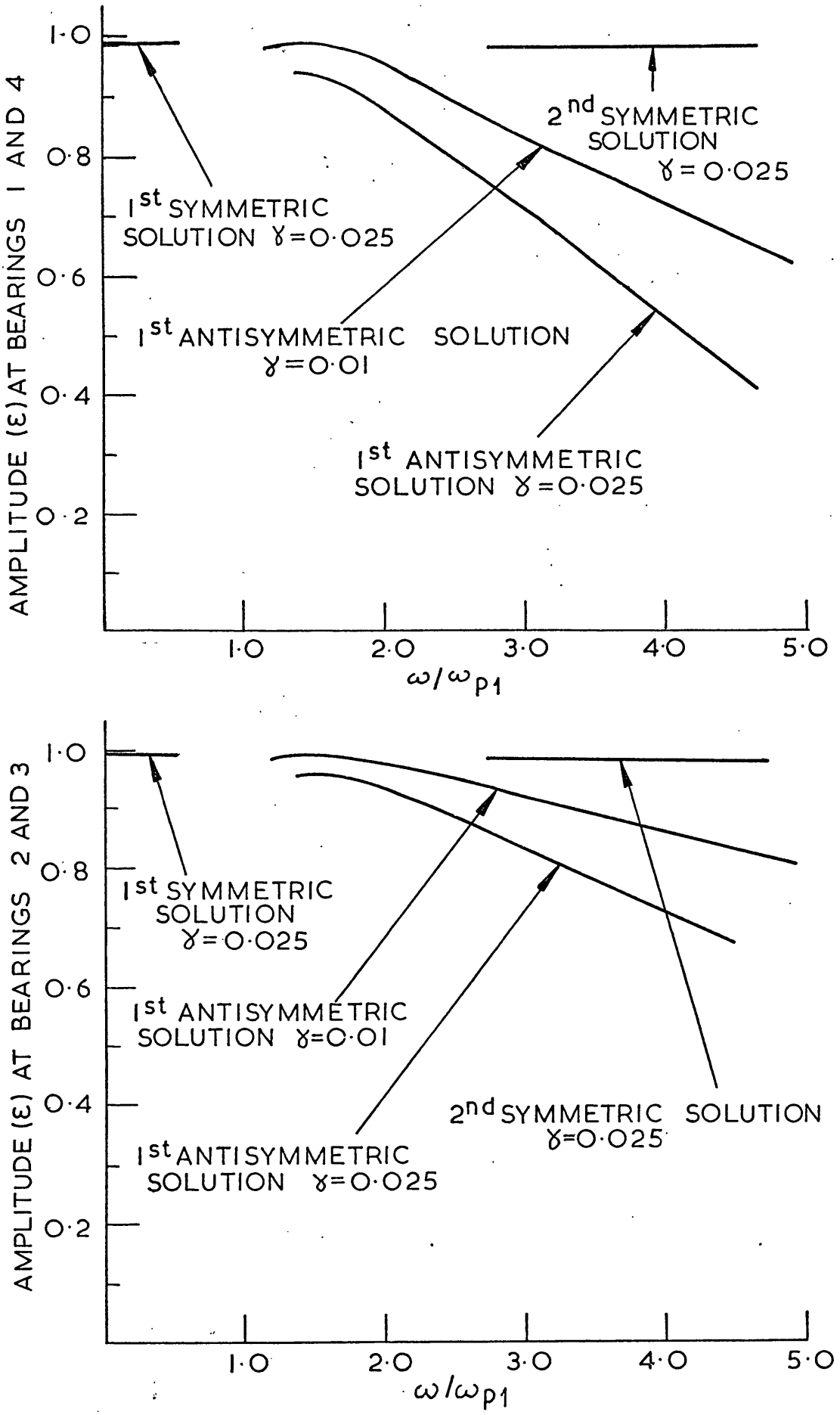


Figure 6.6: The amplitude at the bearings of the vertical two rotor system ($\beta$ = 0.05)

As the shaft stiffness is decreased, a region is reached where stable circular motion does not exist. The most likely explanation for this is that the steady-state motion of the shaft in this region contains more than one frequency component. The nature of the steady-state motion here might be investigated using numerical integration techniques but as the stable solutions on either side of this region indicated that large amplitudes could be expected at the bearings - which would cause the equations of motion to become unmanageably stiff - this was not pursued.

Decreasing the stiffness further gives stable circular motion of the anti-symmetric type. At first, the whirl frequency has a value slightly less than 0.5 $\omega$, but as the shaft stiffness is further decreased and the rotational speed exceeds twice the first pinned natural frequency, the whirl frequency reaches a constant value which, for the lower level of damping, is approximately equal to $\omega_{p_1}$ but for the higher level is approximately 10% below $\omega_{p_1}$. During this transition, the mid-span amplitude increases but just after the whirl frequency has reached a constant value, starts to decrease, as do the bearing amplitudes. These results confirm that, as with a single rotor system, the lowest pinned natural frequency is an important parameter determining the nature of the large amplitude vibration of a multi-rotor system supported upon circular bearings.

For shaft stiffnesses in the range $1.3 < \omega/\omega_{p_1} < 2.75$, the range of principal interest in the work, the only stable circular motion is of the anti-symmetric type. In order to see whether other types of steady-state motion occur in this region, the equations of motion (2.74) for the two rotor system, in which $\nu_{f_3} = 0.128$, $\beta = 0.05$ and $\gamma = 0.025$, were solved using numerical integration. Although several different sets of initial conditions were tried, only the anti-symmetric circular motion was obtained.

The anti-symmetric nature of the motion for shaft stiffnesses in this range is in agreement with the results obtained for the horizontal system.

It may be observed that, for $\omega/\omega_{p_1} > 2.75$, both the anti-symmetric motion and the symmetric motion of the second kind are stable for $\gamma = 0.025$. If it may be assumed that the behaviour of the system would be similar if the variation in $\omega/\omega_{p_1}$ was achieved by changing the shaft rotational speed (tests conducted for a number of cases showed that the variation of $\beta$ due to changes in rotational speed did not qualitatively affect the character of the solutions), then a hysteresis phenomenon could occur. For, if the speed of the shaft were increased until the anti-symmetric solution became unstable, then the shaft might assume the motion corresponding to the second symmetric solution, as this is still stable, and the frequency would increase to $\simeq 0.5\ \omega$. If the speed were then decreased, the motion would remain symmetrical until this became unstable when the shaft would probably revert to the anti-symmetric motion with an accompanying decrease in whirl frequency.

This investigation did not give a complete assessment of the properties of the vertical two rotor system - such an investigation was not relevant to the present work - but the results obtained do, if used with caution, give a valuable insight into the behaviour of multi-rotor systems supported upon circular journal bearings.

### 6.3.7 Assessing the Convergence of the Modal Series

The vertical shaft model provided a computationally economical means of assessing the convergence of the modal series (equations 2.61 to 2.64) for the large amplitude vibration of a shaft supported by journal bearings. For this, the whirl frequency, mid-span and bearing amplitudes of the two rotor system were calculated used successively 8, 10, 12, 14 and

16 free-free modes in the modal expansions. The results for a two rotor system, in which $\nu_{f_3} = 0.128$, $\beta = 0.05$ and $\gamma = 0.025$, are given in Table 6.1.

TABLE 6.1

The whirl frequency and amplitudes for a vertical two rotor system

| Number of Free-Free Modes ($m$) | Non-Dimensional Whirl Frequency ($\nu_w$) | Non-Dimensional Amplitude | | |
|---|---|---|---|---|
| | | Bearings 1 and 4 | Mid-Spans A and B | Bearings 2 and 3 |
| 8 | 0.416 | 0.865 | 5.78 | 0.926 |
| 10 | 0.407 | 0.856 | 5.70 | 0.919 |
| 12 | 0.402 | 0.851 | 5.63 | 0.915 |
| 14 | 0.401 | 0.849 | 5.62 | 0.914 |
| 16 | 0.400 | 0.848 | 5.62 | 0.913 |

It may be seen that increasing the number of modes from 8 to 16 produces small qualitative changes to the calculated values, but the essential character of the motion is unaffected. These results also support the observation made in section 5.6 that a reasonably accurate representation of the shaft for the two rotor system may be achieved using as few as eight free-free modes in the modal series.

## 6.4 HORIZONTAL TWO ROTOR SYSTEM WITH EXTERNAL DAMPING

So far, it has been shown that, in order to predict whirl at frequencies lower than 0.5 $\omega$ for the two rotor system, it is necessary for the rotational speed of the shaft to exceed twice the first pinned natural frequency - this was confirmed using the vertical shaft approximation. But because, for $\omega > 2\omega_{p_1}$, the motion of the (horizontal) shaft is approximately circular at the bearings, these continuously supply energy to the vibrating shaft and a source of dissipation is required in the model if steady-state motion is to be simulated.

Whirl in large turbogenerators commonly occurs at frequencies significantly below 0.5 $\omega$ but the amplitude does not usually become large enough for the machine to be damaged due to loss of internal clearance. Mayes (1973) reported that measurements taken from a turbine rotor of a turbogenerator exhibiting whirl at a frequency of approximately 0.4 $\omega$, revealed that the peak to peak mid-span amplitude was of the order of 3 to 4 times the radial clearance of the turbine bearings. Consideration of the internal clearances of a typical turbogenerator suggested that the maximum peak to peak amplitude in the model should not exceed ten times the radial clearance of the bearings.

The vertical shaft model was used to estimate the amount of external damping required to limit the mid-span amplitude in the two rotor system to the maximum desirable. However, for this level of damping, the equilibrium position of the shaft became so stable (external damping always increases the stability of the equilibrium position) that, except for extreme misalignment of the bearings, whirl could not be induced. Reducing the damping to a level that gave an unstable equilibrium position for reasonable misalignments resulted in steady-state circular whirl of an unacceptably large amplitude. These results suggested that the damping

should be non-linear in nature, only becoming effective during large amplitude motion. Both linear and non-linear damping have been postulated in the literature but no explanation has been given of the physical mechanisms involved.

It was suggested that the required external damping in a turbogenerator might derive from the steam forces acting upon the shaft, but operational experience on large turbogenerators does not support this theory as steady-state whirl, at frequencies below 0.5 $\omega$, has been observed for machines running with zero load, when the steam flow, and hence the forces, are small. (Using data, given by Schlichting (1968) for the drag force experienced by a cylinder moving through a viscous medium, an order of magnitude estimate was made, employing the vertical shaft approximation, of the losses due to "windage" - but these were found to be insignificant.) No other mechanism for providing external damping could be suggested and the only remaining source of dissipation in a turbogenerator were losses within the shaft.

If a rotating shaft whirls at a non-synchronous frequency, then it is subjected to cyclic stresses, and energy is absorbed from the motion due to internal friction. By calculating the maximum bending energy of the shaft, it is possible, by adopting a loss factor approach (see, for example, Lazan (1968)), to esimate the energy loss per stress cycle. The vertical shaft model was used to calculate this loss for a shaft whirling at the maximum permitted amplitude, but even assuming a high loss factor of 0.02 to account for the friction between the shaft and the discs, this mechanism accounted for less than 1% of the required dissipation.

As the level of damping required to simulate steady-state whirl at frequencies less than 0.5 $\omega$ could not be physically justified, the assumptions made for the rotor model were reconsidered. Of these, the

assumption of circular symmety for the bearings was considered to be the most unsatisfactory. Such bearings rarely occur in practice as the circular symmetry of even the nominally circular bore is destroyed by the presence of feed ports, recesses, etc.

Theoretical studies of large amplitude vibration in rotor systems have, to date, been confined to circular bearings. The argument advanced by Someya concerning the energy input to the shaft from the bearings during large amplitude motion explains why finite limit cycles at frequencies less than half shaft speed have not been predicted using classical circular symmetric bearings without recourse to external damping.

It seemed possible that the non-circular bearings invariably used in practice might give realistic limit cycles due to their asymmetry, without the application of heavy (and quite arbitrary) damping to the shaft because, at a certain level of vibration, the bearings either cease to input energy to the shaft or, alternatively, a balance is reached between the input of energy at some bearings and the extraction at others. Therefore, it was decided, in order to test this hypothesis, to develop a non-circular bearing model.

# CHAPTER 7

# DEVELOPMENT OF A LEMON-BORE BEARING MODEL

## 7.1 INTRODUCTION

As stated in Chapter 6, industrial bearings rarely possess circular symmetry. Feed ports for admitting oil to the bearing, and recesses and scallops in the bearing surface designed to reduce the frictional losses in the bearing all contribute to the detraction from circular symmetry. Besides the asymmetries due to these features, further asymmetry is often introduced into the design of a bearing in an attempt to suppress the onset of self-excited vibration. The lemon-bore ("elliptical") bearing, the three-lobe bearing and bearings with off-set halves are examples of this practice (see, for example, Pinkus & Sternlicht (1961) and Tondl (1965)). Of these, the lemon-bore bearing is the one most frequently employed industrially.

An example of a lemon-bore bearing is illustrated in Figure 7.1. In principle, these bearings are made by boring a circular hole of radius $R + C$ through the centre of the bearing whilst the two halves of the bearing are separated by shims of thickness $2d$. Without the shims, the bearing is non-circular although each half is still part of a circular arc. The *ellipticity ratio*, $d/C$, is a measure of the lack of circularity and normally has a value in the range $0.25 < d/C < 0.75$.

Because the lemon-bore bearing has a comparatively simple geometry and is frequently used in large turbogenerators, it was decided to attempt to develop a model of this configuration suitable for use in the numerical integration solution procedure.

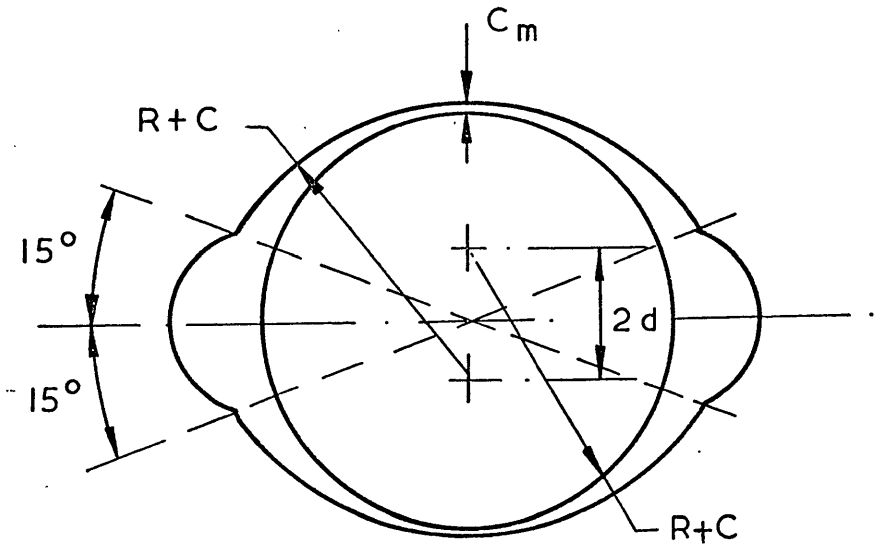


Figure 7.1: Lemon-bore bearing

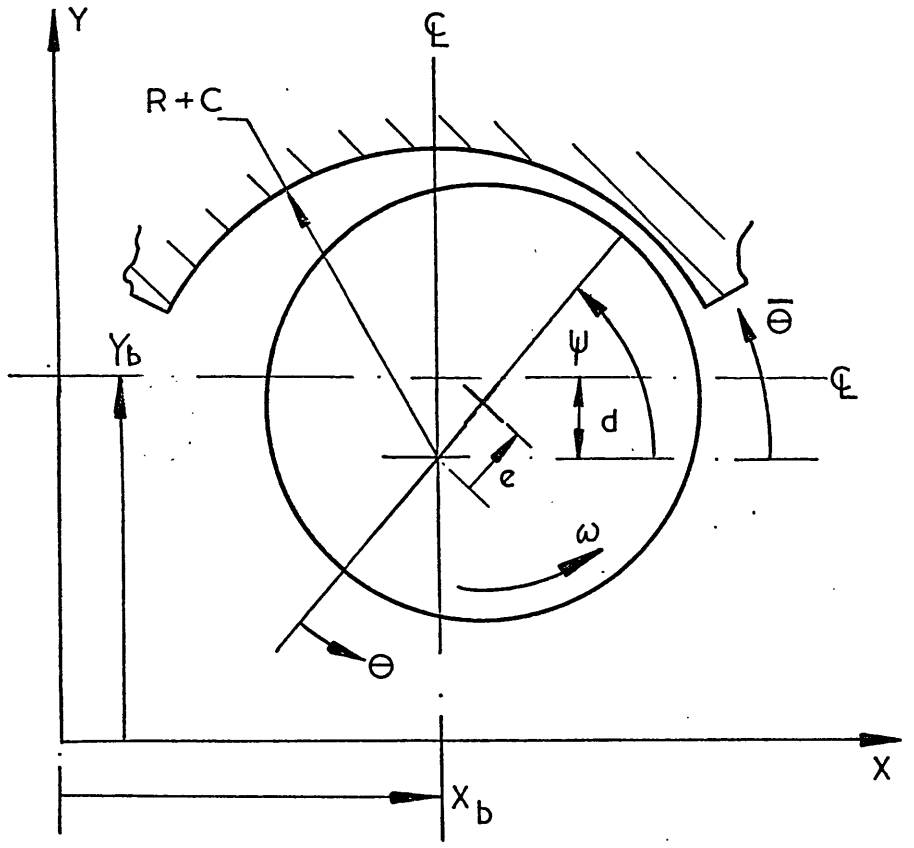


Figure 7.2: Geometry of a preset partial arc

## 7.2 THE PROPOSED MODEL

### 7.2.1 Description

The simple model of a lemon-bore bearing used by Pinkus & Sternlicht was adopted. For this, the bearing is represented by two plain, preset, partial arcs, and it is assumed that the two horizontal axial feed ports extend the entire width of the bearing. The pressure at the sides of the bearing is set to zero (i.e. ambient pressure) and the comparatively low pressure in the feed ports is simulated by setting the pressure at the ends of each arc to zero.

It will be assumed that the oil-film in the bearing cannot sustain sub-ambient pressures and that cavitation occurs. This is a valid assumption for a turbogenerator bearing, where the projected loads (i.e. $W/2BR$) carried by the bearings under static conditions are normally in the range 150 lb.in$^2$ to 250 lb.in$^2$.

Because the axial feed ports extend the entire width of the bearing, the pressure fields developed in the two arcs are independent and therefore the Reynolds equation is solved separately for each arc. The oil-film force components $f_x$ and $f_y$ generated by the bearing are the sum of the respective components generated by each arc.

As each half of the bearing is part of a circular arc, the non-dimensional form of the Reynolds equation (3.10) for a circular bore bearing is applicable if the displacement and velocity of the journal, in polar coordinates, are measured relative to the arc centre instead of the bearing centre.

### 7.2.2 Bearing Geometry

Consideration of the geometry of the "preset" partial arc, illustrated in Figure 7.2, shows that:

$$\varepsilon = \frac{c_r}{C}\sqrt{(x - x_b)^2 + (y - y_b)^2} \tag{7.1}$$

$$\cos\psi = \frac{c_r}{C}\frac{(x - x_b)}{\varepsilon} \tag{7.2}$$

$$\sin\psi = \frac{c_r}{C}\frac{(y - y_b - g_c)}{\varepsilon} \tag{7.3}$$

$$\dot{\varepsilon} = \frac{c_r}{C}(\dot{x}\cos\psi + \dot{y}\sin\psi) \tag{7.4}$$

$$\dot{\psi} = \frac{c_r}{C}\frac{(\dot{y}\cos\psi - \dot{x}\sin\psi)}{\varepsilon} \tag{7.5}$$

where, for the top arc:

$$g_c = -\frac{d}{c_r} = -\frac{C}{c_r}\frac{d}{C} \tag{7.6}$$

and, for the bottom arc:

$$g_c = \frac{d}{c_r} = \frac{C}{c_r}\frac{d}{C} \tag{7.7}$$

In addition to the circumferential coordinate $\theta$, which is measured relative to a line joining the arc and journal centres, another circumferential coordinate, $\bar{\theta}$, measured from a *fixed* axis at the arc centre (see Figure 7.2), is used to define the start and finish of the arc, $\bar{\theta}_s$ and $\bar{\theta}_f$, respectively. The two coordinates are related by:

$$\theta = \bar{\theta} - \psi + \pi \tag{7.8}$$

and so the start and finish of the arc in terms of $\theta$ may be found for a

given position of the journal. (Sometimes, as shown in Figure 7.1, the angular positions for the start and finish of the arc are defined relative to a fixed axis at the bearing centre rather than the arc centre, but as $d << R$ the difference is negligible.)

The minimum radial clearance, $c_m$, in the bearing is the vertical radial clearance given by:

$$c_m = C - d \qquad 7.9$$

Therefore, the reference clearance, $c_r$, for a system supported upon lemon-bore bearings is, in accordance with the definition given in section ~~2.3.1~~ 2.1.4 of Chapter 2, given by:

$$c_r = Min \{(c_m)_k\} \quad , \quad k = 1, \ldots, n \qquad 7.10$$

Finally, the eccentricity of the journal relative to the bearing centre will be denoted by $\bar{e}$, and will be rendered non-dimensional by dividing by the reference clearance of the system, i.e.

$$\bar{\varepsilon} = \frac{\bar{e}}{c_r} = \sqrt{(x - x_b)^2 + (y - y_b)^2} \qquad 7.11$$

### 7.2.3 The Governing Parameters of the Model

The lemon-bore bearing model is uniquely described if the six non-dimensional parameters, $\bar{\theta}_s$, $\bar{\theta}_f$, $C/c_r$, $d/C$, $\alpha$ and $\beta$, are defined for each arc. Normally, all (except $\bar{\theta}_s$ and $\bar{\theta}_f$) have the same value for both the top and the bottom arc.

### 7.2.4 A Criterion for Choosing a Method of Solution for the Reynolds Equation

As stated in section 3.1 of Chapter 3, a closed form solution to the Reynolds equation does not exist for any journal bearing configuration of finite width; and the short bearing approximation used previously is only applicable to bearings possessing circular symmetry. A suitable method for solving the Reynolds equation for the partial arcs of the lemon-bore bearing model was therefore required.

The computational time required to solve the equations of motion for the shaft (2.74) by numerical integration is, principally, governed by the time required to evaluate the oil-film forces $f_x$ and $f_y$. Experience gained using the short circular bearing model indicated that if the solution procedure employing the non-circular bearing model was not to take more than 2-3 times longer than it had using the short circular bearing model* - this being the maximum increase in computational time considered acceptable - then the time required to evaluate the oil-film forces should not increase by more than a factor of ten.

---

* To solve the equations of motion for the two rotor system supported upon short circular bearing, for 64 revolutions of the shaft during steady-state motion (during which the eccentricity ratio $\varepsilon$ had not exceeded 0.9 in any of the bearings) had, typically, required 200 seconds of central processor time using a CDC 6600 computer.

## 7.3 FINITE DIFFERENCE SOLUTIONS

### 7.3.1 Two-Dimensional Finite Difference Solution

A two-dimensional finite difference scheme was developed to solve the Reynolds equation for each partial arc of the lemon-bore bearing. For this, it was computationally simpler to solve the cartesian coordinate form of the Reynolds equation:

$$\frac{\partial}{\partial \bar{\theta}} \left(h^{*3} \frac{\partial P^*}{\partial \bar{\theta}}\right) + \alpha^2 h^{*3} \frac{\partial^2 P^*}{\partial z^{*2}}$$

$$= \frac{c_r}{C} \{0.5 (x - x_b) - \dot{y}\} \sin \bar{\theta} - \frac{c_r}{C} \{0.5 (y - y_b - g_c) + \dot{x}\} \cos \bar{\theta} \qquad 7.12$$

in which the non-dimensional film thickness, $h^*$, is given by:

$$h^* = \frac{h}{C} = 1 - \frac{c_r}{C} \{(x - x_b) \cos \bar{\theta} + (y - y_b - g_c) \sin \bar{\theta}\} \qquad 7.13$$

and where $\bar{\theta}$ is the non-rotating coordinate shown in Figure 7.2. The Reynolds equation in cartesian coordinate form was derived from first principles by Kirk & Gunter (1976). But equation 7.12 may alternatively be derived from the polar coordinate form (3.10) by first substituting for $\theta$ from equation 7.8 and then converting the velocity and displacement of the journal from polar coordinates to cartesian coordinates using equations 7.2 to 7.5. For the non-rotating coordinate system $\bar{\theta}$, the non-dimensional oil-film forces *for each arc* are given by:

$$f_x = -\frac{3}{2} \alpha^2 \beta \left(\frac{c_r}{C}\right)^2 \int_{-1}^{1} \int_{\bar{\theta}_1}^{\bar{\theta}_2} P^* \cos \bar{\theta} \, d\bar{\theta} \, dz^* \qquad 7.14$$

$$f_y = -\frac{3}{2} \alpha^2 \beta \left(\frac{c_r}{C}\right)^2 \int_{-1}^{1} \int_{\bar{\theta}_1}^{\bar{\theta}_2} P^* \sin \bar{\theta} \, d\bar{\theta} \, dz^* \qquad 7.15$$

A uniform, rectangular grid (of mesh size $\Delta\bar{\theta} \times \Delta z^*$) was superimposed on the surface of each arc and, after expanding the first term of equation 7.12, the pressure derivatives were replaced by the finite difference approximations:

$$\frac{\partial P^*}{\partial \bar{\theta}} \simeq \frac{P^*(\bar{\theta} + \Delta\bar{\theta}, z^*) - P^*(\bar{\theta} - \Delta\bar{\theta}, z^*)}{2\Delta\bar{\theta}} \qquad 7.16$$

$$\frac{\partial^2 P^*}{\partial \bar{\theta}^2} \simeq \frac{P^*(\bar{\theta} + \Delta\bar{\theta}, z^*) - 2P^*(\bar{\theta}, z^*) + P^*(\bar{\theta} - \Delta\bar{\theta}, z^*)}{(\Delta\bar{\theta})^2} \qquad 7.17$$

$$\frac{\partial^2 P^*}{\partial z^{*2}} \simeq \frac{P^*(\bar{\theta}, z^* + \Delta z^*) - 2P^*(\bar{\theta}, z^*) - P^*(\bar{\theta}, z^* - \Delta z^*)}{(\Delta z^*)^2} \qquad 7.18$$

The resulting system of algebraic non-linear equations was solved iteratively.

Cavitation was allowed for by setting all negative pressures to zero as they were generated. This gives the boundary condition:

$$P^* = \frac{\partial P^*}{\partial \zeta} = 0 \qquad 7.19$$

at the cavitation boundary of the oil-film, where $\zeta$ is a coordinate in the $\bar{\theta}, z^*$ surface, normal to the cavitation boundary.

By exploiting the symmetry of the pressure field about the mid-axial plane, it was possible (by making the mid-axial plane into a boundary having floating boundary conditions) to reduce the number of finite difference equations to be solved by almost one half.

Successive over-relaxation was employed to accelerate the rate of convergence of the iteration process. For the first twenty iterative sweeps, the relaxation-factor was set to a value that was assumed to be less than the maximum. During this time, an estimate was made of the

optimum relaxation-factor which was then used until convergence was achieved. Details of this method are given by Holmes & Ettles (1975).

Once the pressure field had been found, the oil-film forces were obtained by numerical quadrature.

To test the finite-difference scheme, the equilibrium characteristics of a centrally-loaded partial arc were calculated using a grid of $\Delta\bar{\theta} = (\bar{\theta}_f - \bar{\theta}_s)/40$ and $\Delta z^* = 1/10$. For a given value of the journal equilibrium eccentricity ratio ($\varepsilon_o$), the attitude angle ($\psi$) was adjusted until the horizontal force generated by the bearing was zero; the vertical oil-film force was then equal and opposite to the applied load. The results obtained were in agreement with those given by Pinkus & Sternlicht (1961).

An estimate of the time required to evaluate the oil-film forces for the lemon-bore bearing under dynamic conditions was determined by imposing the circular orbit:

$$\begin{aligned} x - x_b &= 0.7 \cos(0.45\,\tau) \\ y - y_b &= 0.7 \sin(0.45\,\tau) \end{aligned} \qquad 7.20$$

upon the journal of the lemon-bore bearing shown in Figure 7.1 (for which $C/c_r = 1.9$, $d/C = 0.474$, and $\alpha = 1.333$), and evaluating the oil-film forces at five degree intervals around the orbit. For each point on the orbit, the pressure field obtained for the previous oil-film force calculation was used as an initial estimate of the solution to the finite difference equations. The average computational time required to calculate the oil-film forces for two different grid sizes is given in Table 7.1 as a multiple of the time required using the short circular bearing approximation. Clearly, the two-dimensional finite difference

method was unsuitable for use in the numerical integration procedure for the multi-rotor system, even if a comparatively coarse grid was employed.

TABLE 7.1

The comparative computational time required to evaluate the oil-film forces for the lemon-bore bearing using different methods of solution

| Method of Solution | | Time |
|---|---|---|
| (Short circular bearing approximation | | 1.0) |
| Two-dimensional finite difference solution | $\Delta\bar{\theta} = (\bar{\theta}_f - \bar{\theta}_s)/40$ <br> $\Delta z^* = 1/10$ | 7000 |
| | $\Delta\bar{\theta} = (\bar{\theta}_f - \bar{\theta}_s)/20$ <br> $\Delta z^* = 1/4$ | 590 |
| One-dimensional finite difference solution | $\Delta\bar{\theta} = (\bar{\theta}_f - \bar{\theta}_s)/40$ | 380 |
| | $\Delta\bar{\theta} = (\bar{\theta}_f - \bar{\theta}_s)/20$ | 85 |
| Long bearing approximation with side leakage factor obtained using the method of Galerkin | $(\theta_2 - \theta_1)/50$ | 66 |
| | $(\theta_2 - \theta_1)/24$ | 37 |
| Long bearing approximation with side leakage factor obtained using the method of collocation | | 8.4 |

### 7.3.2 One-Dimensional Finite Difference Solution

It may be seen from equation 3.25 that the infinitely narrow bearing has a parabolic pressure profile in the axial direction. A method, first proposed by Frankel (1949), of obtaining a simplified form of the Reynolds equation is to assume that the axial pressure profile in a finite width bearing is also parabolic, i.e. assume:

$$P^* = P_c(\theta)\ (1 - z^{*2}) = \frac{3}{2} P_a(\theta)\ (1 - z^{*2}) \qquad 7.21$$

where $P_c$ and $P_a$ are the non-dimensional centre-line and mean axial pressures, respectively. By substituting the parabolic pressure distribution into equation 3.10, the following one-dimensional form of the Reynolds equation is obtained:

$$\frac{d}{d\theta}\left(h^{*3} \frac{d\overline{P}}{d\theta}\right) - \overline{\gamma}\ \alpha^2\ h^{*3}\ \overline{P} = -\varepsilon\ (0.5 - \dot{\psi})\ \sin\theta + \dot{\varepsilon}\ \cos\theta \qquad 7.22$$

in which: $\overline{\gamma} = 2$ , if $\overline{P} = P_c$

or: $\overline{\gamma} = 3$ , if $\overline{P} = P_a$

Equation 7.22 cannot be integrated directly and so it was converted into cartesian coordinate form and solved using finite difference techniques.

An estimate was made of the computational time required to evaluate the oil-film forces for a lemon-bore bearing under dynamic conditions, using the procedure described in the previous section. The required times for two interval sizes ($\Delta\overline{\theta}$) are given in Table 7.1 as a multiple of the time required by the short circular bearing approximation.

Again, the method of obtaining the oil-film forces did not satisfy the criterion set in section 7.2.4.

## 7.4 SOLUTIONS BASED UPON THE LONG BEARING APPROXIMATION

### 7.4.1 Introduction

As the fastest finite difference method of obtaining the oil-film forces for the lemon-bore bearing was in excess of fifty times slower than the short circular bearing model - and therefore impractical for use in the propagation programme - recourse was made to the long bearing approximation. Although this approximation is somewhat unrealistic for normal turbine bearings, it has the advantage of providing an analytical solution for a partial arc bearing and thus enables the oil-film forces for the lemon-bore bearing to be calculated rapidly.

By using the long bearing approximation, it was hoped to verify the hypothesis that a non-circular bearing model would give finite limit cycles at frequencies below 0.5 $\omega$. Later, if this was successful, a correction factor for the long bearing approximation would be sought to take account of the finite width of realistic bearings.

But first, the long bearing solution for a partial arc bearing will be considered.

### 7.4.2 The Long Bearing Approximation

#### 7.4.2.1 The basic equations

For an infinitely long bearing, the axial pressure gradient is zero and so the Reynolds equation (3.10) reduces to:

$$\frac{d}{d\theta}\left(h^{*3}\frac{dP_l}{d\theta}\right) = -A_\varepsilon \sin\theta + B_\varepsilon \cos\theta \qquad 7.23$$

where, for notational convenience:

$$A_\varepsilon = \varepsilon\,(0.5 - \dot{\psi}) \qquad 7.24$$

$$B_\varepsilon = \dot{\varepsilon} \qquad 7.25$$

and $P_l$ (= $P^*$) is used to indicate that the non-dimesional pressure distribution corresponds to the long bearing approximation. The right hand side of equation 7.23 may alternatively be written as:

$$\frac{d}{d\theta}\left(h^{*3}\frac{dP_l}{d\theta}\right) = -\sqrt{A_\varepsilon^2 + B_\varepsilon^2}\,\sin(\theta + \alpha_\varepsilon) = W_\varepsilon(\theta) \qquad 7.26$$

where: $$\alpha_\varepsilon = \tan^{-1}(B_\varepsilon/A_\varepsilon) \qquad 7.27$$

Equation 7.23 may be integrated once to give:

$$h^{*3}\frac{dP_l}{d\theta} = A_\varepsilon \cos\theta + B_\varepsilon \sin\theta + C_\varepsilon \qquad 7.28$$

and a second time to give:

$$P_l(\theta) - P_l(\theta_1) = \int_{\theta_1}^{\theta} \frac{A_\varepsilon \cos\theta + B_\varepsilon \sin\theta + C_\varepsilon}{h^{*3}}\,d\theta \qquad 7.29$$

where $C_\varepsilon$ and $P_l(\theta_1)$ are constants of integration determined from the boundary conditions for the oil-film. Equation 7.28 may alternatively be written as:

$$h^{*3}\frac{dP_l}{d\theta} = \sqrt{A_\varepsilon^2 + B_\varepsilon^2}\,\cos(\theta + \alpha_\varepsilon) + C_\varepsilon = V_\varepsilon(\theta) + C_\varepsilon \qquad 7.30$$

7.4.2.2 Non-cavitating oil-film

If the boundary conditions:

$$\left.\begin{aligned} P(\theta_s) &= 0 \\ P(\theta_f) &= 0 \end{aligned}\right\} \qquad 7.31$$

are used for the oil-film, where $\theta_s$ and $\theta_f$ are, respectively, the start and finish of the arc in terms of the $\theta$ coordinate, then equation 7.29 becomes:

$$P_l(\theta) = A_\varepsilon \int_{\theta_s}^{\theta} \frac{\cos\theta}{h^{*3}}\,d\theta + B_\varepsilon \int_{\theta_s}^{\theta} \frac{\sin\theta}{h^{*3}} + C_\varepsilon \int_{\theta_s}^{\theta} \frac{d\theta}{h^{*3}} \qquad 7.32$$

with:

$$C_\varepsilon = \frac{-A_\varepsilon \int_{\theta_s}^{\theta_f} \frac{\cos\theta}{h^{*3}}\,d\theta - B_\varepsilon \int_{\theta_s}^{\theta_f} \frac{\sin\theta}{h^{*3}}\,d\theta}{\int_{\theta_s}^{\theta_f} \frac{d\theta}{h^{*3}}} \qquad 7.33$$

Equation 7.32* gives the four types of pressure distribution shown in Figures 7.3a, 7.3b, 7.3c and 7.3d, the type obtained being determined by the displacement and velocity of the journal relative to the arc, i.e. upon the values of $\varepsilon$, $\dot{\varepsilon}$, $\psi$ and $\dot{\psi}$. As regions of sub-ambient pressure are predicted, and it is assumed that the oil-film cannot sustain sub-ambient pressures, then clearly the boundary conditions 7.31 must be modified, for the solution types giving sub-ambient pressure, in order to allow for cavitation.

---

* The integrals in equation 7.32 may be evaluated with the aid of Booker's (1965) table of journal bearing integrals.

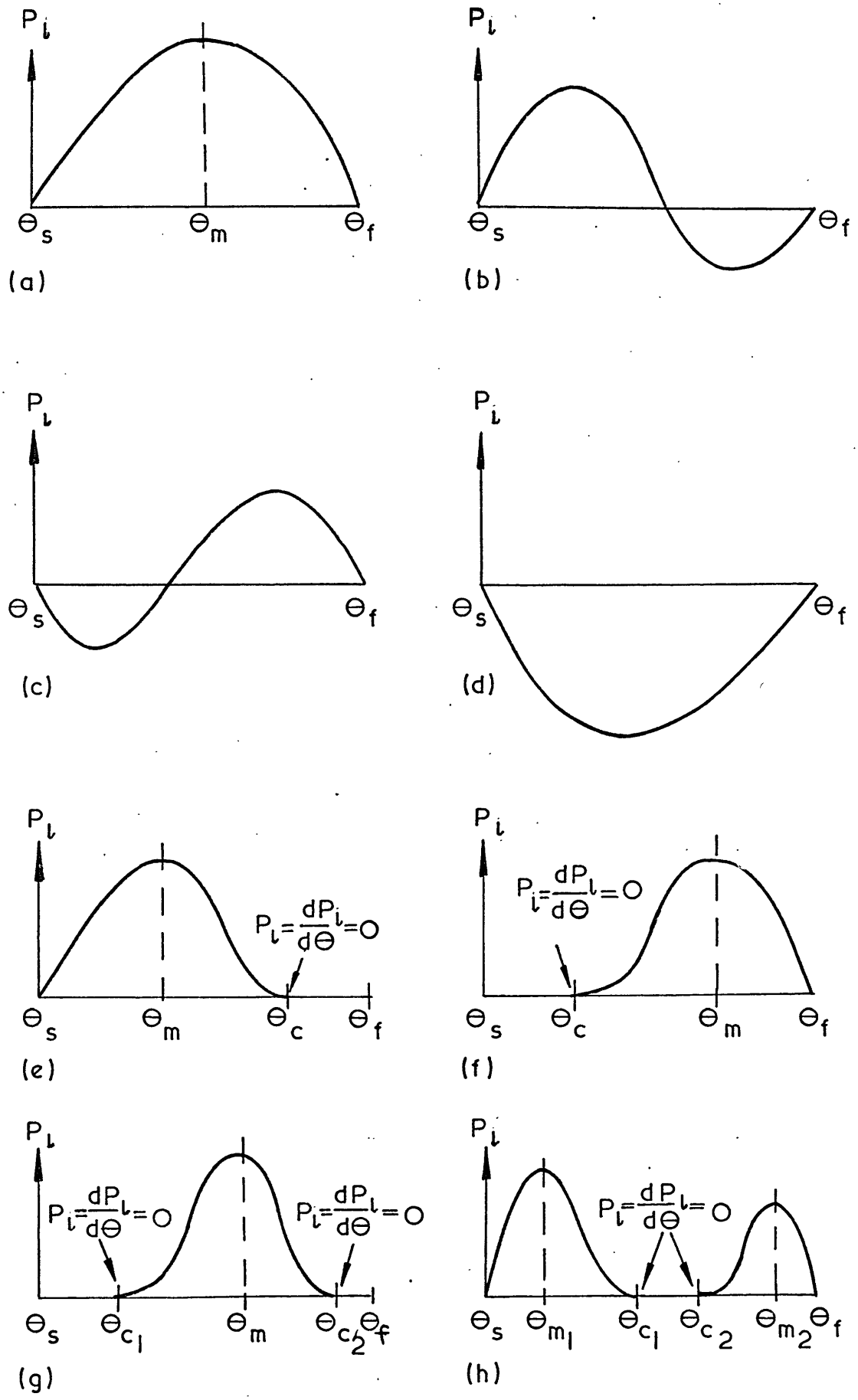


Figure 7.3: Pressure distributions for an infinitely long partial arc bearing

7.4.2.3 Allowance for cavitation

In a region where the oil-film cavitates, the pressure is uniformly zero (i.e. at ambient pressure) and hence the pressure gradient, $dP_l/d\theta$, is uniformly zero. The Reynolds equation is not applicable to this region and so the boundary conditions for the Reynolds equation for the uncavitated region must be applied at the cavitation boundaries. The appropriate boundary conditions for the cavitation boundaries are deduced by considering the oil flow in the bearing.

For the uncavitated region of an infinitely long bearing, the oil flow in the axial direction is zero and the flow rate ($q_\theta$) in the circumferential direction is, if terms of order ($C/R$) are neglected*, given by:

$$q_\theta = R\,C\,\omega\,\left(\frac{h^*}{2} - h^{*3}\,\frac{dP_l}{d\theta}\right) \qquad 7.34$$

Now, as the oil may only enter or leave the arc through the two feed ports situated at $\theta_s$ and $\theta_f$, the oil flow rate through the uncavitated region must be continuous, and therefore, as $h^*$ is continuous and non zero, the pressure gradient $dP_l/d\theta$ must be continuous. (It should be added that the non-dimensional film thickness $h^*$ may only have a value in the range $0 < h^* < 1$.) Physical considerations also require the flow rate across the cavitation boundary to be continuous. Therefore, in order for both the pressure and the flow rate to be continuous across the cavitation boundary, the condition:

---

* It should be noted that terms of order ($C/R$) are neglected in the derivation of the Reynolds equation.

$$P_l(\theta_c) = \left.\frac{dP_l}{d\theta}\right|_{\theta_c} = 0 \qquad 7.35$$

must be satisfied at the point ($\theta_c$) where the oil-film cavitates. This boundary condition is well known (see, for example, Pinkus & Sternlicht (1961)), and is the condition that would be obtained at the point of cavitation, if equation 7.23 was solved using finite difference techniques and all negative pressures were set to zero as they were generated by the iteration procedure.

7.4.2.4 Types of pressure profile occurring for a cavitating oil-film

If an oil-film cannot sustain sub-ambient pressures, then it may, depending upon the velocity and displacement of the journal relative to the arc, be either: uncavitated, in which case it has a pressure distribution of the type shown in Figure 7.3a; completely cavitated, when the pressure is zero over the entire arc; or partially cavitated. For the partially cavitated condition, the pressure distributions of the type shown in Figures 7.3e, 7.3f, 7.3g and 7.3h may be postulated for a partial arc bearing. It will now be shown that the pressure distributions of the type shown in Figures 7.3g and 7.3h cannot occur for an infinitely long partial arc bearing for which $(\theta_f - \theta_s) < 180^0$.

Consider first the pressure distributions shown in Figure 7.3g. This pressure distribution requires the pressure gradient $dP_l/d\theta$ to be zero at the first point of cavitation, $\theta_{c_1}$, the point of maximum pressure, $\theta_m$, and at the second point of cavitation, $\theta_{c_2}$. It may be seen from equation 7.30 that the pressure gradient may not be zero more

than twice in a range of $180^0$. Therefore, this pressure distribution cannot occur if $(\theta_f - \theta_s) < 180^0$.

The pressure distribution shown in Figure 7.3h will now be considered with the aid of Figure 7.4. In Figure 7.4, the point of maximum pressure, $\theta_{m_1}$, and the point of cavitation, $\theta_{c_1}$, for the first uncavitated region are, from equation 7.30, given by the intersection of the horizontal line $a_1b_1$ and the cosine curve $V_\varepsilon(\theta)$. The vertical displacement of the line $a_1b_1$ is governed by the constant of integration, $C_{\varepsilon_1}$, but as $(\theta_{c_1} - \theta_{m_1}) < 180^0$ (which must be the case if $(\theta_f - \theta_s) < 180^0$) and the pressure gradient between $\theta_{m_1}$ and $\theta_{c_1}$ is negative, the line $a_1b_1$ must lie below the $\theta$ axis and be bisected by the normal $(m_1n_1)$ to the local minimum of the curve $V_\varepsilon(\theta)$. For the second uncavitated region, the point of cavitation, $\theta_{c_2}$, and the point of maximum pressure, $\theta_{m_2}$, are given by the intersection of the horizontal line $a_2b_2$ and the curve $V_\varepsilon(\theta)$. A similar argument to the one given above may be used to show that the line $a_2b_2$ must be above the $\theta$ axis and be bisected by the normal $(m_2n_2)$ to the local maximum of the curve $V_\varepsilon(\theta)$. It may thus be seen that $(\theta_{m_2} - \theta_{m_1}) > 180^0$, but as $\theta_s < \theta_{m_1}$ and $\theta_f > \theta_{m_2}$, this type of solution cannot occur if $(\theta_f - \theta_s) < 180^0$.

#### 7.4.2.5 Determination of the type of pressure profile occurring

Having established the four types of pressure profile that may occur for each partial arc of the lemon-bore bearing model, a procedure will now be given for determining the type of profile that occurs for a given displacement and velocity of the journal. First, the pressure gradient at the ends of the arc, $\theta_s$ and $\theta_f$, are calculated for a non-cavitation oil-film using equations 7.28 and 7.33. The type of

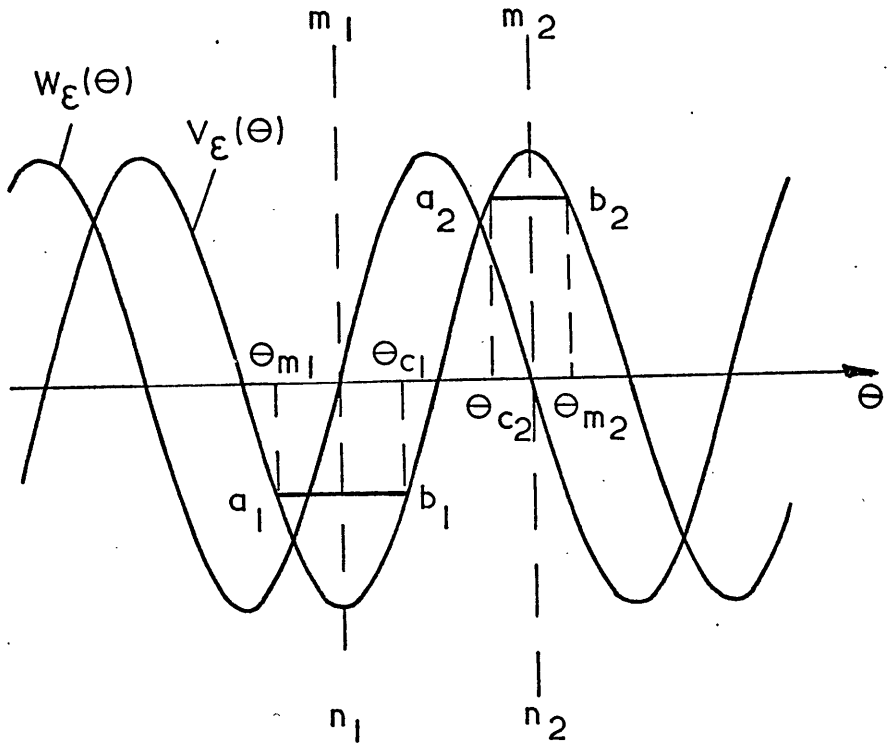


Figure 7.4: The functions $W_\varepsilon(\theta)$ and $V_\varepsilon(\theta)$

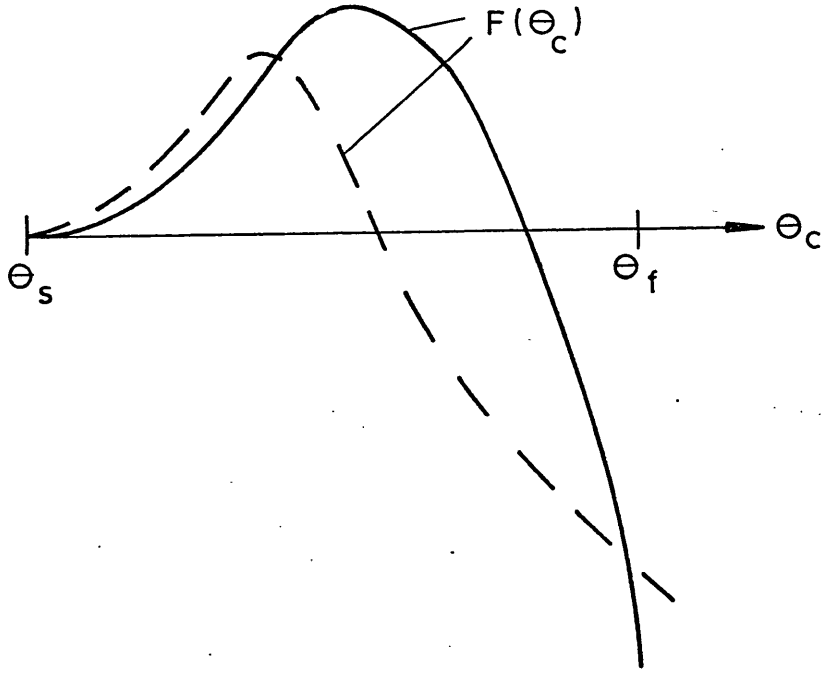


Figure 7.5: The function $F(\theta_c)$

pressure profile obtained for a cavitating oil-film is then determined as follows:

(a) If $dP_l/d\theta|_{\theta_s} > 0$ and $dP_l/d\theta|_{\theta_f} < 0$, the pressure profile is of the type shown in Figure 7.3a and cavitation will not occur.

(b) If $dP_l/d\theta|_{\theta_s} > 0$ and $dP_l/d\theta|_{\theta_f} > 0$, the non-cavitating pressure profile is of the type shown in Figure 7.3b. If cavitation occurs, a partially cavitated pressure profile of the type shown in Figure 7.3e develops.

(c) If $dP_l/d\theta|_{\theta_s} < 0$ and $dP_l/d\theta|_{\theta_f} < 0$, the non-cavitating pressure profile is of the type shown in Figure 7.3c. If cavitation occurs, a partially cavitated pressure profile of the type shown in Figure 7.3f develops.

(d) If $dP_l/d\theta|_{\theta_s} < 0$ and $dP_l/d\theta|_{\theta_f} > 0$, the non-cavitating pressure profile is of the type shown in Figure 7.3d. If cavitation occurs, the oil-film may either completely cavitate or partially cavitate. This is explained as follows.

The term $W_\varepsilon(\theta)$ on the right hand side of equation 7.26 is analogous to the wedge term $(dh/d\theta)$ for a statically loaded bearing. If $W_\varepsilon(\theta)$ is positive for the entire arc (and this is possible since $(\theta_f - \theta_s) < 180^0$), then the oil-film experiences a divergent "wedge" at all points on the arc and only sub-ambient pressures are generated for a non-cavitating oil-film. If, however, for this situation, the oil-film

cavitates, then the completely cavitated condition results. This may be verified from Figure 7.4 where $W_\varepsilon(\theta)$ and $V_\varepsilon(\theta)$ are plotted on the same axis. For, if $W_\varepsilon(\theta_s)$ and $W_\varepsilon(\theta_f)$ are both positive, then the pressure gradient cannot be zero at more than one point on the arc, and hence a partially cavitated condition cannot occur.

A fully sub-ambient pressure profile may also arise for a non-cavitating oil-film when $W_\varepsilon(\theta)$ is positive for most, but not all, of the arc. For this situation, the divergent "wedge" is predominant, but if the oil-film cavitates, then the influence of the divergent "wedge" is nullified, and so the small section of convergent "wedge" is able to generate a region of positive pressure at the end of the arc where $W_\varepsilon(\theta)$ is negative. This may be verified from Figure 7.4 where it may be seen that if $W_\varepsilon(\theta)$ changes sign at a point on the arc, then the pressure gradient may be zero at two points on the arc and so the partially cavitated condition can develop.

The above reasoning may be summarised as follows:

i) If $W_\varepsilon(\theta_s) > W_a$ and $W_\varepsilon(\theta_f) > W_a$, the oil-film completely cavitates.

ii) If $W_\varepsilon(\theta_s) > W_a$ and $W_\varepsilon(\theta_f) < W_a$, the partially cavitated condition of the type shown in Figure 7.3e occurs.

iii) If $W_\varepsilon(\theta_s) < W_a$ and $W_\varepsilon(\theta_f) > W_a$, the partially cavitated condition of the type shown in Figure 7.3f occurs.

iv) If $W_\varepsilon(\theta_s) < W_a$ and $W_\varepsilon(\theta_f) < W_a$, the oil-film does not cavitate. This situation would not occur, since an uncavitated oil-film would have been detected above by (a), and is only given here for completeness.

Where, for computational purposes, $W_a$ had a value slightly less than zero, because it was found that if, for example in (ii), $W_\varepsilon(\theta_s)$ had a value in the range $W_a < W_\varepsilon(\theta_s) < 0$, then the small region of positive pressure generated made an insignificant contribution to the oil-film forces. When calculating the oil-film forces for the numerical integration solution procedure, $W_a$ = -0.01, but for calculating the linearised bearing coefficients by numerical differencing, this increased to $W_a$ = -0.001.

7.4.2.6 Determination of the point of cavitation

If one of the partially cavitated pressure profiles is known to occur, then it is necessary to find the point, $\theta_c$, at which the oil-film cavitates. For the partially cavitated pressure profile of the type shown in Figure 7.3e, the boundary conditions are:

$$P_l(\theta_s) = 0 \qquad 7.36a$$

$$P_l(\theta_c) = 0 \qquad 7.36b$$

$$\left.\frac{dP_l}{d\theta}\right|_{\theta_c} = 0 \qquad 7.36c$$

(Although it may appear that we have three boundary conditions for a second order equation (7.29), it should be remembered that $\theta_c$ is unknown, and this effectively reduces 7.36b and 7.36c to a single condition.)

By using condition 7.36a, equation 7.29 becomes:

$$P_l(\theta) = \int_{\theta_s}^{\theta} \frac{A_\varepsilon \cos\theta + B_\varepsilon \sin\theta + C_\varepsilon}{h^{*3}} d\theta \qquad 7.37$$

and, from equation 7.28, condition 7.36c gives:

$$C_\varepsilon = -A_\varepsilon \cos\theta_c - B_\varepsilon \sin\theta_c \qquad 7.38$$

By requiring the pressure to be zero at $\theta_c$ (i.e. condition 7.36b), equation 7.37 together with equation 7.38 reduce to a single equation in terms of one unknown, $\theta_c$, i.e.

$$F(\theta_c) = \int_{\theta_s}^{\theta_c} \frac{A_\varepsilon (\cos\theta - \cos\theta_c) + B_\varepsilon (\sin\theta - \sin\theta_c)}{h^{*3}} d\theta = 0 \qquad 7.39$$

The derivative of the function $F(\theta_c)$ is given by:

$$F'(\theta_c) = \frac{dF}{d\theta_c} = (A_\varepsilon \sin\theta_c - B_\varepsilon \cos\theta_c) \int_{\theta_s}^{\theta_c} \frac{d\theta}{h^{*3}} \qquad 7.40$$

from which it may be deduced that $F(\theta_c)$ has either of the two forms shown in Figure 7.5 or the mirror image (about the $\theta_c$ axis) of these. From Figure 7.5 it may be seen that equation 7.39 is satisfied at two points on the arc, but one of these is the trivial solution $\theta_c = \theta_s$. Equation 7.39 may be satisfied by other values of $\theta_c$ but these do not lie on the arc.

Newton's method was used to solve equation 7.39, i.e.

$$\theta_{c_{n+1}} = \theta_{c_n} - \frac{F(\theta_{c_n})}{F'(\theta_{c_n})} = \theta_{c_n} - \Delta\theta_{c_n} \qquad 7.41$$

but the initial estimate of the solution, $\theta_{c_o}$, had to be chosen to ensure

that the correct solution was found.

If $F(\theta_c)$ does not have a point of inflection after it has reached its non-zero turning point (this is shown by the full line in Figure 7.5), then $\theta_{c_o} = \theta_f$ is a suitable initial estimate to the solution. If, however, $F(\theta_c)$ has the form shown in Figure 7.5 by the dotted line, then using $\theta_{c_o} = \theta_f$ as an initial estimate for the solution may result in the wrong solution being found; usually the trivial solution. This problem was overcome by using, for both situations, an initial estimate given by:

$$\theta_{c_o} = \theta_f - \alpha \frac{F(\theta_f)}{F'(\theta_f)} \qquad 7.42$$

where $\alpha$ is a number in the range $0 < \alpha < 1$. For all cases cited in this work, an initial estimate obtained using $\alpha = 0.5$ always gave the correct solution. The solution was always tested to ensure that it had a value in the range $\theta_s < \theta_c < \theta_f$ and was hence the correct solution.

The iteration procedure (7.41) was normally continued until $\Delta\theta_{c_n} < 0.86^0$, but if the oil-film forces were being used to find the linearised bearing coefficients, then the procedure was continued until $\Delta\theta_{c_n} < 0.03^0$.

For the partially cavitated pressure profile of the type shown in Figure 7.3f, the boundary conditions are:

$$\left.\begin{aligned} P_l(\theta_f) &= 0 \\ P_l(\theta_c) &= 0 \\ \left.\frac{dP_l}{d\theta}\right|_{\theta_c} &= 0 \end{aligned}\right\} \qquad 7.43$$

The point of cavitation was found in the same manner as described above, except that here:

$$F(\theta_c) = \int_{\theta_c}^{\theta_f} \frac{A_\varepsilon (\cos\theta - \cos\theta_c) + B_\varepsilon (\sin\theta - \sin\theta_c)}{h^{*3}} d\theta \qquad 7.44$$

$$F'(\theta_c) = (A_\varepsilon \sin\theta_c - B_\varepsilon \cos\theta_c) \int_{\theta_c}^{\theta_f} \frac{d\theta}{h^{*3}} \qquad 7.45$$

and

$$\theta_{c_o} = \theta_s - \alpha \frac{F(\theta_s)}{F'(\theta_s)} \qquad 7.46$$

7.4.2.7 The oil-film forces

The general expression (according to the long bearing approximation) for the pressure field developed in a partial arc bearing is:

$$P_l(\theta) = \int_{\theta_1}^{\theta_2} \frac{A_\varepsilon \cos\theta + B_\varepsilon \sin\theta + C_\varepsilon}{h^{*3}} d\theta \qquad 7.47$$

where the oil-film limits $\theta_1$ and $\theta_2$ correspond to the start and finish of the uncavitated oil-film. (For example, $\theta_1 = \theta_c$ and $\theta_2 = \theta_f$ for the partially cavitated oil-film of the type shown in Figure 7.3f.)

From equations 3.18 and 3.19, the non-dimensional oil-film forces generated by a single partial arc bearing are given by:

$$f_e = 3\alpha^2\beta\left(\frac{c_r}{C}\right)^2 \int_{\theta_1}^{\theta_2} P_l(\theta)\cos\theta\, d\theta \qquad 7.48$$

$$f_\psi = 3\alpha^2\beta\left(\frac{c_r}{C}\right)^2 \int_{\theta_1}^{\theta_2} P_l(\theta)\sin\theta\, d\theta \qquad 7.49$$

The above integrals may be evaluated as follows:

$$\int_{\theta_1}^{\theta_2} P_l(\theta) \sin\theta \, d\theta = A_\varepsilon \left(\sin\theta_2 \int_{\theta_1}^{\theta_2} \frac{\cos\theta}{h^{*3}} d\theta - \int_{\theta_1}^{\theta_2} \frac{\sin\theta\cos\theta}{h^{*3}} d\theta\right)$$
$$+ B_\varepsilon \left(\sin\theta_2 \int_{\theta_1}^{\theta_2} \frac{\sin\theta}{h^{*3}} d\theta - \int_{\theta_1}^{\theta_2} \frac{\sin^2\theta}{h^{*3}} d\theta\right)$$
$$+ C_\varepsilon \left(\sin\theta_2 \int_{\theta_1}^{\theta_2} \frac{d\theta}{h^{*3}} - \int_{\theta_1}^{\theta_2} \frac{\sin\theta}{h^{*3}} d\theta\right) \qquad 7.50$$

$$\int_{\theta_1}^{\theta_2} P_l(\theta) \cos\theta \, d\theta = A_\varepsilon \left(\int_{\theta_1}^{\theta_2} \frac{\cos^2\theta}{h^{*3}} d\theta - \cos\theta_2 \int_{\theta_1}^{\theta_2} \frac{\cos\theta}{h^{*3}} d\theta\right)$$
$$+ B_\varepsilon \left(\int_{\theta_1}^{\theta_2} \frac{\cos\theta\sin\theta}{h^{*3}} d\theta - \cos\theta_2 \int_{\theta_1}^{\theta_2} \frac{\sin\theta}{h^{*3}} d\theta\right)$$
$$+ C_\varepsilon \left(\int_{\theta_1}^{\theta_2} \frac{\cos\theta}{h^{*3}} d\theta - \cos\theta_2 \int_{\theta_1}^{\theta_2} \frac{d\theta}{h^{*3}}\right) \qquad 7.51$$

For the completely cavitated oil-film, the oil-film forces are, of course, zero.

### 7.4.3 The Two Rotor System Supported Upon "Long" Lemon-Bore Bearings

The lemon-bore bearing model, in which the long bearing approximation was used to calculate the pressure field developed by each arc, was incorporated into the computer program for the flexible shaft system.

The behaviour of the two rotor, four bearing system was investigated for the three values of $\nu_{f_3}$ given below in Table 7.2. In each case, the shaft was assumed to be balanced and external damping was not applied. All four bearings were identical with $30^0$ axial feed ports, as shown in Figure 7.1, and with $C/c_r = 2.5$ and $d/C = 0.6$. The stability parameter $S_t = 0.4$, and for the aligned system the equilibrium eccentricity ratio $(\bar{\varepsilon}_o)_a = 0.691$.

For each value of $\nu_{f_3}$, and for all vertical misalignments of bearing number 2 investigated, the self-excited vibrations of the shaft remained finite. Although the solution procedure had often to be continued for several hundred revolutions of the shaft to allow the transients of the motion to decay, the shaft centre trajectories eventually formed closed orbit limit cycles. Examples of the steady-state whirl orbits for the three values of $\nu_{f_3}$ are shown in Figures 7.6 to 7.8. The fundamental whirl frequencies ($\omega_{w_1}$) for these are given in Table 7.2.

TABLE 7.2

Fundamental whirl frequencies for a misaligned two rotor system supported upon "long" lemon-bore bearings

| $\nu_{f_3}$ | $\omega/\omega_{p_1}$ | $\Delta y_{b_2}$ | $\omega_{w_1}/\omega$ |
|---|---|---|---|
| 0.128 | 2.15 | 0.5 | 0.375 ± 0.008 |
| 0.160 | 1.72 | 1.0 | 0.406 ± 0.008 |
| 0.200 | 1.37 | 2.0 | 0.438 ± 0.008 |

These results gave clear evidence to support the assertion that: the steady-state large amplitude vibrations, at frequencies below 0.5 $\omega$, which are observed in practice, have not previously been simulated, without recourse to external damping, because the bearing models employed did not take account of the non-circular nature of practical bearings. The results also showed that steady-state whirl at frequencies significantly less than 0.5 $\omega$ could also occur for a shaft rotating at speeds well below twice its first pinned critical speed.

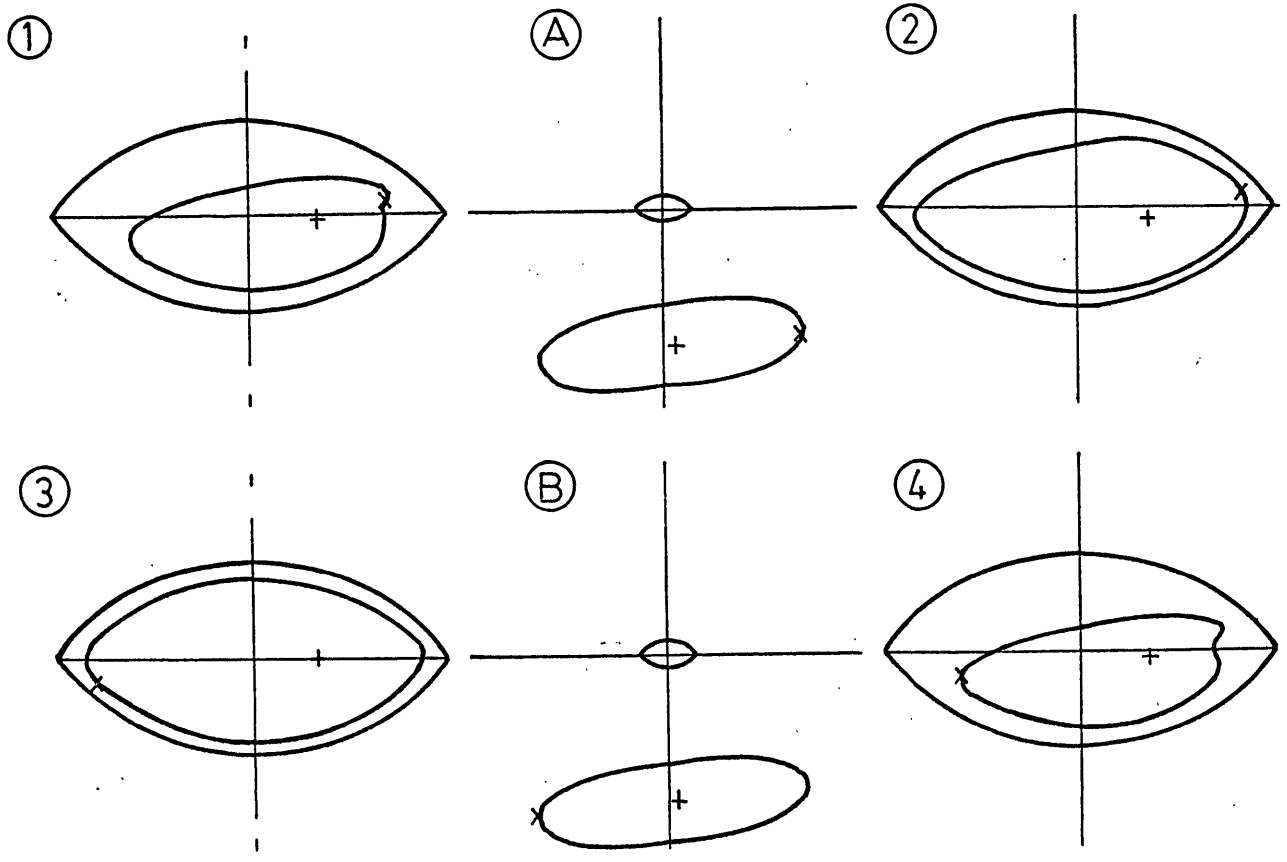


Figure 7.6: The steady-state whirl orbits for the two rotor system supported upon "long" lemon-bore bearings, $\nu_{f_3} = 0.128$, $\Delta y_{b_2} = 0.5$.

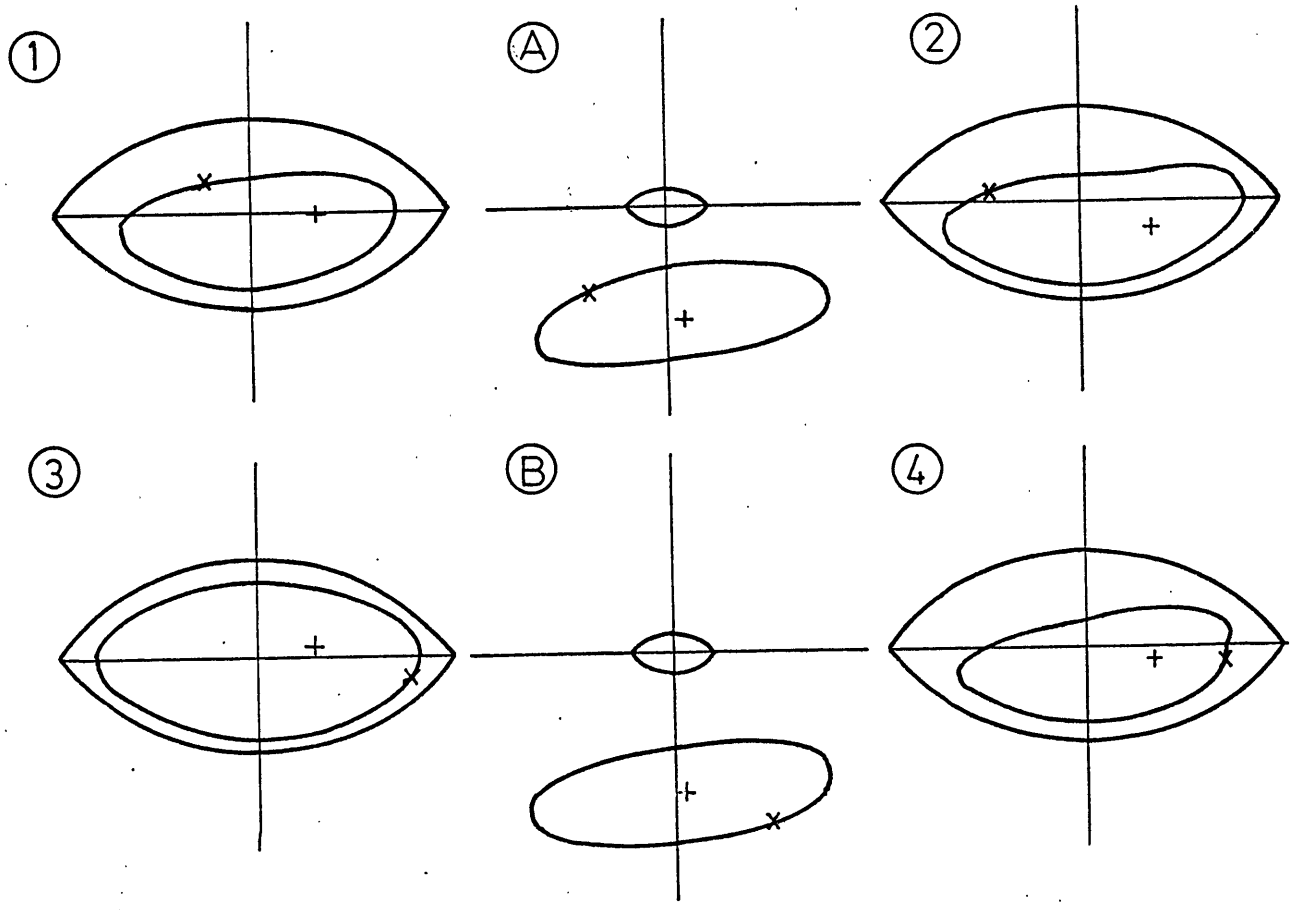


Figure 7.7: The steady-state whirl orbits for the two rotor system supported upon "long" lemon-bore bearings, $\nu_{f_3} = 0.16$, $\Delta y_{b_2} = 1.0$.

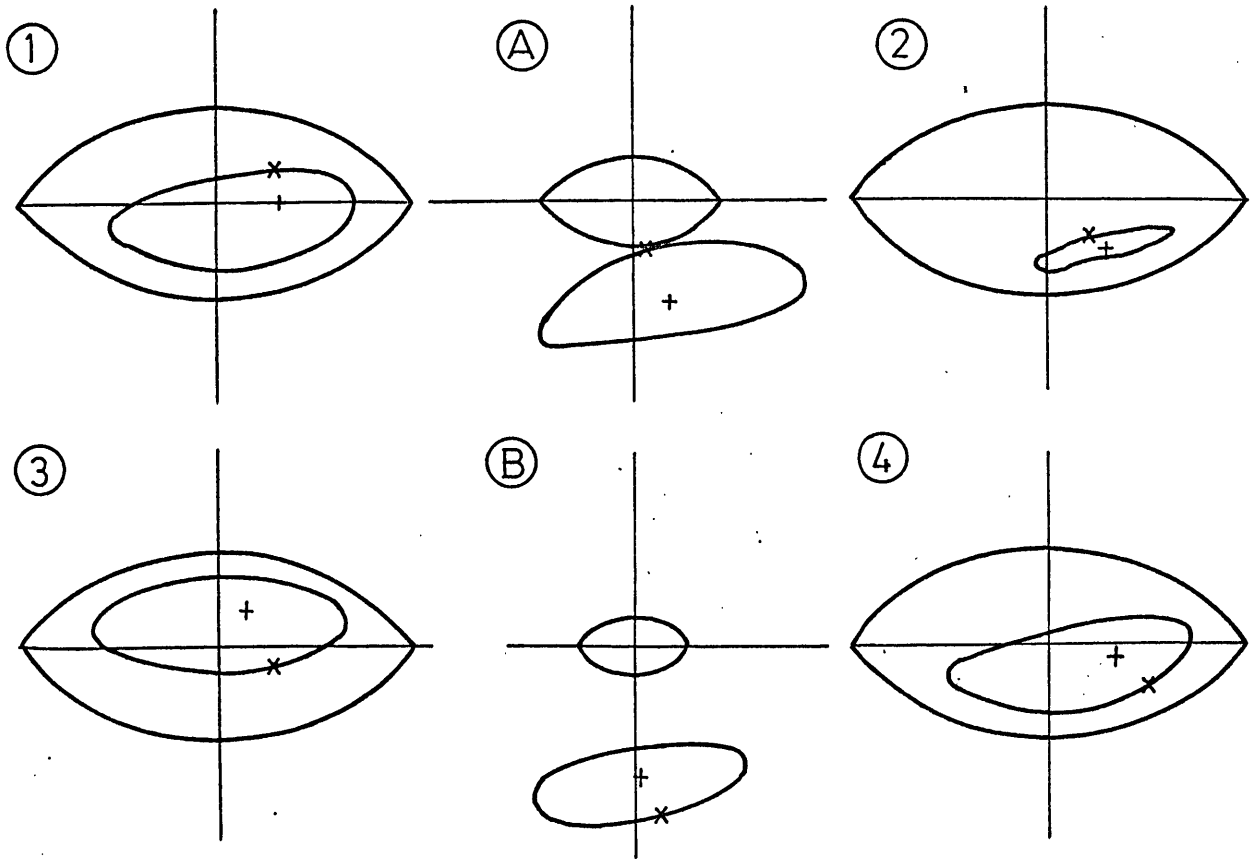


Figure 7.8: The steady-state whirl orbits for the two rotor system supported upon "long" lemon-bore bearings, $\nu_{f_3} = 0.2$, $\Delta y_{b_2} = 2.0$.

### 7.4.4 A Side Leakage Correction Factor

The oil-film forces obtained for the lemon-bore bearing model using the infinitely long bearing approximation needed to be corrected to take account of the finite width of realistic bearings. For this, a modification of a method due to Black & Brown (1976) for determining a side leakage factor was adopted.

By assuming a parabolic axial pressure profile (7.21) in the bearing, the two-dimensional Reynolds equation is reduced to one-dimensional form (7.22). Equation 7.22 cannot be integrated directly and so an approximate method is used, which assumes the solution is of the form:

$$\overline{P} = \kappa P_l(\theta) \qquad 7.52$$

where $P_l(\theta)$ is the long bearing solution for the non-dimensional pressure, and $\kappa$ is a side leakage correction factor. (This is a single term form of the well known method for solving boundary value problems in which the solution is assumed to be a linear combination of a set of trial functions, each of which satisfies the boundary conditions of the problem.) By substituting equation 7.52 in equation 7.22, and invoking equation 7.23, a residual $\overline{R}$ may be formed:

$$\overline{R} = \kappa \overline{\gamma} \alpha^2 h^{*3} P_l(\theta) + (\kappa - 1)(A_\varepsilon \sin\theta - B_\varepsilon \cos\theta) \qquad 7.53$$

If Black & Brown's approach is continued, then $\kappa$ is determined by requiring the residual to be minimised according to the method of Galenkin, i.e. by requiring:

$$\int_{\theta_1}^{\theta_2} P_l(\theta)\, \overline{R}(\theta)\, d\theta = 0 \qquad 7.54$$

where $\theta_1$ and $\theta_2$ are the limits of the uncavitated oil-film, and leads to the following expression for the side leakage correction factor:

$$\kappa = 1 \Big/ \left[ 1 + \frac{\bar{\gamma}\,\alpha^2 \int_{\theta_1}^{\theta_2} P_l^2(\theta)\, h^{*3}\, d\theta}{\int_{\theta_1}^{\theta_2} P_l(\theta)\,(A_\varepsilon \cos\theta - B_\varepsilon \sin\theta)} \right] \qquad 7.55$$

Unfortunately, this requires the evaluation of the integral:

$$\int_{\theta_1}^{\theta_2} P_l^2(\theta)\, h^{*3}\, d\theta \qquad 7.56$$

which, to date, has only been achieved numerically and greatly increases the time required to evaluate the oil-film forces.

At this stage, an alternative argument may be proposed. For, since most of the force generated derives from the region of maximum pressure, it would seem reasonable to set the residual to zero at the point of maximum pressure, $\theta_m$. This method of collocation results in the computationally simpler expression for the side leakage factor:

$$\kappa = 1 \Big/ \left[ 1 + \frac{\bar{\gamma}\,\alpha^2\, h^{*3}(\theta_m)\, P_l(\theta_m)}{A_\varepsilon \sin\theta_m - B_\varepsilon \cos\theta_m} \right] \qquad 7.57$$

It may be verified, by substitution in equations 7.23 and 7.28, that:

$$\cos\theta_m = -(A_\varepsilon C_\varepsilon + B_\varepsilon \sqrt{A_\varepsilon^2 + B_\varepsilon^2 - C_\varepsilon^2})/(A_\varepsilon^2 + B_\varepsilon^2) \qquad 7.58$$

and: $$\sin\theta_m = -(B_\varepsilon C_\varepsilon - A_\varepsilon \sqrt{A_\varepsilon^2 + B_\varepsilon^2 - C_\varepsilon^2})/(A_\varepsilon^2 + B_\varepsilon^2) \qquad 7.59$$

Once the side leakage factor has been found (by whichever

method), the compensated oil-film forces are simply calculated. For example, if the centre-line pressure had been used in equation 7.22, then $\overline{P} = P_c$, and so the non-dimensional pressure distribution is, from equations 7.21 and 7.52, given by:

$$P^* = \kappa P_l(\theta) (1 - z^{*2}) \qquad 7.60$$

which, when substituted into equations 3.18 and 3.19, yields the non-dimensional oil-film forces, i.e.

$$f_e = 2 \alpha^2 \beta \left(\frac{c_r}{C}\right)^2 \kappa \int_{\theta_1}^{\theta_2} P_l(\theta) \cos \theta \, d\theta \qquad 7.61$$

and:

$$f_\psi = 2 \alpha^2 \beta \left(\frac{c_r}{C}\right)^2 \kappa \int_{\theta_1}^{\theta_2} P_l(\theta) \sin \theta \, d\theta \qquad 7.62$$

To test the above assertions, an accurate two-dimensional finite difference solution (with $\Delta\overline{\theta} = (\overline{\theta}_f - \overline{\theta}_s)/40$ and $\Delta z^* = 1/10$) was used to calculate the oil-film forces for the lower arc of the bearing shown in Figure 7.1. The length-to-diameter ratio $1/\alpha = 0.75$, which is typical for turbogenerator bearings.

The error in the force for the centrally loaded arc, when calculated using the compensated long bearing approximation, is shown in Figure 7.9. Both methods for minimising the residual were investigated using both the centre-line and mean axial pressure in equation 7.22. To assess the accuracy under dynamic conditions, the journal was subjected to 100 random conditions of velocity and displacement in the range:

$$0.0 < \varepsilon < 0.9$$

$$-0.2 < \dot{\varepsilon} < 0.2$$

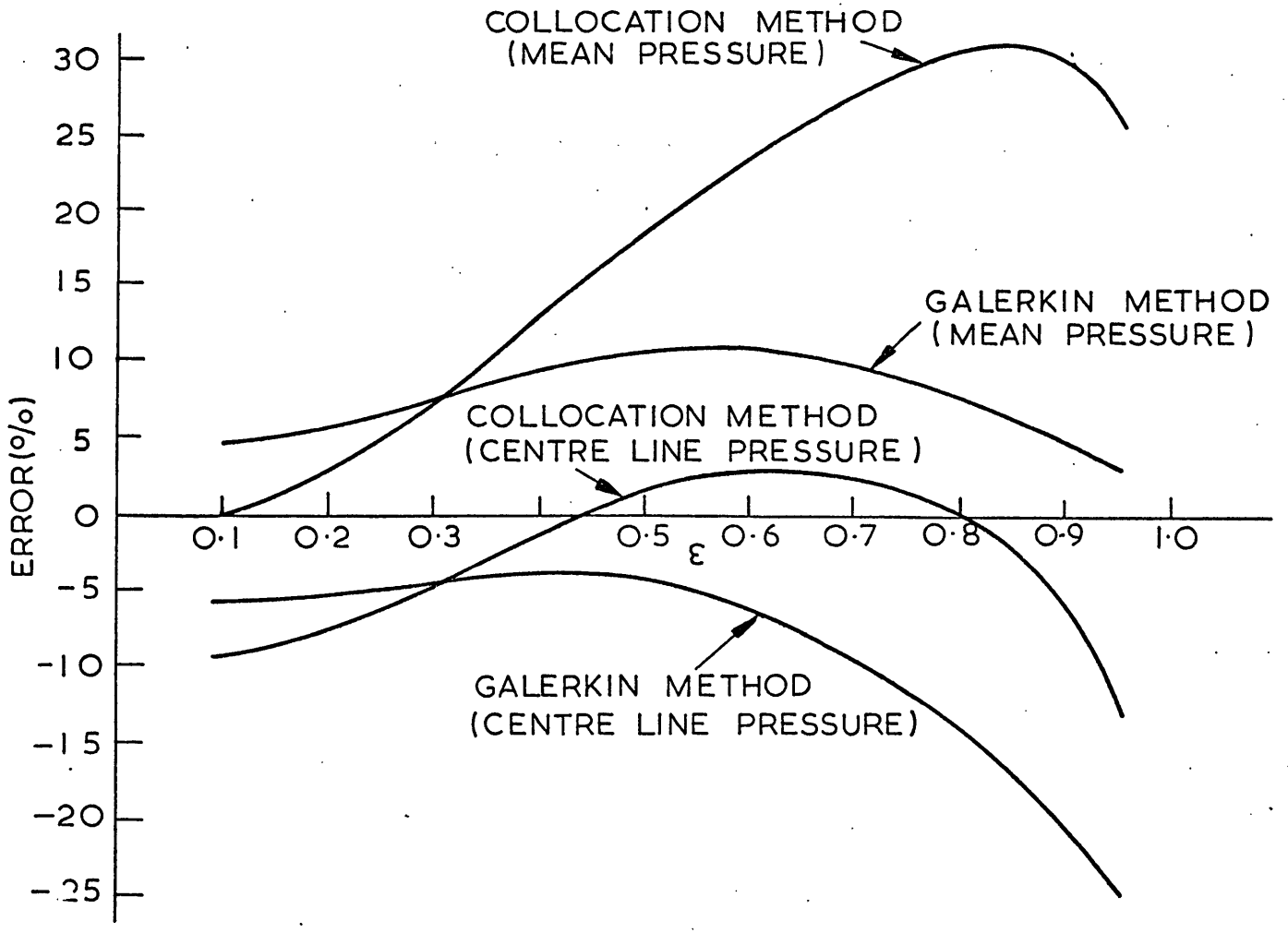


Figure 7.9: The error in the vertical force for a centrally loaded partial arc bearing using various approximate methods

$$-\pi < \psi < 0.0$$

$$-0.2 < \dot{\psi} < 0.6$$

Table 7.3 contains the mean and standard deviation of the error in the resultant force obtained by the approximate methods.

TABLE 7.3

Errors for approximate methods of calculating oil-film forces

| % Error | Method of Collocation | | Method of Galerkin | |
|---|---|---|---|---|
| | Mean Axial Pressure | Centre-Line Pressure | Mean Axial Pressure | Centre-Line Pressure |
| Mean | 22.09 | -4.00 | 9.56 | -12.08 |
| Standard Deviation | 10.03 | 8.07 | 8.33 | 6.18 |

These results showed that the method of collocation using the centre-line pressure could be expected to give the oil-film forces for the lemon-bore bearing to within 20% of those calculated from the two-dimensional finite difference solution and compares favourably with the Galerkin method. This was considered sufficiently accurate to obtain a good approximation to the non-linear limit cycle behaviour.

The method described in section 7.3.1 was used to estimate the computational time required to evaluate the oil-film forces for the lemon-bore bearing using the compensated long bearing solution. Both methods for obtaining the side leakage correction factor were tested, and the results are given in Table 7.1. For Galerkin's method, the integral 7.56 was evaluated using Simpson's quadrature formula, for which two step

sizes, $(\theta_2 - \theta_1)/50$ and $(\theta_2 - \theta_1)/24$, were considered. It may be seen that the method of collocation satisfies the criterion set in section 7.2.4, but Galerkin's method does not. Even for the larger step size, Galerkin's method is in excess of four times slower than the method of collocation.

The stability profile for a rigid shaft supported by two identical bearings, of the type shown in Figure 7.1, and for which $C/c_r$ = 1.9, $d/C$ = 0.474 and $1/\alpha$ = 0.75, was calculated using:

(a) the two-dimensional finite difference solution;

(b) the compensated long bearing solution: method of Galerkin (mean axial pressure);

(c) the compensated long bearing solution: method of collocation (centre-line pressure);

(d) the uncompensated long bearing solution.

The results for this are shown in Figure 7.10. It may be seen that both methods for obtaining the side leakage correction factor improve the estimate of the stability borderline, but a greater improvement is achieved using the method of Galerkin. With both methods, the characteristics of the long bearing solution are retained; this is most marked for the method of collocation at high eccentricity ratios. It should, however, be emphasised that the prediction of the stability threshold is, by its nature, extremely sensitive to small errors in the linearised bearing coefficients. Errors in the bearing forces, which would not have a

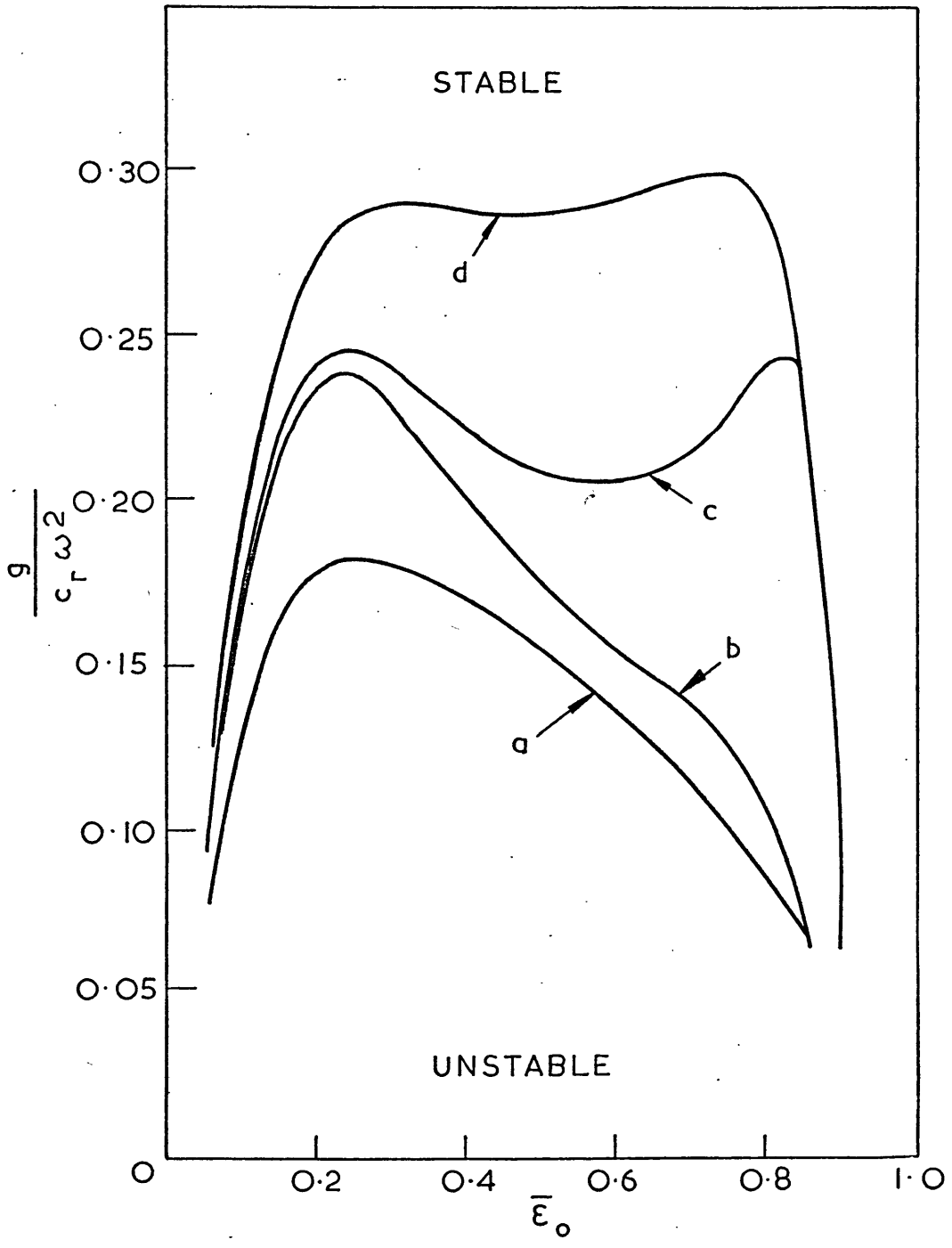


Figure 7.10: Stability profiles for a lemon-bore bearing (rigid shaft). Refer to text for details.

significant effect upon the non-linear limit cycle behaviour, could considerably alter the character of the stability profile. (Mitchell (1967-68) showed that a ±5% error in the linearised bearing coefficients for a short circular bearing supporting a rigid shaft could cause a 100% variation in the value of the stability parameter ($g/C\omega^2$) over the normal range of eccentricity.)

A number of the tests conducted for the two rotor system supported upon "long" lemon-bore bearings were repeated using the compensated long bearing solution, in which the side leakage factor was obtained using the method of collocation. The behaviour was found to be qualitatively in agreement with that observed previously. That is:

i) Without the application of external damping, the self-excited vibrations remained finite when the shaft was rotating at speeds above, as well as below, twice its first pinned critical speed.

ii) Steady-state whirl with a fundamental frequency significantly below 0.5 $\omega$ could be induced in a shaft rotating at speeds substantially below twice its first pinned critical speed.

These observations were in complete contrast to the behaviour observed for the two rotor system supported upon short circular bearings.

Finally, a two rotor system supported upon four identical bearings of the type used for the stability profile calculation above was tested. (This bearing was to be the one used in the series of tests later.) An example of the orbit for the steady-state self-excited vibrations of a shaft running in excess of twice its first pinned critical speed ($\omega/\omega_{p_1} = 2.15$) is shown in Figure 7.11.

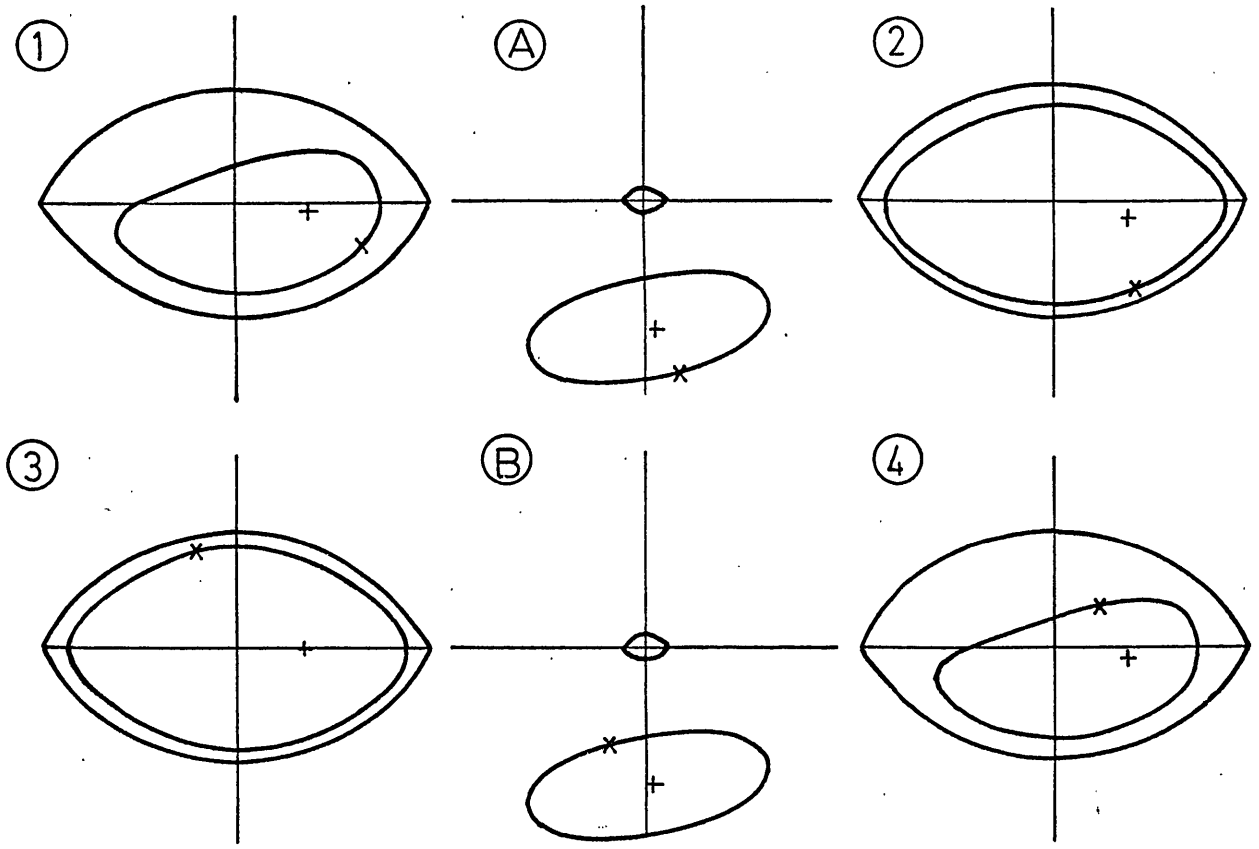


Figure 7.11: The steady-state whirl orbits for a two rotor system supported upon lemon-bore bearings, $\nu_{f_3} = 0.128$, $\Delta y_{b_2} = 0.5$, $(\bar{\varepsilon}_o)_a = 0.623$.

# CHAPTER 8

# THE TWO ROTOR SYSTEM SUPPORTED UPON LEMON-BORE BEARINGS

## 8.1 COMPUTATIONAL PROCEDURE

A series of tests was conducted for the two rotor system supported upon lemon-bore bearings to assess the effect of the vertical misalignment of a bearing upon the self-excited vibrations of the system.

For this, the lowest (flexural) free-free natural frequency of the coupled rotors $\nu_{f_3} = 0.20$, which gave $\omega/\omega_{p_1} = 1.37$. The shaft was assumed to be perfectly balanced, and was not acted upon by external damping. All four bearings were identical with $30^0$ axial feed ports, as shown in Figure 7.1, and with $C/c_r = 1.9$, $d/C = 0.474$ and $1/\alpha = 0.75$. Such a geometry is typical for the lemon-bore bearings used in large turbo-generators. The compensated long bearing solution, in which the side leakage correction factor was calculated according to the method of collocation using the centre-line pressure, was used to obtain the oil-film forces. The stability parameter $S_t = 0.4$, and for the aligned system the equilibrium eccentricity ratio of the shaft relative to the centre of each bearing, $(\bar{\varepsilon}_o)_a = 0.627$. For discussion purposes, it is assumed that for the above conditions the shaft is rotating at design speed, i.e. $\omega/\omega_d = 1.0$.

It was considered that sufficient accuracy would be achieved by using eight free-free modes to represent the shaft. This was confirmed by repeating selected tests using ten modes. As an example (but for a system differing slightly from the one described above in that $C/c_r = 1.75$, $d/C = 0.43$ and $(\bar{\varepsilon}_o)_a = 0.82$), the steady-state orbits at bearing number 2 obtained using 8 and 10 free-free modes are shown in Figure 8.2 for a

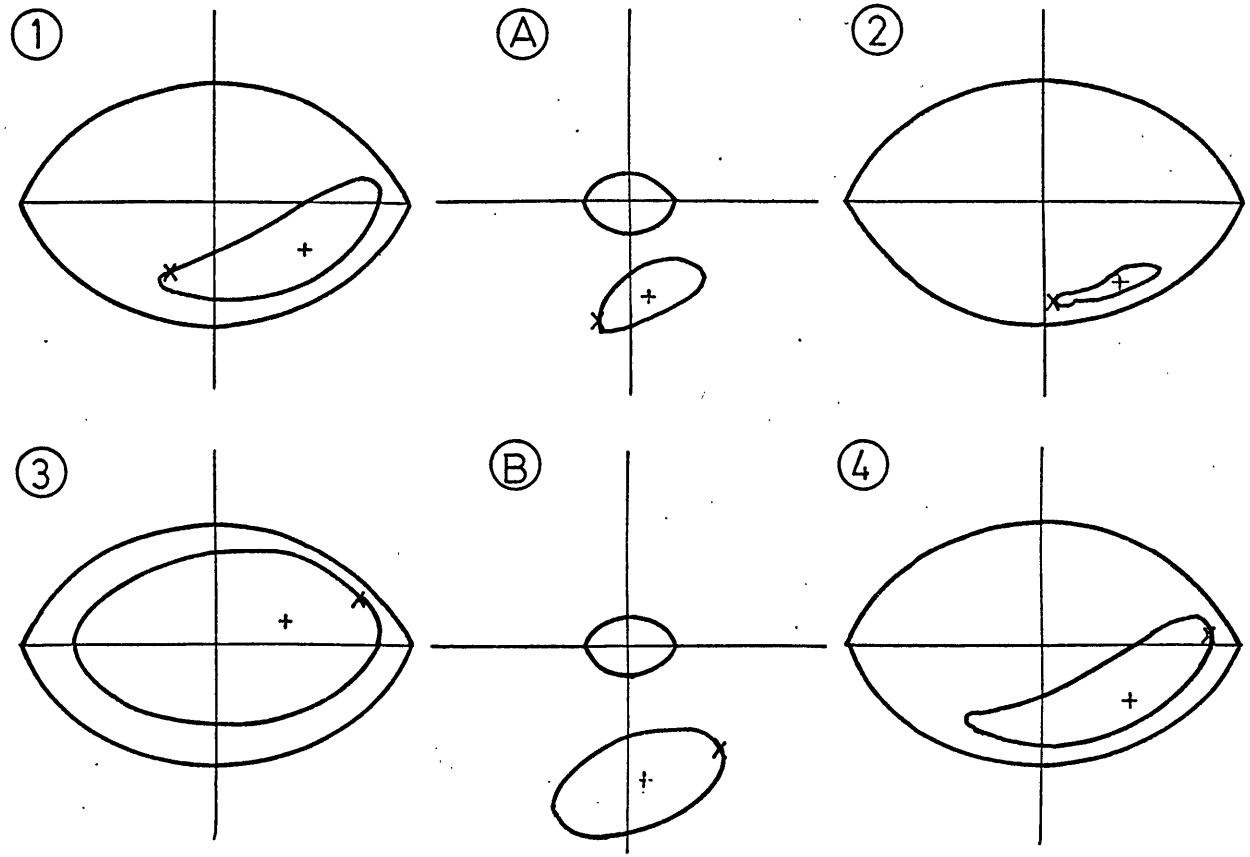


Figure 8.1: The steady-state whirl orbits for the two rotor system supported upon lemon-bore bearings

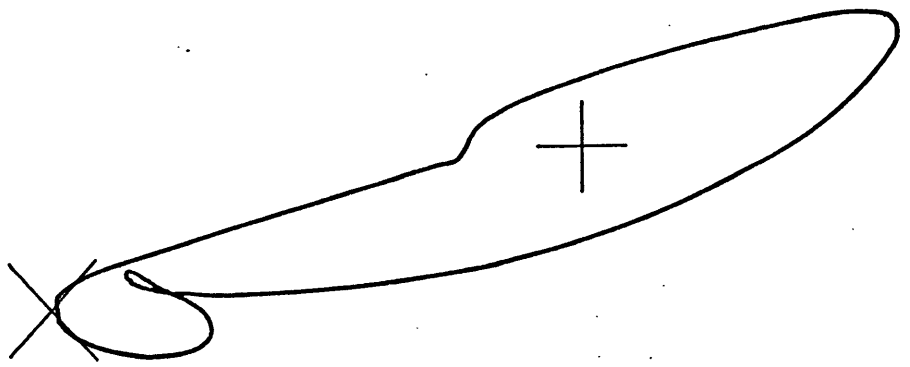

(a)

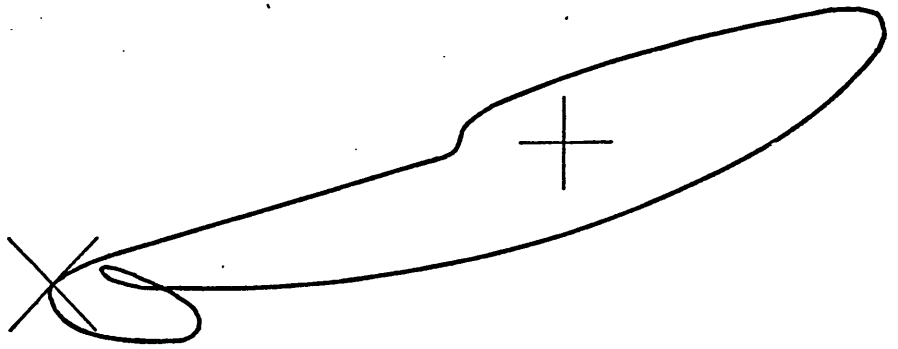

(b)

Figure 8.2: The steady-state whirl orbit at bearing number 2 using (a) 8 modes, and (b) 10 modes in the modal expansion

misalignment of $\Delta y_{b_2} = 1.5$. The steady-state orbits at all six stations, for the calculation employing 10 modes, are shown in Figure 8.1. It may be seen that the orbit at bearing number 2 is the most complex and, although it would be reasonable to assume that any changes to the solution would be most marked here, the details of the orbit are almost unchanged by the addition of two further modes to the modal series. This was corroborated by the frequency analysis.

Except for the initial conditions (which are discussed below), the remaining computational procedure was the same as that given in section 6.1. An interactive version of the computer program used for the tests is given in Appendix 4.

### 8.1.1 Initial Conditions

Previous experience had shown that if the initial conditions for the non-linear solution procedure corresponded to small disturbances of the shaft from its equilibrium position, then the solution procedure had to be continued for several hundred revolutions of the shaft before the steady-state was reached. (This is reasonable considering the increase in energy of the vibrating system and that at 3000 rpm it only takes 5 seconds to complete 250 revolutions.) It was also found to be important to ensure that the steady-state had been fully attained, otherwise misleading results could be obtained.

For small excursions of the shaft about the equilibrium position, the oil-film forces are approximately linear. A considerable saving in computer time was achieved by using the linearised equations of motion (5.25) to determine the unstable motion up to an amplitude where the linear assumption had ceased to be valid, at which point the velocity and displacement of the shaft were used as initial conditions for the non-

linear solution procedure.

Assuming that all the eigenvalues of the matrix $[A]$ are district, then the general solution of equations 5.25 is:

$$\{\bar{u}\} = a_1 \{\bar{u}_1\} e^{\lambda_1 \tau} + a_2 \{\bar{u}_2\} e^{\lambda_2 \tau} + \ldots + a_{4m} \{\bar{u}_{4m}\} e^{\lambda_{4m} \tau} \qquad 8.1$$

where $\{\bar{u}_i\}$ are the eigenvectors of the matrix $[A]$, and $a_i$ are constants determined by the initial conditions. Let $\lambda_1$ and $\lambda_2$ be the complex conjugate pair of eigenvalues that have, algebraically, the maximum real parts. (The eigenvalue with the maximum real part is complex as the unstable motion of the shaft is invariably oscillatory.) If the initial conditions for the shaft are such that:

$$a_2 = a_3 = \ldots\ldots a_{4m} = 0 \qquad 8.2$$

then equation 8.1 reduces to:

$$\{\bar{u}\} = a_1 \{\bar{u}_1\} e^{\lambda_1 \tau} \qquad 8.3$$

which, if the real part of the solution only is considered, becomes:

$$\{\bar{u}\} = a_1 e^{\lambda_R \tau} (\{\bar{u}_R\} \cos \lambda_I \tau - \{\bar{u}_I\} \sin \lambda_I \tau) \qquad 8.4$$

where $\{\bar{u}_R\}$ and $\{\bar{u}_I\}$ are the real and imaginary parts, respectively, of the eigenvector $\{\bar{u}_1\}$, and $\lambda_R$ and $\lambda_I$ are the real and imaginary parts, respectively, of the eigenvalue $\lambda_1$.

From equations 2.61, 2.62, 5.24 and 5.27, the displacement of the shaft from its equilibrium position is:

$$\bar{x}(s) = x(s) - x_o(s) = a_1 e^{\lambda_R \tau} (X_R \cos \lambda_I \tau - X_I \sin \lambda_I \tau) \quad 8.5$$

$$\bar{y}(s) = y(s) - y_o(s) = a_1 e^{\lambda_R \tau} (Y_R \cos \lambda_I \tau - Y_I \sin \lambda_I \tau) \quad 8.6$$

in which:

$$X_R = \sum_{i=1}^{m} \bar{u}_{R_{2m+i}} \phi_i(s) \quad 8.7$$

$$X_I = \sum_{i=1}^{m} \bar{u}_{I_{2m+i}} \phi_i(s) \quad 8.8$$

$$Y_R = \sum_{i=1}^{m} \bar{u}_{R_{3m+i}} \phi_i(s) \quad 8.9$$

$$Y_I = \sum_{i=1}^{m} \bar{u}_{I_{3m+i}} \phi_i(s) \quad 8.10$$

where $\bar{u}_{R_j}$ and $\bar{u}_{I_j}$ are the $j$th elements of the vectors $\{\bar{u}_R\}$ and $\{\bar{u}_I\}$, respectively. Thus, the trajectories of the shaft, corresponding to a single eigenvector, are in the form of "elliptical" spirals.

The modal coefficients for the start of the non-linear solution procedure were, using equations 5.27 and 8.4, given by:

$$\{u\} = \{u\}_o + \bar{a} (\{\bar{u}_R\} \cos \lambda_I \tau - \{\bar{u}_I\} \sin \lambda_I \tau) \quad 8.11$$

where $\bar{a}$ had the largest value possible such that, if the shaft moved in the elliptical orbit:

$$\bar{x}(s) = \bar{a} (X_R \cos \lambda_I \tau - X_I \sin \lambda_I \tau) \quad 8.12$$

$$\bar{y}(s) = \bar{a} (Y_R \cos \lambda_I \tau - Y_I \sin \lambda_I \tau) \quad 8.13$$

then the maximum film thickness in any of the bearings should not be less than 0.25 $C$. As the value of $\tau$ in equation 8.11 is arbitrary, it was set to zero which simplified the initial conditions for the non-linear solution procedure to:

$$\{u\} = \{u\}_o + \bar{\alpha} \{u_R\} \qquad 8.14$$

By using the above procedure, in which the initial conditions are found from the "dominant" eigenvector of the linearised system, it was found that only approximately 60 revolutions of the shaft were required to reach the steady-state, which represented a considerable saving in computer time. It should also be added that the deflected shape of the shaft obtained from the dominant eigenvector was always of the anti-symmetric type shown in Figure 6.4b.

## 8.2 RESULTS AND DISCUSSION

The effect of vertical misalignment of bearing number 2 upon the stability of the equilibrium position of the rotating shaft is shown in Figure 8.3. At the design speed (i.e. $\omega/\omega_d = 1.0$) the system is marginally stable when aligned, but small upward or downward misalignments cause the equilibrium position to become unstable. If the misalignment becomes excessive, the equilibrium position again becomes stable as the initially deloaded bearing becomes loaded in the reverse direction. It may also be seen from Figure 8.3 that, when the system is operating above its design speed at $\omega/\omega_d = 1.2$, the equilibrium position is always unstable and, conversely, when operating below the design speed at $\omega/\omega_d = 0.8$, the equilibrium position remains stable for all misalignments of bearing number 2.

The behaviour of the corresponding non-linear steady-state motion for the system operating at its design speed, and for upward misalignment of bearing number 2, is illustrated in Figures 8.4 to

Although near the aligned condition, the equilibrium position of the shaft is marginally stable, large amplitude self-excited motion could be induced by giving the shaft a sufficiently large disturbance. (The motion of the shaft used for this initial disturbance corresponded to the eigenvector of the linearised system, whose eigenvalue was least damped.) If, however, the shaft was only given a small disturbance from the equilibrium position, then, in accordance with the predictions of linear theory, it returned to its equilibrium position. This hysteresis effect is often observed in practice when the shaft continues to whirl as the rotational speed is reduced below the threshold for the onset of whirl during run-up. A steady-state whirl orbit corresponding to a stable equilibrium position was not found for $\Delta y_{b_2} > 3.25$.

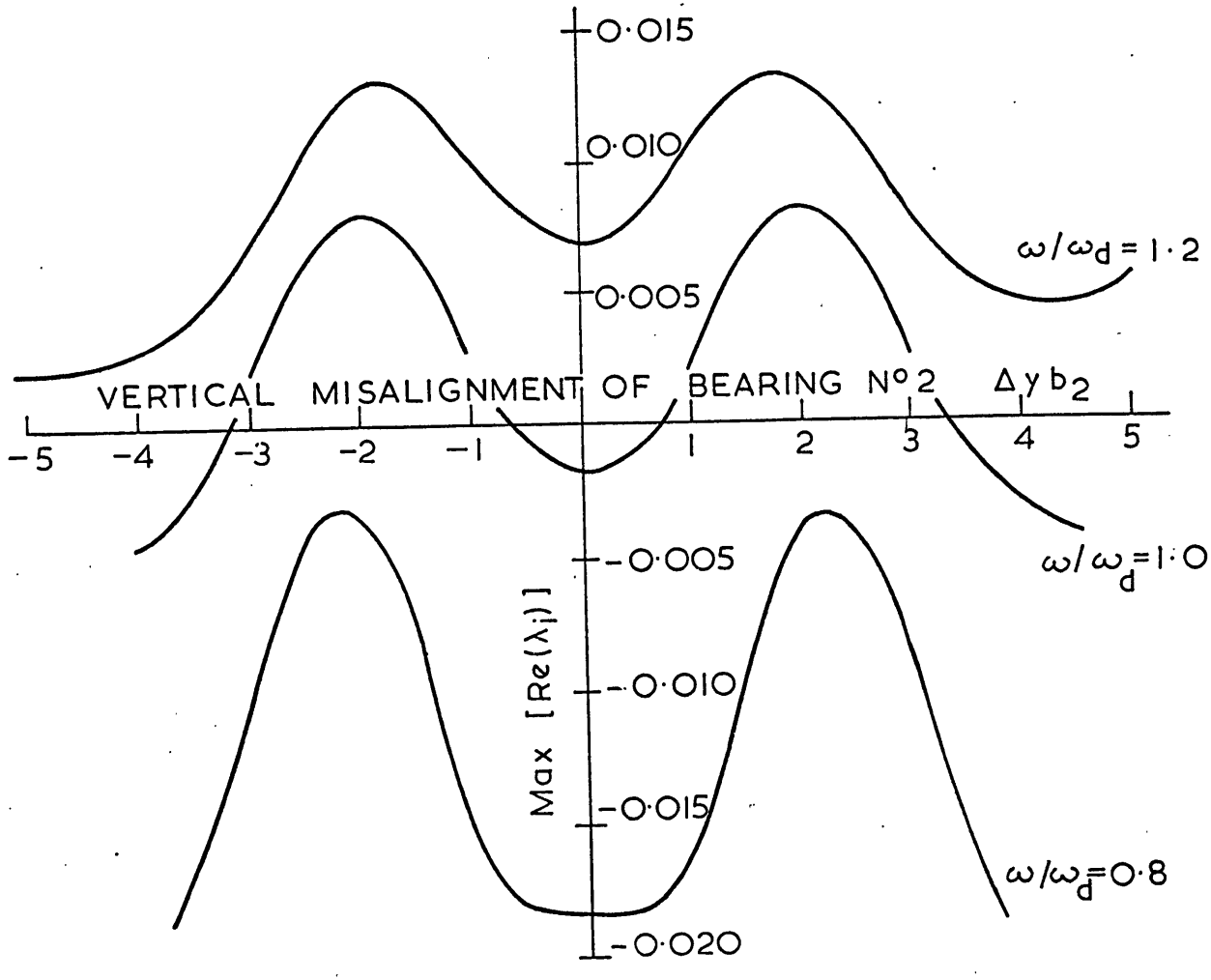


Figure 8.3: The stability of the equilibrium position of the two rotor system. *Max* $\{Re(\lambda_i)\}$ denotes the maximum real part of the eigenvalues of the linearised system.

In the aligned condition, the steady-state motion at each of the three stations (*1*, *A* and *2*) was $180^0$ out of phase to that occurring at the corresponding stations (*3*, *B* and *4*) on the other rotor. The shaft retained this anti-symmetric "mode" shape (which is of the type shown in Figure 6.4b) at all conditions of misalignment but for these the phase relationships were more complex due to the asymmetry of the system. It should also be added that the centre-line of the shaft did not lie in a single plane.

Although the initial conditions for a number of tests were varied, only one limit cycle solution was ever found. The results obtained earlier for the vertical two rotor system supported upon short circular bearings suggest that if the speed of the system were to be increased so that $\omega/\omega_{p_1} > 3.0$, then at some point the anti-symmetric motion would give way to symmetric motion in which the shape of the shaft would be of the form shown in Figure 6.4c. This, however, was not investigated.

The dominant component of the steady-state motion at all stations was at the fundamental whirl frequency, $\omega_{w_1}$. A number of harmonics were present at $2\omega_{w_1}$, $3\omega_{w_2}$, ...., but were usually an order of magnitude smaller than the dominant component. These caused the whirl orbits to be non-elliptical, this being most noticeable at bearing number 2 for larger misalignments. Figure 8.5 shows clearly that the frequency of the steady-state whirl is affected by bearing misalignment. In the aligned condition, the fundamental whirl frequency is a half shaft speed (0.5 $\omega$), but increased misalignment reduces this to 0.44 $\omega$. (Such behaviour was not observed for the horizontal two rotor system supported upon short circular bearings where (for $\nu_{f_3} = 0.2$) the fundamental whirl frequency remained at approximately 0.5 $\omega$ for all misalignment conditions investigated.) When the equilibrium position of the shaft became unstable,

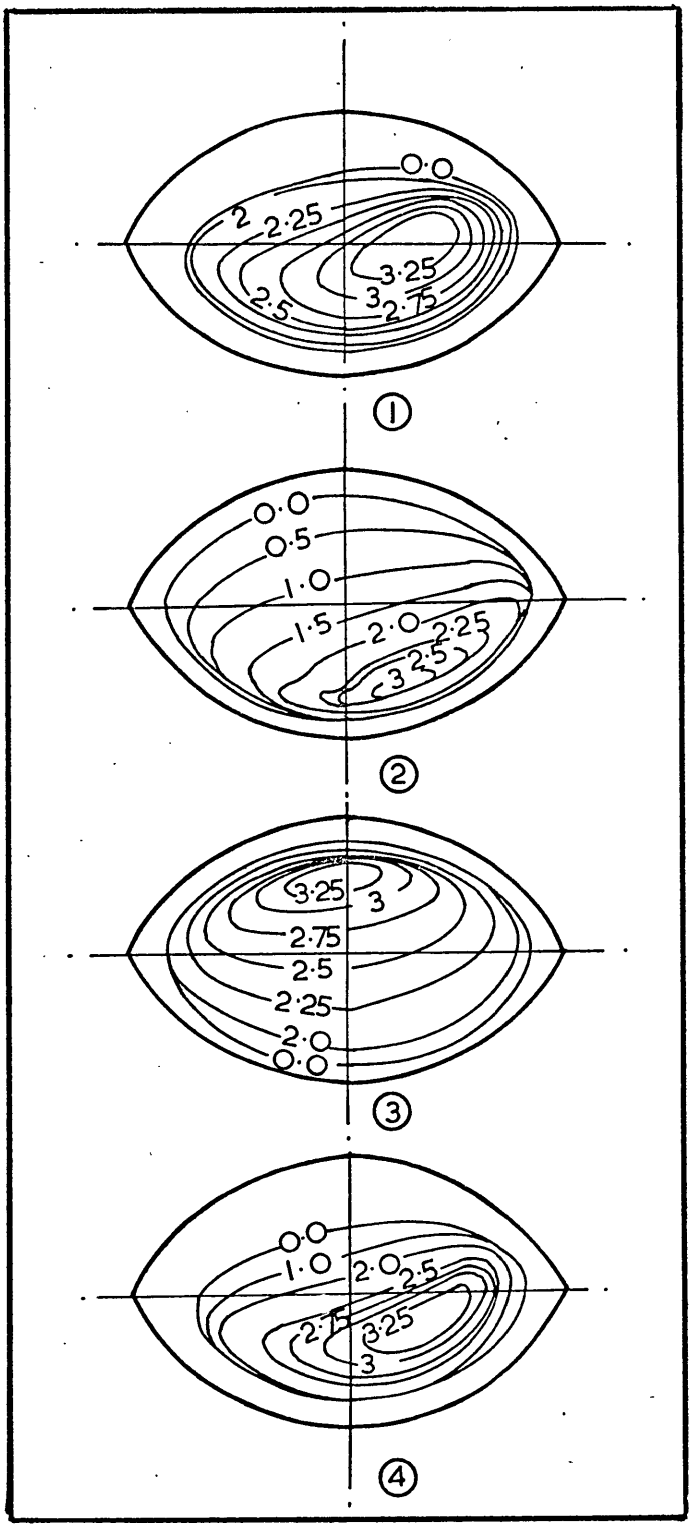


Figure 8.4: Steady-state whirl orbits in each bearing of the two rotor system. Numbers on loci denote the non-dimensional vertical misalignment ($\Delta y_{b_2}$) of bearing number 2.

the whirl initially developed at the lowest damped natural frequency of the linearised system but, as the amplitude of the motion increased, so did the whirl frequency. However, the greater the misalignment, the smaller the difference between the fundamental steady-state whirl frequency and the lowest damped natural frequency of the linearised system, until for $\Delta y_{b_2} = 3.25$ the two frequencies almost coincided.

Increased misalignment brought about a decrease in the amplitude of the whirl, which (in agreement with linear predictions) disappeared for large misalignments as the two central bearings became heavily loaded, but in opposite directions. An explanation for this reduction in amplitude is that any individual misalignment of two closely spaced bearings effectively imposes upon the shaft a "single bearing" that is more non-circular than either bearing individually, and this has a stabilising influence on the large amplitude vibrations. (This effect was also observed with the horizontal two rotor system supported upon short circular bearings.)

For misalignments in the range $0.0 < \Delta y_{b_2} < 1.5$, the vertical load on bearing number 3 was in the downwards direction, and the amplitude of whirl in this bearing remained almost constant. If, however, the misalignment was increased beyond $\Delta y_{b_2} = 1.5$, then the direction of the vertical load carried by bearing number 3 was reversed and the amplitude of whirl in the bearing decreased, becoming at large misalignments marginally smaller than the amplitudes in either of the two out-board bearings. It has sometimes been suggested that the deloaded bearing in a system may be identified because the steady-state amplitude in this bearing is larger than in any other bearing. Subject to the qualification that the bearing is deloaded and not heavily negatively loaded, the results obtained for the two rotor system supporting this assertion. The

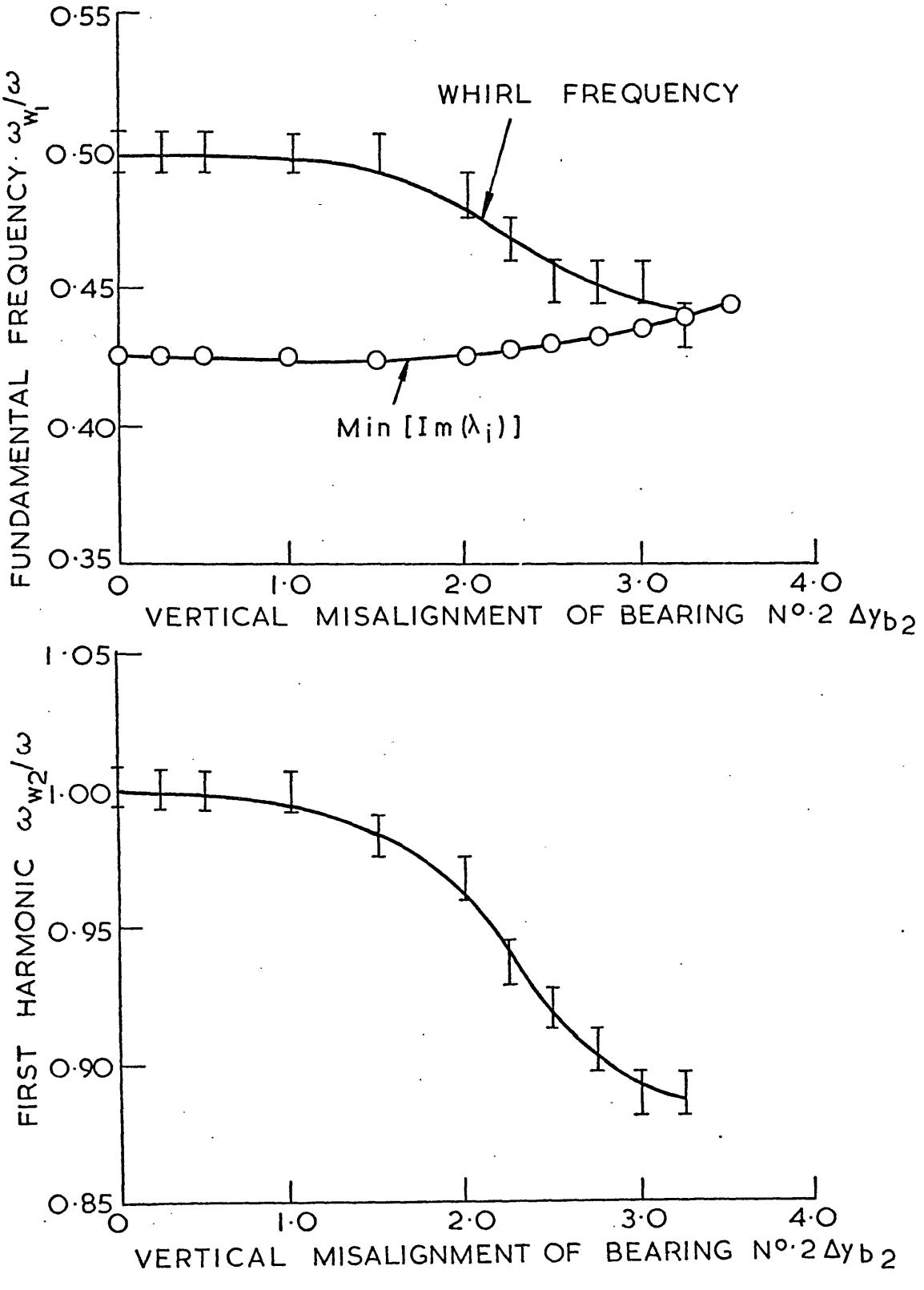


Figure 8.5: Steady-state whirl frequencies of the two rotor system. Also shown are the corresponding lowest damped natural frequencies, *Min* $\{Im(\lambda_i)\}$, of the linearised system.

alternative argument that the smallest steady-state whirl amplitude occurs in the bearing that is most heavily loaded (i.e. bearing number 2) was not always true. It should, however, be added that the steady-state amplitude in bearing number 2 was always smaller than in the adjacent bearing, bearing number 3.

The steady-state motion in the two out-board bearings (numbers 1 and 4) was very similar for all misalignments but, in general, the amplitude in bearing number 1 was slightly larger. A possible explanation for this is that the bending moment imposed upon the shaft by the relative misalignment of the two central bearings always caused bearing number 1 to be marginally less heavily loaded than bearing number 4.

The steady-state motion at the mid-spans of the two rotors was also similar, although the rotor supported by the nominally deloaded bearing (number 3) always had a slightly larger amplitude.

It is a commonly held belief that, if a rotor system becomes unstable due to misalignment of a bearing, then the amplitude of motion at the onset of instability is largest in the deloaded bearing. This would be equivalent to saying that the amplitude, in the bearings, of the elliptical "orbit" (equations 8.12 and 8.13) given by the eigenvector corresponding to the eigenvalue with maximum real part, is largest for the deloaded bearing. The size of the major axis of this elliptical orbit was calculated using the procedure described in Appendix 2, but for all cases of misalignment tested, the major axis was largest for bearing number 4 and not the nominally deloaded bearing, bearing number 3. It was, however, observed that the major axis was always smallest for the heavily loaded bearing, bearing number 2.

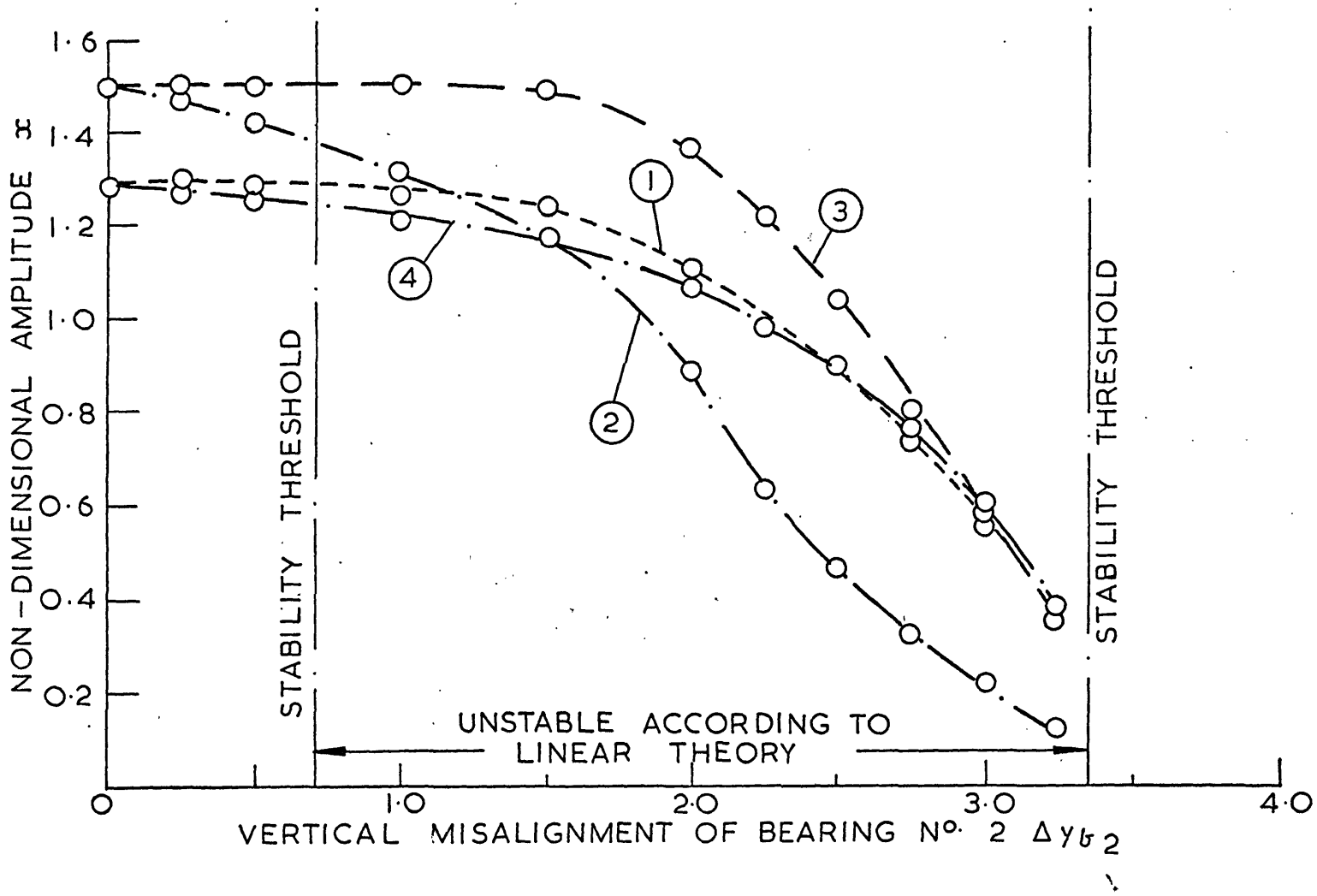


Figure 8.6: The amplitude, in the $X$ direction, of the dominant component of the steady-state whirl at each bearing of the two rotor system.

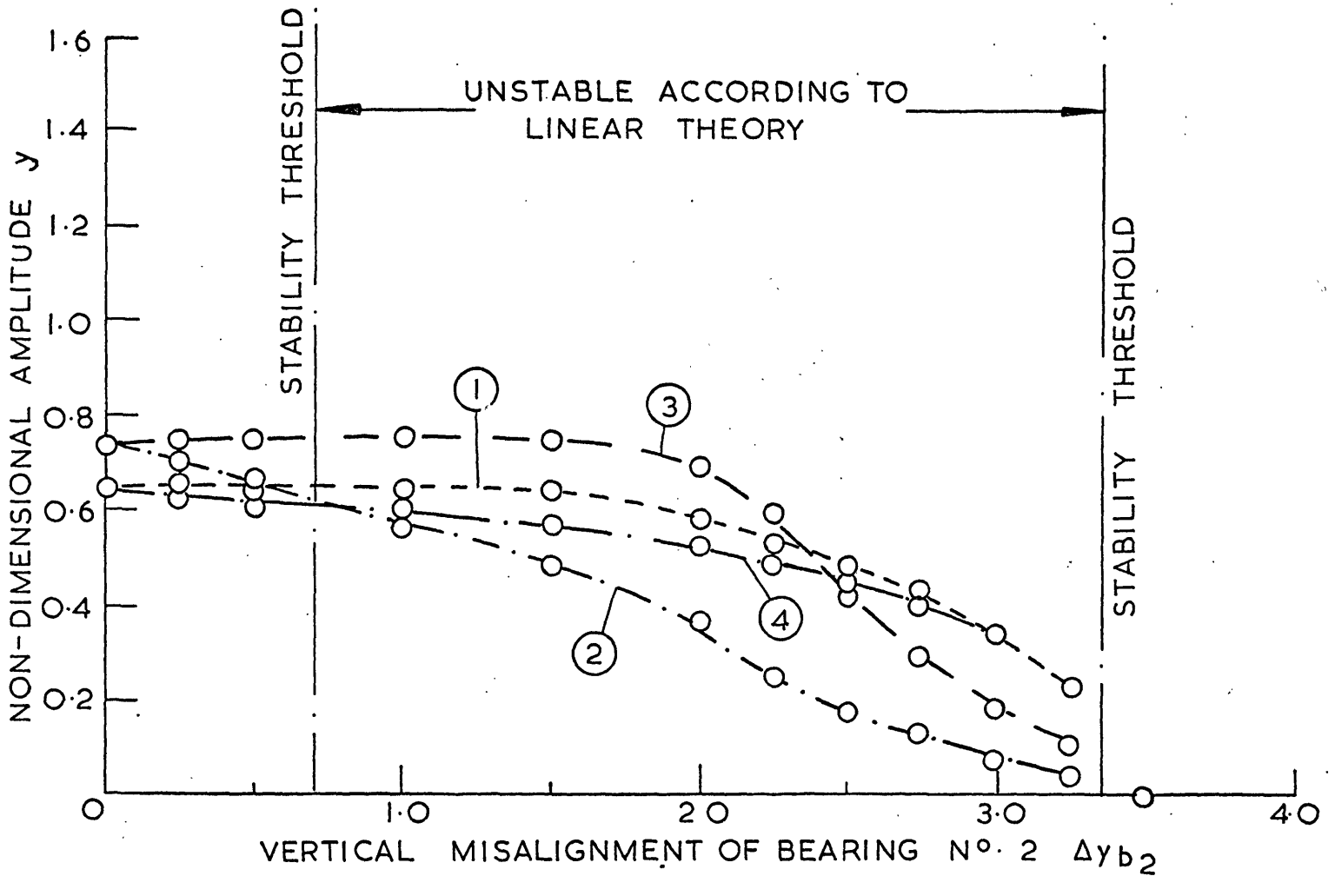


Figure 8.7: The amplitude, in the $Y$ direction, of the dominant component of the steady-state whirl at each bearing of the two rotor system.

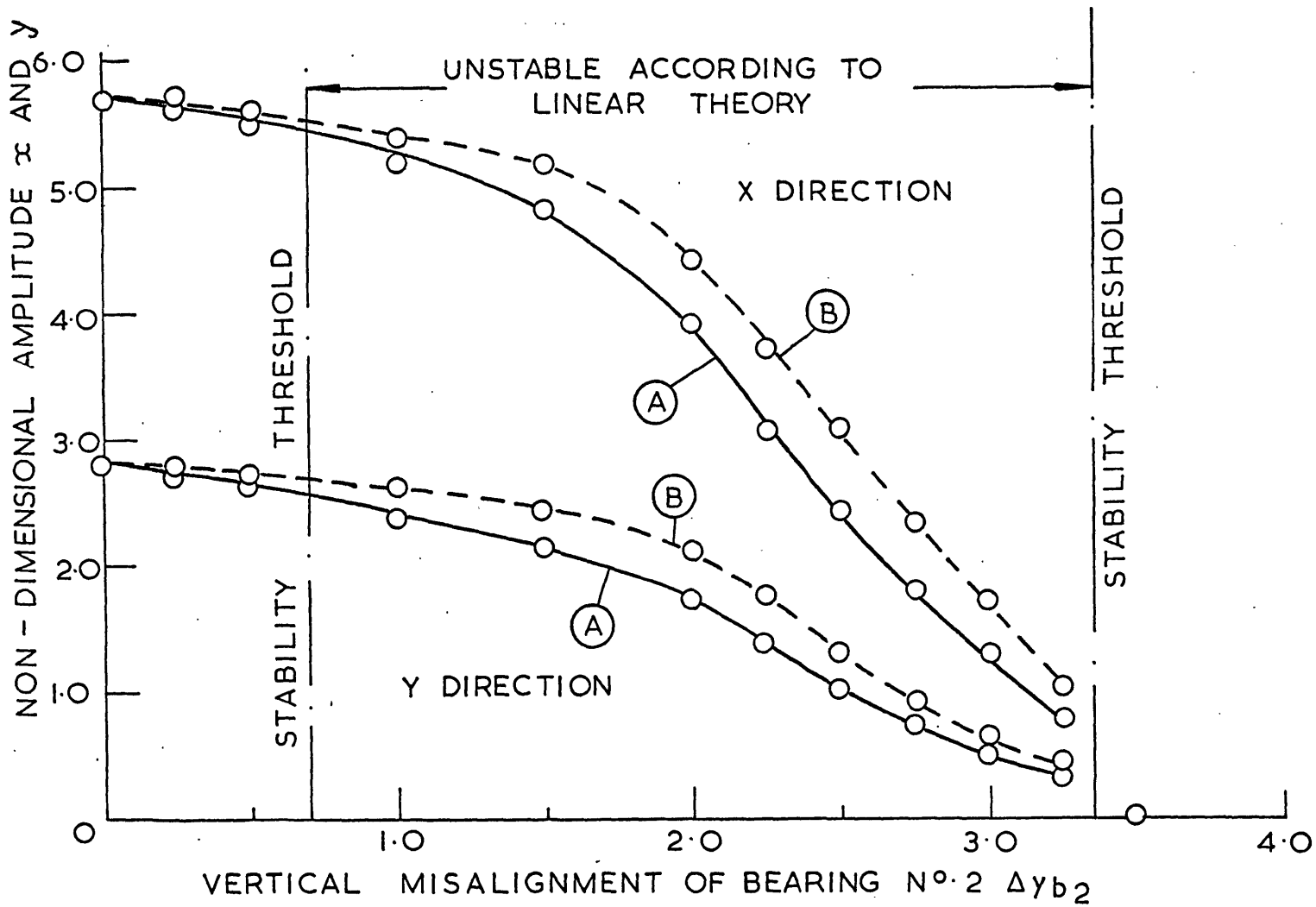


Figure 8.8: The amplitude, in the $X$ and $Y$ directions, of the dominant component of the steady-state whirl at the mid-span stations A and B of the two rotor system.

### 8.2.1 Energy Interchange Between the Shaft and the Bearings

For steady-state, self-excited motion to exist, the net energy input from the bearings to the shaft over a complete cycle must be zero. An investigation was undertaken to determine whether, during the steady-state motion, the net input of energy from each bearing to the shaft over a complete cycle is zero, or whether, alternatively, some bearings put a net amount of energy into the shaft over a complete cycle, whilst an equivalent amount of energy is extracted by the others.

From a knowledge of the oil-film forces acting on the shaft and its position at each time step ($\Delta\tau$) on the steady-state orbit, the cumulative energy ($E_c$) input to the shaft from the $k$th bearing up to a time $\tau_j$ was obtained by numerical integration using the formula:

$$E_c(\tau_j) = M c_r^2 \omega^2 \sum_{i=1}^{j} \{0.5 (f_{x_k}(\tau_j) + f_{x_k}(\tau_{j-1}))$$

$$(x(s_k, \tau_j) - x(s_k, \tau_{j-1})) + 0.5 (f_{y_k}(\tau_j) + f_{x_k}(\tau_{j-1}))$$

$$(y(s_k, \tau_j) - y(s_k, \tau_{j-1}))\} \qquad 8.15$$

in which:

$$\tau_j = \tau_s + j \Delta\tau \qquad 8.16$$

where $\tau_s$ is an arbitrary time during the steady-state motion when the cumulative energy is assumed to be zero.

For the aligned system, the net energy input by each bearing after a complete cycle was, to the accuracy obtainable, found to be zero, but during the cycle there was an interchange of energy between each bearing and the shaft. However, for a misaligned system (see Figure 8.9), individual bearings could have a net exciting or damping effect upon the

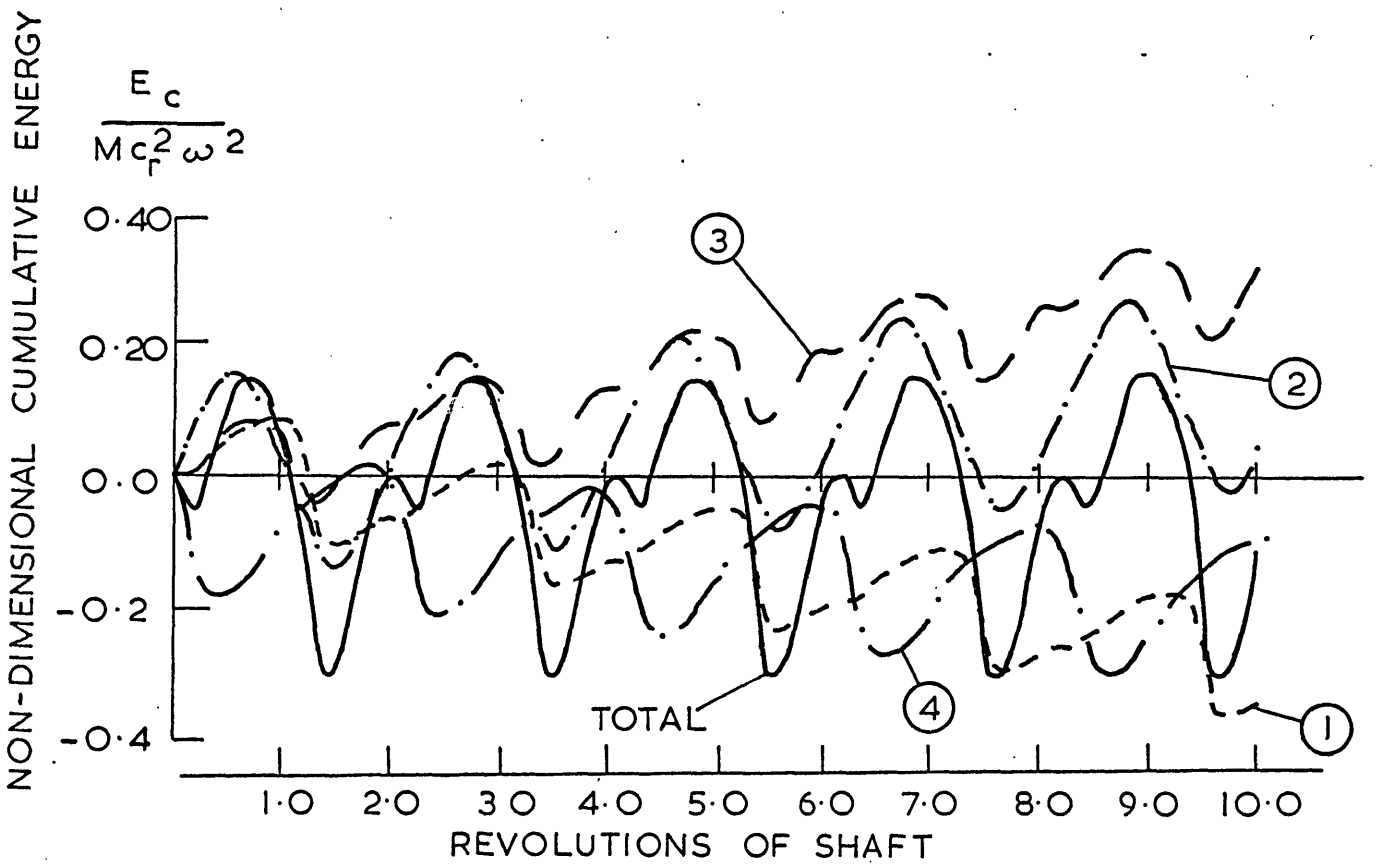


Figure 8.9: Cumulative energy input to the whirling shaft from the bearings during the steady-state motion. Two rotor system misaligned at bearing number 2 by $\Delta y_{b_2} = 2.0$.

system. In all cases, the nominally deloaded bearing put energy into the system while the damping was provided by the two end bearings, principally bearing number 1. The misaligned bearing (number 2), which was heavily loaded, either put energy into the system or remained passive.

# CHAPTER 9

# CLOSURE

## 9.1 SUMMARY AND CONCLUSIONS

### 9.1.1 General

(1) A method has been developed for predicting the non-linear flexural vibrations of a multi-rotor system. The equations of motion are in terms of the free-free modes of the coupled rotors and the modal coefficients are propagated in time using numerical initial-value-problem techniques. The method is general and may be used for any shaft for which the free-free modes and natural frequencies are known, and for any number of bearings. The modal approach effectively separates the linear dynamic characteristics of the shaft from the non-linear properties of the bearings, and allows the shaft to be represented by relatively few degrees of freedom. By using the free-free modes, the "inertia" matrix in the equations of motion is diagonalised and the equations of motion are thus in a form suitable for solution by standard numerical initial-value-problem techniques. The free-free modes also allow the relocation, insertion, removal or modification of a bearing for an existing shaft, without the need to compute a new set of modes.

(2) An adaptation of the basic method was used to calculate the horizontal and vertical bearing settings required to align the system; the equilibrium position of the rotating shaft for given bearing settings; the stability of the equilibrium

position; and the forced response of the linearised system.

(3) A computationally efficient model of a lemon-bore bearing has been developed, suitable for use in the numerical integration procedure for solving the equations of motion of the shaft. The model takes account of the region of comparatively low pressure occurring at the axial feed ports, and cavitation of the oil-film is allowed for.

(4) Frequency analysis was used to determine the amplitude and frequency of the components of the predicted steady-state motion.

(5) A considerable saving in computer time was achieved by obtaining the initial conditions for the solution procedure from the "dominant" eigenvector of the linearised system.

9.1.2 Two Rotor System Supported Upon Short Circular Bearings

(6) The non-linear behaviour of the two rotor system supported upon short circular bearings was, even with bearing misalignment, found to be essentially the same as that of a single rotor system supported upon plain circular-bore bearings, reported in the literature.

(7) In order to predict steady-state whirl at frequencies less than 0.5 $\omega$ (and closer to those normally occurring in large turbogenerators), the flexibility of the shaft had to be increased so that the rotational speed was in excess of twice

its first pinned critical speed, and external damping had to be imposed on the shaft to limit the amplitude of vibration.

(8) Tondl's vertical shaft model, the equations of motion for which may (assuming circular motion) be solved as a system of non-linear algebraic equations, was extended to treat the case of a shaft bearing distributed mass and elasticity, and supported upon more than two bearings.

(9) Using the vertical shaft model, the behaviour observed for the horizontal two rotor system was confirmed, and estimates were made of the amount of external damping required to limit the amplitude to maximum that could occur in practice without loss of internal clearance. However, the level of dissipation required could not be physically accounted for.

9.1.3 Two Rotor System Supported Upon Lemon-Bore Bearings

(10) If the two rotor system was supported upon lemon-bore bearings, the self-excited vibrations remained finite, without the application of external damping, when the shaft was rotating at speeds both above and below twice its first pinned critical speed.

(11) The amplitude and frequency of the steady-state self-excited motion was affected by parallel misalignment of the bearings. Increased misalignment tended to reduce both the amplitude and the frequency of the motion.

(12) Steady-state whirl at frequencies significantly below 0.5 $\omega$ could be induced in a shaft rotating at speeds substantially below twice its first pinned critical speed.

(13) During the steady-state, limit cycle motion, the net energy input from *each* bearing to the shaft over a complete cycle was, for the aligned condition, found to be zero. For a misaligned system, however, some bearings put a net amount of energy into the shaft whilst others extracted an equivalent amount of energy, thus maintaining the zero net input required for steady-state motion. For both situations, there was an interchange of energy between each bearing the the shaft during each cycle.

9.1.4 Principal Conclusion

(14) The steady-state self-excited motion at frequencies less than half the rotational frequency of the shaft, observed in practice, cannot be predicted without recourse to heavy external damping unless the bearing model used to obtain the oil-film forces takes account of the circumferential asymmetry of practical bearings.

## 9.2 SUGGESTIONS FOR FURTHER WORK

A method for improving the accuracy of the compensated long bearing solution, in which the side leakage factor is obtained using the method of collocation, would be desirable in order to obtain better estimates of the stability threshold for a system supported upon lemon-bore bearings. It is doubtful whether such an improvement in the accuracy of the oil-film forces would have an appreciable effect upon the results obtained for the large amplitude limit cycle behaviour of the system and so it is important that the computational time required should not increase significantly.

A comparison of the results given in Figure 7.9 and Table 7.3 would suggest that the error in the oil-film forces is principally a function of the eccentricity ratio of the journal, and are comparatively insensitive to its attitude angle or velocity. One possible method of improving the accuracy of the oil-film forces would be to obtain a further correction factor in the form of a polynomial in terms of the eccentricity ratio, i.e. (cf. equation 7.61):

$$f_e = 2\alpha^2 \beta \left(\frac{c_r}{C}\right)^2 \kappa \left(a_o + a_1 \varepsilon + a_2 \varepsilon^2 + \ldots\right) \int_{\theta_1}^{\theta_2} P_l(\theta) \cos\theta \, d\theta \qquad 9.1$$

etc. The constants $a_i$ would be obtained by curve fitting, using values of the oil-film forces obtained from finite difference solutions.

Another method for improving the accuracy would be to increase the number of trial functions in equations 7.52, but the choice of suitable trial functions, or the additional places in the pressure field where the residual should be set to zero, are not immediately obvious.

## REFERENCES

BADGLEY, R.H., & BOOKER, J.F. (1969)

"Turbogenerator Instability: Effect of Initial Transients on Plane Motion",

*J. Lubr. Technol., Trans. ASME*, Series F, 91, (4), pp. 625-633.

BISHOP, R.E.D., & JOHNSON, D.C. (1960)

"The Mechanics of Vibration",

Cambridge University Press, London.

BLACK, H.F., BROWN, R.D., FRANCE, D., & JENSSEN, D.N. (1972)

"Theoretical and Experimental Investigations Relating to Centrifugal Pump Rotor Vibrations",

Vibrations in Rotating Systems Conf., Inst. Mech. Eng., London.

BLACK, H.F., & LOCH, N.E. (1973)

"Computation of Lateral Vibration and Stability of Pump Rotors",

Computer Aided Design of Pumps and Fans Conf., Inst. Mech. Eng., Newcastle.

BLACK, H.F., & BROWN, R.D. (1976)

"Fast Dynamic Calculations for Non-Circular Bearings",

Tribology Conv., Inst. Mech. Eng., Durham.

BOOKER, J.F. (1965)

"A Table of Journal Bearing Integrals",

*J. Bas. Eng., Trans. ASME*, Series D, 87, (2), pp. 533-535.

BROWN, R.D. (1977)

Private communication,

Mechanical Engineering Department, Heriot-Watt University.

DIMENTBERG, F.M. (1961)

"Flexural Vibrations of Rotating Shafts",

Butterworths, London.

DOSTAL, M., ROBERTS, J.B., & HOLMES, R. (1974)

"Stability Control of Flexible Shafts Supported on Oil-Film Bearings",

*J. Sound & Vib.*, 35, (3), pp. 361-377.

ETTLES, C., WELLS, D.E., STOKES, M., & MATTHEWS, J.C. (1974)

"Investigation of Bearing Misalignment Problems in a 500 MW Turbo-Generator Set",

*Proc. I. Mech. E.*, 188, pp. 403-414.

FRÄNKEL, A. (1949)

"Berechnung von Zylindrischen Gleitlagern",

Diss. ETH Zürich (in German).

GEAR, C.W. (1971)

"Numerical Initial Value Problems in Ordinary Differential Equations",

Prentice-Hall, Englewood Cliffs, New Jersey, U.S.A.

GLADWELL, G.M.L., & BISHOP, R.E.D. (1959)

"The Receptances of Uniform and Non-Uniform Rotating Shafts",

*J. Mech. Eng. Sci.*, 1, (1), pp. 78-91.

GLIENECKE, J. (1966-67)

"Experimental Investigation of the Stiffness and Damping Coefficients of Turbine Bearings",

*Proc. Inst. Mech. Eng.*, 181, (3B), p. 116.

GREATHEAD, S.H. (1976)

"Investigations Into Load Dependent Vibrations of the High Pressure Rotor on Large Turbo-Generators",

Vibrations in Rotating Machinery Conf., Inst. Mech. Eng., Cambridge.

GUNTER, E.J. (1967)

"The Influence of Internal Friction on the Stability of High Speed Rotors",

*J. Eng. Ind. Trans. ASME*, Series B, 89, (4), pp. 683-688.

HAGG, A.C., & SANKEY, G.O. (1956)

"Some Dynamic Properties of Oil-Film Journal Bearings With Reference to Unbalance Vibration of Rotors",

*Trans. ASME*, 78, (June), pp. 302-305.

HAGG, A.C., & SANKEY, G.O. (1958)

"Elastic and Damping Properties of Oil-Film Journal Bearings for Application to Unbalance Vibration Calculations",

*J. Appl. Mech., Trans. ASME*, 25, p. 141.

HOLMES, A.G., & ETTLES, C.M.M. (1975)

"A Study of Iterative Solution Techniques for Elliptic Partial Differential Equations with Particular Reference to Reynolds Equation",

*Comp. Meth. Appl. Mech. Eng.*, 5, pp. 309-328.

HOLMES, R. (1960)

"The Vibration of a Rigid Shaft on Short Sleeve Bearings",

*J. Mech. Eng. Sci.*, 2, (4), pp. 337-341.

HOLMES, R. (1970)

"Non-Linear Performance of Turbine Bearings",

*J. Mech. Eng. Sci.*, 12, (6), pp. 377-380.

HORI, Y. (1959)

"A Theory of Oil Whip",

*J. Appl. Mech., Trans. ASME*, Series E, 26, (2), pp. 189-198.

HUGGINS, N.J. (1963-64)

"Non-Linear Modes of Vibration of a Rigid Rotor in Short Journal Bearings",

*Proc. Inst. Mech. Eng.*, 178, (3N), pp. 238-245.

JENNINGS, U.D., & OCVIRK, F.W. (1962)

"The Simulation of Bearing Whirl on an Electronic-Analog Computer",

*J. Bas. Eng., Trans. ASME*, Series D, 84, (4), pp. 503-510.

KIRK, R.G., & GUNTER, E.J. (1976)

"Short Bearing Analysis Applied to Rotor Dynamics" (Part 1),

*J. Lubr. Technol., Trans. ASME*, Series F, 98, (1), pp. 47-56.

LAZAN, B.J. (1968)

"Damping of Materials and Members in Structural Mechanics",

Pergamon, Oxford.

LUND, J.W. (1964)

"Spring and Damping Coefficients for the Tilting Pad Journal Bearing",

*Trans. ASLE*, 7, pp. 342-352.

LUND, J.W. (1966)

"Self-Excited Stationary Whirl Orbits of a Journal in a Sleeve Bearing",

Ph.D. Thesis, Rensselaer Polytechnic Institute, Troy, New York, U.S.A.

LUND, J.W., & ORCUTT, F.K. (1967)

"Calculations and Experiments on the Unbalance Response of a Flexible Rotor",

*J. Eng. Ind., Trans. ASME*, Series B, 89, (4), pp. 785-796.

LUND, J.W. (1974)

"Stability and Damped Critical Speeds of a Flexible Rotor in Fluid-Film Bearings",

*J. Eng. Ind., Trans. ASME*, Series B, 96, (2), pp. 509-517.

MacDUFF, J.N., & FELGAR, R.P. (1957)

"Vibration Design Charts",

*Trans. ASME*, 79, (October), pp. 1459-1475.

MAYES, I.W. (1974)

Private communication,

Midlands Region Scientific Services Department, Central Electricity Generating Board.

MEIROVITCH, L. (1967)

"Analytical Methods in Vibrations",

Macmillan, New York, U.S.A.

MITCHELL, J.R., HOLMES, R., & VAN BALLYGOOYEN, H. (1965-66)

"Experimental Determination of a Bearing Oil-Film Stiffness",

*Proc. Inst. Mech. Eng.*, 180, (3K), p. 90.

MITCHELL, J.R. (1967-68)

Discussion following Session 2, Lubrication and Wear Conf., London,

*Proc. Inst. Mech. Eng.*, 182, (3A), pp. 146-148.

MORTON, P.G. (1965-66)

"On the Dynamics of Large Turbo-Generator Rotors",

*Proc. Inst. Mech. Eng.*, 180, (1), pp. 295-329.

MORTON, P.G. (1971)

"Measurement of the Dynamic Characteristics of Large Sleeve Bearings",

*J. Lubr. Technol., Trans. ASME*, Series F, 93, (1), pp. 143-150.

MORTON, P.G. (1972)

"Analysis of Rotors Supported Upon Many Bearings",

*J. Mech. Eng. Sci.*, 14, (1), pp. 25-33.

MORTON, P.G. (1974)

"The Derivation of Bearing Characteristics by Means of Transient Excitation Applied Directly to a Rotating Shaft",

IUTAM Symp., Dynamics of Rotors, Lyngby, Denmark.

NAG (1973)

Numerical Algorithms Group, Fortran Subroutine Library Mk 3 (updated 1976 to Mk 4),

NAG Central Office, 7 Banbury Road, Oxford, U.K.

NEWKIRK, B.L., & TAYLOR, H.D. (1925)

"Shaft Whipping Due to Oil Action in Journal Bearings",

*Gen. Elect. Rev.*, 28, pp. 559-568.

NEWKIRK, B.L. (1957)

"Journal Bearing Instability",

Lubrication and Wear Conf., Inst. Mech. Eng., London.

OCVIRK, F.W. (1952)

"Short-Bearing Approximation for Full Journal Bearings",

N.A.C.A. Tech. Note, No. 2808.

PESTEL, E.C., & LECKIE, F.A. (1963)

"Matrix Methods in Elastomechanics",

McGraw-Hill, New York, U.S.A.

PINKUS, O. (1956)

"Experimental Investigation of Resonant Whip",

*Trans. ASME*, 78, (July), pp. 975-983.

PINKUS, O., & STERNLICHT, B. (1961)

"Theory of Hydrodynamic Lubrication",

McGraw-Hill, New York, U.S.A.

REDDI, M.M., & TRUMPLER, P.R. (1962)

"Stability of the High-Speed Journal Bearing Under Steady Load",

*J. Eng. Ind., Trans. ASME*, Series B, 84, (3), pp. 351-358.

SCHLICHTING, H. (1968)

"Boundary Layer Theory",

6th Edition, McGraw-Hill, New York, U.S.A.

SEERY, T.J., COLDIRON, W.B., & MARKOWSKY, J. (1972)

"Analyzing Turbine Alignment and Bearing Problems by Monitoring Oil-Film Pressure",

ASME Paper No. 72-WA/Pwr-6.

SMITH, D.M. (1969)

"Journal Bearings in Turbomachinery",

Chapman & Hall, London.

SNEDDON, I.N. (1961)

"Fourier Series",

Routledge & Kegan Paul, London.

SOMEYA, T. (1963-64)

"Stability of a Balanced Shaft Running in Cylindrical Journal Bearings",

*Proc. Inst. Mech. Eng.*, 178, (3N), pp. 196-214.

STERNLICHT, B. (1959)

"Elastic and Damping Properties of Cylindrical Journal Bearings",

*J. Bas. Eng., Trans. ASME*, Series D, 81, pp. 101-108.

STERNLICHT, B. (1967)

"Rotor Stability",

Lubrication and Wear Conf., Inst. Mech. Eng., London.

TIMOSHENKO, S.P., YOUNG, D.H., & WEAVER, W.Jnr. (1974)

"Vibration Problems in Engineering",

4th Edition, John Wiley & Son, New York, U.S.A.

TONDL, A. (1965)

"Some Problems of Rotor Dynamics",

Chapman & Hall, London.

WITTE, A.F. (1968)

"A Theoretical Modal Study for the Lateral Vibrations of Bars Having Variable Cross-Section and Free End Conditions",

*Shock & Vib. Bull.*, 38, (1), pp. 67-85.

WOODCOCK, J.S., & HOLMES, R. (1969-70)

"The Determination and Application of the Dynamic Properties of a Turbo-Rotor Bearing Oil-Film",

*Proc. Inst. Mech. Eng.*, 184, (3L), p. 111.

WRONSKI, G., DAVIES, A., & BURROWS, B.D. (1973)

"Behaviour of Turbo-Generator Bearings Under the Influence of Varying Operational Conditions",

Conv. on Steam Plant Operation, Inst. Mech. Eng., London.

# APPENDIX 1

## AN ALTERNATIVE DERIVATION OF THE EQUATIONS OF MOTION - LUMPED MASS APPROACH

An outline is given here of the derivation of the modal equations of motion for a shaft by direct consideration of the lumped mass approximation. The notation used here differs slightly from that used elsewhere in the text.

A shaft is represented by $p$ point masses connected by light elastic shaft elements. Let the mass at the $i$th station be given by $M_i$ and its transverse displacement in the horizontal and vertical directions be given by $X_i$ and $Y_i$, respectively. Let $[K]$ be a matrix of stiffness influence coefficients for the shaft, where an element of the matrix $K_{ij}$ is the force required at the $i$th station to produce unit deflection at the $j$th station and zero deflection elsewhere. It should be noted that $[K]$ is a symmetric matrix due to the reciprocity relationship, but is singular as the shaft is unconstrained.

If the external damping acting on the shaft and the unbalance forces are omitted (for the sake of brevity), then the equations of motion for the rotor system are:

$$\left.\begin{aligned} [M]\frac{d^2\{X\}}{dt^2} + [K]\{X\} &= \{F_X\} \\ [M]\frac{d^2\{Y\}}{dt^2} + [K]\{Y\} &= \{F_Y\} - g[M]\{1\} \end{aligned}\right\} \quad \text{A1.1}$$

where $[M]$ is a diagonal matrix containing the point masses; $\{F_X\}$ and $\{F_Y\}$ contain the bearing reactions at the relevant stations; and $\{1\}$ is a vector whose elements are all equal to unity.

These equations may be rendered dimensionless by dividing through each

equation by $M_T c_m \omega^2$, where $M_T$ ($= \sum_{i=1}^{p} M_i$) is the total mass of the shaft. The non-dimensional equations are:

$$\left.\begin{aligned} [m]\ \{\ddot{x}\} + [k]\ \{x\} &= \{f_x\} \\ [m]\ \{\ddot{y}\} + [k]\ \{y\} &= \{f_y\} - S_t\ [m]\ \{1\} \end{aligned}\right\} \quad \text{A1.2}$$

where:

$$x_i = X_i/c_r \quad \text{A1.3}$$

$$y_i = Y_i/c_r \quad \text{A1.4}$$

$$m_{ij} = M_{ij}/M_T \quad \text{A1.5}$$

$$k_{ij} = K_{ij}/M_T\ \omega^2 \quad \text{A1.6}$$

$$f_{x_i} = F_{X_i}/M_T\ c_r\ \omega^2 \quad \text{A1.7}$$

$$f_{y_i} = F_{Y_i}/M_T\ c_r\ \omega^2 \quad \text{A1.8}$$

Consider now the free-free vibration of the unconstrained shaft described by the homogeneous form of equations A1.2. As the equations for the horizontal and vertical directions are identical, only the one for the horizontal direction will be considered, i.e.

$$[m]\ \{\ddot{x}\} + [k]\ \{x\} = 0 \quad \text{A1.9}$$

Assume a solution of the form:

$$\{x\} = \{\Phi\}\ e^{\underline{i}\,\nu_f \tau} \quad \text{A1.10}$$

which, upon substituting into equation A1.9, leads to the eigenvalue

problem:

$$[k]\ \{\Phi^{(i)}\} = \nu_{f_i}{}^2\ [m]\ \{\Phi^{(i)}\} \qquad \text{A1.11}$$

The eigenvectors $\{\Phi^{(i)}\}$ are normalised with respect to $[m]$ by setting:

$$\{\Phi^{(i)}\}^T\ [m]\ \{\Phi^{(i)}\} = 1 \qquad \text{A1.12}$$

from which it follows directly from equation A1.11 that:

$$\{\Phi^{(i)}\}^T\ [k]\ \{\Phi^{(i)}\} = \nu_{f_i}{}^2 \qquad \text{A1.13}$$

If $\{\Phi^{(i)}\}$ and $\{\Phi^{(j)}\}$ are eigenvectors corresponding to eigenvalues $\nu_{f_i}$ and $\nu_{f_j}$, respectively, then, as $[k]$ and $[m]$ are both symmetric matrices, the following orthogonality relationship exists between them (see, for example, Timoshenko et al (1974)):

$$\{\Phi^{(i)}\}^T\ [m]\ \{\Phi^{(j)}\} = 0 \quad , \quad \text{if } \nu_{f_i} \neq \nu_{f_j} \qquad \text{A1.14}$$

$$\{\Phi^{(i)}\}^T\ [k]\ \{\Phi^{(j)}\} = 0 \quad , \quad \text{if } \nu_{f_i} \neq \nu_{f_j} \qquad \text{A1.15}$$

All the non-zero eigenvalues of equation A1.11 are, by physical consideration, necessarily distinct but as the shaft is unconstrained, it has two zero eigenvalues. For $\nu_f = 0$, equation A1.11 reduces to:

$$[k]\ \{\Phi\} = 0 \qquad \text{A1.16}$$

which is satisfied by *any* rigid body displacement of the shaft. However, it is desirable that the two rigid body eigenvectors should also be

mutually orthogonal and normalised according to equation A1.12. This is achieved by choosing them to be:

$$\{\Phi^{(1)}\} = \{1\} \qquad \text{A1.17}$$

$$\{\Phi^{(2)}\} = \frac{(\sum_{i=1}^{p} m_i s_i)\{1\} - \{s_i\}}{\sqrt{(\sum_{i=1}^{p} m_i s_i^2) - (\sum_{i=1}^{p} m_i s_i)^2}} \qquad \text{A1.18}$$

where $s_i$ is the non-dimensional displacement along the shaft to the $i$th mass station, and $\{s_i\}$ is a vector containing these.

Returning now to the situation of the shaft supported upon bearings and whose motion is expressed by equations A1.2. As the eigenvectors of equation A1.11 are mutually orthogonal, they may be used to form a basis in $p$-dimensional space and so any displacement of the shaft may be represented as a linear combination of these. This may be expressed as:

$$\{x(\tau)\} = \sum_{j=1}^{p} (q_{x_j}(\tau)\{\Phi^{(j)}\}) = [A]\{q_x(\tau)\} \qquad \text{A1.19}$$

$$\{y(\tau)\} = \sum_{j=1}^{p} (q_{y_j}(\tau)\{\Phi^{(j)}\}) = [A]\{q_y(\tau)\} \qquad \text{A1.20}$$

where: $$[A] = |\{\Phi^{(1)}\}, \{\Phi^{(2)}\}, \ldots, \{\Phi^{(p)}\}| \qquad \text{A1.21}$$

As a consequence of the orthogonality relationship existing between its columns, $[A]$ has the properties:

$$[A]^T [m] [A] = [I] \qquad \text{A1.22}$$

and: $$[A]^T [k] [A] = [\Omega] \qquad \text{A1.23}$$

where $[I]$ is the unit matrix, and $[\Omega]$ is a diagonal matrix whose elements along the diagonal are $\nu_{f_i}{}^2$. (It should be remembered that $\nu_{f_1} = \nu_{f_2} = 0$.)

Substituting equations A1.19 and A1.20 into equations A1.2 and pre-multiplying each equation by $[A]^T$ leads to:

$$\left.\begin{aligned} \{\ddot{q}_x\} + [\Omega]\{q_x\} &= [A]^T\{f_x\} \\ \{\ddot{q}_y\} + [\Omega]\{q_y\} &= [A]^T\{f_y\} - S_t[A]^T[m]\{1\} \end{aligned}\right\} \quad \text{A1.24}$$

which, upon expansion, gives:

$$\left.\begin{aligned} \ddot{q}_{x_i} + \nu_{f_i}{}^2 q_{x_i} &= \sum_{j=1}^{p} (\Phi_j^{(i)} f_{x_j}) \\ \ddot{q}_{y_i} + \nu_{f_i}{}^2 q_{y_i} &= \sum_{j=1}^{p} (\Phi_j^{(i)} f_{y_j}) - \delta_{i1} S_t \\ &, \quad (i = 1, 2, \ldots, p) \end{aligned}\right\} \quad \text{A1.25}$$

It may be seen that, but for the absence of terms for external damping and unbalance forces, these equations would have an identical *form* to equations 2.66 for a continuous shaft.

# APPENDIX 2

## A SCHEME FOR DETERMINING THE SIZE AND ORIENTATION OF THE ELLIPTICAL ORBITS OBTAINED FOR A LINEARISED SYSTEM

Equations 5.55 and 5.56, which describe an ellipse, may be written in simplified form as:

$$x = E \cos \tau - F \sin \tau \qquad \text{A2.1}$$

$$y = G \cos \tau - H \sin \tau \qquad \text{A2.2}$$

Let a new coordinate system $(x',y')$ be coincident with the principal axes of the ellipse, and let the angle between the $x$ and $x'$ axes be $\theta$. The two coordinate systems are identical except for a rotation by $\theta$ and are therefore related as follows:

$$\begin{Bmatrix} x' \\ y' \end{Bmatrix} = \begin{bmatrix} \cos \theta & \sin \theta \\ -\sin \theta & \cos \theta \end{bmatrix} \begin{Bmatrix} x \\ y \end{Bmatrix} \qquad \text{A2.3}$$

Transforming A2.1 and A2.2 into the $(x',y')$ coordinate system gives:

$$x' = (E \cos \theta + G \sin \theta) \cos \tau - (F \cos \theta + H \sin \theta) \sin \tau \qquad \text{A2.4}$$

$$y' = (G \cos \theta - E \sin \theta) \cos \tau - (H \cos \theta - F \sin \theta) \sin \tau \qquad \text{A2.5}$$

but, as the principal axes of the ellipse are coincident with the $(x',y')$ coordinates, the equation of the ellipse may be written as:

$$x' = A \cos (\tau + \beta) = A \cos \beta \cos \tau - A \sin \beta \sin \tau \qquad \text{A2.6}$$

$$y' = B \sin (\tau + \beta) = B \sin \beta \cos \tau + B \cos \beta \sin \tau \qquad \text{A2.7}$$

Therefore, equating coefficients of $\cos \tau$ and $\sin \tau$ in equations A2.4 to A2.7 gives:

$$A \cos \beta = E \cos \theta + G \sin \theta \qquad \text{A2.8}$$

$$A \sin \beta = F \cos \theta + H \sin \theta \qquad \text{A2.9}$$

$$B \sin \beta = G \cos \theta - E \sin \theta \qquad \text{A2.10}$$

$$-B \cos \beta = H \cos \theta - F \sin \theta \qquad \text{A2.11}$$

Eliminating $A$, $B$, $\cos \beta$ and $\sin \beta$ from equations A2.8 to A2.11 leads to:

$$\tan 2\theta = \frac{2\,(FH + GE)}{(F^2 + E^2) - (G^2 + H^2)} \qquad \text{A2.12}$$

from which $\theta$ may be determined.

Once $\theta$ is known, the phase angle $\beta$ may be obtained from equations A2.8 and A2.9 (or A2.10 and A2.11) and then the semi-axis $A$ is determined from equation A2.8 (or A2.9) and the semi-axis $B$ from equation A2.10 (or A2.11). If $|B| > |A|$, then $B$ is the major semi-axis and $\pi/2$ must be added to $\theta$ (adjusted to the range $-\pi/2 < \theta < \pi/2$ if necessary) to give the angle of inclination of the major axis of the ellipse to the $x$ axis. It should be noted that if $(A/B) < 0.0$ (i.e. $A$ and $B$ are of different signs), then the shaft at that station exhibits "backwards" precession.

## APPENDIX 3

## THE PARTIAL DERIVATIVES REQUIRED FOR THE VERTICAL ROTOR MODEL

The oil-film forces for a circular bearing are a function of the three variables $\varepsilon$, $\dot{\varepsilon}$ and $\dot{\psi}$ only, i.e.

$$f_e = f_e(\varepsilon, \dot{\varepsilon}, \dot{\psi}) \qquad \text{A3.1}$$

and:

$$f_\psi = f_\psi(\varepsilon, \dot{\varepsilon}, \dot{\psi}) \qquad \text{A3.2}$$

From A3.1, A3.2 and equations 6.11 to 6.17, it may be shown that the partial derivatives required to linearise equations 6.18 are given by:

$$\frac{\partial g_{R_i}}{\partial \dot{a}_{R_j}} = \sum_{k=1}^{n} \left\{ \frac{\phi_i \phi_j}{\varepsilon^2} \left( A_R^2 \frac{\partial f_e}{\partial \dot{\varepsilon}} - \frac{A_R A_I}{\varepsilon} \frac{\partial f_e}{\partial \dot{\psi}} - A_R A_I \frac{\partial f_\psi}{\partial \dot{\varepsilon}} + \frac{A_I^2}{\varepsilon} \frac{\partial f_\psi}{\partial \dot{\psi}} \right) \right\}_{s_k} - \delta_{ij} 2\gamma \qquad \text{A3.3}$$

$$\frac{\partial g_{R_i}}{\partial \dot{a}_{I_j}} = \sum_{k=1}^{n} \left\{ \frac{\phi_i \phi_j}{\varepsilon^2} \left( A_R A_I \frac{\partial f_e}{\partial \dot{\varepsilon}} + \frac{A_R^2}{\varepsilon} \frac{\partial f_e}{\partial \dot{\psi}} - A_I^2 \frac{\partial f_\psi}{\partial \dot{\varepsilon}} - \frac{A_R A_I}{\varepsilon} \frac{\partial f_\psi}{\partial \dot{\psi}} \right) \right\}_{s_k} + \delta_{ij} 2\nu_w \qquad \text{A3.4}$$

$$\frac{\partial g_{I_i}}{\partial \dot{a}_{R_j}} = \sum_{k=1}^{n} \left\{ \frac{\phi_i \phi_j}{\varepsilon^2} \left( A_R A_I \frac{\partial f_e}{\partial \dot{\varepsilon}} - \frac{A_I^2}{\varepsilon} \frac{\partial f_e}{\partial \dot{\psi}} + A_R^2 \frac{\partial f_\psi}{\partial \dot{\varepsilon}} - A_R A_I \frac{\partial f_\psi}{\partial \dot{\psi}} \right) \right\}_{s_k} - \delta_{ij} 2\nu_w \qquad \text{A3.5}$$

$$\frac{\partial g_{I_i}}{\partial \dot{a}_{I_j}} = \sum_{k=1}^{n} \left[ \frac{\phi_i \, \phi_j}{\varepsilon^2} \left( A_I^{\,2} \frac{\partial f_e}{\partial \dot{\varepsilon}} + \frac{A_R \, A_I}{\varepsilon} \frac{\partial f_e}{\partial \dot{\psi}} + A_R \, A_I \frac{\partial f_\psi}{\partial \dot{\varepsilon}} + \frac{A_R^{\,2}}{\varepsilon} \frac{\partial f_\psi}{\partial \dot{\psi}} \right) \right]_{s_k} - \delta_{ij} \, 2\gamma \qquad \text{A3.6}$$

$$\frac{\partial g_{R_i}}{\partial a_{R_j}} = \sum_{k=1}^{n} \left[ \frac{\phi_i \, \phi_j}{\varepsilon^2} \left( A_R^{\,2} \frac{\partial f_e}{\partial \varepsilon} + \varepsilon \, f_e - A_R \, A_I \frac{\partial f_\psi}{\partial \varepsilon} - A_R \left\{ \frac{A_R \, f_e - A_I \, f_\psi}{\varepsilon} \right\} \right) \right]_{s_k} - \delta_{ij} \left( \nu_w^{\,2} - \nu_{f_i}^{\,2} \right) \qquad \text{A3.7}$$

$$\frac{\partial g_{R_i}}{\partial a_{I_j}} = \sum_{k=1}^{n} \left[ \frac{\phi_i \, \phi_j}{\varepsilon^2} \left( A_R \, A_I \frac{\partial f_e}{\partial \varepsilon} - \varepsilon \, f_\psi - A_I^{\,2} \frac{\partial f_\psi}{\partial \varepsilon} - A_I \left\{ \frac{A_R \, f_e - A_I \, f_\psi}{\varepsilon} \right\} \right) \right]_{s_k} + \delta_{ij} \, 2\gamma \, \nu_w \qquad \text{A3.8}$$

$$\frac{\partial g_{I_i}}{\partial a_{R_j}} = \sum_{k=1}^{n} \left[ \frac{\phi_i \, \phi_j}{\varepsilon^2} \left( A_R \, A_I \frac{\partial f_e}{\partial \varepsilon} + \varepsilon \, f_\psi + A_R^{\,2} \frac{\partial f_\psi}{\partial \varepsilon} - A_R \left\{ \frac{A_I \, f_e + A_R \, f_\psi}{\varepsilon} \right\} \right) \right]_{s_k} - \delta_{ij} \, 2\gamma \, \nu_w \qquad \text{A3.9}$$

$$\frac{\partial g_{I_i}}{\partial a_{I_j}} = \sum_{k=1}^{n} \left[ \frac{\phi_i \, \phi_j}{\varepsilon^2} \left( A_I^{\,2} \frac{\partial f_e}{\partial \varepsilon} + \varepsilon \, f_e + A_R \, A_I \frac{\partial f_\psi}{\partial \varepsilon} - A_I \left\{ \frac{A_I \, f_e + A_R \, f_\psi}{\varepsilon} \right\} \right) \right]_{s_k} + \delta_{ij} \left( \nu_w^{\,2} - \nu_{f_i}^{\,2} \right) \qquad \text{A3.10}$$

and the partial derivatives needed to form the jacobean matrix used for the solution of equations 6.19 are:

$$\frac{\partial h_{R_i}}{\partial a_{R_j}} = \frac{\partial g_{R_i}}{\partial a_{R_j}} \qquad \text{A3.11}$$

$$\frac{\partial h_{R_i}}{\partial a_{I_j}} = \frac{\partial g_{R_i}}{\partial a_{I_j}} \qquad \text{A3.12}$$

$$\frac{\partial h_{I_i}}{\partial a_{R_j}} = \frac{\partial g_{I_i}}{\partial a_{R_j}} \qquad \text{A3.13}$$

$$\frac{\partial h_{I_i}}{\partial a_{I_j}} = \frac{\partial g_{I_i}}{\partial a_{I_j}} \qquad \text{A3.14}$$

$$\frac{\partial h_{R_i}}{\partial \nu_w} = 2\nu_w\, a_{R_i} + 2\gamma\, a_{I_i} + \sum_{k=1}^{n} \left[ \frac{\phi_i}{\varepsilon} \left( A_R \frac{\partial f_e}{\partial \dot{\psi}} - A_I \frac{\partial f_\psi}{\partial \dot{\psi}} \right) \right]_{s_k} \qquad \text{A3.15}$$

$$\frac{\partial h_{I_i}}{\partial \nu_w} = -2\gamma\, a_{R_i} + 2\nu_w\, a_{I_i} + \sum_{k=1}^{n} \left[ \frac{\phi_i}{\varepsilon} \left( A_I \frac{\partial f_e}{\partial \dot{\psi}} + A_R \frac{\partial f_\psi}{\partial \dot{\psi}} \right) \right]_{s_k} \qquad \text{A3.16}$$

where, for a short circular bearing in which $\dot{\varepsilon} = 0$ and $\dot{\psi} = \nu_w$:

$$\frac{\partial f_e}{\partial \varepsilon} = -\beta\,(0.5 - \nu_w)\, \frac{4\varepsilon\,(1 + \varepsilon^2)}{(1 - \varepsilon^2)^3} \qquad \text{A3.17}$$

$$\frac{\partial f_\psi}{\partial \varepsilon} = \beta\,(0.5 - \nu_w)\, \frac{\pi\,(1 + 2\varepsilon^2)}{2\,(1 - \varepsilon^2)^{5/2}} \qquad \text{A3.18}$$

$$\frac{\partial f_e}{\partial \dot{\varepsilon}} = -\beta\, \frac{\pi\,(1 + 2\varepsilon^2)}{2\,(1 - \varepsilon^2)^{5/2}} \qquad \text{A3.19}$$

$$\frac{\partial f_\psi}{\partial \dot{\varepsilon}} = \beta\, \frac{2\varepsilon}{(1 - \varepsilon^2)^2} \qquad \text{A3.20}$$

$$\frac{\partial f_e}{\partial \dot{\psi}} = \beta \frac{2\varepsilon^2}{(1 - \varepsilon^2)^2} \qquad \text{A3.21}$$

$$\frac{\partial f_\psi}{\partial \dot{\psi}} = - \beta \frac{\pi \varepsilon}{2 (1 - \varepsilon^2)^{3/2}} \qquad \text{A3.22}$$

## APPENDIX 4

## COMPUTER PROGRAM

### Namelist of Input and Principal Variables

AJ1(J) : $\int_0^{s_j} m_l(\eta)\, d\eta$ (c.f. equations 5.9)

AJ2(J) : $\int_0^{s_j}\int_0^{\xi} m_l(\eta)\, d\eta\, d\xi$ (c.f. equations 5.9)

ALPHA(K,I) : value of $\alpha$ for $k$th bearing, $i$th arc

AMU(I) : $\mu_i$

ANU(I) : $\nu_{f_i}$

A2NU(I) : $\nu_{f_i}^2$

ARCS(K,I) : value of $\overline{\theta}_s$ for $k$th bearing, $i$th arc (degrees)

ARCF(K,I) : value of $\overline{\theta}_f$ for $k$th bearing, $i$th arc (degrees)

BETA(K,I) : value of $\beta$ for $k$th bearing, $i$th arc

BGSHPE(K,I) : value of $\phi_i(s)$ at $k$th bearing

COEFLN(I,K) : for $k$th bearing contains linearised bearing force coefficients $\partial f_x/\partial \dot{x}$, $\partial f_x/\partial x$, $\partial f_x/\partial \dot{y}$, $\partial f_x/\partial y$, $\partial f_y/\partial \dot{x}$, $\partial f_y/\partial x$, $\partial f_y/\partial \dot{y}$, $\partial f_y/\partial y$, in that order

CAVCC : convergence criterion ($\Delta\theta_{c_n}$) for solving equation 7.41

DAMP : $2\gamma$

DELXB(K) : $\Delta x_{b_k}$

DELYB(K) : $\Delta y_{b_k}$

DATAFQ : used to store data for frequency analysis

FF3 : $\nu_{f_3}$

FX(K) : $f_{x_k}$

FY(K) : $f_{y_k}$

FQSHPE(J,I) : value of $\phi_i(s)$ at $j$th monitor point

GAMMA : $\gamma$

GC(K,I) : value of $g_c$ at $k$th bearing, $i$th arc

NBRG : $n$ - number of bearings

NCPL : number of couplings

NFRQ : number of monitor points

NMODE : $m$ - number of free-free modes in modal expansion

QQ(1,I) : $u_{x_i} = \dot{q}_{x_i}$

QQ(2,I) : $q_{x_i}$

QQ(3,I) : $u_{y_i} = \dot{q}_{y_i}$

QQ(4,I) : $q_{y_i}$

QEXI(I) : $Q_{\xi_i}$

QETA(I) : $Q_{\eta_i}$

RACSC(K,I) : value of $C/c_r$ for $k$th bearing, $i$th arc

RELAX : "$a$" in equation 7.42

SBRG(K) : $s_k$ - non-dimensional displacement along shaft to $k$th bearing

SCPL(J) : non-dimensional displacement along shaft to $j$th coupling

SFRQ(J) : non-dimensional displacement along shaft to $j$th monitor point

ST : $S_t$

T, TAU : $\tau$

WFACT : $W_a$ (see section 7.4.2.5)

W1, W2, W3, etc. : working arrays used by NAG routines

XBRG(K) : $x_{b_k}$

XDIS : $x(s,\tau)$

XDOT : $\dot{x}(s,\tau)$

YBRG(K) : $y_{b_k}$

YDIS : $y(s,\tau)$

YDOT : $\dot{y}(s,\tau)$

```
      PROGRAM MAIN(INPUT,OUTPUT,TAPE5,TAPE6)                            0001
C                                                                       0002
C**** THE NUMERICAL INTEGRATION OF THE NON-LINEAR EQUATIONS             0003
C     OF MOTION FOR THE FLEXURAL VIBRATIONS OF A ROTATING               0004
C     SHAFT SUPPORTED UPON JOURNAL BEARINGS.                            0005
C                                                                       0006
C**** AUTHOR                    A.G.HOLMES                              0007
C                                                                       0008
C**** DATE                    SEPTEMBER  1977                           0009
C                                                                       0010
C**** THE THEORY UPON WHICH THIS PROGRAMME IS BASED IS GIVEN IN         0011
C                                                                       0012
C         THE LARGE AMPLITUDE VIBRATION OF MULTI-ROTOR SYSTEMS          0013
C               SUPPORTED UPON OIL-FILM BEARINGS.                       0014
C                                                                       0015
C                                BY                                     0016
C                                                                       0017
C                             A.G.HOLMES                                0018
C                                                                       0019
C               PH.D. THESIS  LONDON UNIVERSITY  1977/78                0020
C                                                                       0021
C                                                                       0022
C                                                                       0023
C**** THE PROGRAMME IS (SUBJECT TO THE ASSUMPTIONS STATED IN CHAPTER 2) 0024
C     GENERALLY APPLICABLE TO ANY ROTOR SYSTEM FOR WHICH THE FREE-FREE  0025
C     MODES AND NATURAL FREQUENCIES ARE KNOWN AND A SUITABLE MODEL      0026
C     FOR THE BEARINGS FORCES IS AVAILABLE. THE BEARING FORCES ARE      0027
C     CALCULATED BY SUBROUTINE FILMXY AND THE VERSION OF THIS           0028
C     SUBROUTINE GIVEN HERE IS FOR A LEMON BORE BEARING.                0029
C                                                                       0030
C**** THIS VERSION OF THE PROGRAMME IS DESIGNED TO BE USED IN           0031
C     CONJUNCTION WITH AN ON-LINE PLOTING FACILITY.                     0032
C                                                                       0033
C**** THE PROGRAMME HAS BEEN DIMENSIONED FOR                            0034
C                                                                       0035
C                        NMODE .LE. 10                                  0036
C                         NBRG .LE. 6                                   0037
C                         NCPL .LE. 2                                   0038
C                         NFRQ .LE. 6                                   0039
C                                                                       0040
C     IF VALUES LARGER THAN THE ABOVE MAXIMA ARE REQUIRED THEN THE      0041
C     THE PROGRAMME DIMENSIONS MUST BE INCREASED AND THE FOLLOWING      0042
C     STATEMENTS MODIFIED AS SHOWN WHERE EVER THEY APPEAR               0043
C                                                                       0044
C            M=NMODE , N=NBRG , J=NCPL , K=NFRQ                         0045
C                                                                       0046
C                                                                       0047
C     BLANK COMMON                                                      0048
C     ------------                                                      0049
C                                                                       0050
C     QQ(4,M),A2NU(M),SBRG(N),XBRG(N),YBRG(N),BGSHPE(N,M),SCPL(J)       0051
C     AJ1(J),AJ2(J),SFRQ(K),FQSHPE(K,M),QEXI(M),QETA(M),FX(N),FY(N)     0052
C     COEFLN(8,N),DATAFQ(2048*K)                                        0053
C                                                                       0054
C     COMMON /BRGSET/                                                   0055
C     ---------------                                                   0056
C                                                                       0057
C     BETA(N,2),GC(N,2),RSCAC(N,2),ARCL(N,2),ALGAM(N,2)                 0058
C     SCOS(N,2),SSIN(N,2),FCOS(N,2),FSIN(N,2)                           0059
C                                                                       0060
C     DIMENSION, EQUIVALENCE AND CALLS TO SUBROUTINES                   0061
C     -----------------------------------------------                   0062
C                                                                       0063
C     DETAILS ARE GIVEN IN THE RELEVANT SUBROUTINES                     0064
C                                                                       0065
C                                                                       0066
C                                                                       0067
C**** THE PROGRAMME CALLS THE FOLLOWING NAG LIBRARY SUBROUTINES         0068
C                                                                       0069
C     C06AAF  CALCULATES THE FINITE FOURIER TRANSFORM OF A SET OF       0070
C             REAL DATA VALUES USING THE COOLEY-TUKEY ALGORITHM.        0071
C                                                                       0072
C     D02ABF  INTEGRATES A SYSTEM OF ORDINARY DIFFERENTIAL EQUATIONS    0073
C             OVER A RANGE,USING MERSONS METHOD.                        0074
C                                                                       0075
C     F02AFF  FINDS ALL THE EIGENVALUES OF A REAL UNSYMMETRIC MATRIX.   0076
C                                                                       0077
C     F02AGF  CALCULATES ALL THE EIGENVALUES AND EIGENVECTORS OF A      0078
C             REAL UNSYMMETRIC MATRIX.                                  0079
C                                                                       0080
```

```
C     F04ATF  SOLVES A SET OF REAL LINEAR ALGEBRAIC EQUATIONS,          0081
C             BY CROUTS FACTORIZATION METHOD.                           0082
C                                                                       0083
C     M01AAF  PERFORMS A DETACHED KEY SORT,SORTING AN INDEX ARRAY TO    0084
C             GIVE THE ASCENDING ORDER OF A REAL ARRAY. (USED TO SORT   0085
C             THE DAMPED EIGENVALUES OF THE LINEARIZED SYSTEM INTO      0086
C             ORDER OF ASCENDING FREQUENCY.)                            0087
C                                                                       0088
      COMMON QQ(4,10),A2NU(10),NMODE,ST,DAMP,NBRG,SBRG(6),XBRG(6)       0089
     +,YBRG(6),BGSHPE(6,10),NCPL,SCPL(2),AJ1(2),AJ2(2),NFRQ,SFRQ(6)     0090
     +,FQSHPE(6,10),QEXI(10),QETA(10),FX(6),FY(6),COEFLN(8,6)           0091
     +,XDOT,XDIS,YDOT,YDIS,DATAFQ(12288)                                0092
      DIMENSION DELXB(6),DELYB(6)                                       0093
C                                                                       0094
C**** STATEMENT MODIFICATIONS FOR INCREASED PROGRAMME DIMENSIONS        0095
C                                                                       0096
C     DIMENSION                                                         0097
C     ---------                                                         0098
C                                                                       0099
C     DELXB(N),DELYB(N)                                                 0100
C                                                                       0101
C**** READ IN ALL DATA EXCEPT SHAFT AND BEARING DATA                    0102
C                                                                       0103
      READ(5,5010) NMODE,NBRG,NCPL,NFRQ,ISTART                          0104
      READ(5,5020) ST,GAMMA                                             0105
      READ(5,5020) (SBRG(N),N=1,NBRG)                                   0106
      READ(5,5020) (XBRG(N),YBRG(N),N=1,NBRG)                           0107
      READ(5,5020) (DELXB(N),DELYB(N),N=1,NBRG)                         0108
      IF(NCPL.NE.0) READ(5,5020) (SCPL(I),I=1,NCPL)                     0109
      READ(5,5020) (QEXI(I),QETA(I),I=1,NMODE)                          0110
      READ(5,5020) (SFRQ(I),I=1,NFRQ)                                   0111
C                                                                       0112
C**** MANIPULATE DATA WHERE NECESSARY AND WRITE OUT PROGRAMME VARIABLES  0113
C                                                                       0114
      DAMP=2.0*GAMMA                                                    0115
      WRITE(6,6010)                                                     0116
      WRITE(6,6020) NMODE,NBRG,NCPL,ST,GAMMA                            0117
C                                                                       0118
C**** CALL ASHAFT TO READ IN DATA FOR SHAFT TO SET UP                   0119
C     ARRAYS A2NU,BGSHPE,FQSHPE,AJ1,AJ2                                 0120
C                                                                       0121
      CALL ASHAFT                                                       0122
C                                                                       0123
C**** CALL SETBRG TO READ IN BEARING DATA AND SET UP ARRAYS USED        0124
C     IN OBTAINING OIL-FILM FORCES                                      0125
C                                                                       0126
      CALL SETBRG                                                       0127
C                                                                       0128
C**** CALL ALIGNM TO DETERMINE AND SET HORIZONTAL AND VERTICAL POSITION 0129
C     OF THE BEARINGS IN ORDER TO GIVE A CORRECTLY ALIGNED SYSTEM. SET  0130
C     NCPL=0 IN INPUT DATA TO PREVENT A CALL TO THIS ROUTINE.           0131
C                                                                       0132
      IF(NCPL.NE.0) CALL ALIGNM                                         0133
C                                                                       0134
C**** WRITE OUT BEARING LOCATIONS AND MISALIGNMENTS                     0135
C                                                                       0136
      WRITE(6,6030)                                                     0137
      WRITE(6,6040) (N,SBRG(N),XBRG(N),YBRG(N),N=1,NBRG)                0138
      WRITE(6,6050)                                                     0139
      WRITE(6,6060) (N,DELXB(N),DELYB(N),N=1,NBRG)                      0140
C                                                                       0141
C**** MISALIGN BEARINGS                                                 0142
C                                                                       0143
      DO 10 N=1,NBRG                                                    0144
      XBRG(N)=XBRG(N)+DELXB(N)                                          0145
      YBRG(N)=YBRG(N)+DELYB(N)                                          0146
10    CONTINUE                                                          0147
C                                                                       0148
C**** WRITE OUT GENERALIZED UNBALANCE COMPONENTS AND LOCATION OF        0149
C     MONITOR POINTS                                                    0150
C                                                                       0151
      WRITE(6,6070)                                                     0152
      WRITE(6,6080) (I,QEXI(I),QETA(I),I=1,NMODE)                       0153
      WRITE(6,6090)                                                     0154
      WRITE(6,6100) (I,SFRQ(I),I=1,NFRQ)                                0155
C                                                                       0156
C**** CALL STATIC TO FIND EQUILIBRIUM POSITION OF SHAFT                 0157
C                                                                       0158
      CALL STATIC                                                       0159
C                                                                       0160
C**** ROUTINES LNSVEC AND LNSTAB BOTH CALCULATE THE EIGENVALUES OF      0161
```

```
C     THE LINEARIZED SYSTEM AT THE EQUILIBRIUM POSITION OF THE SHAFT.      0162
C     IF THE INITIAL CONDITIONS FOR THE NON-LINEAR SOLUTION PROCEDURE      0163
C     ARE TO BE GIVEN BY THE EIGENVECTOR CORRESPONDING TO THE              0164
C     EIGENVALUE WITH MAXIMUM REAL PART THEN LNSVEC SHOULD BE CALLED.      0165
C     THIS IS ACHIEVED BY SETTING ISTART=1 IN THE INPUT DATA. OTHERWISE    0166
C     LNSTAB IS CALLED AND THE INITIAL CONDITIONS CORRESPOND TO            0167
C     STARTING FROM REST AT THE EQUILIBRIUM POSITION.                      0168
C                                                                          0169
      IF(ISTART.EQ.1) CALL LNSVEC                                          0170
      IF(ISTART.NE.1) CALL LNSTAB                                          0171
C                                                                          0172
C**** CALL PROPGT TO INTEGRATE THE EQUATIONS UNTIL THE STEADY-STATE        0173
C     IS REACHED AND THEN FOR A FUTHER 64 REVOLUTIONS TO OBTAIN DATA       0174
C     FOR FREQUENCY ANALYSIS                                               0175
C                                                                          0176
      CALL PROPGT                                                          0177
C                                                                          0178
C**** CALL FORIER TO FREQUENCY ANALYSE DATA OBTAINED FOR STEADY-STATE      0179
C     MOTION AT MONITOR POINTS.                                            0180
C                                                                          0181
      CALL FORIER                                                          0182
C                                                                          0183
      STOP                                                                 0184
C                                                                          0185
5010  FORMAT(5I10)                                                         0186
5020  FORMAT(8F10.0)                                                       0187
6010  FORMAT(1H1///5X                                                      0188
     +,53HTHE NUMERICAL INTEGRATION OF THE NON-LINEAR EQUATIONS/5X         0189
     +,51HOF MOTION FOR THE FLEXURAL VIBRATIONS OF A ROTATING/5X           0190
     +,38HSHAFT SUPPORTED UPON JOURNAL BEARINGS.)                          0191
6020  FORMAT(//5X,20HGOVERNING PARAMETERS/5X,20H--------------------//5X   0192
     +,7HNMODE =,I13/5X                                                    0193
     +,7HNBRG  =,I13/5X                                                    0194
     +,7HNCPL  =,I13//5X                                                   0195
     +,7HST    =,E13.5/5X                                                  0196
     +,7HGAMMA =,E13.5)                                                    0197
6030  FORMAT(///5X,20HLOCATION OF BEARINGS/5X,20H--------------------//    0198
     +,6X,1HN,19X,26HPOSITION RELATIVE TO DATUM//22X                       0199
     +,3H(S),12X,3H(X),12X,3H(Y)/)                                         0200
6040  FORMAT(5X,I2,8X,E13.5,2X,E13.5,2X,E13.5)                             0201
6050  FORMAT(//5X,40HBEARING MISALIGNMENT FROM ABOVE SETTINGS//15X         0202
     +,3H(X),12X,3H(Y)/)                                                   0203
6060  FORMAT(5X,I2,2X,E13.5,2X,E13.5)                                      0204
6070  FORMAT(//5X,32HGENERALIZED UNBALANCE COMPONENTS/5X                   0205
     +,32H--------------------------------//6X,1HI,9X,7HQEXI(I),10X       0206
     +,7HQETA(I)/)                                                         0207
6080  FORMAT(5X,I2,4X,E13.5,4X,E13.5)                                      0208
6090  FORMAT(//5X,49HLOCATION OF MONITOR POINTS FOR FREQUENCY ANALYSIS/    0209
     +         5X,49H-------------------------------------------------/    0210
     +//17X,3H(S)/)                                                        0211
6100  FORMAT(5X,I2,3X,E13.5)                                               0212
      END                                                                  0213
```

```
      SUBROUTINE ASHAFT                                                  0214
C                                                                        0215
C**** ASHAFT SETS UP ARRAYS A2NU,BGSHPE,FQSHPE,AJ1,AJ2                   0216
C                                                                        0217
C**** STATEMENT MODIFICATIONS FOR INCREASED PROGRAMME DIMENSIONS         0218
C                                                                        0219
C     DIMENSION                                                          0220
C     ---------                                                          0221
C                                                                        0222
C     SHPE(M),ANU(M)                                                     0223
C                                                                        0224
      COMMON QQ(4,10),A2NU(10),NMODE,ST,DAMP,NBRG,SBRG(6),XBRG(6)        0225
     +,YBRG(6),BGSHPE(6,10),NCPL,SCPL(2),AJ1(2),AJ2(2),NFRQ,SFRQ(6)      0226
     +,FQSHPE(6,10),QEXI(10),QETA(10),FX(6),FY(6),COEFLN(8,6)            0227
     +,XDOT,XDIS,YDOT,YDIS,DATAFQ(12288)                                 0228
      DIMENSION SHPE(10),ANU(10)                                         0229
C                                                                        0230
C**** READ IN A DATA CARD. IF ISHAFT=1  A UNIFORM SHAFT IS ASSUMED       0231
C     AND THE REQUIRED SHAFT DATA IS OBTAINED ANALYTICALLY FROM          0232
C     ROUTINE UNIFRM. OTHERWISE THE REQUIRED DATA IS READ IN. NOTE       0233
C     THE VALUE OF FF3 IS ONLY RELEVANT IF THE UNIFORM SHAFT OPTION      0234
C     IS CHOSEN                                                          0235
C                                                                        0236
      READ(5,5010) ISHAFT,FF3                                            0237
      IF(ISHAFT.EQ.1) GO TO 20                                           0238
C                                                                        0239
C**** READ DATA INTO ARRAYS ANU,BGSHPE,FQSHPE,AJ1,AJ2                    0240
C                                                                        0241
      READ(5,5020) (ANU(I),I=1,NMODE)                                    0242
      READ(5,5020) ((BGSHPE(N,I),I=1,NMODE),N=1,NBRG)                    0243
      READ(5,5020) ((FQSHPE(K,I),I=1,NMODE),K=1,NFRQ)                    0244
      IF(NCPL.NE.0) READ(5,5020) (AJ1(J),AJ2(J),J=1,NCPL)                0245
C                                                                        0246
      WRITE(6,6010)                                                      0247
      DO 10 I=1,NMODE                                                    0248
      A2NU(I)=ANU(I)*ANU(I)                                              0249
      WRITE(6,6020) I,ANU(I)                                             0250
10    CONTINUE                                                           0251
      RETURN                                                             0252
C                                                                        0253
C**** CALCULATE THE SHAFT DATA FOR A UNIFORM SHAFT                       0254
C                                                                        0255
20    DO 22 N=1,NBRG                                                     0256
      CALL UNIFRM(NMODE,SBRG(N),SHPE,1)                                  0257
      DO 24 M=1,NMODE                                                    0258
      BGSHPE(N,M)=SHPE(M)                                                0259
24    CONTINUE                                                           0260
22    CONTINUE                                                           0261
      DO 26 I=1,NFRQ                                                     0262
      CALL UNIFRM(NMODE,SFRQ(I),SHPE,1)                                  0263
      DO 28 M=1,NMODE                                                    0264
      FQSHPE(I,M)=SHPE(M)                                                0265
28    CONTINUE                                                           0266
26    CONTINUE                                                           0267
      IF(NCPL.EQ.0) GO TO 32                                             0268
      DO 30 J=1,NCPL                                                     0269
      AJ1(J)=SCPL(J)                                                     0270
      AJ2(J)=0.5*SCPL(J)*SCPL(J)                                         0271
30    CONTINUE                                                           0272
C                                                                        0273
32    CALL UNIFRM(NMODE,FF3,ANU,0)                                       0274
      WRITE(6,6010)                                                      0275
      DO 34 I=1,NMODE                                                    0276
      A2NU(I)=ANU(I)*ANU(I)                                              0277
      WRITE(6,6020) I,ANU(I)                                             0278
34    CONTINUE                                                           0279
      RETURN                                                             0280
C                                                                        0281
5010  FORMAT(I10,F10.0)                                                  0282
5020  FORMAT(8F10.0)                                                     0283
6010  FORMAT(///5X                                                       0284
     +,58HNON-DIMENSIONAL FREE-FREE NATURAL FREQUENCIES OF THE SHAFT/5X  0285
     +,58H-----------------------------------------------------///)      0286
6020  FORMAT(5X,I2,3X,E13.5)                                             0287
      END                                                                0288
```

```
      SUBROUTINE SETBRG                                                 0289
C                                                                       0290
C**** SETBRG READS IN THE DATA FOR A LEMON BORE BEARING AND SETS        0291
C     UP THE ARRAYS NEEDED BY FILMXY FOR OBTAINING THE OIL-FILM FORCES. 0292
C                                                                       0293
C**** STATEMENT MODIFICATIONS FOR INCREASED PROGRAMME DIMENSIONS        0294
C                                                                       0295
C     DIMENSION                                                         0296
C     ---------                                                         0297
C                                                                       0298
C     RACSC(N,2),ARCS(N,2),ARCF(N,2),ALPHA(N,2)                         0299
C                                                                       0300
      COMMON QQ(4,10),A2NU(10),NMODE,ST,DAMP,NBRG,SBRG(6),XBRG(6)       0301
     +,YBRG(6),BGSHPE(6,10),NCPL,SCPL(2),AJ1(2),AJ2(2),NFRQ,SFRQ(6)     0302
     +,FQSHPE(6,10),QEXI(10),QETA(10),FX(6),FY(6),COEFLN(3,6)           0303
     +,XDOT,XDIS,YDOT,YDIS,DATAFQ(12288)                                0304
      COMMON /SRQSET/ BETA(6,2),GC(6,2),RSCAC(6,2),ARCL(6,2),ALGAM(6,2) 0305
     +,FXA(2),FYA(2),SCOS(6,2),SSIN(6,2),FCOS(6,2),FSIN(6,2),CAVCC,WFACT 0306
      DIMENSION RACSC(6,2),ARCS(6,2),ARCF(6,2),ALPHA(6,2)               0307
C                                                                       0308
      PI=3.14159265358979                                               0309
C                                                                       0310
      READ(5,5010) ((BETA(N,K),ARCS(N,K),ARCF(N,K),GC(N,K),RACSC(N,K)   0311
     +              ,ALPHA(N,K),K=1,2),N=1,NBRG)                        0312
      WRITE(6,6010)                                                     0313
      WRITE(6,6020) ((N,K,BETA(N,K),ARCS(N,K),ARCF(N,K),GC(N,K)         0314
     +               ,RACSC(N,K),ALPHA(N,K),K=1,2),N=1,NBRG)            0315
C                                                                       0316
      DO 10 N=1,NBRG                                                    0317
      DO 12 NA=1,2                                                      0318
      ARCL(N,NA)=(ARCF(N,NA)-ARCS(N,NA)-1.0)*PI/180.0                   0319
      SCOS(N,NA)=COS(ARCS(N,NA)*PI/180.0)                               0320
      SSIN(N,NA)=SIN(ARCS(N,NA)*PI/180.0)                               0321
      FCOS(N,NA)=COS(ARCF(N,NA)*PI/180.0)                               0322
      FSIN(N,NA)=SIN(ARCF(N,NA)*PI/180.0)                               0323
      RSCAC(N,NA)=1.0/RACSC(N,NA)                                       0324
      ALGAM(N,NA)=2.0*ALPHA(N,NA)*ALPHA(N,NA)                           0325
      BETA(N,NA)=ALGAM(N,NA)*RSCAC(N,NA)*RSCAC(N,NA)*BETA(N,NA)         0326
12    CONTINUE                                                          0327
10    CONTINUE                                                          0328
C                                                                       0329
      CAVCC=0.015                                                       0330
      WFACT=-0.01                                                       0331
C                                                                       0332
      RETURN                                                            0333
C                                                                       0334
5010  FORMAT(6F10.0)                                                    0335
6010  FORMAT(//5X,8HBEARINGS/5X,8H--------//6X,1HN,2X,3HARC,6X,4HBETA   0336
     +      ,6X,4HARCS,6X,4HARCF,7X,2HCG,5X,5HRACSC,4X,5HALPHA/)        0337
6020  FORMAT(5X,I2,3X,I1,4X,F7.3,4X,F6.2,3X,F7.2,3X,F7.3,3X,F6.3,3X,F6.3 0338
     +  /5X,I2,3X,I1,4X,F7.3,3X,F7.2,3X,F7.2,3X,F7.3,3X,F6.3,3X,F6.3/)  0339
      END                                                               0340
```

```
      SUBROUTINE PROPGT                                                 0341
C                                                                       0342
C**** PROPGT INTEGRATES THE EQUATIONS OF MOTION (2.74) UNTIL THE        0343
C     STEADY-STATE HAS BEEN REACHED AND THEN FOR A FURTHER 64           0344
C     REVOLUTIONS OF THE SHAFT TO OBTAIN DATA FOR FREQUENCY ANALYSIS.   0345
C     DURING BOTH STAGES DATA IS GENERATED FOR THE ON-LINE GRAPH        0346
C     FACILITY TO PLOT THE TRAJECTORIES OF THE SHAFT AT THE MONITOR     0347
C     STATIONS. IT SHOULD BE NOTED THAT THIS ROUTINE OPERATES           0348
C     INTERACTIVELY TO ENABLE THE USER - WHO BY INSPECTION OF THE       0349
C     PLOTTED TRAJECTORIES ASCERTAINS WHEN THE STEADY-STATE HAS BEEN    0350
C     REACHED - TO SPECIFY WHEN DATA COLLECTION FOR THE FREQUENCY       0351
C     ANALYSIS SHOULD BEGIN. THE NUMBER OF DATA INTERVALS FOR BOTH      0352
C     STAGES OF THE SOLUTION PROCEDURE HAS BEEN SET TO 16               0353
C     I.E.  NPOINT=16 .                                                 0354
C                                                                       0355
C**** STATEMENT MODIFICATIONS FOR INCREASED PROGRAMME DIMENSIONS        0356
C                                                                       0357
C     DIMENSION                                                         0358
C     ---------                                                         0359
C                                                                       0360
C     Q(4*M),ER(4*M),W1(4*M),W2(4*M),W3(4*M),W4(4*M),W5(4*M),W6(4*M)    0361
C     X(N),Y(N)                                                         0362
C                                                                       0363
      COMMON QQ(4,10),A2NU(10),NMODE,ST,DAMP,NBRG,SBRG(6),XBRG(6)       0364
     +,YBRG(6),BGSHPE(6,10),NCPL,SCPL(2),AJ1(2),AJ2(2),NFRQ,SFRQ(6)     0365
     +,FQSHPE(6,10),QEXI(10),QETA(10),FX(6),FY(6),COEFLN(8,6)           0366
     +,XDOT,XDIS,YDOT,YDIS,DATAFQ(12288)                                0367
      DIMENSION Q(40),ER(40),W1(40),W2(40),W3(40),W4(40),W5(40),W6(40)  0368
     +,X(6),Y(6)                                                        0369
      EXTERNAL DERIVT                                                   0370
C                                                                       0371
C**** INITIALIZE AND SET VARIABLES                                      0372
C                                                                       0373
      PI=3.14159265358979                                               0374
      NPOINT=16                                                         0375
      N5REV=5*NPOINT                                                    0376
      H0=2.0*PI/FLOAT(NPOINT)                                           0377
      H=0.05*H0                                                         0378
      NEQ=4*NMODE                                                       0379
C                                                                       0380
C**** FOR ROUTINE D02ABF THE VARIABLES TO BE PROPOGATED MUST BE         0381
C     CONTAINED IN A ONE DIMENSIONAL ARRAY SO DEFINE A NEW ARRAY Q      0382
C     AS                                                                0383
C                                                                       0384
C     Q(I+4*(M-1))=QQ(I,M) ,   I=1,..,4 ,  M=1,....,NMODE               0385
C                                                                       0386
C                                                                       0387
      DO 12 I=1,NEQ                                                     0388
      Q(I)=QQ(I,1)                                                      0389
      ER(I)=1.0E-5                                                      0390
12    CONTINUE                                                          0391
      T=0.0                                                             0392
      IFAIL=0                                                           0393
      IT=1                                                              0394
      NDATA=0                                                           0395
      NSTEP=0                                                           0396
10    NSTEP=NSTEP+1                                                     0397
C                                                                       0398
C**** CALL D02ABF TO INTEGRATE EQUATIONS OF MOTION OVER INTERVAL H0     0399
C                                                                       0400
      CALL D02ABF(T,Q,ER,IT,NEQ,IFAIL,H0,H,DERIVT,W1,W2,W3,W4,W5,W6)    0401
      DO 16 I=1,NEQ                                                     0402
      QQ(I,1)=Q(I)                                                      0403
16    CONTINUE                                                          0404
C                                                                       0405
C**** CALCULATE DISPLACEMENTS IN HORIZONTAL AND VERTICAL DIRECTIONS     0406
C     AT MONITOR STATIONS                                               0407
C                                                                       0408
      DO 20 K=1,NFRQ                                                    0409
      X(K)=0.0                                                          0410
      Y(K)=0.0                                                          0411
      DO 22 I=1,NMODE                                                   0412
      X(K)=X(K)+QQ(2,I)*FQSHPE(K,I)                                     0413
      Y(K)=Y(K)+QQ(4,I)*FQSHPE(K,I)                                     0414
22    CONTINUE                                                          0415
20    CONTINUE                                                          0416
C                                                                       0417
C**** CALL PLOTTING ROUTINE TO PLOT THE NEXT LINE-SEGMENT OF THE        0418
C     SHAFT TRAJECTORIES.                                               0419
C                                                                       0420
      CALL PLOTER(X,Y)                                                  0421
```

```
C                                                                       0422
      IF(NDATA.GT.0) GO TO 32                                           0423
C                                                                       0424
C**** EVERY FIVE REVOLUTIONS OF THE SHAFT ASK (INTERACTIVELY) IF        0425
C     STEADY-STATE HAS BEEN REACHED, IF YES START STORING DATA.         0426
C                                                                       0427
      IF(MOD(NSTEP,N5REV),NE.0) GO TO 10                                0428
C                                                                       0429
      PRINT 1000                                                        0430
      READ*,IFRQ                                                        0431
      IF(IFRQ.NE.1) GO TO 10                                            0432
C                                                                       0433
C**** STORE DATA FOR FREQUENCY ANALYSIS                                 0434
C                                                                       0435
32    NDATA=NDATA+1                                                     0436
      DO 30 K=1,NFRQ                                                    0437
      J=(K-1)*2048                                                      0438
      DATAFQ(J     +NDATA)=X(K)                                         0439
      DATAFQ(J+1024+NDATA)=Y(K)                                         0440
30    CONTINUE                                                          0441
C                                                                       0442
C**** IF ALL STEADY-STATE DATA HAS BEEN OBTAINED RETURN TO              0443
C     MAIN PROGRAMME FOR CALL TO FREQUENCY ANALYSIS ROUTINE             0444
C                                                                       0445
      IF(NDATA.LT.1024) GO TO 10                                        0446
C                                                                       0447
      RETURN                                                            0448
1000  FORMAT(40H P/I .+1 IF STEADY-STATE HAS BEEN REACHED)              0449
C                                                                       0450
      END                                                               0451
```

```
      SUBROUTINE DERIVT(F,Q,T)                                          0452
C                                                                       0453
C**** DERIVT IS CALLED BY NAG ROUTINE D02ABF TO CALCULATE THE           0454
C     RHS OF EQUATIONS 2.74                                             0455
C                                                                       0456
C**** STATEMENT MODIFICATIONS FOR INCREASED PROGRAMME DIMENSIONS        0457
C                                                                       0458
C     DIMENSION                                                         0459
C     ---------                                                         0460
C                                                                       0461
C     Q(4*M),F(4*M)                                                     0462
C                                                                       0463
      COMMON QQ(4,10),A2NU(10),NMODE,ST,DAMP,NBRG,SBRG(6),XBRG(6)       0464
     +,YBRG(6),BGSHPE(6,10),NCPL,SCPL(2),AJ1(2),AJ2(2),NFRQ,SFRQ(6)     0465
     +,FQSHPE(6,10),QEXI(10),QETA(10),FX(6),FY(6),COEFLN(8,6)           0466
     +,XDOT,XDIS,YDOT,YDIS,DATAFQ(12288)                                0467
      DIMENSION Q(40),F(40)                                             0468
C                                                                       0469
      DO 12 N=1,NBRG                                                    0470
      XDOT=0.0                                                          0471
      XDIS=-XBRG(N)                                                     0472
      YDOT=0.0                                                          0473
      YDIS=-YBRG(N)                                                     0474
      DO 16 M=1,NMODE                                                   0475
      MEQ=4*(M-1)                                                       0476
      SHAPE=BGSHPE(N,M)                                                 0477
      XDOT=XDOT+Q(1+MEQ)*SHAPE                                          0478
      XDIS=XDIS+Q(2+MEQ)*SHAPE                                          0479
      YDOT=YDOT+Q(3+MEQ)*SHAPE                                          0480
      YDIS=YDIS+Q(4+MEQ)*SHAPE                                          0481
16    CONTINUE                                                          0482
      CALL FILMXY(N)                                                    0483
12    CONTINUE                                                          0484
C                                                                       0485
      TAU=AMOD(T,6.28318530717959)                                      0486
      COST=COS(TAU)                                                     0487
      SINT=SIN(TAU)                                                     0488
C                                                                       0489
      DO 18 M=1,NMODE                                                   0490
      SUMX=0.0                                                          0491
      SUMY=0.0                                                          0492
      DO 20 N=1,NBRG                                                    0493
      SUMX=SUMX+FX(N)*BGSHPE(N,M)                                       0494
      SUMY=SUMY+FY(N)*BGSHPE(N,M)                                       0495
20    CONTINUE                                                          0496
      MEQ=4*(M-1)                                                       0497
      F(1+MEQ)=SUMX-A2NU(M)*Q(2+MEQ)-DAMP*Q(1+MEQ)                      0498
     +        +QEXI(M)*COST-QETA(M)*SINT                                0499
      F(2+MEQ)=Q(1+MEQ)                                                 0500
      F(3+MEQ)=SUMY-A2NU(M)*Q(4+MEQ)-DAMP*Q(3+MEQ)                      0501
     +        +QEXI(M)*SINT+QETA(M)*COST                                0502
      F(4+MEQ)=Q(3+MEQ)                                                 0503
18    CONTINUE                                                          0504
      F(3)=F(3)-ST                                                      0505
C                                                                       0506
      RETURN                                                            0507
      END                                                               0508
```

```
      SUBROUTINE FILMXY(N)                                                  0509
C                                                                           0510
C**** FILMXY CALCULATES THE NON-DIMENSIONAL OIL-FILM FORCES FX(N)            0511
C     AND FY(N) FOR THE NTH BEARING, THE CONFIGURATION MODELLED IS          0512
C     A LEMON BORE BEARING REPRESENTED BY TWO PRESET INFINITELY             0513
C     LONG PARTIAL ARCS. THE METHOD OF COLLOCATION IS USED TO OBTAIN        0514
C     A SIDE LEAKAGE FACTOR. (REF. CHAPTER 7 )                              0515
C                                                                           0516
      COMMON QQ(4,10),A2NU(10),NMODE,ST,DAMP,NBRG,SBRG(6),XBRG(6)           0517
     +,YBRG(6),BQSHPE(6,10),NCPL,SCPL(2),AJ1(2),AJ2(2),NFRQ,SFRQ(6)         0518
     +,FQSHPE(6,10),QEXT(10),QETA(10),FX(6),FY(6),COEFLN(8,6)               0519
     +,XDOT,XDIS,YDOT,YDIS,DATAFQ(12289)                                    0520
      COMMON /BRGSET/ BETA(6,2),GC(6,2),RSCAC(6,2),ARCL(6,2),ALGAM(6,2)     0521
     +,FXA(2),FYA(2),SCOS(6,2),SSIN(6,2),FCOS(6,2),FSIN(6,2),CAVCC,WFACT    0522
      DATA PI,P2I/3.14159265358979,6.28318530717959/                        0523
      MXITER=50                                                             0524
C                                                                           0525
C                                                                           0526
      DO 50 NA=1,2                                                          0527
      RELAX=0.5                                                             0528
C                                                                           0529
      X=RSCAC(N,NA)*XDIS                                                    0530
      Y=RSCAC(N,NA)*(YDIS-GC(N,NA))                                         0531
      E2S=X*X+Y*Y                                                           0532
      EE=1.0-E2S                                                            0533
      EPS=SQRT(E2S)                                                         0534
      IF(EPS.LT.1.0E-4 .OR. EPS.GT.0.999) GO TO 16                          0535
      SQRTEE=SQRT(EE)                                                       0536
      COSPSI=X/EPS                                                          0537
      SINPSI=Y/EPS                                                          0538
      AA=0.5*EPS-RSCAC(N,NA)*(YDOT*COSPSI-XDOT*SINPSI)                      0539
      BB=RSCAC(N,NA)*(XDOT*COSPSI+YDOT*SINPSI)                              0540
      COSS=-SCOS(N,NA)*COSPSI-SSIN(N,NA)*SINPSI                             0541
      SINS= SCOS(N,NA)*SINPSI-SSIN(N,NA)*COSPSI                             0542
      COSF=-FCOS(N,NA)*COSPSI-FSIN(N,NA)*SINPSI                             0543
      SINF= FCOS(N,NA)*SINPSI-FSIN(N,NA)*COSPSI                             0544
C                                                                           0545
      ANGS=ATAN2(SQRTEE*SINS,EPS+COSS)                                      0546
      S1I00=ANGS/SQRTEE                                                     0547
      RHS=1.0/(1.0+EPS*COSS)                                                0548
      S2I00=(S1I00-EPS*SINS*RHS)/EE                                         0549
      S3I00=(3.0*S2I00-S1I00-EPS*SINS*RHS*RHS)/(2.0*EE)                     0550
      S3I01=(S2I00-S3I00)/EPS                                               0551
      S3I10=0.5*RHS*RHS/EPS                                                 0552
C                                                                           0553
      ANGF=ATAN2(SQRTEE*SINF,EPS+COSF)                                      0554
      ADD2PI=0.0                                                            0555
      IF(ANGF.LT.ANGS) ADD2PI=P2I                                           0556
      ANGF=ANGF+ADD2PI                                                      0557
      F1I00=ANGF/SQRTEE                                                     0558
      RHF=1.0/(1.0+EPS*COSF)                                                0559
      F2I00=(F1I00-EPS*SINF*RHF)/EE                                         0560
      F3I00=(3.0*F2I00-F1I00-EPS*SINF*RHF*RHF)/(2.0*EE)                     0561
      F3I01=(F2I00-F3I00)/EPS                                               0562
      F3I10=0.5*RHF*RHF/EPS                                                 0563
C                                                                           0564
      A3I00=F3I00-S3I00                                                     0565
      A3I10=F3I10-S3I10                                                     0566
      A3I01=F3I01-S3I01                                                     0567
C                                                                           0568
      MS=-1                                                                 0569
      MF=3                                                                  0570
      C1=-(AA*A3I01+BB*A3I10)/A3I00                                         0571
      IF(AA*COSS+BB*SINS+C1.LT.0.0) MS=1                                    0572
      IF(AA*COSF+BB*SINF+C1.LT.0.0) MF=2                                    0573
      MF=MF+MS                                                              0574
      GO TO (10,20,30,40),MF                                                0575
C                                                                           0576
C          COMPLETE FILM                                                    0577
C                                                                           0578
10    A3I02=(A3I00-2.0*(F2I00-S2I00)+F1I00-S1I00)/E2S                       0579
      A3I20=A3I00-A3I02                                                     0580
      A3I11=((RHF-RHS)/EPS-A3I10)/EPS                                       0581
C                                                                           0582
      FE=AA*(SINF*A3I01-A3I11)+BB*(SINF*A3I10-A3I20)                        0583
     +  +C1*(SINF*A3I00-A3I10)                                              0584
      FP=AA*(A3I02-COSF*A3I01)+BB*(A3I11-COSF*A3I10)                        0585
     +  +C1*(A3I01-COSF*A3I00)                                              0586
C                                                                           0587
      A2B2=AA*AA+BB*BB                                                      0588
      SQTABC=SQRT(A2B2-C1*C1)                                               0589
```

```
      COSF=-(AA*C1+BB*SQTABC)/A2B2                                      0590
      SINF= (AA*SQTABC-BB*C1)/A2B2                                      0591
C                                                                       0592
      ANGF=ATAN2(SQRTEE*SINF,EPS+COSF)                                  0593
      IF(ANGF.LT.ANGS) ANGF=ANGF+P2I                                    0594
      F1I00=ANGF/SQRTEE                                                 0595
      RHF=1.0/(1.0+EPS*COSF)                                            0596
      F2I00=(F1I00-EPS*SINF*RHF)/EE                                     0597
      F3I00=(3.0*F2I00-F1I00-EPS*SINF*RHF*RHF)/(2.0*EE)                 0598
      F3I01=(F2I00-F3I00)/EPS                                           0599
      F3I10=0.5*RHF*RHF/EPS                                             0600
      A3I00=F3I00-S3I00                                                 0601
      A3I10=F3I10-S3I10                                                 0602
      A3I01=F3I01-S3I01                                                 0603
C                                                                       0604
      TEMP1=ALGAM(N,NA)*(AA*A3I01+BB*A3I10+C1*A3I00)/(RHF*RHF*RHF)      0605
      FCOL=1.0/(1.0+TEMP1/(AA*SINF-BB*COSF))                            0606
C                                                                       0607
      FXA(NA)=FCOL*(FE*COSPSI-FP*SINPSI)                                0608
      FYA(NA)=FCOL*(FE*SINPSI+FP*COSPSI)                                0609
      GO TO 50                                                          0610
C                                                                       0611
C          FIRST PARTIALLY CAVITATED CONDITION                          0612
C                                                                       0613
20    NITER=0                                                           0614
      SUMDEL=0.0                                                        0615
22    NITER=NITER+1                                                     0616
      DELTH=RELAX*(AA*A3I01+BB*A3I10-(AA*COSF+BB*SINF)*A3I00)           0617
     +     /((AA*SINF-BB*COSF)*A3I00)                                   0618
      COSDEL=COS(DELTH)                                                 0619
      SINDEL=SIN(DELTH)                                                 0620
      SUMDEL=SUMDEL+DELTH                                               0621
      TEMP1=COSF                                                        0622
      TEMP2=SINF                                                        0623
      COSF=TEMP1*COSDEL+TEMP2*SINDEL                                    0624
      SINF=TEMP2*COSDEL-TEMP1*SINDEL                                    0625
C                                                                       0626
      ANGF=ATAN2(SQRTEE*SINF,EPS+COSF)                                  0627
      IF(ANGF.LT.ANGS) ANGF=ANGF+P2I                                    0628
      F1I00=ANGF/SQRTEE                                                 0629
      RHF=1.0/(1.0+EPS*COSF)                                            0630
      F2I00=(F1I00-EPS*SINF*RHF)/EE                                     0631
      F3I00=(3.0*F2I00-F1I00-EPS*SINF*RHF*RHF)/(2.0*EE)                 0632
      F3I01=(F2I00-F3I00)/EPS                                           0633
      F3I10=0.5*RHF*RHF/EPS                                             0634
      A3I00=F3I00-S3I00                                                 0635
      A3I10=F3I10-S3I10                                                 0636
      A3I01=F3I01-S3I01                                                 0637
      IF(ABS(DELTH).LT.CAVCC) GO TO 24                                  0638
      IF(NITER.GE.MXITER) GO TO 18                                      0639
      RELAX=1.0                                                         0640
      GO TO 22                                                          0641
24    A3I02=(A3I00-2.0*(F2I00-S2I00)+F1I00-S1I00)/E2S                   0642
      A3I20=A3I00-A3I02                                                 0643
      A3I11=((RHF-RHS)/EPS-A3I10)/EPS                                   0644
      C1=-AA*COSF-BB*SINF                                               0645
C                                                                       0646
      IF(SUMDEL.LT.0.0 .OR. SUMDEL.GT.ARCL(N,NA)) GO TO 14              0647
C                                                                       0648
      FE=AA*(SINF*A3I01-A3I11)+BB*(SINF*A3I10-A3I20)                    0649
     +  +C1*(SINF*A3I00-A3I10)                                          0650
      FP=AA*(A3I02-COSF*A3I01)+BB*(A3I11-COSF*A3I10)                    0651
     +  +C1*(A3I01-COSF*A3I00)                                          0652
C                                                                       0653
      A2B2=AA*AA+BB*BB                                                  0654
      SQTABC=SQRT(A2B2-C1*C1)                                           0655
      COSF=-(AA*C1+BB*SQTABC)/A2B2                                      0656
      SINF= (AA*SQTABC-BB*C1)/A2B2                                      0657
C                                                                       0658
      ANGF=ATAN2(SQRTEE*SINF,EPS+COSF)                                  0659
      IF(ANGF.LT.ANGS) ANGF=ANGF+P2I                                    0660
      F1I00=ANGF/SQRTEE                                                 0661
      RHF=1.0/(1.0+EPS*COSF)                                            0662
      F2I00=(F1I00-EPS*SINF*RHF)/EE                                     0663
      F3I00=(3.0*F2I00-F1I00-EPS*SINF*RHF*RHF)/(2.0*EE)                 0664
      F3I01=(F2I00-F3I00)/EPS                                           0665
      F3I10=0.5*RHF*RHF/EPS                                             0666
      A3I00=F3I00-S3I00                                                 0667
      A3I10=F3I10-S3I10                                                 0668
      A3I01=F3I01-S3I01                                                 0669
C                                                                       0670
```

```
      TEMP1=ALGAM(N,NA)*(AA*A3I01+BB*A3I10+C1*A3I00)/(RHF*RHF*RHF)          0671
      FCOL=1.0/(1.0+TEMP1/(AA*SINF-BB*COSF))                                0672
C                                                                           0673
      FXA(NA)=FCOL*(FE*COSPSI-FP*SINPSI)                                    0674
      FYA(NA)=FCOL*(FE*SINPSI+FP*COSPSI)                                    0675
      GO TO 50                                                              0676
C                                                                           0677
C          SECOND PARTIALLY CAVITATED CONDITION                             0678
C                                                                           0679
30    NITER=0                                                               0680
      SUMDEL=0.0                                                            0681
32    NITER=NITER+1                                                         0682
      DELTH=RELAX*(AA*A3I01+BB*A3I10-(AA*COSS+BB*SINS)*A3I00)               0683
     +     /((AA*SINS-BB*COSS)*A3I00)                                       0684
      COSDEL=COS(DELTH)                                                     0685
      SINDEL=SIN(DELTH)                                                     0686
      SUMDEL=SUMDEL-DELTH                                                   0687
      TEMP1=COSS                                                            0688
      TEMP2=SINS                                                            0689
      COSS=TEMP1*COSDEL+TEMP2*SINDEL                                        0690
      SINS=TEMP2*COSDEL-TEMP1*SINDEL                                        0691
C                                                                           0692
      ANGS=ADD2PI+ATAN2(SQRTEE*SINS,EPS+COSS)                               0693
      IF(ANGF.LT.ANGS) ANGS=ANGS-P2I                                        0694
      S1I00=ANGS/SQRTEE                                                     0695
      RHS=1.0/(1.0+EPS*COSS)                                                0696
      S2I00=(S1I00-EPS*SINS*RHS)/EE                                         0697
      S3I00=(3.0*S2I00-S1I00-EPS*SINS*RHS*RHS)/(2.0*EE)                     0698
      S3I01=(S2I00-S3I00)/EPS                                               0699
      S3I10=0.5*RHS*RHS/EPS                                                 0700
      A3I00=F3I00-S3I00                                                     0701
      A3I10=F3I10-S3I10                                                     0702
      A3I01=F3I01-S3I01                                                     0703
      IF(ABS(DELTH).LT.CAVCC) GO TO 34                                      0704
      IF(NITER.GE.MXITER) GO TO 18                                          0705
      RELAX=1.0                                                             0706
      GO TO 32                                                              0707
34    A3I02=(A3I00-2.0*(F2I00-S2I00)+F1I00-S1I00)/E2S                       0708
      A3I20=A3I00-A3I02                                                     0709
      A3I11=((RHF-RHS)/EPS-A3I10)/EPS                                       0710
      C1=-AA*COSS-BB*SINS                                                   0711
C                                                                           0712
      IF(SUMDEL.LT.0.0 .OR. SUMDEL.GT.ARCL(N,NA)) GO TO 14                  0713
C                                                                           0714
      FE=AA*(SINF*A3I01-A3I11)+BB*(SINF*A3I10-A3I20)                        0715
     +  +C1*(SINF*A3I00-A3I10)                                             0716
      FP=AA*(A3I02-COSF*A3I01)+BB*(A3I11-COSF*A3I10)                        0717
     +  +C1*(A3I01-COSF*A3I00)                                             0718
C                                                                           0719
      A2B2=AA*AA+BB*BB                                                      0720
      SQTABC=SQRT(A2B2-C1*C1)                                               0721
      COSF=-(AA*C1+BB*SQTABC)/A2B2                                          0722
      SINF= (AA*SQTABC-BB*C1)/A2B2                                          0723
C                                                                           0724
      ANGF=ATAN2(SQRTEE*SINF,EPS+COSF)                                      0725
      IF(ANGF.LT.ANGS) ANGF=ANGF+P2I                                        0726
      F1I00=ANGF/SQRTEE                                                     0727
      RHF=1.0/(1.0+EPS*COSF)                                                0728
      F2I00=(F1I00-EPS*SINF*RHF)/EE                                         0729
      F3I00=(3.0*F2I00-F1I00-EPS*SINF*RHF*RHF)/(2.0*EE)                     0730
      F3I01=(F2I00-F3I00)/EPS                                               0731
      F3I10=0.5*RHF*RHF/EPS                                                 0732
      A3I00=F3I00-S3I00                                                     0733
      A3I10=F3I10-S3I10                                                     0734
      A3I01=F3I01-S3I01                                                     0735
C                                                                           0736
      TEMP1=ALGAM(N,NA)*(AA*A3I01+BB*A3I10+C1*A3I00)/(RHF*RHF*RHF)          0737
      FCOL=1.0/(1.0+TEMP1/(AA*SINF-BB*COSF))                                0738
C                                                                           0739
      FXA(NA)=FCOL*(FE*COSPSI-FP*SINPSI)                                    0740
      FYA(NA)=FCOL*(FE*SINPSI+FP*COSPSI)                                    0741
      GO TO 50                                                              0742
C                                                                           0743
C          COMPLETELY CAVITATED CONDITION                                   0744
C                                                                           0745
40    MS=1                                                                  0746
      M4=3                                                                  0747
      RELAX=0.5                                                             0748
      IF(BB*COSS-AA*SINS.LT.WFACT) MS=-1                                    0749
      IF(BB*COSF-AA*SINF.LT.WFACT) M4=2                                     0750
      M4=M4+MS                                                              0751
```

```
      GO TO (14,20,30,42),M4                                                0752
42    FXA(NA)=0.0                                                           0753
      FYA(NA)=0.0                                                           0754
C                                                                           0755
50    CONTINUE                                                              0756
C                                                                           0757
C          SUM FORCES FOR BOTH ARCS                                         0758
C                                                                           0759
      FX(N)=BETA(N,1)*FXA(1)+BETA(N,2)*FXA(2)                               0760
      FY(N)=BETA(N,1)*FYA(1)+BETA(N,2)*FYA(2)                               0761
C                                                                           0762
      RETURN                                                                0763
14    WRITE(6,1014) N,NA                                                    0764
      STOP                                                                  0765
16    WRITE(6,1016) EPS,N,NA                                                0766
      STOP                                                                  0767
18    WRITE(6,1018) N,NA                                                    0768
      STOP                                                                  0769
C                                                                           0770
1014  FORMAT(40H ***************************************//10X,             0771
     +36HWRONG SOLUTION OBTAINED FOR BEARING ,I2,5H ARC ,I1//)              0772
1016  FORMAT(40H ***************************************//10X,             0773
     +,20HFILMXY FAILS AS EPS=,E13.5,13H FOR BEARING ,I2,5H ARC ,I1//)      0774
1018  FORMAT(40H ***************************************//10X,             0775
     +37HCONVERGENCE NOT ACHIEVED FOR BEARING ,I2,5H ARC ,I1//)             0776
      END                                                                   0777
```

```
      SUBROUTINE LNCOEF(N,NL)                                                  0778
C                                                                              0779
C**** LNCOEF CALCULATES THE COEFFICIENTS (COEFLN(I,N) ,I=1,..,8)               0780
C     OF THE LINEARIZED BEARING FORCES FOR THE NTH BEARING BY                  0781
C     NUMERICAL DIFFERENCING. IF NL=4 ONLY THE DISPLACEMENT                    0782
C     COEFFICIENTS ARE CALCULATED (I.E. COEFLN(2,N),COEFLN(4,N),               0783
C     COEFLN(6,N),AND COEFLN(8,N) ) OTHERWISE ALL EIGHT ARE                    0784
C     CALCULATED.                                                              0785
C                                                                              0786
      COMMON QQ(4,10),A2NU(10),NMODE,ST,DAMP,NBRG,SBRG(6),XBRG(6)              0787
     +,YBRG(6),BGSHPE(6,10),NCPL,SCPL(2),AJ1(2),AJ2(2),NFRQ,SFRQ(6)            0788
     +,FQSHPE(6,10),QEXI(10),QETA(10),FX(6),FY(6),COEFLN(8,6)                  0789
     +,XDOT,XDIS,YDOT,YDIS,DATAFQ(12288)                                       0790
      COMMON /BRGSET/ BETA(6,2),GC(6,2),RSCAC(6,2),ARCL(6,2),ALGAM(6,2)        0791
     +,FXA(2),FYA(2),SCOS(6,2),SSIN(6,2),FCOS(6,2),FSIN(6,2),CAVCC,WFACT       0792
      DIMENSION XY(4)                                                          0793
      EQUIVALENCE (XY(1),XDOT)                                                 0794
      STORE1=CAVCC                                                             0795
      STORE2=WFACT                                                             0796
      CAVCC=0.0005                                                             0797
      WCONV=-0.001                                                             0798
      CALL FILMXY(N)                                                           0799
      FX0=FX(N)                                                                0800
      FY0=FY(N)                                                                0801
      M=1                                                                      0802
      IF(NL.EQ.4) M=2                                                          0803
      DO 10 I=M,4,M                                                            0804
      DELXY=0.0001*ABS(XY(I))                                                  0805
      IF(DELXY.LT.1.0E-5) DELXY=1.0E-5                                         0806
      TEMP=XY(I)                                                               0807
      XY(I)=XY(I)+DELXY                                                        0808
      CALL FILMXY(N)                                                           0809
      COEFLN(I  ,N)=(FX(N)-FX0)/DELXY                                          0810
      COEFLN(I+4,N)=(FY(N)-FY0)/DELXY                                          0811
      XY(I)=TEMP                                                               0812
10    CONTINUE                                                                 0813
      FX(N)=FX0                                                                0814
      FY(N)=FY0                                                                0815
      CAVCC=STORE1                                                             0816
      WFACT=STORE2                                                             0817
      RETURN                                                                   0818
      END                                                                      0819
```

```
      SUBROUTINE UNIFRM(NMODE,A,UNFM,IFLAG)                                 0820
C                                                                           0821
C**** IF IFLAG .EQ. 1 UNIFRM CALCULATES THE VALUE OF THE MODES              0822
C     AT STATION S=A FOR A FREE-FREE UNIFORM SHAFT.                         0823
C     IF IFLAG .NE. 1 UNIFRM RETURNS THE NATURAL FREQUENCIES OF THE         0824
C     FREE-FREE UNIFORM SHAFT ADJUSTED SO THAT AMU(3)=FF3 .                 0825
C     (REF. SECTION 4.2)                                                    0826
C                                                                           0827
C**** STATEMENT MODIFICATIONS FOR INCREASED PROGRAMME DIMENSIONS            0828
C                                                                           0829
C     DOUBLE PRECISION                                                      0830
C     ----------------                                                      0831
C                                                                           0832
C     AMU(M) .... BUT ONLY FOR  M .GT. 16                                   0833
C                                                                           0834
C     FOR M .GT. 16   AMU(M) = 0.5*((2*M)-3)*PI  ,WHERE PI=3.1415....      0835
C                                                                           0836
C                                                                           0837
      DIMENSION UNFM(NMODE)                                                 0838
      DOUBLE PRECISION AMU(16),COSH,SINH,RHOS,AMUS,S,X                      0839
      DATA AMU/0.0D0,0.0D0                                                  0840
     +,0.47300407448627040260D+01                                           0841
     +,0.78532046240958375564D+01                                           0842
     +,0.10995607838001670906D+02                                           0843
     +,0.14137165491257464177D+02                                           0844
     +,0.17278759657399481438D+02                                           0845
     +,0.20420352245626061090D+02                                           0846
     +,0.23561944902040455075D+02                                           0847
     +,0.26703537555508186248D+02                                           0848
     +,0.29845130209103254267D+02                                           0849
     +,0.32986722862692819561D+02                                           0850
     +,0.36128315516282622650D+02                                           0851
     +,0.39269908169872415463D+02                                           0852
     +,0.42411500823462208720D+02                                           0853
     +,0.45553093477052001957D+02/                                          0854
      COSH(X)=0.5D0*(DEXP(X)+DEXP(-X))                                      0855
      SINH(X)=0.5D0*(DEXP(X)-DEXP(-X))                                      0856
      S=A                                                                   0857
      IF(IFLAG.NE.1) GO TO 12                                               0858
      UNFM(1)=1.0                                                           0859
      UNFM(2)=(1.0D0-2.0D0*S)*DSQRT(3.0D0)                                  0860
      IF(NMODE.LT.3) RETURN                                                 0861
      DO 10 M=3,NMODE                                                       0862
      AMUS=AMU(M)                                                           0863
      RHOS=(DCOS(AMUS)-COSH(AMUS))/(DSIN(AMUS)-SINH(AMUS))                  0864
      AMUS=AMU(M)*S                                                         0865
      UNFM(M)=DCOS(AMUS)+COSH(AMUS)-RHOS*(DSIN(AMUS)+SINH(AMUS))            0866
10    CONTINUE                                                              0867
      RETURN                                                                0868
C                                                                           0869
12    FACTOR=AMU(3)*AMU(3)                                                  0870
      FACTOR=FACTOR/A                                                       0871
      DO 14 M=1,NMODE                                                       0872
      UNFM(M)=AMU(M)*AMU(M)                                                 0873
      UNFM(M)=UNFM(M)/FACTOR                                                0874
14    CONTINUE                                                              0875
      RETURN                                                                0876
      END                                                                   0877
```

```
      SUBROUTINE ALIGNM                                                 0878
C                                                                       0879
C**** ALIGNM DETERMINES AND SETS THE HORIZONTAL AND VERTICAL POSITION   0880
C     OF EACH BEARING IN ORDER TO PRODUCE A CORRECTLY ALIGNED SYSTEM.   0881
C     THE ROUTINE IS ONLY APPLICABLE TO SYSTEMS HAVING AN EVEN NUMBER   0882
C     OF BEARINGS GREATER THAN TWO. (REF. SECTION 5.2)                  0883
C                                                                       0884
C**** STATEMENT MODIFICATIONS FOR INCREASED PROGRAMME DIMENSIONS        0885
C                                                                       0886
C     DIMENSION                                                         0887
C     ---------                                                         0888
C                                                                       0889
C     ARRAY(N+M,N+M),BVEC(M+N),XVEC(M+N),W1(M+N,M+N),W2(M+N),W3(M+N)    0890
C                                                                       0891
C     EQUIVALENCE                                                       0892
C     -----------                                                       0893
C                                                                       0894
C     (W1(1,1),DATAFQ(1+(N+M)**2))                                      0895
C                                                                       0896
C     CALLS TO SUBROUTINES                                              0897
C     --------------------                                              0898
C                                                                       0899
C     F04ATF( ,M+N, , , , ,M+N, , , )                                   0900
C                                                                       0901
      COMMON QQ(4,10),A2NU(10),NMODE,ST,DAMP,NBRG,SBRG(6),XBRG(6)       0902
     +,YBRG(6),BGSHPE(6,10),NCPL,SCPL(2),AJ1(2),AJ2(2),NFRQ,SFRQ(6)     0903
     +,FQSHPE(6,10),QEXI(10),QETA(10),FX(6),FY(6),COEFLN(8,6)           0904
     +,XDOT,XDIS,YDOT,YDIS,DATAFQ(12288)                                0905
      DIMENSION ARRAY(16,16),BVEC(16),XVEC(16),W1(16,16)                0906
     +,W2(16),W3(16)                                                    0907
      EQUIVALENCE (ARRAY(1,1),DATAFQ(1)),(W1(1,1),DATAFQ(257))          0908
C                                                                       0909
      IF((NBRG+1)/2-NBRG/2.NE.0 .OR. NBRG.EQ.2) GO TO 50                0910
      IF(NBRG/2-1.NE.NCPL) GO TO 52                                     0911
      M1=NMODE                                                          0912
      MN=NMODE+NBRG                                                     0913
C                                                                       0914
      XDOT=0.0                                                          0915
      YDOT=0.0                                                          0916
C                                                                       0917
      DO 10 I=1,MN                                                      0918
      BVEC(I)=0.0                                                       0919
      DO 12 J=1,MN                                                      0920
      ARRAY(I,J)=0.0                                                    0921
12    CONTINUE                                                          0922
10    CONTINUE                                                          0923
      BVEC(1)=ST                                                        0924
      DO 14 I=1,M1                                                      0925
      ARRAY(   I,I)=-A2NU(I)                                            0926
      ARRAY(MN-1,I)=BGSHPE(1,I)                                         0927
      ARRAY(  MN,I)=BGSHPE(NBRG,I)                                      0928
      DO 16 N=1,NBRG                                                    0929
      ARRAY(I,M1+N)=BGSHPE(N,I)                                         0930
16    CONTINUE                                                          0931
14    CONTINUE                                                          0932
      DO 18 J=1,NCPL                                                    0933
      BVEC(     M1+J)=ST*AJ1(J)                                         0934
      BVEC(NCPL+M1+J)=ST*AJ2(J)                                         0935
      DO 20 N=1,NBRG                                                    0936
      IF(SCPL(J).LT.SBRG(N)) GO TO 20                                   0937
      ARRAY(     M1+J,M1+N)=1.0                                         0938
      ARRAY(NCPL+M1+J,M1+N)=SCPL(J)-SBRG(N)                             0939
20    CONTINUE                                                          0940
18    CONTINUE                                                          0941
C                                                                       0942
      IFAIL=0                                                           0943
C                                                                       0944
      CALL F04ATF(ARRAY,16,BVEC,MN,XVEC,W1,16,W2,W3,IFAIL)              0945
C                                                                       0946
      WRITE(6,1010)                                                     0947
C                                                                       0948
      MXITER=50                                                         0949
      DO 22 N=1,NBRG                                                    0950
      XBRG(N)=0.7                                                       0951
      YBRG(N)=-0.3                                                      0952
      NITER=0                                                           0953
24    NITER=NITER+1                                                     0954
      XDIS=XBRG(N)                                                      0955
      YDIS=YBRG(N)                                                      0956
      CALL FILMXY(N)                                                    0957
      CALL LNCOEF(N,4)                                                  0958
```

```
      DENOM=COEFLN(2,N)*COEFLN(8,N)-COEFLN(4,N)*COEFLN(6,N)                0959
      XBRG(N)=XBRG(N)-(COEFLN(8,N)*FX(N)-COEFLN(4,N)*(FY(N)-XVEC(M1+N)))   0960
     +       /DENOM                                                        0961
      YBRG(N)=YBRG(N)-(COEFLN(2,N)*(FY(N)-XVEC(M1+N))-COEFLN(6,N)*FX(N))   0962
     +       /DENOM                                                        0963
      IF(ABS(XBRG(N)-XOLD)+ABS(YBRG(N)-YOLD).LT.1.0E-8) GO TO 26           0964
      IF(NITER.GT.MXITER) GO TO 54                                         0965
      GO TO 24                                                             0966
26    EQEPS=SQRT(XBRG(N)**2+YBRG(N)**2)                                    0967
      WRITE(6,1020) N,XBRG(N),YBRG(N),EQEPS                                0968
22    CONTINUE                                                             0969
C                                                                          0970
      N=NBRG                                                               0971
      DENOM=BGSHPE(1,1)*BGSHPE(N,2)-BGSHPE(1,2)*BGSHPE(N,1)                0972
      QX1=(BGSHPE(N,2)*XBRG(1)-BGSHPE(1,2)*XBRG(N))/DENOM                  0973
      QX2=(BGSHPE(1,1)*XBRG(N)-BGSHPE(N,1)*XBRG(1))/DENOM                  0974
      XVEC(1)=XVEC(1)+(BGSHPE(N,2)*YBRG(1)-BGSHPE(1,2)*YBRG(N))/DENOM      0975
      XVEC(2)=XVEC(2)+(BGSHPE(1,1)*YBRG(N)-BGSHPE(N,1)*YBRG(1))/DENOM      0976
C                                                                          0977
      DO 30 N=1,NBRG                                                       0978
      Y=0.0                                                                0979
      DO 32 I=1,NMODE                                                      0980
      Y=Y+XVEC(I)*BGSHPE(N,I)                                              0981
32    CONTINUE                                                             0982
      X=QX1*BGSHPE(N,1)+QX2*BGSHPE(N,2)                                    0983
      XBRG(N)=X-XBRG(N)                                                    0984
      YBRG(N)=Y-YBRG(N)                                                    0985
      IF(ABS(XBRG(N)).LT.1.0E-8) XBRG(N)=0.0                               0986
      IF(ABS(YBRG(N)).LT.1.0E-8) YBRG(N)=0.0                               0987
30    CONTINUE                                                             0988
      RETURN                                                               0989
C                                                                          0990
50    WRITE(6,1030) NBRG                                                   0991
      STOP                                                                 0992
52    WRITE(6,1040)                                                        0993
      STOP                                                                 0994
54    WRITE(6,1050)                                                        0995
      STOP                                                                 0996
C                                                                          0997
1010  FORMAT(//5X                                                          0998
     +,58HEQUILIBRIUM POSITION OF THE SHAFT RELATIVE TO EACH BEARING/5X    0999
     +,58H----------------------------------------------------------/5X    1000
     +,22HFOR THE ALIGNED SYSTEM/5X                                        1001
     +,22H----------------------//6X                                      1002
     +,1HN,10X,3H(X),14X,3H(Y),13X,5HEQEPS//)                              1003
1020  FORMAT(5X,I2,3(4X,E13.5))                                            1004
1030  FORMAT(40H ***************************************//                1005
     +5X,36HALIGNMENT ROUTINE NOT APPLICABLE TO ,I2,16H BEARING SYSTEMS)   1006
1040  FORMAT(40H ***************************************//                1007
     +5X,40HINCORRECT NUMBER OF COUPLINGS DESIGNATED)                      1008
1050  FORMAT(40H ***************************************//                1009
     +5X,45HCONVERGENCE NOT ACHIEVED IN SUBROUTINE ALIGNM)                 1010
      END                                                                  1011
```

```
      SUBROUTINE STATIC                                                 1012
C                                                                       1013
C**** STATIC CALCULATES THE EQUILIBRIUM POSITION OF THE ROTATING        1014
C     SHAFT, IT IS APPLICABLE TO ANY SYSTEM HAVING TWO OR MORE          1015
C     BEARINGS. (REF. SECTION 5.3)                                      1016
C                                                                       1017
C**** STATEMENT MODIFICATIONS FOR INCREASED PROGRAMME DIMENSIONS        1018
C                                                                       1019
C     DIMENSION                                                         1020
C     ---------                                                         1021
C                                                                       1022
C     ARRAY(2*M,2*M),HQQ(2*M),DELQQ(2*M),W1(2*M,2*M),W2(2*M),W3(2*M)    1023
C                                                                       1024
C     EQUIVALENCE                                                       1025
C     -----------                                                       1026
C                                                                       1027
C     (W1(1,1),DATAFQ(1+(2*M)**2))                                      1028
C                                                                       1029
C     CALLS TO SUBROUTINES                                              1030
C     --------------------                                              1031
C                                                                       1032
C     F04ATF( ,2*M, , , , ,2*M, , , )                                   1033
C                                                                       1034
C                                                                       1035
      COMMON QQ(4,10),A2NU(10),NMODE,ST,DAMP,NBRG,SBRG(6),XBRG(6)       1036
     +,YBRG(6),BGSHPE(6,10),NCPL,SCPL(2),AJ1(2),AJ2(2),NFRQ,SFRQ(6)     1037
     +,FQSHPE(6,10),QEXI(10),QETA(10),FX(6),FY(6),COEFLN(8,6)           1038
     +,XDOT,XDIS,YDOT,YDIS,DATAFQ(12288)                                1039
      DIMENSION ARRAY(20,20),HQQ(20),DELQQ(20),W1(20,20)                1040
     +,W2(20),W3(20)                                                    1041
      EQUIVALENCE (ARRAY(1,1),DATAFQ(1)),(W1(1,1),DATAFQ(401))          1042
C                                                                       1043
      IF(NBRG.LT.2 .OR. NMODE.LT.NBRG) GO TO 64                         1044
      XDOT=0.0                                                          1045
      YDOT=0.0                                                          1046
      DO 62 M=1,NMODE                                                   1047
      QQ(1,M)=0.0                                                       1048
      QQ(2,M)=0.0                                                       1049
      QQ(3,M)=0.0                                                       1050
      QQ(4,M)=0.0                                                       1051
62    CONTINUE                                                          1052
C                                                                       1053
      DO 52 I=1,NBRG                                                    1054
      HQQ(I)=XBRG(I)+0.7                                                1055
      DO 54 J=1,NBRG                                                    1056
      ARRAY(I,J)=BGSHPE(I,J)                                            1057
54    CONTINUE                                                          1058
52    CONTINUE                                                          1059
      N1=NBRG                                                           1060
      IFAIL=0                                                           1061
      CALL F04ATF(ARRAY,20,HQQ,N1,DELQQ,W1,20,W2,W3,IFAIL)              1062
      DO 56 I=1,NBRG                                                    1063
      QQ(2,I)=DELQQ(I)                                                  1064
      HQQ(I)=YBRG(I)-0.3                                                1065
      DO 58 J=1,NBRG                                                    1066
      ARRAY(I,J)=BGSHPE(I,J)                                            1067
58    CONTINUE                                                          1068
56    CONTINUE                                                          1069
      CALL F04ATF(ARRAY,20,HQQ,N1,DELQQ,W1,20,W2,W3,IFAIL)              1070
      DO 60 I=1,NBRG                                                    1071
      QQ(4,I)=DELQQ(I)                                                  1072
60    CONTINUE                                                          1073
C                                                                       1074
      MXITER=50                                                         1075
      NITER=0                                                           1076
10    NITER=NITER+1                                                     1077
      DO 12 N=1,NBRG                                                    1078
      XDIS=-XBRG(N)                                                     1079
      YDIS=-YBRG(N)                                                     1080
      DO 14 M=1,NMODE                                                   1081
      XDIS=XDIS+QQ(2,M)*BGSHPE(N,M)                                     1082
      YDIS=YDIS+QQ(4,M)*BGSHPE(N,M)                                     1083
14    CONTINUE                                                          1084
      CALL LNCOEF(N,4)                                                  1085
12    CONTINUE                                                          1086
C                                                                       1087
      DO 16 I=1,NMODE                                                   1088
      SUMX=0.0                                                          1089
      SUMY=0.0                                                          1090
      DO 20 N=1,NBRG                                                    1091
      SUMX=SUMX+FX(N)*BGSHPE(N,I)                                       1092
```

```
      SUMY=SUMY+FY(N)*BGSHPE(N,I)                                       1093
20    CONTINUE                                                          1094
      HQQ(I)       =SUMX-A2NU(I)*QQ(2,I)                                1095
      HQQ(NMODE+I)=SUMY-A2NU(I)*QQ(4,I)                                 1096
      DO 18 J=1,NMODE                                                   1097
      SUMKXX=0.0                                                        1098
      SUMKXY=0.0                                                        1099
      SUMKYX=0.0                                                        1100
      SUMKYY=0.0                                                        1101
      DO 22 N=1,NBRG                                                    1102
      BGIJ=BGSHPE(N,I)*BGSHPE(N,J)                                      1103
      SUMKXX=SUMKXX+BGIJ*COEFLN(2,N)                                    1104
      SUMKXY=SUMKXY+BGIJ*COEFLN(4,N)                                    1105
      SUMKYX=SUMKYX+BGIJ*COEFLN(6,N)                                    1106
      SUMKYY=SUMKYY+BGIJ*COEFLN(8,N)                                    1107
22    CONTINUE                                                          1108
      ARRAY(I,J)=SUMKXX                                                 1109
      ARRAY(I,NMODE+J)=SUMKXY                                           1110
      ARRAY(NMODE+I,J)=SUMKYX                                           1111
      ARRAY(NMODE+I,NMODE+J)=SUMKYY                                     1112
18    CONTINUE                                                          1113
16    CONTINUE                                                          1114
      HQQ(NMODE+1)=HQQ(NMODE+1)-ST                                      1115
      DO 24 I=1,NMODE                                                   1116
      ARRAY(I,I)=ARRAY(I,I)-A2NU(I)                                     1117
      IM=NMODE+I                                                        1118
      ARRAY(IM,IM)=ARRAY(IM,IM)-A2NU(I)                                 1119
24    CONTINUE                                                          1120
C                                                                       1121
      M2=NMODE+NMODE                                                    1122
      IFAIL=0                                                           1123
C                                                                       1124
      CALL F04ATF(ARRAY,20,HQQ,M2,DELQQ,W1,20,W2,W3,IFAIL)              1125
C                                                                       1126
      QXMAX=0.0                                                         1127
      QYMAX=0.0                                                         1128
      DO 26 I=1,NMODE                                                   1129
      QQ(2,I)=QQ(2,I)-DELQQ(I)                                          1130
      QQ(4,I)=QQ(4,I)-DELQQ(NMODE+I)                                    1131
      IF(ABS(QQ(2,I)).GT.QXMAX) QXMAX=ABS(QQ(2,I))                      1132
      IF(ABS(QQ(4,I)).GT.QYMAX) QYMAX=ABS(QQ(4,I))                      1133
26    CONTINUE                                                          1134
      DO 32 I=1,NMODE                                                   1135
      IF(ABS(QQ(2,I)/QXMAX).LT.1.0E-6) GO TO 34                         1136
      IF(ABS(DELQQ(I)/QQ(2,I)).GT.1.0E-8) GO TO 28                      1137
34    IF(ABS(QQ(4,I)/QYMAX).LT.1.0E-6) GO TO 32                         1138
      IF(ABS(DELQQ(NMODE+I)/QQ(4,I)).GT.1.0E-8) GO TO 28                1139
32    CONTINUE                                                          1140
      WRITE(6,42)                                                       1141
      DO 44 N=1,NBRG                                                    1142
      XDIS=-XBRG(N)                                                     1143
      YDIS=-YBRG(N)                                                     1144
      DO 46 M=1,NMODE                                                   1145
      XDIS=XDIS+QQ(2,M)*BGSHPE(N,M)                                     1146
      YDIS=YDIS+QQ(4,M)*BGSHPE(N,M)                                     1147
46    CONTINUE                                                          1148
      EQEPS=SQRT(XDIS**2+YDIS**2)                                       1149
      WRITE(6,48) N,XDIS,YDIS,EQEPS                                     1150
44    CONTINUE                                                          1151
      RETURN                                                            1152
28    IF(NITER.LT.MXITER) GO TO 10                                      1153
      WRITE(6,1020)                                                     1154
      STOP                                                              1155
64    WRITE(6,1030)                                                     1156
      STOP                                                              1157
C                                                                       1158
42    FORMAT(//5X                                                       1159
     +,55HPREDICTED EQUILIBRIUM POSITION RELATIVE TO EACH BEARING/5X    1160
     +,55H----------------------------------------------------//6X      1161
     +,1HN,10X,3H(X),14X,3H(Y),13X,5HEQEPS//)                           1162
48    FORMAT(5X,I2,3(4X,E13.5))                                         1163
1020  FORMAT(40H ************************************//                1164
     +5X,46H CONVERGENCE NOT ACHIEVED IN SUBROUTINE STATIC)             1165
1030  FORMAT(40H ************************************//                1166
     +5X,41HEXECUTION TERMINATED IN SUBROUTINE STATIC/                  1167
     +5X,40H AS VALUE OF NBRG OR NMODE IS UNSUITABLE)                   1168
      END                                                               1169
```

```
      SUBROUTINE LNSTAB                                                 1170
C                                                                       1171
C**** LNSTAB CALCULATES, USING NAG ROUTINE F02AFF, THE EIGENVALUES      1172
C     OF THE LINEARIZED SYSTEM. (REF. SECTION 5.4)                      1173
C                                                                       1174
C**** STATEMENT MODIFICATIONS FOR INCREASED PROGRAMME DIMENSIONS        1175
C                                                                       1176
C     DIMENSION                                                         1177
C     ---------                                                         1178
C                                                                       1179
C     ARRAY(4*M,4*M),AREAL(4*M),AJMAG(4*M),IW(4*M),INDEX(4*M)           1180
C     SORTR(4*M),SORTI(4*M)                                             1181
C                                                                       1182
C     CALLS TO SUBROUTINES                                              1183
C     --------------------                                              1184
C                                                                       1185
C     F02AFF( ,4*M, , , , , )                                           1186
C                                                                       1187
      COMMON QQ(4,10),A2NU(10),NMODE,ST,DAMP,NBRG,SBRG(6),XBRG(6)       1188
     +,YBRG(6),BGSHPE(6,10),NCPL,SCPL(2),AJ1(2),AJ2(2),NFRQ,SFRQ(6)     1189
     +,FQSHPE(6,10),QEXI(10),QETA(10),FX(6),FY(6),COEFLN(8,6)           1190
     +,XDOT,XDIS,YDOT,YDIS,DATAFQ(12288)                                1191
      DIMENSION ARRAY(40,40),AREAL(40),AJMAG(40),IW(40)                 1192
     +,INDEX(40),SORTR(40),SORTI(40)                                    1193
      EQUIVALENCE (ARRAY(1,1),DATAFQ(1))                                1194
C                                                                       1195
      M1=NMODE                                                          1196
      M2=M1+M1                                                          1197
      M3=M1+M2                                                          1198
      M4=M1+M3                                                          1199
      XDOT=0.0                                                          1200
      YDOT=0.0                                                          1201
      DO 10 N=1,NBRG                                                    1202
      XDIS=-XBRG(N)                                                     1203
      YDIS=-YBRG(N)                                                     1204
      DO 12 M=1,NMODE                                                   1205
      XDIS=XDIS+QQ(2,M)*BGSHPE(N,M)                                     1206
      YDIS=YDIS+QQ(4,M)*BGSHPE(N,M)                                     1207
12    CONTINUE                                                          1208
      CALL LNCOEF(N,8)                                                  1209
10    CONTINUE                                                          1210
C                                                                       1211
      DO 14 I=1,NMODE                                                   1212
      DO 16 J=1,NMODE                                                   1213
      SUMCXX=0.0                                                        1214
      SUMCXY=0.0                                                        1215
      SUMCYX=0.0                                                        1216
      SUMCYY=0.0                                                        1217
      SUMKXX=0.0                                                        1218
      SUMKXY=0.0                                                        1219
      SUMKYX=0.0                                                        1220
      SUMKYY=0.0                                                        1221
      DO 18 N=1,NBRG                                                    1222
      BGIJ=BGSHPE(N,I)*BGSHPE(N,J)                                      1223
      SUMCXX=SUMCXX+BGIJ*COEFLN(1,N)                                    1224
      SUMCXY=SUMCXY+BGIJ*COEFLN(3,N)                                    1225
      SUMCYX=SUMCYX+BGIJ*COEFLN(5,N)                                    1226
      SUMCYY=SUMCYY+BGIJ*COEFLN(7,N)                                    1227
      SUMKXX=SUMKXX+BGIJ*COEFLN(2,N)                                    1228
      SUMKXY=SUMKXY+BGIJ*COEFLN(4,N)                                    1229
      SUMKYX=SUMKYX+BGIJ*COEFLN(6,N)                                    1230
      SUMKYY=SUMKYY+BGIJ*COEFLN(8,N)                                    1231
18    CONTINUE                                                          1232
      ARRAY(   I,J   )=SUMCXX                                           1233
      ARRAY(   I,M1+J)=SUMCXY                                           1234
      ARRAY(M1+I,J   )=SUMCYX                                           1235
      ARRAY(M1+I,M1+J)=SUMCYY                                           1236
      ARRAY(   I,M2+J)=SUMKXX                                           1237
      ARRAY(   I,M3+J)=SUMKXY                                           1238
      ARRAY(M1+I,M2+J)=SUMKYX                                           1239
      ARRAY(M1+I,M3+J)=SUMKYY                                           1240
16    CONTINUE                                                          1241
14    CONTINUE                                                          1242
C                                                                       1243
      M2P1=M2+1                                                         1244
      DO 20 I=M2P1,M4                                                   1245
      DO 22 J=1,M4                                                      1246
      ARRAY(I,J)=0.0                                                    1247
22    CONTINUE                                                          1248
20    CONTINUE                                                          1249
      DO 24 I=1,NMODE                                                   1250
```

```
      ARRAY(   I,M2+I)=ARRAY(   I,M2+I)-A2NU(I)                          1251
      ARRAY(M1+I,M3+I)=ARRAY(M1+I,M3+I)-A2NU(I)                          1252
      ARRAY(   I,I   )=ARRAY(   I,I   )-DAMP                             1253
      ARRAY(M1+I,M1+I)=ARRAY(M1+I,M1+I)-DAMP                             1254
      ARRAY(M2+I,I   )=1.0                                               1255
      ARRAY(M3+I,M1+I)=1.0                                               1256
24    CONTINUE                                                           1257
C                                                                        1258
      IFAIL=0                                                            1259
      CALL F02AFF(ARRAY,40,M4,AREAL,AJMAG,IW,IFAIL)                      1260
C                                                                        1261
      REALMX=-1.0E20                                                     1262
      DO 26 I=1,M4                                                       1263
      IF(AREAL(I).GT.REALMX) REALMX=AREAL(I)                             1264
      SORTI(I)=ABS(AJMAG(I))                                             1265
26    CONTINUE                                                           1266
      WRITE(6,1012) REALMX                                               1267
      WRITE(6,1014)                                                      1268
      IFAIL=0                                                            1269
      CALL M01AAF(SORTI,1,M4,INDEX,IW,IFAIL)                             1270
      DO 32 I=1,M4                                                       1271
      J=INDEX(I)                                                         1272
      SORTR(J)=AREAL(I)                                                  1273
      SORTI(J)=AJMAG(I)                                                  1274
32    CONTINUE                                                           1275
      WRITE(6,1016) (SORTR(I),SORTI(I),I=1,M4)                           1276
      RETURN                                                             1277
C                                                                        1278
1012  FORMAT(///5X,16HLINEAR STABILITY/5X                                1279
     +           ,16H----------------//5X                                1280
     +,56HTHE MAXIMUM REAL PART OF THE ROOTS TO THE CHARACTERISTIC//5X    1281
     +,35HEQUATION OF THE LINEARIZED SYSTEM =,E13.5)                     1282
1014  FORMAT(///5X,36HEIGENVALUES OF THE LINEARIZED SYSTEM/5X            1283
     +           ,37H------------------------------------//14X           1284
     +,9HREAL PART,6X,9HIMAG PART/)                                      1285
1016  FORMAT(10X,E13.5,2X,E13.5)                                         1286
      END                                                                1287
```

```
      SUBROUTINE LNSVEC                                                 1288
C                                                                       1289
C**** LNSVEC CALCULATES, USING NAG ROUTINE F02AGF, THE EIGENVALUES      1290
C     AND EIGENVECTORS OF THE LINEARIZED SYSTEM. THE INITIAL CONDITIONS 1291
C     FOR THE NON-LINEAR SOLUTION PROCEDURE ARE SET TO THE EIGENVECTOR  1292
C     CORRESPONDING TO THE EIGENVALUE WITH MAXIMUM REAL PART. THE       1293
C     EIGENVECTOR IS SCALED SO THAT THE MINIMUM FILM THICKNESS          1294
C     FOR ANY POINT ON THE LINEARIZED ELLIPTIC ORBIT IS NOT LESS        1295
C     THAN 0.25 OF THE ARC RADIAL CLEARANCE IN ANY OF THE BEARINGS.     1296
C     (REF. SECTIONS 5.4 AND 8.1)                                       1297
C                                                                       1298
C**** STATEMENT MODIFICATIONS FOR INCREASED PROGRAMME DIMENSIONS        1299
C                                                                       1300
C     DIMENSION                                                         1301
C     ---------                                                         1302
C                                                                       1303
C     ARRAY(4*M,4*M),VR(4*M,4*M),VI(4*M,4*M),AREAL(4*M),AJMAG(4*M)      1304
C     IW(4*M),INDEX(4*M),SORTR(4*M),SORTI(4*M),XODIS(N),YODIS(N)        1305
C     XR(N),XI(N),YR(N),YI(N)                                           1306
C                                                                       1307
C     EQUIVALENCE                                                       1308
C     -----------                                                       1309
C                                                                       1310
C     (VR(1,1),DATAFQ(1+(4*M)**2)),(VI(1,1),DATAFQ(1+2*((4*M)**2)))     1311
C                                                                       1312
C     CALLS TO SUBROUTINES                                              1313
C     --------------------                                              1314
C                                                                       1315
C     F04AGF( ,4*M, , , , ,4*M, ,4*M, , )                               1316
C                                                                       1317
      COMMON QQ(4,10),A2NU(10),NMODE,ST,DAMP,NBRG,SBRG(6),XBRG(6)       1318
     +,YBRG(6),BGSHPE(6,10),NCPL,SCPL(2),AJ1(2),AJ2(2),NFRQ,SFRQ(6)     1319
     +,FQSHPE(6,10),QEXI(10),QETA(10),FX(6),FY(6),COEFLN(8,6)           1320
     +,XDOT,XDIS,YDOT,YDIS,DATAFQ(12288)                                1321
      COMMON /BRGSET/ BETA(6,2),GC(6,2),RSCAC(6,2),ARCL(6,2),ALGAM(6,2) 1322
     +,FXA(2),FYA(2),SCOS(6,2),SSIN(6,2),FCOS(6,2),FSIN(6,2),CAVCC,WFACT 1323
      DIMENSION ARRAY(40,40),VR(40,40),VI(40,40)                        1324
     +,AREAL(40),AJMAG(40),IW(40),INDEX(40),SORTR(40),SORTI(40)         1325
     +,XODIS(6),YODIS(6),XR(6),XI(6),YR(6),YI(6)                        1326
     +,AMAJN(6),RATIO(6),THETAN(6)                                      1327
      EQUIVALENCE (ARRAY(1,1),DATAFQ(1)),(VR(1,1),DATAFQ(1601))         1328
     +           ,(VI(1,1),DATAFQ(3201))                                1329
C                                                                       1330
      PI=3.14159265358979                                               1331
      M1=NMODE                                                          1332
      M2=M1+M1                                                          1333
      M3=M1+M2                                                          1334
      M4=M1+M3                                                          1335
      XDOT=0.0                                                          1336
      YDOT=0.0                                                          1337
      DO 10 N=1,NBRG                                                    1338
      XDIS=-XBRG(N)                                                     1339
      YDIS=-YBRG(N)                                                     1340
      DO 12 M=1,NMODE                                                   1341
      XDIS=XDIS+QQ(2,M)*BGSHPE(N,M)                                     1342
      YDIS=YDIS+QQ(4,M)*BGSHPE(N,M)                                     1343
12    CONTINUE                                                          1344
      XODIS(N)=XDIS                                                     1345
      YODIS(N)=YDIS                                                     1346
      CALL LNCOEF(N,8)                                                  1347
10    CONTINUE                                                          1348
C                                                                       1349
      DO 14 I=1,NMODE                                                   1350
      DO 16 J=1,NMODE                                                   1351
      SUMCXX=0.0                                                        1352
      SUMCXY=0.0                                                        1353
      SUMCYX=0.0                                                        1354
      SUMCYY=0.0                                                        1355
      SUMKXX=0.0                                                        1356
      SUMKXY=0.0                                                        1357
      SUMKYX=0.0                                                        1358
      SUMKYY=0.0                                                        1359
      DO 18 N=1,NBRG                                                    1360
      BGIJ=BGSHPE(N,I)*BGSHPE(N,J)                                      1361
      SUMCXX=SUMCXX+BGIJ*COEFLN(1,N)                                    1362
      SUMCXY=SUMCXY+BGIJ*COEFLN(3,N)                                    1363
      SUMCYX=SUMCYX+BGIJ*COEFLN(5,N)                                    1364
      SUMCYY=SUMCYY+BGIJ*COEFLN(7,N)                                    1365
      SUMKXX=SUMKXX+BGIJ*COEFLN(2,N)                                    1366
      SUMKXY=SUMKXY+BGIJ*COEFLN(4,N)                                    1367
      SUMKYX=SUMKYX+BGIJ*COEFLN(6,N)                                    1368
```

```
      SUMKYY=SUMKYY+BGIJ*COEFLN(8,N)                                    1369
18    CONTINUE                                                          1370
      ARRAY(   I,J   )=SUMCXX                                           1371
      ARRAY(   I,M1+J)=SUMCXY                                           1372
      ARRAY(M1+I,J   )=SUMCYX                                           1373
      ARRAY(M1+I,M1+J)=SUMCYY                                           1374
      ARRAY(   I,M2+J)=SUMKXX                                           1375
      ARRAY(   I,M3+J)=SUMKXY                                           1376
      ARRAY(M1+I,M2+J)=SUMKYX                                           1377
      ARRAY(M1+I,M3+J)=SUMKYY                                           1378
16    CONTINUE                                                          1379
14    CONTINUE                                                          1380
C                                                                       1381
      M2P1=M2+1                                                         1382
      DO 20 I=M2P1,M4                                                   1383
      DO 22 J=1,M4                                                      1384
      ARRAY(I,J)=0.0                                                    1385
22    CONTINUE                                                          1386
20    CONTINUE                                                          1387
      DO 24 I=1,NMODE                                                   1388
      ARRAY(   I,M2+I)=ARRAY(   I,M2+I)-A2NU(I)                         1389
      ARRAY(M1+I,M3+I)=ARRAY(M1+I,M3+I)-A2NU(I)                         1390
      ARRAY(   I,I   )=ARRAY(   I,I   )-DAMP                            1391
      ARRAY(M1+I,M1+I)=ARRAY(M1+I,M1+I)-DAMP                            1392
      ARRAY(M2+I,I   )=1.0                                              1393
      ARRAY(M3+I,M1+I)=1.0                                              1394
24    CONTINUE                                                          1395
C                                                                       1396
      IFAIL=0                                                           1397
      CALL F02AGF(ARRAY,40,M4,AREAL,AJMAG,VR,40,VI,40,IW,IFAIL)         1398
C                                                                       1399
      REALMX=-1.0E20                                                    1400
      DO 26 I=1,M4                                                      1401
      IF(AREAL(I).GT.REALMX) MXR=I                                      1402
      IF(AREAL(I).GT.REALMX) REALMX=AREAL(I)                            1403
      SORTI(I)=ABS(AJMAG(I))                                            1404
26    CONTINUE                                                          1405
      WRITE(6,1012) REALMX                                              1406
      WRITE(6,1014)                                                     1407
      IFAIL=0                                                           1408
      CALL M01AAF(SORTI,1,M4,INDEX,IW,IFAIL)                            1409
      DO 32 I=1,M4                                                      1410
      J=INDEX(I)                                                        1411
      SORTR(J)=AREAL(I)                                                 1412
      SORTI(J)=AJMAG(I)                                                 1413
32    CONTINUE                                                          1414
      WRITE(6,1016) (SORTR(I),SORTI(I),I=1,M4)                          1415
C                                                                       1416
      AXISMX=0.0                                                        1417
      DO 40 N=1,NBRG                                                    1418
      SUMXR=0.0                                                         1419
      SUMXI=0.0                                                         1420
      SUMYR=0.0                                                         1421
      SUMYI=0.0                                                         1422
      DO 42 I=1,NMODE                                                   1423
      SHAPE=BGSHPE(N,I)                                                 1424
      SUMXR=SUMXR+VR(M2+I,MXR)*SHAPE                                    1425
      SUMXI=SUMXI+VI(M2+I,MXR)*SHAPE                                    1426
      SUMYR=SUMYR+VR(M3+I,MXR)*SHAPE                                    1427
      SUMYI=SUMYI+VI(M3+I,MXR)*SHAPE                                    1428
42    CONTINUE                                                          1429
      XR(N)=SUMXR                                                       1430
      XI(N)=SUMXI                                                       1431
      YR(N)=SUMYR                                                       1432
      YI(N)=SUMYI                                                       1433
      X2AMP=SUMXR*SUMXR+SUMXI*SUMXI                                     1434
      Y2AMP=SUMYR*SUMYR+SUMYI*SUMYI                                     1435
      THETA=0.5*ATAN(2.0*(SUMXI*SUMYI+SUMXR*SUMYR)/(X2AMP-Y2AMP))       1436
      CTHETA=COS(THETA)                                                 1437
      STHETA=SIN(THETA)                                                 1438
      PHASE=ATAN2(SUMXI*CTHETA+SUMYI*STHETA,SUMXR*CTHETA+SUMYR*STHETA)  1439
      CPHASE=COS(PHASE)                                                 1440
      AMAJ=(SUMXR*CTHETA+SUMYR*STHETA)/CPHASE                           1441
      AMNR=(SUMXI*STHETA-SUMYI*CTHETA)/CPHASE                           1442
      IF(ABS(AMAJ).GT.ABS(AMNR)) GO TO 44                               1443
      TEMP=AMAJ                                                         1444
      AMAJ=AMNR                                                         1445
      AMNR=TEMP                                                         1446
      THETA=THETA+0.5*PI                                                1447
      IF(THETA.GT.0.5*PI) THETA=THETA-PI                                1448
44    IF(ABS(AMAJ).GT.AXISMX) AXISMX=ABS(AMAJ)                          1449
```

```
      AMAJN(N)=AMAJ                                                          1450
      RATIO(N)=AMNR/AMAJ                                                     1451
      THETAN(N)=THETA*180.0/PI                                               1452
40    CONTINUE                                                               1453
      CONST=0.05/AXISMX                                                      1454
C                                                                            1455
      COSDEL=COS(PI/18.0)                                                    1456
      SINDEL=SIN(PI/18.0)                                                    1457
64    CONST=CONST+0.05/AXISMX                                                1458
      COST=1.0                                                               1459
      SINT=0.0                                                               1460
      DO 60 I=1,36                                                           1461
      TEMP1=COST                                                             1462
      TEMP2=SINT                                                             1463
      COST=TEMP1*COSDEL-TEMP2*SINDEL                                         1464
      SINT=TEMP2*COSDEL+TEMP1*SINDEL                                         1465
      DO 62 N=1,NBRG                                                         1466
      X=RSCAC(N,1)*(X0DIS(N)+CONST*(XR(N)*COST-XI(N)*SINT))                  1467
      Y=RSCAC(N,1)*(Y0DIS(N)-GC(N,1)+CONST*(YR(N)*COST-YI(N)*SINT))          1468
      IF(X*X+Y*Y.GE.0.563) GO TO 66                                          1469
      Y=RSCAC(N,2)*(Y0DIS(N)-GC(N,2)+CONST*(YR(N)*COST-YI(N)*SINT))          1470
      IF(X*X+Y*Y.GE.0.563) GO TO 66                                          1471
62    CONTINUE                                                               1472
60    CONTINUE                                                               1473
      GO TO 64                                                               1474
66    CONST=CONST-0.05/AXISMX                                                1475
C                                                                            1476
      WRITE(6,1018)                                                          1477
      DO 72 N=1,NBRG                                                         1478
      AMAJN(N)=CONST*AMAJN(N)                                                1479
      WRITE(6,1020) N,AMAJN(N),RATIO(N),THETAN(N)                            1480
72    CONTINUE                                                               1481
C                                                                            1482
      DO 70 I=1,NMODE                                                        1483
      QQ(1,I)=QQ(1,I)+CONST*VR(   I,MXR)                                     1484
      QQ(2,I)=QQ(2,I)+CONST*VR(M2+I,MXR)                                     1485
      QQ(3,I)=QQ(3,I)+CONST*VR(M1+I,MXR)                                     1486
      QQ(4,I)=QQ(4,I)+CONST*VR(M3+I,MXR)                                     1487
70    CONTINUE                                                               1488
      RETURN                                                                 1489
C                                                                            1490
1012  FORMAT(///5X,16HLINEAR STABILITY/5X                                    1491
     +           ,16H----------------//5X                                    1492
     +,56HTHE MAXIMUM REAL PART OF THE ROOTS TO THE CHARACTERISTIC//5X       1493
     +,35HEQUATION OF THE LINEARIZED SYSTEM =,E13.5)                         1494
1014  FORMAT(///5X,36HEIGENVALUES OF THE LINEARIZED SYSTEM/5X                1495
     +           ,37H-------------------------------------//14X              1496
     +,9HREAL PART,6X,9HIMAG PART/)                                          1497
1016  FORMAT(10X,E13.5,2X,E13.5)                                             1498
1018  FORMAT(////5X,24HTHE ELLIPTICAL MOTION AT                              1499
     +,39H THE BEARINGS GIVEN BY THE EIGENVECTOR,/5X                         1500
     +,60HCORRESPONDING TO THE EIGENVALUE WITH MAXIMUM REAL PART, USED/      1501
     +,5X,59HAS INITIAL CONDITIONS FOR THE NON-LINEAR SOLUTION PROCEDURE     1502
     +//12X,13HMAJ.SEMI-AXIS,4X,14HRATIO(MIN/MAJ),4X,12HANG.MAJ.AXIS//)      1503
1020  FORMAT(5X,I2,6X,E11.5,6X,E11.5,9X,F6.2)                                1504
      END                                                                    1505
```

```
      SUBROUTINE FORIER                                                 1506
C                                                                       1507
C**** FORIER ARRANGES THE DATA COLLECTED FOR THE STEADY-STATE           1508
C     MOTION, AT THE MONITOR POINTS, IN A FORM SUITABLE FOR             1509
C     PRESENTATION TO THE NAG ROUTINE C06AAF - WHICH THEN PERFORMS      1510
C     A FINITE FOURIER TRANSFORM ON EACH SET OF DATA.                   1511
C                                                                       1512
      COMMON QQ(4,10),A2NU(10),NMODE,ST,DAMP,NBRG,SBRG(6),XBRG(6)       1513
     +,YBRG(6),BGSHPE(6,10),NCPL,SCPL(2),AJ1(2),AJ2(2),NFRQ,SFRQ(6)     1514
     +,FQSHPE(6,10),QEXI(10),QETA(10),FX(6),FY(6),COEFLN(8,6)           1515
     +,XDOT,XDIS,YDOT,YDIS,DATAFQ(12288)                                1516
      DIMENSION FRCOS(513),FRSIN(513),ILST(20)                          1517
C                                                                       1518
      PI=3.14159265358979                                               1519
      MFOR=9                                                            1520
      NFOR=2**MFOR                                                      1521
      M1FOR=2*MFOR+2                                                    1522
      N1FOR=NFOR+1                                                      1523
      DO 20 NSTN=1,NFRQ                                                 1524
      NXY=1HX                                                           1525
      DO 18 IXY=1,2                                                     1526
      NCOS=2*NFOR*(2*NSTN+IXY-3)                                        1527
      NSIN=NCOS+NFOR                                                    1528
      DO 22 I=1,NFOR                                                    1529
      FRCOS(I)=DATAFQ(NCOS+I)                                           1530
      FRSIN(I)=DATAFQ(NSIN+I)                                           1531
22    CONTINUE                                                          1532
      WRITE(6,6010) NSTN,NXY                                            1533
C                                                                       1534
      CALL C06AAF(FRCOS,FRSIN,N1FOR,.FALSE.,M1FOR,ILST)                 1535
C                                                                       1536
      FRCOS(1)=FRCOS(1)*0.5                                             1537
      DO 12 I=1,201                                                     1538
      IHAR=I-1                                                          1539
      FORAMP=SQRT(FRCOS(I)**2+FRSIN(I)**2)                              1540
      FORPHA=ATAN2(-FRSIN(I),FRCOS(I))*180.0/PI                         1541
      WRITE(6,6020) IHAR,FRCOS(I),FRSIN(I),FORAMP,FORPHA                1542
12    CONTINUE                                                          1543
      NXY=1HY                                                           1544
18    CONTINUE                                                          1545
20    CONTINUE                                                          1546
      RETURN                                                            1547
C                                                                       1548
6010  FORMAT(1H1/15X,48HFOURIER COEFFICIENTS FOR MOTION AT MONITOR POINT 1549
     +,I3,5X,A1,10H-DIRECTION///13X,1HK,14X,6HCOSINE,17X,4HSINE,18X     1550
     +,9HAMPLITUDE,15X,5HPHASE////)                                     1551
6020  FORMAT(10X,I5,6X,4(E17.9,7X))                                     1552
      END                                                               1553
```

```
      SUBROUTINE PLOTER                                                 1554
C                                                                       1555
C**** THIS ROUTINE PLOTS OUT A LINE-SEGMENT OF THE SHAFT TRAJECTORIES   1556
C     AT THE MONITOR POINTS. DETAILS ARE NOT GIVEN AS THE REQUIRED      1557
C     PROGRAMMING CODE IS INSTALLATION DEPENDENT.                       1558
C                                                                       1559
C**** STATEMENT MODIFICATIONS FOR INCREASED PROGRAMME DIMENSIONS        1560
C                                                                       1561
C     DIMENSION                                                         1562
C     ---------                                                         1563
C                                                                       1564
C     X(N),Y(N)                                                         1565
C                                                                       1566
      DIMENSION X(6),Y(6)                                               1567
C                                                                       1568
      RETURN                                                            1569
      END                                                               1570
```